



The University of  
**Nottingham**

UNITED KINGDOM • CHINA • MALAYSIA

Faculty of Engineering – Civil Engineering Department

# **Characterization of Rubberized Cement-Stabilized Roadbase Mixtures**

**By**

**Ahmed Hilal Farhan**

**B.Sc. Civil Eng., M.Sc. Highways and Airports Eng.**

**Thesis submitted to the University of Nottingham for the degree of  
Doctor of Philosophy in Civil Engineering**

**April 2016**

## Abstract

Due to urbanization, industrialization and population increase, a substantial increase occurred in the number of vehicles and hence large numbers of end-of-use tires are being disposed every year. The vast majority of these tires are stockpiled or used as a fuel for combustion which, in both cases, affects the environment detrimentally. The use of tire rubber in cement-stabilized aggregate mixtures (CSAMs) will ensure beneficial use of large quantities of these waste materials, saving natural resources and may enhance the properties of CSAMs especially these related to brittleness and sensitivity to fatigue failure.

Research was undertaken to investigate, at macro and mesoscale levels, the effect of both rubber and degree of stabilization and their combination on the behaviour of CSAMs in terms of the most influential pavement design properties under different static and dynamic modes of loading. These properties are strength, stiffness and fatigue. A range of testing equipment, methodologies and tools was developed, suggested and implemented to perform this investigation. Further investigation was also conducted to provide better understanding of the damage and failure mechanism through quantitative studying of the fractured surface, internal structure and surface cracking patterns under different testing modes.

The results of this study revealed that the addition of rubber has a negative effect on the compaction efficiency, compressive, flexural and tensile strengths while the stiffness, under different testing modes, was slightly reduced. In addition, a tougher mixture was produced after rubber-modification which means a change from a brittle to a more ductile behaviour. This behaviour was observed through different stiffness modulus evaluation methods. On the other hand, increase in cementation level has resulted in an increase in both strength and stiffness for both reference and rubberized mixtures. However, the decrease in the mixtures' strength due to rubberization was more obvious in highly cemented mixtures than the lightly cemented ones. On the other hand, a greater decline in the mixtures' stiffness, due to rubber incorporation, was observed at low cement contents. This behaviour is related to the void-like behaviour which depends, to large extent, on the relative stiffness between rubber and surrounding matrix.

Quantification of the fractured surfaces and cracking pattern utilizing the photogrammetry and fractal dimension concepts, respectively, revealed that the addition of rubber resulted in rougher and more tortuous cracks and increases disperse-ability of these cracks. This means the rubber-modification changed the cracking pattern which implies better load transfer through the cracks and less risk of reflection cracking.

The investigation of the internal structure, at mesoscale level, showed that the cracks were propagated through the rubber particles at all investigated cementation levels. This contributed to a lengthening of the crack path and to the delaying of crack propagation by absorbing and relieving the stresses at the crack tip, especially at the microcrack level. The latter mechanisms are behind toughness and fatigue improvement. Evaluation of rubber distribution revealed uniform distribution and this decrease as rubber content increases.

The results also indicated an improvement in the fatigue life for all rubber replacement levels. This was valid at all cementation levels. In terms of modulus degradability, rubberization of the cemented mixture has only a slight effect on this property while larger permanent deformation was accumulated after rubber inclusion. It was observed that the poorly cemented mixtures showed greater stiffness modulus degradation. Pavement analysis and design study showed that the decrease in the mixtures' strength overshadowed any improvement due to both mitigation of mixtures' stiffnesses or fatigue life enhancement. However, this is not the case for poor rubber mixtures where this mixture showed better behaviour than the reference mixtures.

## **Dedication**

*At the feet of my mother and my father*

## Acknowledgement

All thanks, glory, praise and adoration is due to God almighty, the most gracious the most merciful. O Allah you gave me the patience and strength to tackle with the hardships I have faced and guided me to finish this research.

First of all I would like to express my deep thanks for my supervisors: Mr. Andrew Dawson and Dr. Nick Thom for their motivation, encouragement and guidance throughout this project. I can say that I still hear your encouragement statements which indeed were like a charger to continue in this project after many difficulties that I faced. Big thank is also due to Mr. Andrew (particularly) due to his effort in reviewing my thesis chapters. They really gave me an excellent experience. Mr. Andrew and Dr. Nick I would say I am sorry for the many virtual five minutes that I frequently took during my PhD program to discuss some issues which always become half an hour.

I appreciate the kind advices from Dr. Luis Neves, my internal assessor, especially at the beginning of this project. Thanks Dr. Luis for your kindness and encouragement.

Sincere appreciation is due to the Higher Committee for Education Development in Iraq (HCED) for providing a scholarship to conduct this PhD study.

At this point, I can say that conducting such research with this type of mixture that share some properties of concrete (as cementitious material) and the others with the asphaltic mixtures (as a compacted material with relatively small stabilizer content) used in pavement structure is not an easy task. This is because this requires an understanding of both cement and asphalt concrete mixtures as well as cement-stabilized mixtures and their testing and most importantly higher level of independency in terms of sample manufacturing and testing. The independency in conducting this research was quit hard and useful at the same time. No doubt this comprehensive study required different tests and tools at different places. So, I would like to thank the following people who helped me by different means:

- Mr. Nigel Rook (concrete laboratory) for his kindness by providing cement, moulds and some technical demonstration (at the start of my study).
- Balbir Loyla (structures laboratory) for helping during the development of fatigue testing machine, kind advices to start with instrumentation process and for strain gauging.
- Mr. Richard Blackmore (Nottingham Transportation Engineering Centre-NTEC) for his technical discussion and demonstration.
- Mr. Jon Watson (NTEC) for his friendship, helping in X-raying some trials and scanning some samples and his continuous encouragement and support.
- Mr. Steve Elesbrook (Servocone Company) for his technical advice (in spite of his extremely limited time) during my struggling with cyclic testing facility
- Mr. Andrew Cooper (Cooper Company) for his cooperation and discussion when I started using the NAT machine to characterize my stiff mixtures.
- Mr. Tom Buss (senior technical manager at the Faculty of Engineering) for his technical discussion during some testing.
- Mr. Martyn Barret, Mr. Mathew Thomas and Miss. Laura (all from NTEC) for their help in samples trimming.
- Mr. Mark Dale (rock mechanics laboratory) for coring and testing my rock samples.

Thanks must go to Dr. Mathew Hall (the University of Nottingham) for providing me with the waste rubber and due to his discussion during my flexural program. Special thanks are also extended to Prof. Kypros Pilakoutas and Dr. Harris Angelakopoulos (both from Sheffield University) for providing me with some materials and their kind encouragement at the beginning of this project. Also, I am grateful to Dr. Martin Smith (Geospatial Institute at the University of Nottingham) and Dr. Sarhat Adam for their cooperation and involving me in scanning of my fractured surfaces samples. I must appreciate the help from Mr. Chris Fox (senior technician at Faculty of Engineering) for scanning some of samples. Special thanks to Dr. Alvaro Garcia for his friendship and support. I also appreciate the support from Dr. James Grenfell for helping in some ITS trials. My appreciation also goes to Mrs. Kathryn Sanderson for her encouragement and support in my conference administrative work. I must give special thanks for the reviewers of my papers for providing me with a useful feedback that contributed to raise the quality of this PhD study.

Thanks is also to my colleagues at the Nottingham Transportation Engineering Centre Dr. Ameer, Dr. Mahmood Al-Nasri, Dr. Chibuzor, Ahmed Nassar, Waleed, Ayad, Gustavo, Dr. Mahmoud, Rami, Bilal, Sydney, Venon, Hamed, Ahmed Ibrahim, Hasan, Abdulshafi, Yasameen, Haneen, Harith and Tariq. I am grateful to Dr. Ameer for his help when I first came to the UK.

I would like also to thank Dr. Jamal A. Farhan, the Assistance Prof. at Al-Anbar University for his continuous support and encouragement during my academic and practical lives and for keeping in touch during my PhD study. Also, I am grateful due Dr. Juma'ah Al-Sumaida'ai for his encouragement.

Now it is the time to thank my wife and my daughter: the tax payers of my success. You really struggled a lot (especially my daughter Haya) during my PhD study. Haya I know that I was not a perfect father because of my busy time but I will be a father to be proud of. All thanks to my mother and my father for their prayers and encouragements during the whole of my life. I have also to give big thanks to my brothers and my sisters for their support during my study. Finally, I would say I am sorry for both my big and small families because I know that the three years of my study without any visit to my country, due to my continuous work in this project, was hard and long time for both of you.

## **Declaration**

This research described in this thesis was conducted at the Civil Engineering Department, the University of Nottingham between October 2012 and February 2016. I declare that the work is my own and has not been submitted for a degree at another university.

Ahmed Hilal Farhan

The University of Nottingham

## Table of Contents

Abstract

Dedication

Acknowledgement

Declaration

Table of contents

List of figures

List of tables

List of abbreviations

List of notations

**Chapter 1..... Introduction ..... 1**

1.1 Background and problem statement..... 1

1.2 Aim and objectives ..... 6

1.3 Novelty of research .....8

1.4 Research Methodology and structure of thesis .....9

1.5 Research significance and contribution ..... 13

1.6 Publications, Prizes and achievements..... 16

1.7 References.....18

<b>Chapter 2.....</b>	<b>Cement-stabilized materials.....</b>	<b>2</b>
2.1	Introduction.....	23
2.2	Pavement types.....	24
2.3	Pavement structural components.....	25
2.4	Soil Stabilization.....	26
2.4.1	Methods of stabilization.....	26
2.5	Base Course Materials.....	27
2.6	Cement based pavement materials: classification and practice.....	28
2.6.1	PCA practice.....	30
2.6.2	South African practice.....	31
2.6.3	The UK practice.....	32
2.6.4	International practices.....	33
2.7	CBGMs constitute and mix design criteria .....	36
2.7.1	Cement .....	36
2.7.2	Aggregate.....	38
2.8	Mix design .....	39
2.9	Compaction .....	40
2.10	Curing .....	43
2.11	Characterization of cement-stabilized mixtures and their typical properties .....	43
2.11.1	Unconfined compressive strength (UCS) .....	43
2.11.2	Tensile strength .....	44

2.11.3	Stiffness modulus .....	45
2.11.4	Fatigue performance and damage.....	50
2.11.5	X-Ray Computed Tomography .....	52
2.11.5.1	Image analysis technique.....	53
2.11.5.2	X-ray applications.....	53
2.12	Previous suggested correlations.....	54
2.13	Concluding remarks.....	56
2.14	Reference.....	58
 <b>Chapter 3..... Rubberized cementitious mixtures.....</b>		<b>3</b>
3.1	Introduction.....	68
3.2	Waste tyres .....	69
3.2.1	Scrap tyre recycling.....	69
3.2.2	Size based classification.....	70
3.3	Review of rubberized cementitious mixtures studies.....	73
3.3.1	Rubberized concrete .....	73
3.3.1.1	Air-voids and density.....	73
3.3.1.2	Compressive, flexural and tensile strengths.....	75
3.3.1.3	Modulus of elasticity, toughness and ductility.....	80
3.3.1.4	Rubberized concrete under repeated loading .....	82
3.3.2	Cracking and failure patterns.....	83

3.3.3	Other rubberized cementitious materials.....	86
3.3.3.1	Rubberized cement-stabilized materials .....	86
3.3.3.2	Rubberized roller-compacted concrete.....	88
3.4	Concluding remarks.....	89
3.5	Reference.....	91

**Chapter 4..... Mixture design and initial investigation..... 4**

4.1	Introduction.....	96
4.2	Materials used.....	97
4.2.1	Aggregates.....	97
4.2.2	Crumb Rubber.....	98
4.2.3	Cement.....	99
4.3	Tests on Aggregates.....	100
4.3.1	Particle size distribution.....	100
4.3.2	Particle specific gravity and water absorption.....	100
4.3.3	Aggregate surface roughness.....	101
4.3.4	Aggregate strength and stiffness.....	104
4.4	Mix design methodology.....	105
4.5	Samples preparation and curing.....	109
4.6	Some properties related to mixture design.....	111
4.6.1	Bulk density determination.....	111

4.6.2	Compacity.....	112
4.6.2.1	Compacity by mathematical method as per BS EN 14227-1:2013.....	112
4.6.2.2	Compacity by experimental method.....	114
4.7	Results and discussion.....	115
4.7.1	Bulk density.....	115
4.7.2	Compacity.....	117
4.7.2.1	Effect of rubber content on the compacity of CSAMs.....	117
4.7.2.2	Effect of cement content on the compacity of CSAMs and RCSAMs.....	118
4.7.2.3	Comparison between theoretical and experimental procedures.....	119
4.8	Concluding remarks.....	121
4.9	References.....	123

**Chapter 5...Behaviour under unconfined compressive and indirect tensile testing.. 5**

5.1	Introduction.....	126
5.2	Materials, mixture design and samples preparation.....	128
5.3	Experimental Procedures.....	129
5.3.1	Unconfined Compressive Strength (UCS) Testing.....	129
5.3.2	Compressive stress-strain relationship.....	129
5.3.3	Static indirect tensile testing.....	133

5.3.3.1	Indirect tensile static modulus .....	134
5.3.3.1.1	Deformation measurement setup development.....	134
5.3.3.2	Toughness based on indirect tensile testing.....	137
5.3.3.3	Quantification of damage through fractal analysis.....	138
5.3.3.3.1	Fractal dimension .....	139
5.3.3.3.2	Fracture energy and fracture toughness based on fractal analysis.....	141
5.3.4	Cyclic indirect tensile testing .....	143
5.3.5	Mesostructural investigation.....	147
5.4	Results and discussion.....	148
5.4.1	Unconfined Compressive Strength (UCS) Test.....	148
5.4.1.1	Effect of rubber content on UCS.....	148
5.4.1.2	Combined effect of rubber and cement contents on UCS.....	149
5.4.2	Compressive stress-strain relationship.....	152
5.4.3	Indirect tensile strength (ITS) .....	151
5.4.3.1	Effect of rubber content on ITS.....	154
5.4.3.2	Combined effect of rubber and cement contents on ITS.....	154
5.4.3.3	Failure patterns.....	157
5.4.4	Load-deformation curves and toughness.....	159
5.4.4.1	Effect of rubber content on load-deformation curves and toughness.....	159
5.4.4.2	Combined effect of rubber and cement contents on load-deformation relationships and toughness.....	164

5.4.5	Indirect tensile elastic modulus of elasticity (Eit) .....	168
5.4.5.1	Effect of rubber content on static modulus of elasticity.....	168
5.4.5.2	Combined effect of rubber and cement contents on elastic elasticity modulus.....	169
5.4.6	Damage quantification.....	172
5.4.7	Comparison fracture energy.....	175
5.4.8	Overall discussion of failure mechanism.....	176
5.4.9	Cyclic indirect tensile testing.....	177
5.5	Concluding Remarks.....	181
5.6	References.....	185

**Chapter 6..... Flexural characterization and understanding .....6**

6.1	Introduction.....	191
6.2	Materials, mixture design and samples preparation.....	193
6.3	Testing equipment and procedure.....	196
6.4	Methods of analysis.....	197
6.4.1	Flexural strength and static flexural modulus.....	197
6.4.2	Flexural toughness.....	198
6.5	Flexural testing results and discussion.....	199
6.5.1	Flexural strength .....	199
6.5.2	Load-deformation relationships and flexural toughness.....	202

6.5.3	Static flexural modulus of elasticity.....	206
6.5.4	Failure patterns.....	210
6.6	Quantification of the flexural induced fractured surfaces.....	211
6.6.1	Quantification parameters.....	211
6.6.1.1	Volumetric Surface Texture Ratio (VSTR) .....	211
6.6.1.2	3D tortuosity.....	212
6.6.1.3	Arithmetic mean roughness (Ra) .....	213
6.6.2	Fractured surfaces characterization methods.....	214
6.6.3	Photogrammetric method.....	219
6.6.4	Fractured surface quantification findings.....	215
6.6.5	Implications of fractured surface study.....	225
6.7	Failure mechanism .....	226
6.8	Rubber distribution study.....	227
6.8.1	Experimental procedure and image analysis .....	228
6.8.1.1	Interval of X-ray scanning .....	229
6.8.1.2	Filtration and thresholding .....	229
6.8.1.3	Image analysis methodology.....	230
6.8.1.4	Segregation analysis.....	231
6.8.2	Rubber distribution and segregation results and discussion.....	234
6.8.2.1	Vertical and radial rubber distribution.....	234
6.8.2.2	Rubber segregation analysis.....	236
6.9	Concluding remarks.....	240

6.10	References.....	244
------	-----------------	-----

**Chapter 7..... Non-destructive evaluation and their correlation..... 7**

7.1	Introduction.....	249
7.2	Importance of the non-destructive testing for pavement design.....	250
7.3	Materials, mixture design and samples preparation.....	251
7.4	Experimental Procedures.....	251
7.4.1	Ultrasonic Pulse Velocity (UPV) .....	252
7.4.2	Resonant-frequency testing.....	253
7.5	Results and discussion.....	255
7.5.1	Uniformity of different samples densities.....	255
7.5.2	Ultrasonic pulse velocity (UPV) .....	258
7.5.2.1	Effect of combined effect of cement and rubber on UPV .....	261
7.5.3	Dynamic modulus of elasticity.....	265
7.5.4	Dynamic modulus of elasticity, dynamic shear moduli and dynamic Poisson's ratio.....	266
7.5.4.1	Effect of sample size on stiffness and shear moduli form resonant-frequency testing.....	270
7.6	New proposed application for non-destructive testing .....	271
7.7	Concluding Remarks.....	274
7.8	References.....	277

**Chapter 8.....Development of fatigue testing facility..... 8**

8.1	Introduction.....	280
8.2	Fatigue testing configuration and previous studies.....	281
8.3	Wave form and fatigue testing mode.....	282
8.4	Fatigue failure analysis criteria.....	283
8.5	Initial stiffness.....	285
8.6	Development of fatigue testing facility .....	285
8.6.1	Actuator installation and set-up .....	286
8.6.2	Manufacturing and aligning test fittings .....	287
8.6.3	Data acquisition system and instruments calibration.....	288
8.6.4	Instrumentation mounting and LVDTs Calibration .....	292
8.6.5	Initial investigations results.....	293
8.6.6	Data handling and processing.....	298
8.7	Concluding remarks.....	299
8.8	References .....	301

**Chapter 9..... Fatigue and dynamic modulus performance ..... 9**

9.1	Introduction.....	304
9.2	Pavement fatigue failure .....	305
9.3	Interpretation of fatigue performance.....	306

9.3.1	Stiffness reduction approach.....	307
9.3.2	Dissipated energy approach.....	307
9.3.2.1	Dissipated energy ratio (DER) .....	310
9.4	Materials, mixture design and samples preparation.....	312
9.5	Load application and configuration.....	312
9.6	Resilience, permanent and total deformation, and dynamic modulus.....	313
9.7	Testing methodology and procedures.....	314
9.7.1	Estimation the actual strength of the mixture.....	314
9.7.2	Flexural dynamic modulus and fatigue testing .....	314
9.8	Flexural dynamic modulus and comparison with other methods.....	318
9.9	Fatigue testing program.....	322
9.9.1	Effect of rubber and cement on phase angle of cement-stabilized aggregate.....	322
9.10	Fatigue testing program results.....	323
9.10.1	Fatigue lives.....	323
9.10.1.1	Effect of rubber on the fatigue behaviour of CSAMs.....	323
9.10.1.2	Combined effect of cement and rubber on the fatigue behaviour of CSAMs .....	327
9.11	Dynamic deformations.....	329
9.12	Stress ratio-Number of cycles to failure (S-N) curves.....	330
9.13	Endurance limits and fatigue strength.....	331
9.14	Evaluation of Damage accumulation .....	332
9.14.1	Permanent deformation accumulation.....	332

9.14.2	Dynamic modulus degradation.....	339
9.14.3	Dynamic load-deformation hysteresis loops.....	345
9.14.4	Fatigue damage accumulation assessment through dissipated energy approach.....	346
9.15	Concluding remarks.....	349
9.16	References.....	353

**Chapter 10..... Pavement analysis and design ..... 10**

10.1	Introduction.....	356
10.2	Pavement arrangements and properties.....	357
10.3	Traffic loads and analysis software.....	359
10.4	Pavement failure criteria.....	360
10.5	Methodology and Mechanistic pavement design.....	361
10.6	Pavement analysis results.....	362
10.6.1	Vertical stresses and strains distributions.....	362
10.6.2	Horizontal stress and strain distributions.....	365
10.7	Pavement design sensitivity analysis.....	367
10.8	Overall discussion regarding pavement design.....	370
10.9	Effect of stiffness degradation on pavement analysis and design .....	372
10.10	Effect of difference between laboratory and field results on pavement design.....	374
10.11	Suggested design approach.....	378

10.12	Concluding remarks.....	380
10.13	References.....	382

**Chapter 11..... Conclusions and recommendations ..... 11**

11.1	Introduction.....	384
11.2	Main Conclusions .....	385
11.3	Conclusions related to mix design and sample preparation.....	388
11.4	Conclusions related to static mechanical characterization.....	389
11.5	Conclusions related to fracture pattern, internal structure and mechanism of failure.....	390
11.6	Conclusions related to nondestructive testing of cementitious materials and comparison with static and dynamic testing.....	392
11.7	Conclusions related to fatigue testing facility and characterization tests and techniques.....	394
11.8	Conclusions related to fatigue performance and pavement analysis and design.....	395
11.9	Recommendations for future research.....	396

**Appendix A:** Vertical deformation histories under cyclic loading

**Appendix B:** Load-deformation hysteresis loops

**Appendix C:** Dissipated energy approach results

**Appendix D:** Dynamic moduli relationships

## List of Figures

### Chapter 1

Figure 1.1: Main problems undertaken in this research : a. environmental; b. Natural resources scarcity and c. Cement-stabilization problems.....	5
---	---

### Chapter 2

Figure 2.1: Types of highway pavements structures.....	25
Figure 2.2: Stresses distribution on subgrade.....	28
Figure 2.3: Various types of cement based materials.....	31
Figure 2.4: Fatigue crushing at the top of lightly cemented layer.....	38
Figure 2.5: Cement stabilized materials mixture design sequence.....	40
Figure 2.6: Pavement structure containing CSAM base under traffic loading (exaggerated deflection).....	51
Figure 2.7: Elements of an X-Ray setup.....	53

### Chapter 3

Figure 3.1: Illustration of ambient granulating for scrap tyre recycling system	71
Figure 3.2: Illustration of cryogenic grinding for scrap tyre recycling system	71
Figure 3.3: Illustration of different sizes of recycled crumb rubber .....	72
Figure 3.4: Air-voids distribution through concrete samples.....	74
Figure 3.5: Relationship between density and fine rubber percentages .....	74
Figure 3.6: Relationship between density and coarse rubber percentages .....	75

Figure 3.7: Relationship between Compressive strength and rubber percentages: coarse aggregate replacement.....	76
Figure 3.8: Relationship between strength and rubber percentages: Fine aggregate replacement .....	76
Figure 3.9: Rubber distribution in rubberized concrete (a) and roller-compacted concrete (b).....	79
Figure 3.10: Relationship between tensile strength and rubber percentages: fine and coarse aggregate replacement.....	80
Figure 3.11: Load- Deflection for concrete with different rubber contents .....	80
Figure 3.12: Relationship between elastic modulus and rubber percentages: fine and coarse aggregate replacement .....	80
Figure 3.13: Fatigue line for different mixtures reported by.....	83
Figure 3.14: Failure pattern under static compressive loading for plain (left) and rubberized (right) concrete.....	84
Figure 3.15: Modelling rubberized concrete under compressive loading (Redrawn from .....	85
Figure 3.16: Finite element analysis of rubberized concrete samples under indirect tensile testing .....	85

## **Chapter 4**

Figure 4.1: Different sizes of aggregate fractions.....	97
Figure 4.2: Crumb rubber appearance .....	98
Figure 4.3: Particle size distribution of natural aggregate fractions and crumb rubber.....	101
Figure 4.4: Surface roughness apparatus at the University of Nottingham.....	103

Figure 4.5: a. Aggregate cores and b. testing set-up for UCS of aggregate.....	104
Figure 4.6: Stress-strain relationship for different aggregate samples.....	105
Figure 4.7: Design gradation of cement stabilized mixture used in this study...	106
Figure 4.8: Sample preparation: a. batching aggregate for each sample and b. details of moulds and compaction equipment.....	110
Figure 4.9: Samples appearance for different rubber contents at 5% cement...	110
Figure 4.10: Density measurement arrangement.....	111
Figure 4.11: Porosity measurement arrangement.....	115
Figure 4.12: Effect of rubber replacement level on dry density.....	116
Figure 4.13: Effect of cement content on density of RCSAMs and CSAMs .....	116
Figure 4.14: Effect of rubber content on compacity value.....	118
Figure 4.15: Effect of cement content on compacity value of RCSAMs and CSAMs.....	119
Figure 4.16: Mechanism of water penetration and cement paste film coating aggregate particles.....	121

## **Chapter 5**

Figure 5.1: Large cylinders > 300 mm height; b. samples curing.....	128
Figure 5.2: UCS testing machine used in this study.....	130
Figure 5.3: Sample preparation and instrumentation setup: a. checking instrumentation alignment; b. LDPs setup and c. LVDTs setup.....	131
Figure 5.4a: Preparations for test face of samples for video gauge testing.....	132
Figure 5.4b: Instron machine and test configuration used for compressive test with video gauge .....	132

Figure 5.5: Instron machine and configuration used for indirect tensile testing.....	133
Figure 5.6: Trial arrangement for lateral deformation measurement.....	136
Figure 5.7: Manufactured gluing jig parts.....	136
Figure 5.8: Fixing LVDTs holders through the new instrumentation setup.....	136
Figure 5.9: Sample cracking pattern traced from failed samples showing application of box counting methodology.....	140
Figure 5.10: A plot of log of box size versus the log of box count.....	140
Figure 5.11: Cyclic indirect tensile testing NAT machine with close-up view of test configuration.....	146
Figure 5.12: Cyclic load wave applied by NAT machine and corresponding deformation .....	146
Figure 5.13: Figure 2.13: X-Ray CT machine parts and alignment of sample....	147
Figure 5.14: Effect of rubber content on UCS at 7, 28 and 365 days.....	149
Figure 5.15: Effect of cement content on UCS of control and rubberized mixtures at 7, 28 and 365 days.....	151
Figure 5.16: Variation of UCS at 28 days with UCS at 7 and 360 days .....	152
Figure 5.17: Load-axial deformation relationship for different mixtures. ....	153
Figure 5.18: Effect of rubber content on ITS at 7, 28 and 365 days.....	155
Figure 5.19: Effect of cement content on ITS at 7 and 28 days.....	155
Figure 5.20: Variation of UCS with ITS for different ages, cement and rubber contents.....	156
Figure 5.21: Failure pattern of ITS samples containing different rubber contents and 5% cement.....	158

Figure 5.22: Failure patterns of ITS samples containing different combinations of rubber and cement contents. ....	158
Figure 5.23: Failure patterns of UCS samples containing different rubber contents and 5% cement.....	158
Figure 5.24: Failure patterns of UCS samples containing different combinations of rubber and cement contents. ....	159
Figure 5.25: Load-deformation curve for C5R0.....	160
Figure 5.26: Load-deformation curve for C5R15.....	160
Figure 5.27: load-deformation curve for C5R30.....	160
Figure 5.28: Load-deformation curve for C5R45.....	160
Figure 5.29: Effect of rubber content on toughness indices.....	161
Figure 5.30: Cracks propagation mechanism for C5R15.....	163
Figure 5.31: Cracks propagation mechanism for C5R30.....	163
Figure 5.32: Cracks propagation mechanism for C5R45.....	163
Figure 5.33: Schematic illustration of fracture process .....	164
Figure 5.34: load-deformation curve for C3R0.....	165
Figure 5.35: load-deformation curve for C3R30.....	165
Figure 5.36: load-deformation curve for C7R0.....	165
Figure 5.37: load-deformation curve for C7R30.....	165
Figure 5.38: Effect of cement content on toughness indices. ....	166
Figure 5.39: Effect of cement content on toughness indices: a. C3R30; b. C5R30 and c. C7R30.....	167-168
Figure 5.40: Effect of rubber content on indirect tensile static modulus .....	169

Figure 5.41: Effect of cement content on indirect tensile static modulus.....	170
Figure 5.42: Variation of indirect tensile static stiffness modulus versus ITS...	171
Figure 5.43: Variation of indirect tensile static stiffness modulus versus UCS	171
Figure 5.44: A graph of log of box count against the log of box size for mixtures of different rubber contents .....	173
Figure 5.45: A graph of log of box count against the log of box size for reference and rubberized mixtures of different cement contents.....	174
Figure 5.46: Effect of different rubber contents on indirect tensile resilient modulus.....	178
Figure 5.47: Effect of cement content on indirect tensile resilient modulus...	178
Figure 5.48: Correlation of indirect tensile moduli under static and cyclic loading.....	180
Figure 5.49: Variation of ITST versus ITS.....	180
Figure 5.50: Variation of ITST versus UCS.....	181

## **Chapter 6**

Figure 6.1: Samples preparation: a. mixing of materials; b. Sample moulds and moulding; c. compaction procedure and d. samples curing.....	195
Figure 6.2: sample preparations (a) sawing prismatic samples. (b) Sawed specimens.....	196
Figure 6.3: Static flexural testing configuration.....	197
Figure 6.4: Toughness determination methodology.....	199
Figure 6.5: Effect of rubber replacement on flexural strength.....	200
Figure 6.6: Effect of cement content on flexural strength.....	201
Figure 6.7: Flexural strength and UCS relationship.....	202

Figure 6.8:	Flexural strength and ITS relationship.....	202
Figure 6.9:	Load-deformation curves for C5R0.....	203
Figure 6.10:	Load-deformation curves for C5R15.....	203
Figure 6.11:	Load-deformation curves for C7R30.....	203
Figure 6.12:	Load-deformation curves for C7R45.....	203
Figure 6.13:	Load-deformation curves for C3R0.....	204
Figure 6.14:	Load-deformation curves for C3R30.....	204
Figure 6.15:	Load-deformation curves for C7R0.....	204
Figure 6.16:	Load-deformation curves for C7R30.....	204
Figure 6.17:	Toughness indices for CSAMs containing different amounts of rubber and 5% cement.....	205
Figure 6.18:	Toughness indices for CSAMs containing different amounts of cement and 30% rubber.....	206
Figure 6.19:	Effect of rubber replacement on static flexural stiffness.....	207
Figure 6.20:	Effect of cement content on static flexural stiffness.....	208
Figure 6.21:	Static flexural modulus and UCS relationship.....	209
Figure 6.22:	Static flexural modulus and ITS relationship.....	209
Figure 6.23:	Flexural strength and modulus relationship.....	209
Figure 6.24:	Failure pattern of CSAMs at different binding degrees: A.3% cement, B. 5% cement and C.7% cement (Red and black arrows indicate failure through and around aggregate, respectively) .....	210
Figure 6.25:	Illustration of fractured surface and the plane surface. ....	212
Figure 6.26:	Surface area estimation methodology .....	213

Figure 6.27: A flow diagram of the photogrammetric and structure from motion processes.....	216
Figure 6.28: Photogrammetric procedure preparation steps: a. painted fractured samples; b. fixing references; c. image capturing from different angles and d. surveying references coordinates on fractured surfaces.....	217
Figure 6.29: Samples of fractured surface scan of C5R0-1.....	220
Figure 6.30: Samples of fractured surface scan of C5R0-2.....	220
Figure 6.31: Samples of fractured surface scan of C5R15-1.....	221
Figure 6.32: Samples of fractured surface scan of C5R15-2.....	221
Figure 6.33: Samples of fractured surface scan of C5R30-1.....	222
Figure 6.34: Samples of fractured surface scan of C5R30-2.....	222
Figure 6.35: Samples of fractured surface scan of C45R0-1.....	223
Figure 6.36: Samples of fractured surface scan of C45R0-2.....	223
Figure 6.37: Effect of cement content on 3D tortuosity.....	224
Figure 6.38: Effect of rubber content on roughness number.....	224
Figure 6.39: Effect of rubber content on VSTR.....	225
Figure 6.40: Analysis of rubber quantity through fractures surface: a. captured image, b. thresholded image and c. thresholding process.....	227
Figure 6.41: Effect of replacement level on amount of rubber across the fractured surfaces.....	227
Figure 6.42: Samples x-ray images showing the rubber clustering in cemented mixtures.....	231
Figure 6.43: Methodology for radial (a) and vertical (b) segregation evaluation.....	233

Figure 6.44: Vertical rubber distribution for different RCSAMs.....	234
Figure 6.45: Radial rubber distribution in external and internal parts of C5R15 sample.....	235
Figure 6.46: Radial rubber distribution in external and internal parts of C5R30 sample.....	236
Figure 6.47: Radial rubber distribution in external and internal parts of C5R45 sample.....	236
Figure 6.48: Sample of 3D distribution for RCSAMs containing 30% rubber replacement.....	238
Figure 6.49: Samples of rubber distribution in prismatic specimens containing (a) 15%, (b) 30% and (d) 45% replacement levels.....	239
Figure 6.50: Samples of rubber distribution in prismatic specimen containing 30% rubber replacement at (a) top, (b) middle and (d) bottom levels.....	239

## **Chapter 7**

Figure 7.1: PUNDIT-Plus Apparatus and measuring arrangement.....	252
Figure 7.2: Resonant frequency test configuration: a. Torsional mode arrangement; b. longitudinal mode arrangement.....	255
Figure 7.3: Effect of rubber content on densities of different samples types....	256
Figure 7.4: Effect of cement content on densities of different samples types...	257
Figure 7.5: Effect of age and rubber content on the UPVs .....	258
Figure 7.6: Effect of rubber content on UPVs of different samples.....	260
Figure 7.7: Effect of cement content on UPVs of different samples.....	261
Figure 7.8: Effect of age and cement content on the UPVs.....	262
Figure 7.9: Variation of UPVs versus UCSs.....	264
Figure 7.10: Variation of UPVs versus ITS.....	264

Figure 7.11: Variation of UPVs versus flexural strength @ 5% cement content.	265
Figure 7.12: Variation of UPVs versus flexural strength @3% and 7% cement content.....	265
Figure 7.13: Variation of UPVs versus static flexural modulus.....	265
Figure 7.14: Variation of UPVs versus static indirect tensile modulus.....	265
Figure 7.15: Effect of rubber replacement level on dynamic modulus of elasticity and shear modulus.....	267
Figure 7.16: Effect of cementation level on dynamic modulus of elasticity and shear modulus.....	268
Figure 7.17: Effect of rubber replacement level on dynamic Poisson's ratio.....	269
Figure 7.18: Effect of cement content on dynamic Poisson's ratio.....	270
Figure 7.19: Dynamic moduli for large cylinders versus prismatic samples for different rubberized and reference samples under different stabilization degrees..	271

## **Chapter 8**

Figure 8.1: Different fatigue test arrangements.....	282
Figure 8.2: Idealized illustration of stress and strain controlled failure points...	284
Figure 8.3: Installing testing frame and actuator and the hydraulics.....	287
Figure 8.4: Manufacturing and installation of test fittings: a. top and bottom parts; b. installation and alignment.....	288
Figure 8.5: Fatigue test facility developed during the course of this study.....	290
Figure 8.6: Schematic technical representation for the developed fatigue test facility.....	291

Figure 8.7:	Instrumentation mounting arrangement.....	292
Figure 8.8:	Illustration of LVDT calibration using blocks of known thickness.....	293
Figure 8.9:	Calibration curves for LVDT 1 and LVDT 2.....	293
Figure 8.10:	Load waveform generated during fatigue testing of constant amplitude.....	295
Figure 8.11:	Deformation waveform corresponding to the load waveform.....	295
Figure 8.12:	Strain gauging: a. Strain gauges and wired sample; b. Electrical circuit testing.....	296
Figure 8.13:	On-sample instrumentation arrangement.....	297
Figure 8.14:	Comparison between different instrumentation arrangements.....	298

## **Chapter 9**

Figure 9.1:	Stiffness reduction approach illustration.....	307
Figure 9.2:	Typical hysteresis loop and dissipated energy concept.....	309
Figure 9.3:	Total, elastic and permanent deformation during cyclic loading....	313
Figure 9.4:	Testing planning for fatigue testing program.....	317
Figure 9.5:	Effect of rubber contents on fatigue lives of CSAMs .....	328
Figure 9.6:	Effect of cement content on fatigue lives of reference and rubberized mixtures @ 90% and 85% stress ratios.....	328
Figure 9.7:	Vertical deformation under cyclic loading for C3R0@90% stress ratio.....	329
Figure 9.8:	Vertical deformation under cyclic loading for C3R30@85% stress ratio.....	329

Figure 9.9: Vertical deformation under cyclic loading for C5R0@85% stress ratio.....	330
Figure 9.10: Vertical deformation under cyclic loading for C5R30@85% stress ratio.....	330
Figure 9.11: Vertical deformation under cyclic loading for C7R0@85% stress ratio.....	330
Figure 9.12: Vertical deformations under cyclic loading for C7R30@85% stress ratio.....	330
Figure 9.13: S-N curve for reference and rubberized mixtures @ 5% cement content.....	332
Figure 9.14: Permanent deformation accumulation for mixtures containing different rubber contents @ 90% stress ratio.....	334
Figure 9.15: Permanent deformation accumulation for mixtures containing different rubber contents @85% stress ratio.....	334
Figure 9.16: Permanent deformation accumulation for rubberized mixtures containing different cement contents @ 90% stress ratio.....	336
Figure 9.17: Permanent deformation accumulation for rubberized mixtures containing different cement contents @ 85% stress ratio.....	336
Figure 9.18: Permanent deformation accumulation for reference mixtures containing different cement contents @ 90% stress ratio.....	337
Figure 9.19: Permanent deformation accumulation for reference mixtures containing different cement contents @85% stress ratio.....	337
Figure 9.20: Evolution of dynamic modulus of elasticity for CSAMs of different rubber replacement @90% stress ratio.....	342
Figure 9.21: Evolution of dynamic modulus of elasticity for CSAMs of different rubber replacement @85% stress ratio.....	342

Figure 9.22: Evolution of dynamic modulus of elasticity for RCSAMs of different cement contents @90% stress ratio.....	343
Figure 9.23 Evolution of dynamic modulus of elasticity for RCSAMs of different cement contents @85% stress ratio.....	343
Figure 9.24: Evolution of dynamic modulus of elasticity for CSAMs of different cement contents @90% stress ratio.....	344
Figure 9.25: Evolution of dynamic modulus of elasticity for CSAMs of different cement contents @85% stress ratio.....	344
Figure 9.26: Load-deformation hysteresis loops for C3R0@90% stress ratio....	345
Figure 9.27: Load-deformation hysteresis loops C3R30@90% stress ratio.....	345
Figure 9.28: Load-deformation hysteresis loops for C5R0@90% stress ratio.....	346
Figure 9.29: Load-deformation hysteresis loops for C5R30@90% stress ratio..	346
Figure 9.30: Load-deformation hysteresis loops for C7R0@90% stress ratio....	346
Figure 9.31: Load-deformation hysteresis loops for C7R30@90% stress ratio...	346
Figure 9.32: Variation in energy ratio versus cycles number for C3R30@85%..	348
Figure 9.33: Variation in energy ratio versus cycles number for C5R30@85%..	348
Figure 9.34: Variation in energy ratio versus cycles number for C7R30@85....	348
Figure 9.35: Fatigue life based on energy ratio versus cycles number to break the sample.....	349

## **Chapter 10**

Figure 10.1: Pavement structure configuration .....	358
Figure 10.2: Pavement structure critical responses for design .....	361
Figure 10.3: Pavement analysis and design adopted Methodology .....	363
Figure 10.4: Effect of different layer properties on vertical stresses .....	364

Figure 10.5: Effect of different layer properties on vertical strains .....	364
Figure 10.6: Effect of different layer properties on horizontal stresses.....	365
Figure 10.7: Effect of different layer properties on horizontal strains.....	366
Figure 10.8: Allowable load applications for 40 mm surface course and variable cement-stabilized base thicknesses.....	367
Figure 10.9: Allowable load applications for 50 mm surface course and variable cement-stabilized base thicknesses .....	368
Figure 10.10: Allowable load applications for 40 mm surface course and variable cement-stabilized base thicknesses .....	369
Figure 10.11: Allowable load applications for 50 mm surface course and variable cement-stabilized base thicknesses .....	369
Figure 10.12: Effect of cemented mixture stiffness on pavement critical responses (no bond between layers) .....	377
Figure 10.13: Effect of cemented mixture stiffness reduction on pavement critical responses (Fully bonded).....	377
Figure 10.14: Schematic illustration of the effect the cemented base modulus degradation on the stresses applied on the subgrade.....	378

## List of Tables

### Chapter 2

Table 2.1: Properties of modified, lightly bound and heavily bound materials.....	30
Table 2.2: Different categories of cemented materials as defined by South African mechanistic pavement design method.....	32
Table 2.3: Practices and criteria used by different countries for cement stabilized materials .....	34-35
Table 2.4: Approximate range of cement contents for various materials.....	37
Table 2.5: Tentative range of optimum moisture contents for various materials.....	39
Table 2.6: Elastic moduli estimated by different methods for different materials and binder contents with their typical values.....	48-49
Table 2.7: Previous fatigue correlation extracted from the literature.....	52
Table 2.8: Previous developed correlation extracted from literature.....	55

### Chapter 4

Table 4.1: Chemical composition of crumb rubber .....	99
Table 4.2: Physical properties of crumb rubber .....	99
Table 4.3: Physical and chemical properties of cement.....	100
Table 4.4: Properties of aggregate included in this study.....	101
Table 4.5: Surface roughness characterization results.....	103
Table 4.6: Optimum moisture contents and maximum dry densities.....	107
Table 4.7: Investigated mixtures.....	108

## **Chapter 5**

Table 5.1: Fracture energies and toughness indices based on fractal analysis and experimental procedures .....	175
--	-----

## **Chapter 6**

Table 6.1: RMSE of the residuals at the control points on the fractured surface.....	218
--	-----

Table 6.2: Rubber segregation analysis for CSAMs containing different amount of rubber.....	237
---	-----

## **Chapter 9**

Table 9.1: Densities, UPVs and estimation of the actual flexural strength for dynamic flexural modulus test samples.....	320
--	-----

Table 9.2: Summary of comparison between different stiffness modulus characterization methods.....	321
--	-----

Table 9.3: The relationships between moduli of elasticity estimated under static, dynamic and nondestructive testing.....	322
---	-----

Table 9.4: Densities, UPVs and estimation of the actual flexural strength for fatigue test samples.....	325
---	-----

Table 9.5: Densities, UPVs and estimation of the actual flexural strength for fatigue test samples.....	326
---	-----

Table 9.6: Regression coefficients for permanent deformation of investigated mixtures.....	339
--	-----

## **Chapter 10**

Table 10.1: Analysis and design matrix .....	358
--	-----

Table 10.2: Typical properties for surface, subbases and subgrades course.....	359
--	-----

## List of Abbreviations

CSAM	Cement-Stabilized Aggregate Mixture.
RCSAM	Rubberized Cement-Stabilized Aggregate Mixture.
MEPDG	Mechanistic-Empirical Pavement Design Guide.
UCS	Unconfined Compressive strength
ITS	Indirect Tensile Strength
LVDT	Linear Variable Differential Transducer
LDP	Linear Displacement Potentiometers.
NAT	Nottingham Asphalt Tester
RAP	Recycled Asphalt Pavement
ASTM	American Society of Testing Materials
VSTR	Volumetric Surface Texture Ratio
VST	Volumetric Surface Texture
RMSE	Root Mean Square Error
RGB	Red Green Blue
UPV	Ultrasonic Pulse Velocity
AASHTO	American Association of State Highway and Transportation Officials
BS EN	British European Standards
S-N	Stress Ratio- Number of cycles
SR	Stress Ratio
N	Number of cycles
HMA	Hot mix Asphalt
ALF	Accelerated Load Facility
PCA	American Portland Concrete Association
DER	Dissipated Energy Ratio

## List of Notations

$\rho_b$	Bulk density
$w_a$	Weight of specimen in air
$w_w$	Weight of specimen in water
$C$	Compacity factor
$\gamma_m$	Maximum dry density of the mixture
$\gamma_A$	Particle density of material A
$\gamma_B$	Particle density of material B
$\gamma_C$	Particle density of material C
$p$	Porosity
$m_s$	Mass of saturated specimen in air
$m_d$	Mass of oven dried specimen
$m_{ss}$	Mass of saturated specimen in water
$E_r$	Resilient modulus measured under indirect tensile cyclic loading.
$E_{it}$	Static modulus of elasticity measured via indirect tensile testing.
$E_r$	Resilient modulus under indirect tensile loading.
$D_s$	Fractal dimension.
$P$	Ultimate load
$A$	Cross sectional area of the sample
$CxRy$	Cement-stabilized mixture that contain x% cement and y% rubber.
$h$	Thickness of specimen
$d$	Diameter of specimen
$\Delta H_T$	Lateral deformation
$D_g$	LVDTs gauge distance
$\nu$	Poisson's ratio
$A_D$	Area under normalized load-deformation curve up to a specific deformation
$A_p$	Area under normalized load-deformation curve up to deformation at a peak
$D$	Deformation
$D_p$	Deformation at failure
$J_{IC}$	Fracture energy
$L$	Scale of observation
$S_y$	Ultimate strength
$E$	Modulus of elasticity
$D_s$	Fractal dimension
$K_{IC}$	Toughness of the material
$D_{1-d}$	Two dimensional fractal dimension
$\delta_o$	Scale of observation
$z$	Horizontal deformation amplitude
$W_s$	energy dissipated at the surface of the crack

$G_f$	Fracture energy at the observation scale
ITST	Indirect tensile stiffness modulus under cyclic indirect tensile loading
$F_s$	Flexural strength
$b$	Width of the prism
$h$	Height of the prism
$P_d$	Applied dynamic load
$E_f$	Static flexural modulus of elasticity
$a$	Span between load application points
$\delta$	Deflection at mid-span
Ra	Roughness number
$R_i$	Distance above mean plan
$S_j$	Distance below mean plane
$A_i$	Projected area of each grid above mean plan
$A_j$	Projected area of each grid below mean plane
$Z_{av}$	Average surface height
$R_{vu}$	Volumetric ratio of rubber in upper half
$V_{vu}$	Volume of aggregate in upper half
$V_{af}$	Volume of aggregate in whole sample
$n'$	Fundamental longitudinal frequency
$n''$	Fundamental torsional frequency
$M$	Mass of sample
$L$	Length of the sample
$d$	Diameter of the cylindrical sample
$A$	Area of specimen cross-section
$R$	Shape factor
$E_d$	Dynamic modulus of elasticity
$G_d$	Dynamic modulus of rigidity
$\nu_d$	Dynamic Poisson's ratio
$\omega_n$	Energy dissipated in cycle $n$
$\sigma_n$	Stress amplitude in cycle $n$
$\epsilon_n$	Strain amplitude in cycle $n$
$\theta_n$	Phase angle in cycle $n$
$f$	Loading frequency
$\Delta t$	Time interval between maximum load and maximum deflection
$w_0$	Initial dissipated energy at the start of test
$W_n$	Dissipated energy at cycle $n$
$D_m$	Dynamic stiffness modulus
$D_{m0}$	Dynamic stiffness modulus at the start of test
$D_{mn}$	Dynamic stiffness modulus $n^{\text{th}}$ cycle
$\delta_r$	Recoverable dynamic deformation
$I$	Beam cross section moment of inertia
$\Delta_p$	Permanent deformation
$\Delta_{pmax}$	Total accumulated permanent deformation at failure

$c_1$ and $c_2$	Regression constants
$N_i$	Cycles number up to cycle $i$ .
$N_f$	Total number of cycles up to failure
$L_f$	Fatigue life determined on the basis of specimen collapse
$L_e$	Fatigue life determined by dissipated energy approach
$\varepsilon_t$	Horizontal strain at the bottom of asphalt layer
$E_{du}$	Dynamic modulus measured by ultrasonic method

# Chapter One

## Introduction

### 1.1 Background and problem statement

Due to urbanization, industrialization and the large increase of populations, accompanied with an uplift in the standard of living, road vehicle number have increased dramatically which, consequently, has resulted in a lot of end-of-use tires every year. The estimated number of tires manufactured in the world per annum is about 1.5 billion tires. Millions of these are discarded. According to estimations, around 1000 million tires reach the end of their service life yearly and half of these are stockpiled without any use. It was estimated, recently, that the latter number will escalate to around 1200 by the end of 2030 which means there would then be about 5000 million tires, including the stockpiled ones (Thomas and Gupta 2015). This has

a negative impact on the environment and is a real threat to humans since these stockpiles can harbour vermin and represent possible combustion sites (Zheng et al. 2008). Therefore, it is necessary to make use of these waste materials. The majority of the current use of such waste materials is by using them as fuel for combustion which becomes, especially in the light of increasing concerns about the climate change, an unfavourable solution from the environmental point of view.

Development of the modern world has increased the number of the construction projects conducted every year which, in turn, is resulting in a depletion of natural resources. Over the years, many researchers (Khatib and Bayomy 1999; Güneyisi et al. 2004; Papakonstantinou and Tobolski 2006; Balaha et al. 2007; Gesoğlu and Güneyisi 2007; Zheng et al. 2007; Khaloo et al. 2008; Taha et al. 2008; Zheng et al. 2008; Topçu and Bilir 2009; Güneyisi 2010; Nguyen et al. 2010; Pelisser et al. 2011; Najim and Hall 2012; Eiras et al. 2014; Güneyisi et al. 2014) have attempted to make use of these waste tires in concrete mixtures by replacing the natural aggregate by either fine or coarse tire-driven aggregate, or both. Their results revealed reductions in the strength and stiffness modulus of rubber-modified mixtures. Toughness and impact resistance, on the other hand, improved substantially. The degree of decline or improvement of the mentioned properties was different depending on the size of rubber and whether coarse or fine aggregate fractions, or both, were replaced.

Based on their findings and justifications, other researchers (Güneyisi et al. 2004; Pelisser et al. 2011; Najim and Hall 2013) attempted treating the rubber particles with sodium hydroxide or using silica fume to enhance their interaction with the other constituents of the concrete mixtures. Their investigations claimed better

performance because these treatments improved the bond between rubber and the surrounding cement matrix. Despite the lower number of studies performed to assess the behaviour of such modified concrete mixtures under cyclic loading, the investigations conducted by [Wang et al. \(2010\)](#) and [Liu et al. \(2013\)](#) showed an improvement in the fatigue life of such mixtures.

Owing to the fact that the construction of highways consumes a large volume of natural resources as compared with other civil engineering projects ([Cao 2007](#); [Barišić et al. 2014](#)), the recycling of waste tires into such projects represents greater sustainability than discarding or burning or using in other civil engineering ,at the same time, it saves natural aggregate resources. This was the driving force behind several investigations conducted to utilize these waste tires in the construction of asphaltic mixtures. In these investigations, rubber has been used either as a bitumen modifier through the wet process or to replace the aggregate through the dry process ([Rahman 2004](#); [Cao 2007](#); [Chiu and Lu 2007](#); [Xiao et al. 2007](#); [Chiu 2008](#); [Fontes et al. 2010](#)). Others ([Pincus et al. 1994](#); [Cecich et al. 1996](#); [Foose et al. 1996](#); [Masad et al. 1996](#); [Liu et al. 2000](#); [Youwai and Bergado 2003](#); [Kim et al. 2005](#); [Humphrey 2007](#)) studied the possible use of tire-derived rubber materials in geotechnical applications as fill materials for embankments and behind retaining walls.

Unfortunately, very few studies were conducted to investigate the possibility of using crumb rubber within cement-stabilized aggregate mixtures typically used as base and/or subbase courses in flexible composite pavement structures. The usage in this case might be more feasible than in asphaltic mixtures used as base or surface courses, since the latter two layers usually have a limited thickness (due to their high

cost) as compared with the greater thickness of cement-stabilized layers achievable due to their lower unit cost.

Cement-stabilized mixtures are normally used as base or subbase courses within pavement structures so as to improve the structural capacity of pavement structures in terms of strength and stiffness. [Lim and Zollinger \(2003\)](#) described cement-stabilized mixtures as a mixture of aggregate and Portland cement moisturized with small quantities of water for compaction and cement hydration purposes.

Utilization of cement-stabilized base in a pavement structure provides an excellent foundation for asphaltic surface course. This is because cement-stabilized mixtures are less water sensitive, stronger and more uniform ([Adaska et al. 2004](#)). Due to their rigidity, cement stabilized base courses ensure distribution of the applied load over a large area which in turn reduces the stresses applied on the top of subgrade as well as bridging the pavement over weak locations. It hence acts to control rutting. In addition, such layers minimize the fatigue cracking that may happen in the surface layer. However, stabilization with cement can, unfortunately, make this layer sensitive to overloading and to fatigue failure and cause shrinkage. This, in turn, can be considered the main cause of reflection cracking in the surface course. These cracks are inherent characteristics of cement stabilized aggregate materials/mixtures (CSAMs). Reflection crack width is normally less than 3 mm and does not affect the riding quality ([Adaska et al. 2004](#)). However, such cracks may reduce the stiffness and the strength of the layer. A crack width of more than 6 mm can cause problems ranging from negative impacts on riding quality to permitting the surface water to ingress into the underlying layers (especially subgrade) and hence accelerating

premature failure. All the above problems are governed by the crack width in the cement-stabilized layer since a wider crack, as reported by [Adaska et al. \(2004\)](#), will cause stress concentrations in the surface layer especially in the absence of a stress relieving layer (such as a granular material) between the stabilized layer and the asphaltic layer. Figure 1.1 illustrates graphically the main research problems.

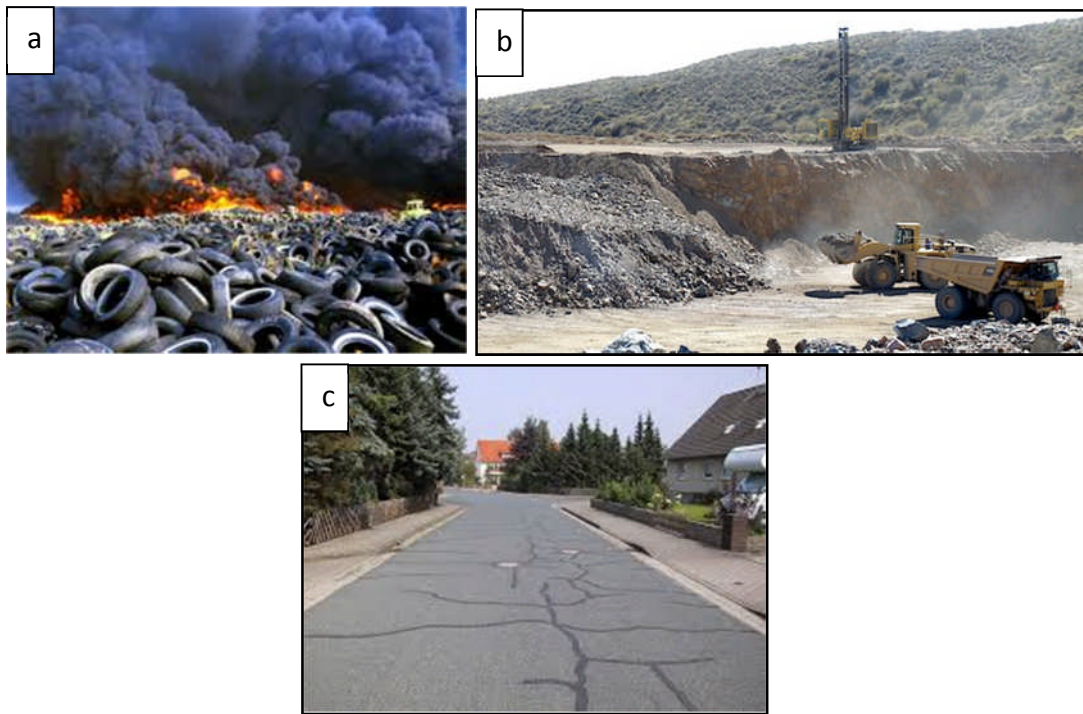


Figure 1.1: Main problems undertaken in this research : a. environmental; b. natural resources scarcity and c. cement-stabilization problems

Therefore, the use of rubber from post-consumed tires in cement-stabilized aggregate mixtures to replace fine aggregate may ensure, firstly, disposing of large quantities of environmentally detrimental materials, secondly, saving natural resources and finally mitigating the problems related to cement-stabilization.

## **1.2 Aim and objectives**

The aim of this research is to investigate the effect of waste tire rubber and degree of cementation on the behaviour of cement-stabilized aggregate mixtures intended to be used as a base course within the pavement structure. This is to be achieved by developing adequate testing equipment, suggesting testing methodologies, implementation of quantification procedures and using these to adequately assess the materials' properties, in terms of the most influential pavement design properties, and to understand their behaviour and the mechanisms of their failure. Then the different experimental properties will be utilized and combined in an analytical study to best quantify their implications for pavement analysis and design.

The specific objectives of this study include, but not limited, to the following:

1. Investigation of the effect of crumb rubber and the degree of stabilization on the properties of CSAMs under different static and dynamic testing modes related to pavement analysis and design. This will be performed mainly in terms of tensile strength, stiffness and fatigue evaluations.
2. Evaluate the behaviour of modified mixtures, due to rubber and cement, under nondestructive testing so as to accurately estimate the fatigue performance and dynamic stiffness modulus.
3. Development of a four-point loading test system to evaluate fatigue performance and monitoring the permanent deformation, modulus degradation and damage accumulation during the fatigue life. Then utilizing this equipment to determine

the fatigue performance and degradation of rubberized and reference cement-stabilized aggregate mixtures under cyclic flexural loading.

4. Assemble correlations between results from the above tests that will permit estimation of parameters needed for the pavement design process in an efficient and cost-effective manner to facilitate the pavement design process and provide default values for different properties
5. Quantitative characterization of the fractured surfaces and the cracking patterns obtained in the different modified mixtures. Various techniques are to be assessed so as to better understand the effect of both rubber and cement on cracking mechanisms and so as to identify possible relationships between damage manifestation and mechanical properties and so as to deduce implications for pavement performance.
6. Investigation, quantitatively at mesoscale level, of the rubber distribution and the crack propagation mechanism using X-ray CT scanning (of internal structure) and image processing techniques. The findings are to be used to interpret and understand the macro-scale behaviour.
7. Conducting analytical study through a numerical multilayer elastic solution (KENLAYER) to identify the effect of rubber and cement and their combination on the critical stresses/strains of a pavement structure and, hence, on the layer thicknesses.

### **1.3 Novelty of research**

A comprehensive literature review revealed that, according to the author's best knowledge, the research presented in this thesis newly, or more deeply than before, addresses (at minimum) the following areas:

1. The performance of rubberized cement stabilized mixtures. Very few previous studies have addressed these materials. There is no existing comprehensive evaluation of these mixtures in terms of popular testing modes under static and dynamic loading.
2. Evaluation of the effect of cement content on the properties of rubberized cement-stabilized aggregate mixtures. In spite of extensive research of the properties of concrete mixtures, it is not easy to find research that has studied this aspect.
3. The failure mechanisms of rubberized cement-stabilized aggregate mixtures. At present, this is still unclear even for rubberized concrete. In this study, various techniques were used to evidence this mechanism.
4. Quantitative characterization of the fractured surfaces of cement-stabilized materials. This is presented for the first time in this thesis. Moreover, using the photogrammetric procedure to acquire fractured surface information has rarely been presented in previous studies.
5. Quantification of the cracking damage in cement stabilized mixtures in general and rubberized mixture in particular. Fractal analysis is used in this research for the first time for such quantification.

6. Analytical modelling of pavement structures to evaluate effect of different modified mixtures on the pavement responses and design, incorporating strength, stiffness and fatigue characteristics. Unfortunately, previous research in concrete mixtures was limited to evaluating the properties of rubberized mixtures without implementing these properties in the analysis and design of structural member to assess the benefit of modified mixtures.
7. Investigate and compare different testing modes used to obtain the modulus of elasticity, as this is the main input for pavement analysis. For cement stabilized aggregate, there is no comprehensive study at present.
8. Quantitative quantification of rubber distribution of cement-stabilized aggregate materials containing various rubber contents. This is the first time for such quantification for rubberized cementitious materials (including concrete).

#### **1.4 Research Methodology and structure of thesis**

To achieve the above aim and objectives, the following methodology consisting of ten tasks was adopted:

##### **Task 1: Review of literature**

In this task, an extensive literature review was conducted. The purpose of this task is to review the previous literature to identify and differentiates between different stabilized mixtures and rubberized cementitious mixtures and their typical properties. This also helped to identify the current state of knowledge and the gaps in literature. Due to the lack of the standardized test, there was a necessity to review the

characterization techniques that were used by previous researchers and prepare some suggestion to develop others. To validate the outcomes of this project, it was important to compare them with previous findings of other researchers therefore necessitating a review of the previous results and the relationships between different parameters. The majority of these issues are presented in **Chapters 2 and 3**.

**Task 2: Materials characterization, mixture design and manufacturing methodology**

The purpose of this task is to characterize the mixtures' materials and waste tire rubber. Also, it is to design the compacted mixtures in such a way that ensures comparable results by eliminating any variability between different mixtures. This was achieved through the manufacturing process. A further purpose is to check how rubber and cement may affect the compactibility of the mixtures using two different approaches. This is going to be explained in **Chapter 4**.

**Task 3: Behaviour under monotonic loading at different curing periods**

In this task, the behaviour of reference and modified mixtures is evaluated under monotonic loading in terms of strength and stiffness. As bound mixtures are normally under tensile action at the bottom of the layer, tensile testing will be used as the main testing mode in this study. Flexural and indirect tensile testing methods are employed. However, as there is a possibility for crushing at the top of the cemented layer, the unconfined compressive strength will also be evaluated. The evaluation of toughness represents another subtask. This task is presented in **Chapters 5 and 6**.

**Task 4: Evaluation of cracking pattern, fractured surfaces and internal structure**

To understand the failure mechanism, quantitatively, the cracking patterns for different modified mixtures are investigated utilizing the fractal dimension concept. This quantification also includes the study of the fractured surfaces (3D fracturing) of these mixtures through the implementation of close-range photogrammetry. The final subtask is to study the cracking propagation and the rubber distribution at the mesoscale level. This is conducted through X-ray CT scanning combined with image processing techniques. This is reported in **Chapter 5 and 6**.

**Task 5: Investigation of the performance under non-destructive testing procedures**

This task was to study how rubber and cement and their combination may affect the non-destructive properties in terms of ultrasonic and resonant frequency testing methods and assess the effect of curing time. Also, these methods are utilized to more accurately measure the properties under cyclic testing. **Chapter 7** presents the findings.

**Task 6: Development of fatigue test facility and testing tools and methodologies**

The purpose of this task is, firstly, to manufacture the necessary tools that help in sample manufacturing and to improve the accuracy of instrumentation. Secondly its purpose is to develop a cyclic testing system, specimen preparation and adequate instrumentation and data logging arrangements. Thirdly it is to develop the necessary

software to handle and analyse the huge amount of data and perform the necessary calculations. **Chapter 8** focuses on this task.

**Task 7: Comparison between different methods used for elastic modulus estimation**

Investigated mixtures represent a broad range of mixtures of different aggregate composition and degrees of cementation. Therefore, it is intended in this task to compare different methods (static, dynamic and nondestructive) for characterization of the stiffness modulus of cementitious mixtures. The results are included as **Chapter 9**.

**Task 8: Investigating the performance under cyclic loading**

This task comprises an investigation of the behaviour of rubberized reference and modified mixtures (due to rubber and cement and their combination) under cyclic flexural loading in terms of fatigue performance and dynamic flexural modulus. In addition, it evaluates the damage accumulation throughout the fatigue life. The latter is assessed by evaluating the permanent deformation and the degradability of the dynamic flexural modulus. Finally, it includes preparation of the laboratory transfer functions which will be used in Task 9. In addition, this task suggests a testing methodology and performs a study to evaluate the behaviour under indirect tensile cyclic loading. The latter is evaluated through indirect tensile stiffness test. This is also useful in evaluating the suitability of the NAT machine for testing the wide range of cemented mixtures. This is the focus of **Chapter 9**

**Task 9: Analytical pavement and design**

Perform an analytical study using KENLAYER software utilizing the results from experimental investigation. This combines properties, in terms of stiffness modulus, strength and fatigue performance, to investigate the effect of both rubber and cement on stresses, strains and fatigue life of a pavement structural system. This is reported in **Chapter 10**.

**Task 10: Analysis of results and reporting**

Perform the analysis of the testing results in parallel with the experimental program to ensure the reliability of test results and the suitability of the other laboratory issues such as instrumentation and also to provide the necessary information for the analytical study. At the end of the experimental program, synthesize all experimental results to provide a comprehensive picture of the whole project. Then, draw overall conclusions and practical implications of the study. This task is the focus **Chapters 11**.

**1.5 Research significance and contribution**

If the results of this investigation showed an enhancement in the modified mixture performance, this will be considered as an optimal solution for both industry and environment as it will be possible to produce a more sustainable “green” pavement structure. This is because the utilization of such materials will save the environment by ensuring proper disposal, protection of the natural resources and reduction in related issues especially those concerning the consequences of stockpiling. Furthermore, such modification may produce different mixture with less sensitivity

to fatigue loading and having different cracking tendencies. Therefore, this research will demonstrate how rubber and its combination with cement may affect the behaviour of cement-stabilized aggregate subjected to static and dynamic loading and will provide an understanding regarding the mechanism of failure and fracturing of such modified mixtures at both macro and meso scale levels.

In case of asphaltic mixtures, most of their tests are standardized and certain machines are manufactured and programmed to perform a specific type of testing such as four- and two-point fatigue and modulus or indirect tensile stiffness modulus evaluations. However, no standardization, especially under dynamic loading, is available yet to characterize the cementitious materials in general and it is not possible to use some of the asphalt-designed equipment due to their limited load capacity or the unsuitability of testing methodology. No doubt, the right characterization depends, to large extent, on the right testing. Therefore, a considerable part of this research was directed to suggest, develop and implement testing equipment, techniques and methodologies to better characterize these modified mixtures. The study can, therefore, also be considered as a guide for testing such materials in the future.

Quantification of the fracturing process and mode is important to understand the damage mechanism of the modified mixtures. This is not important for rubberized cemented mixtures only, but for cementitious mixtures in general where changes occur in terms of aggregate composition and degree of stabilization.

The merit of this research is its multi-benefits; i.e., in addition to the main objective of each research element, other side benefits are simultaneously achieved. Examples of these are:

1. Since the rubber reduces the density of resulting mixtures, it can be said that this research also investigates the performance of cement-stabilized mixtures of different achieved densities and their combination with the degree of cementation.
2. The manufacturing and sample preparation methods, suggested testing procedures and developed testing equipment, can be considered as a guide for other researches using different stabilized materials.
3. This research evaluates the performance of a wide range of cement-stabilized mixtures under different testing types and modes and finds the relationship between them. These can be utilized to estimate, reliably, different parameters from each other which will save time and effort during pavement design.
4. This research also investigates how a small change in the aggregate composition combined with degree of stabilization may affect the final performance and the mechanism of failure of cement-stabilized aggregate mixtures.

In summary, by studying how the crumb rubber and the degree of stabilization may affect the properties of cement-stabilized aggregate mixtures, their relationships and failure mechanism, the investigation presented in this thesis will provide important information about sustainable pavement mixtures and, in parallel, will enrich and

broaden the current knowledge, understanding and testing of cementitiously stabilized materials intended to be used in pavement structures.

### **1.6 Publications, Prizes and achievements**

To validate the findings of this research, gain an approval and acquire suggestions from different academics to develop this study, five papers were published or are under review in prestigious civil engineering journals as well as one conference paper. In addition, some further achievements were also made during the course of this study. All of these are listed as follows:

- **Ahmed Hilal Farhan**, Andrew Robert Dawson and Nicholas Howard Thom, (2016) “Characterization of cement-stabilized mixtures using indirect tensile testing and fractal dimension” **Published**. [Construction and Building Materials Journal \(Elsevier\)](#).
- **Ahmed Hilal Farhan**, Andrew Robert Dawson, Nicholas Howard Thom, Adam Sarhat and Martin J. Smith, (2015) “Flexural characteristics of rubberized cement-stabilized crushed aggregate for pavement structure” **Published**. [Materials and Design Journal \(Elsevier\)](#).
- **Ahmed Hilal Farhan**, Andrew Robert Dawson and Nicholas Howard Thom, (2016) “Effect of cementation degree on performance of rubberized cement-bound aggregate mixtures” **Published**. [Materials and Design Journal \(Elsevier\)](#).

- **Ahmed Hilal Farhan**, Andrew Robert Dawson and Nicholas Howard Thom, (2015) “Rubber modification of cement- stabilized aggregate: delivering more sustainable pavement mixes” **Accepted and Presented at 9<sup>th</sup> international conference on road and airfield pavements (ICPT2015)**, Dalian, China.
- **Ahmed Hilal Farhan**, Andrew Robert Dawson and Nicholas Howard Thom, “Effect of Rubber incorporation on the behaviour of cement stabilized aggregate mixtures under cyclic flexural loading” **to be Submitted to Materials and Design Journal (Elsevier)**.
- **Ahmed Hilal Farhan**, Andrew Robert Dawson, Nicholas Howard Thom, “Rubberized cementitious materials: an overview” **to be Submitted to Construction and Building Materials Journal (Elsevier)**.
- **Ahmed Hilal Farhan**, “Cement-stabilized flexible pavement structure incorporating waste tire materials”, **Poster Winner**, Infrastructure, Geomatics and Architecture (IGA2015), 21<sup>st</sup> January 2015, **The University of Nottingham**.
- **Ahmed Hilal Farhan**, “Cement-stabilized flexible pavement structure incorporating waste tire materials”, **Finalist in the Engineering Research Showcase**, 6<sup>th</sup> May 2015, **The University of Nottingham**.

An M.Sc. thesis entitled “RAP stabilized with cement and fly ash as a base layer” by Al-Shandokhi (2015) was supported by the author during the course of this PhD study.

### 1.7 References:

- Adaska, W. S., D. R. Luhr, C. Petit, I. Al-Qadi and A. Millien (2004). Control of reflective cracking in cement stabilized pavements. Fifth International RILEM Conference on Reflective Cracking in Pavements, RILEM Publications SARL.
- Al-Shandokhi, M. S. (2015). RAP stabilized with cement and fly ash as a base layer. M.Sc., Civil Engineering Department, The University of Nottingham
- Balaha, M. M., A. A. M. Badawy and M. Hashish (2007). "effect of using ground waste tire rubber on the behavior of concrete mixes." *Indian journal of Engineering and Materials Science* 14: 427-435.
- Barišić, I., S. Dimter and T. Rukavina (2014). "Strength properties of steel slag stabilized mixes." *Composites Part B: Engineering* 58: 386-391.
- Cao, W. (2007). "Study on properties of recycled tire rubber modified asphalt mixtures using dry process." *Construction and Building Materials* 21(5): 1011-1015.
- Cecich, V., L. Gonzales, A. Hoisaeter, J. Williams and K. Reddy (1996). "Use of shredded tires as lightweight backfill material for retaining structures." *Waste Management & Research* 14(5): 433-451.
- Chiu, C.-T. (2008). "Use of ground tire rubber in asphalt pavements: Field trial and evaluation in Taiwan." *Resources, conservation and recycling* 52(3): 522-532.
- Chiu, C.-T. and L.-C. Lu (2007). "A laboratory study on stone matrix asphalt using ground tire rubber." *Construction and Building Materials* 21(5): 1027-1033.
- Eiras, J., F. Segovia, M. Borrachero, J. Monzó, M. Bonilla and J. Payá (2014). "Physical and mechanical properties of foamed Portland cement composite containing crumb rubber from worn tires." *Materials & Design* 59: 550-557.

Farhan, A. H., A. R. Dawson and N. H. Thom (2015). Rubber modification of cement-stabilized aggregate delivering more sustainable pavement mixes. 9th international conference on road and airfield pavements (ICPT2015). Dalian, China.

Farhan, A. H., A. R. Dawson and N. H. Thom (2016 a). "Characterization of rubberized cement bound aggregate mixtures using indirect tensile testing and fractal analysis." *Construction and Building Materials* 105: 94-102.

Farhan, A. H., A. R. Dawson and N. H. Thom (2016 b). "Effect of cementation level on performance of rubberized cement-stabilized aggregate mixtures." *Materials & Design*.

Farhan, A. H., A. R. Dawson, N. H. Thom, S. Adam and M. J. Smith (2015). "Flexural characteristics of rubberized cement-stabilized crushed aggregate for pavement structure." *Materials & Design* 88: 897-905.

Fontes, L. P., G. Trichês, J. C. Pais and P. A. Pereira (2010). "Evaluating permanent deformation in asphalt rubber mixtures." *Construction and Building Materials* 24(7): 1193-1200.

Foose, G. J., C. H. Benson and P. J. Bosscher (1996). "Sand reinforced with shredded waste tires." *Journal of Geotechnical Engineering* 122(9): 760-767.

Gesoğlu, M. and E. Güneyisi (2007). "Strength development and chloride penetration in rubberized concretes with and without silica fume." *Materials and Structures* 40(9): 953-964.

Güneyisi, E. (2010). "Fresh properties of self-compacting rubberized concrete incorporated with fly ash." *Materials and Structures* 43(8): 1037-1048.

Güneyisi, E., M. Gesoğlu, K. Mermerdaş and S. İpek (2014). "Experimental investigation on durability performance of rubberized concrete."

- Güneyisi, E., M. Gesoğlu and T. Özturan (2004). "Properties of rubberized concretes containing silica fume." *Cement and Concrete Research* 34(12): 2309-2317.
- Humphrey, D. (2007). Tire derived aggregate as lightweight fill for embankments and retaining walls. *Proceedings International Workshop on Scrap Tire Derived Geomaterials*, Yokosuka, Japan.
- Khaloo, A. R., M. Dehestani and P. Rahmatabadi (2008). "Mechanical properties of concrete containing a high volume of tire-rubber particles." *Waste Management* 28(12): 2472-2482.
- Khatib, Z. K. and F. M. Bayomy (1999). "Rubberized Portland cement concrete." *Journals of Materials in Civil Engineering, ASCE* 11: 206-213.
- Kim, B., M. Prezzi and R. Salgado (2005). "Geotechnical properties of fly and bottom ash mixtures for use in highway embankments." *Journal of geotechnical and geoenvironmental engineering* 131(7): 914-924.
- Lim, S. and D. G. Zollinger (2003). "Estimation of the compressive strength and modulus of elasticity of cement-treated aggregate base materials." *Transportation Research Record: Journal of the Transportation Research Board* 1837(1): 30-38.
- Liu, F., W. Zheng, L. Li, W. Feng and G. Ning (2013). "Mechanical and fatigue performance of rubber concrete." *Construction and Building Materials* 47: 711-719.
- Liu, H., J. Mead and R. Stacer (2000). "Environmental effects of recycled rubber in light-fill applications." *Rubber chemistry and technology* 73(3): 551-564.
- Masad, E., R. Taha, C. Ho and T. Papagiannakis (1996). "Engineering properties of tire/soil mixtures as a lightweight fill material." *Geotechnical Testing Journal*(19).
- Najim, K. B. and M. R. Hall (2012). "Mechanical and dynamic properties of self-compacting crumb rubber modified concrete." *Construction and Building Materials* 27(1): 521-530.

- Najim, K. B. and M. R. Hall (2013). "Crumb rubber aggregate coatings/pre-treatments and their effects on interfacial bonding, air entrapment and fracture toughness in self-compacting rubberised concrete (SCRC)." *Materials and Structures*.
- Nguyen, T., A. Toumi and A. Turatsinze (2010). "Mechanical properties of steel fibre reinforced and rubberised cement-based mortars." *Materials & Design* 31(1): 641-647.
- Papakonstantinou, C. G. and M. J. Tobolski (2006). "Use of waste tire steel beads in Portland cement concrete." *Cement and Concrete Research* 36(9): 1686-1691.
- Pelisser, F., N. Zavarise, T. A. Longo and A. M. Bernardin (2011). "Concrete made with recycled tire rubber: Effect of alkaline activation and silica fume addition." *Journal of Cleaner Production* 19(6-7): 757-763.
- Pincus, H., T. Edil and P. Bosscher (1994). "Engineering properties of tire chips and soil mixtures."
- Rahman, M. (2004). "characterisation of dry process crumb rubber modified asphalt mixtures." PhD Thesis, University of Nottingham.
- Taha, M. M. R., A. S. El-Dieb, M. A. Abd El-Wahab and M. E. Abdel-Hameed (2008). "Mechanical, Fracture, and Microstructural Investigations of Rubber Concrete." *Journal of Materials in Civil Engineering, ASCE* 20: 640-649.
- Thomas, B. S. and R. C. Gupta (2015). "Long term behaviour of cement concrete containing discarded tire rubber." *Journal of Cleaner Production*.
- Topçu, İ. B. and T. Bilir (2009). "Experimental investigation of some fresh and hardened properties of rubberized self-compacting concrete." *Materials & Design* 30(8): 3056-3065.

Wang, C., Y. Zhang and A. Ma (2010). "Investigation into the fatigue damage process of rubberized concrete and plain concrete by AE analysis." *Journal of Materials in Civil Engineering* 23(7): 953-960.

Xiao, F., S. Amirkhanian and C. H. Juang (2007). "Rutting resistance of rubberized asphalt concrete pavements containing reclaimed asphalt pavement mixtures." *Journal of Materials in Civil Engineering* 19(6): 475-483.

Youwai, S. and D. T. Bergado (2003). "Strength and deformation characteristics of shredded rubber tire sand mixtures." *Canadian Geotechnical Journal* 40(2): 254-264.

Zheng, L., X. S. Huo and Y. Yuan (2008). "Strength, modulus of elasticity, and brittleness index of rubberized concrete." *Journal of Materials in Civil Engineering* 20(11): 692-699.

Zheng, L., X. Sharon Huo and Y. Yuan (2007). "Experimental investigation on dynamic properties of rubberized concrete." *Construction and Building Materials* 22(5): 939-947.

Zheng, L., X. Sharon Huo and Y. Yuan (2008). "Strength, Modulus of Elasticity, and Brittleness Index of Rubberized Concrete." *Journal of Civil Engineering* , ASCE.

## **Chapter Two**

### **Cement-stabilized mixtures**

#### **2.1 Introduction**

This chapter discussing three main aspects relating to the cement-stabilized materials. These are the terminology used to define and differentiate between different cemented mixtures and the general procedure for the design of these mixtures as well as the practices adopted in different countries. The majority of previous investigations do not rely on a standardized test due to the absence of such specifications, except the basic tests, for the cement-stabilized mixtures. Therefore, another purpose of this chapter is to review different characterization methods. To understand how rubber particles as well as their combination with cement may affect the properties of cement-stabilized mixtures, it was necessary to review the typical properties of these mixtures. The final goal of this literature review is to identify the gaps in knowledge in these themes.

## 2.2 Pavement types

According to Design Manual for Roads and Bridges ([Highway England 2009](#)), there are four pavement types which are:

1. Flexible pavement: in this type, both surface and base courses are bituminous bound mixtures.
2. Flexible composite pavement: this type consists of surface and may be upper base course bound with bituminous materials resting on roadbase made from cement-bound materials.
3. Rigid pavement: the surface course of this type is a normal concrete layer resting on subbase course. Concrete surface may be :
  - a. Jointed unreinforced (URC)
  - b. Jointed reinforced (JRC)
  - c. Continuously reinforced (CRCP)
4. Rigid composite: this type includes bituminous bound mixture surface course on continuously reinforced concrete roadbase.

Figure 2.1 gives a diagrammatic representation of the different types. Sometimes the subbase course is comprised of stabilized rather than the base course which, in such pavement types, is unstabilized granular materials. The use of this system is described as upside-down ([Lay, 1986](#)) or inverted pavement ([PIARC, 1991](#)) pavement. The latter arrangement is sometimes used to delay the crack propagation, after its formation in the cemented layer, to the surface layer

### 2.3 Pavement structural components

The components of a highway pavement in accordance with the UK terminology are (Sunarjono 2008):

1. Foundation: this consists of underlying roadbed soil, capping (if used) and subbase course. It represents the platform for other layers.
2. Roadbase: it represents the main structural layer within highway structure. The main function of this layer is to distribute the traffic load in such a way that the stresses on underlying layer are minimized.
3. Surface (wearing) course: this layer represents the top of pavement structure. The purpose of this layer is to make it possible for the pavement structure to provide good ride quality and skid resistance. In addition, it enables crack propagation resistance.

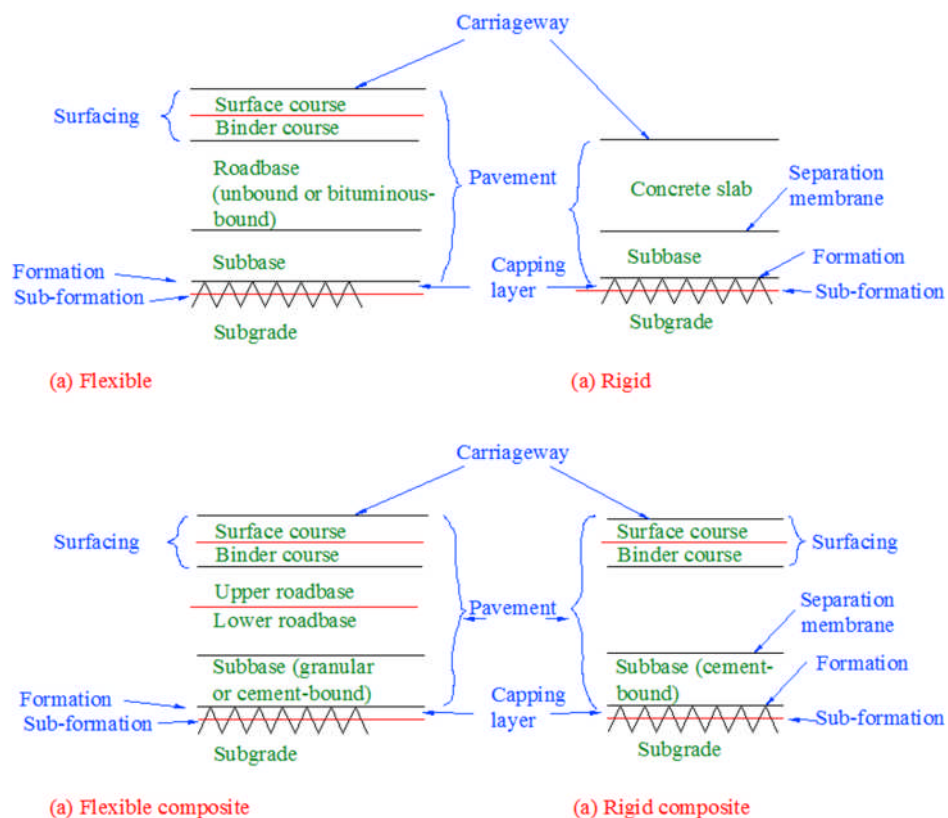


Figure 2.1: Types of highway pavements structures. Drawn based on (O'Flaherty 2002)

## **2.4 Soil Stabilization**

Soil stabilization is defined as the improvement of the strength and durability of a soil by adding binding agents and/or blending and mixing materials with that soil (TRL 2003). The blending process includes adjusting gradation to meet the target requirements. There are many advantages that may come from stabilization. Firstly, it enhances the shear resistance within the layer. Secondly, it decreases the elastic deflection that may result in fatigue cracking in the layer or layer(s) above. Thirdly, by means of densification, the stabilization helps to prevent permanent deformation. In addition, improving the structural quality of the stabilized layer will ensure the ability of that layer to spread the applied load over a large area and minimize the tensile stress at the bottom of asphaltic layer which in turn secures thickness reduction of the stabilized layer and also, potentially, of the surface course (Grilli et al. 2013).

### **2.4.1 Methods of stabilization**

Basically, there are two methods for stabilization which are mechanical and chemical. Mechanical stabilization can be achieved by blending two or more gradations so that the final mixture meets the required specifications. Bituminous stabilization may be considered as a type of mechanical stabilization. This is because the latter does not contain any chemical reactions. Although the compaction can be considered as another type of mechanical stabilization, in some cases this alone is insufficient to deliver the required properties.

Unlike mechanical stabilization, it depends on reactions which take place after stabilizer addition which may, or may not, involve chemical reaction with the soil or aggregate being treated. If such reactions do occur, then soil modification rather than stabilization may be the preferred term. By far the most common stabilizers are the hydraulic binders such as cement, lime, fly ash, etc. where, these, provide hydraulic stabilization.

## **2.5 Base Course Materials**

Generally, base course can be classified either as unbound materials such as crushed rock, natural or crushed gravel, granular materials, etc. or, on the other hand, as bound materials which are hydraulically stabilized or treated with other types of chemical additives. Base courses comprised of different material types (bound or unbound) have different behaviour characteristics, failure mechanism and performance. In terms of behaviour, unbound mixtures are stress-dependent. In addition, they resist the applied loads by shear strength developed through cohesion, which is negligible in the case of granular materials, and internal friction between particles. With regard to distress mechanism, deformation (rutting) resulting from shear distortion and densification that results from particle breakdown due to additional compaction is the main distress mode for unbound materials.

On the other hand, bound materials withstand the traffic loads through shear strength, particle interlock, chemical bonding and cohesion. Unlike the unbound mixtures, significant tensile strength and rigidity may exist in case of bound materials which enables them, as shown in Figure 2.2, to distribute the loads over a wide area which,

in turn, ensures protection of the subgrade soils from excessive rutting by reducing the applied vertical stress upon it. Besides, use of bound materials may reduce the possibility of fatigue failure that may happen in the surface course because the former will reduce the pavement deflection. These above advantages are still provided as long as the layer is intact. However, shrinkage cracking may reduce the load spreading capacity of this layer (Gnanendran and Piratheepan 2009). Also, it achieves its load spreading ability by attracting stress to itself, thereby promoting the possibility of fatigue cracking which may occur at the bottom of this layer. In the light of above discussion, the structural design criteria and philosophy for bound or unbound materials are significantly different.

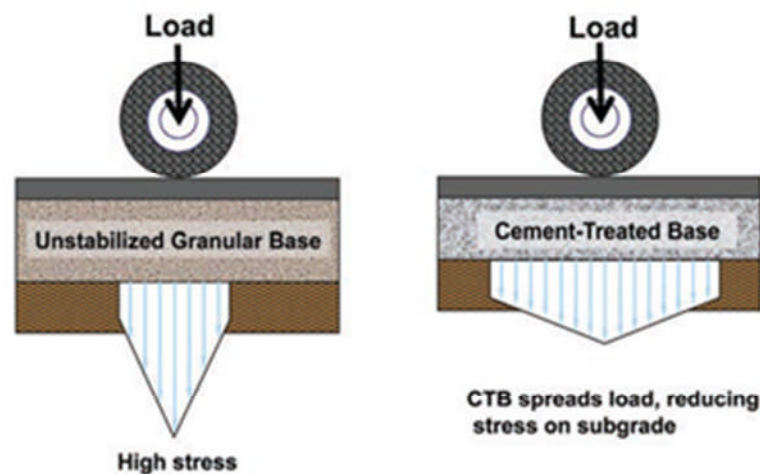


Figure 2.2: Stresses distribution on subgrade (Garber et al. 2011).

## 2.6 Cement based pavement materials: classification and practice

The use of cement-based materials as construction materials for bases, subbases and subgrade for different types of pavements is well known world-wide. Some differences are found in the literatures in describing the broad range of stabilized and similar materials such as cement-treated aggregate, cement-stabilized aggregate,

cement-modified and cement bound materials. Some authors classified these materials based on their cement content while others grouped them in accordance with material strength. [Baghdadi \(1982\)](#) used two terms for the materials treated with cement which are soil-cement and cement-modified soils. The former contains enough cement and water to achieve both strength and durability. This type is usually utilized in the base and subbase construction. The latter, on the other hand, is used to describe the materials in which only a small quantity of cement is used to reduce both plasticity and potential volume change. Subgrade construction is the field of application of this type. [Halsted \(2010\)](#) used cement stabilized base term to describe both soil cement and cement treated aggregate. [Little \(1995\)](#) classified the materials to which the cement was added into lightly, moderately, heavily stabilized materials and stabilised subgrade, based on the amount of added cement. These contain less than 2%, between 2-4%, more than 4% of cement for lightly, moderately and heavily stabilized materials, respectively. However, [Paul and Gnanendran \(2012\)](#) considered the mixture that contain less than 5% cement as a lightly stabilized material. Stabilized subgrade includes the subgrade soils in which a small amount of cement is added just to alter their constructability or to reduce swelling and shrinkage potential. On the other hand, other researchers ([Foley 2002](#)) discriminated between various materials depending on their strength as illustrated in Table 2.1.

In fact, it seems logical that the behaviour, regardless of the terminology, is controlled by the cement content rather than the strength of the mixtures. This is because the strength depends, to large extent, on the strength of the parent materials i.e., the strength of aggregate itself. This is clear if a comparison is made between the

strength of two mixtures with the same cement-contents but with one manufactured from virgin and the other from recycled aggregates.

Table 2.1: Properties of modified, lightly bound and heavily bound materials (Foley 2002)

Degree of binding	Design strength (MPa)	Design flexural modulus (MPa)
Modified	UCS < 1.0	<1,000
Lightly bound	UCS=1-4	1,500-3,000
Heavily bound	UCS > 4	>5,000

### 2.6.1 PCA practice

PCA (2005) classifies various cement based materials into different categories, as shown in Figure 2.3 depending on both water and cement contents. These include conventional concrete, roller-compacted concrete, soil cement and flowable fill. It can be seen from this figure that soil cement includes both cement-treated base in which a sufficient amount of cement is used to satisfy the required structural capacity and cement-modified soil in which a small quantity of cement is added to improve some properties.

Although, at low water contents, both roller compacted concrete (RCC) and soil cement are constructed by rolling, the former has a strength comparable to that of normal concrete (Balbo 1997; Adaska et al. 2004). Furthermore, some differences in terms of the construction practices such as using admixtures in RCC e.g. retarders

also exists (Adaska et al. 2004). Choi and Hansen (2005) reported that the cement-treated aggregate falls between the RCC and soil cement.

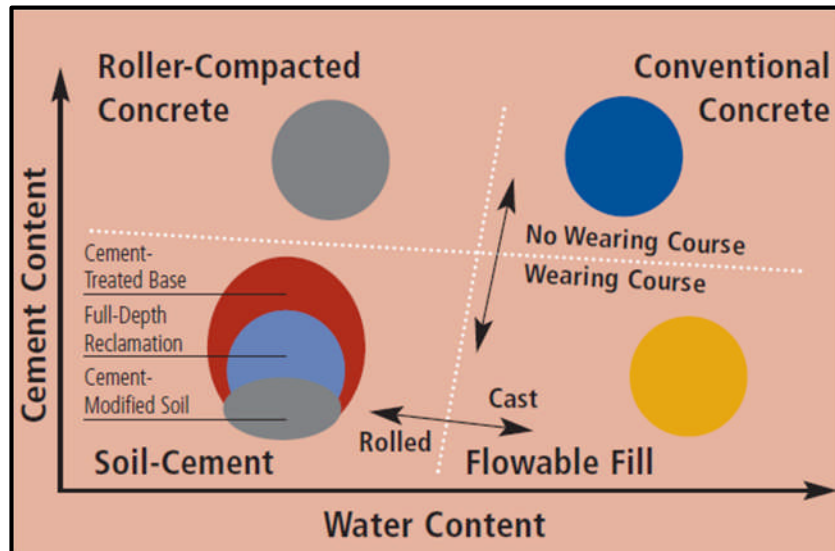


Figure 2.3: Various types of cement based materials (PCA 2005)

### 2.6.2 South African practice

Unlike other terminology used, South African specifications, as reported by Theyse et al. (1996), utilise the term *cemented materials* to describe all materials to which the cement is added. They classify these materials into four categories (C1, C2, C3 and C4) based on their strength as shown in Table 2.2. In addition, they also put certain limitations on the types of aggregate being used for each of which.

Table 2.2: Different categories of cemented materials as defined by South African mechanistic pavement design method (Theyse et al. 1996)

Category	UCS, MPa	Parent material
C1	6 - 12	Crushed stone
C2	3 - 6	Crushed stone
C3	1.5 - 3	Gravel
C4	0.75 – 1.5	Gravel

### 2.6.3 The UK practice

When cement is used as additive, the UK specification, illustrated in [BS EN 14227-1:2004](#) and [BS EN14227-10:2006](#), groups the materials into two main categories. When the materials fall within a specific range of gradations, they are classified as cement bound granular materials (CBGMs) which in turn also contain many subgroups depending on their strength. Otherwise, they are classified as cement-stabilised soils or soil-cement. Similarly, [Choi and Hansen \(2005\)](#) define soil-cement as the materials derived from those that occur naturally. Unlike other classification systems, the UK specifications consider the material which is cemented so as to improve its workability and compactibility without improving any structural property as a part of earthwork process. According to [Manual of Highway Work \(Highway England 2009\)](#) cement-bound granular materials is divided based on the gradation of aggregate into CBGM A, CBGM B and CBGM C. Europeans standards in the recently issued specification ([BS EN 14227-1:2013](#)) has classified the cement bound mixtures in to five types. Each of these types has a specific gradation and other requirements.

#### **2.6.4 International practices**

Regardless of the terminology used, when these materials are used in the pavement structure, different countries have different requirements especially those concerning minimum strength, cement content, curing, gradation, etc. Table 2.3 summarizes the requirements of different countries concerning the materials used in the construction of a semi-rigid pavement where the stabilized materials are used as a base or subbase layers. It can be concluded from this table, that the gradation of materials to be used in base course construction is carefully controlled. This ensures maximum density which will lead to increasing strengths and stiffness.

Table 2.3: Practices and criteria used by different countries for cement stabilized materials (Thøgersen et al. 2004)

Country	Austria	Belgium		Switzerland	Germany		Spain		
Pavement layer	Sub-base/base	Base			sub-base		sub-base	base	
		Light traffic	Heavy traffic		Light traffic	Heavy traffic		Light traffic	Heavy traffic
Minimum strength C (compression) or st (splitting tensile) (days)	$R_{c7} \geq 2.5$	$R_{c90} \geq 10$ (average)	$R_{c90} \geq 10$ (single value)	$R_{c7} \geq 2-4$	$R_{c28} \sim 7$		$R_{c7} \geq 2.5$ Or $R_{c28} \geq 3.8$	$R_{c7} \geq 6$ or $R_{c90} \geq 9$ $R_{st7} \geq 0.5$ or $R_{st7} \geq 0.75$	
Cement content (kg/m <sup>3</sup> )	Min. 90	Min. 100		Min. 60	Uniform sand ~ 180 Well-graded aggregate ~ 95		Usually 100-120	Usually 90-100	
Cement type	CEM II 32.5	CEM I OR CEM III/A 32.5 or CEM III/A 42.5		CEM II 32.5	CEM II 32.5		CEM IV/B 32.5		
Fly ash/ slag content (%)	$\leq 35$	$\leq 35$		0	0		36-55		
Gradation prescribed	NO	NO			NO		NO	YES	
Crushed aggregate prescribed	NO	YES			NO		NO	NO	YES MIN. 50%
Compaction (% Proctor)	Min. 97			97	Min. 98		100	97 mod.	
Curing	Bitumen emulsion	Bitumen emulsion +sand		Bitumen emulsion	Keep moist		Bitumen emulsion +sand		
Groove joints	no	no		no	Per 2.5 m (asphalt <14cm)	Per 5 m (asphalt <14cm)	no	no	Since 1997
Asphalt cover (cm)	15-17 (heavy traffic)	15	17-18		$\geq 12$	30		12	15
CTB thickness (cm)	25-30	20	20			15-20	20	20	22-25
Reflection cracking	yes	often		often	None when groove joint			Often when no groove joints	
Experience	35 years	25 years		30 years	Groove joint since 1982			Since 1988 300 km with groove joints	
Max. axle load (kN)	105	130		100	115		130		

Table 2.3: Continue...

Country	France			UK			Italy
Pavement layer	Sub-base	Base		Sub-bases	base		sub-base for heavy traffic
		Light traffic	Heavy traffic		Light traffic	Heavy traffic	
Minimum strength C (compression) or st (splitting tensile) (days)	$R_{st360} \geq 1.1$ ( $R_{st28} \geq 0.66$ )			$R_{c7} \geq 2-4$	$R_{c28} \sim 7$		$R_{c7} \geq 2.5-4.5$ Or $R_{st7} 0.25$
Cement content (kg/m <sup>3</sup> )	Min. 70						60-100
Cement type	CEM I, II or III 32.5						CEM 32.5
Fly ash/ slag content (%)	$\leq 80$						40 FA
Gradation prescribed	partly	yes	yes	no	yes		yes
Crushed aggregate prescribed	no	partly	yes	no	yes		yes
Compaction (% Proctor)	95 mod.		98 mod.	Min. 95			100 (mod. AASHTO)
Curing	Bitumen emulsion +sand			Bitumen emulsion			Bitumen emulsion
Groove joints	no	Per 3m		Being investigated			no
Asphalt cover (cm)		6-8	14	0	10-15	20	20-25
CTB thickness (cm)	15-25	15-25 Depending on traffic and subbase		Min. 15	15-25 Depending on traffic and CTB type		20-30 Depending on subbase
Reflection cracking	no			Yes, with no groove joints			no
Experience	25 years, 5000 km main road, 1500 km motorways			25 years			20 years, 3500 km
Max. axle load (kN)	130			105			120

## 2.7 CBGMs constitute and mix design criteria

### 2.7.1 Cement

Portland cement type I, or CEM 1, class 32.5 N, 42.5 N or 52.5 N, is usually used in soil stabilization applications. Its amount is usually estimated based on strength and/or durability requirements. On the other hand, some specifications ([PCA, US corps of engineers](#)) have specific ranges of cement contents for each soil type. Table 2.4 illustrates the approximate range of cement for different types of materials.

Generally, the unconfined compressive strength test is most widely used as a strength criterion for cement content determination. Although it does not simulate the field condition ([Brown et al. 1993](#)), UCS is most commonly adopted by many authors, organizations and specifications due to its simplicity and availability. However, some countries adopt more advanced tests as additional criteria which better simulate what will actually happen in the field. For example, Spain and Czechoslovakia use flexural strength while Italy and France adopt indirect tensile strength and direct tensile strength, respectively ([PIARC Permanent International Association of Road Congresses, 1991](#)).

In the UK specification ([BS EN 14227-1:2004](#)), there are two systems for strength evaluation and further classification of cement bound granular materials. In System I, compressive strength is utilized while a combination of direct or indirect tensile strength and modulus of elasticity are adopted within System II. According to this specification no correlation between the above two systems exists. It seems that the

above specification tries to transfer from the old system, where the UCS test is used for strength evaluation, to a more precisely simulative test which is used by other European countries.

Table 2.4: Approximate range of cement contents for various materials (Shahid 1997)

Material description	Possible range of cement content ( percentage by mass of dry aggregate), Kg/m <sup>3</sup>
Well-graded hard granular materials	80 - 120
Pulverised Fuel ash	80 - 240
Poorly graded/ uniform hard granular materials and well graded weak materials such as shale	130 – 190
Brickearths	170 – 200
Soft chalk	180 - 225

In fact, since the stabilized layer in the reality is subjected to tensile stresses approximately at its bottom, it is more logical to adopt the tensile stress as a criterion for mix design in lieu of the UCS test. However, Theyse et al. (1996) reported that if the stabilized layer is lightly cemented, crushing may occur on the top of the layer (Figure 2.4). . It can be inferred from the above information that when the layer is lightly cemented it may behave like unbound materials since the crushing will results in rutting as in the case of unbound materials. Because of that, in the mechanistic design of cement stabilized layer, the crushing of at the top of cemented layer is considered as a design failure mode that should be taken in consideration.

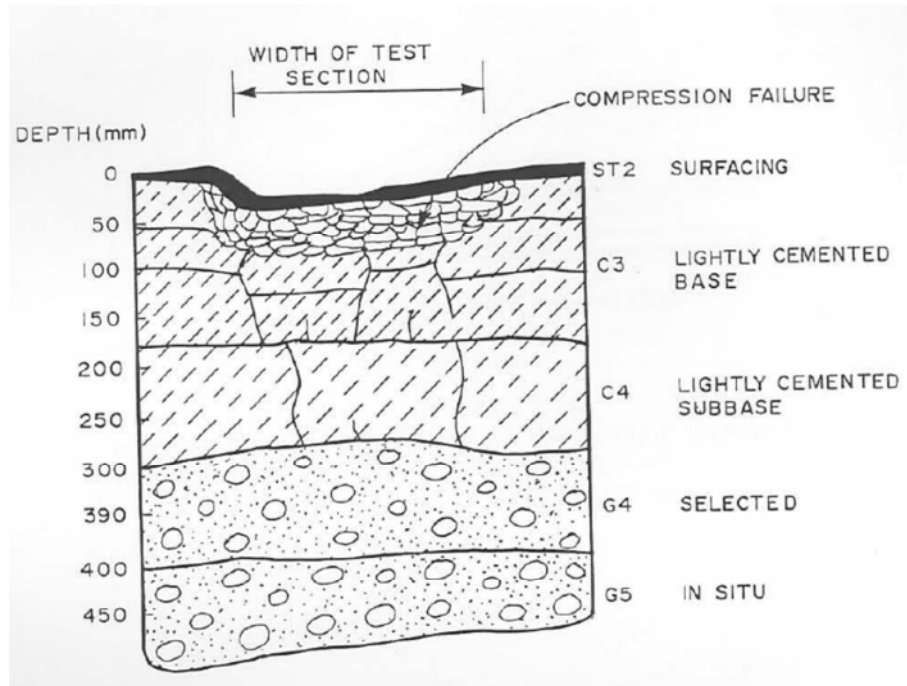


Figure 2.4: Fatigue crushing at the top of lightly cemented layer (De Beer 1990)

### 2.7.2 Aggregate

Several types of aggregate can be used in cement-treated base construction. These consist of either natural high quality or marginal and recycled aggregates. Even though high quality aggregate has a good structural capacity, nevertheless it may be utilized in a stabilized form especially if heavy traffic loads are expected and/or weak subgrades exist (PARIC, 1991). On the other hand, there are many reasons to use recycled aggregate. For example, recycled concrete aggregate or recycled asphalt concrete may be available as high quality aggregates having environmental benefits, saving natural resources and saving cost, especially if these types are available in the vicinity of the project (PIARC 1991).

## 2.8 Mix design

Since the elements of cement-treated materials are granular materials/aggregates, the design of such mixtures requires an exact determination of water, cement and appropriate gradation. However, as stated earlier in this chapter (Table 2.2), some specifications do not require specific gradations to be used. When a specific gradation is demanded the selection of aggregate is controlled by that desired mixture gradation and aggregate from different fractions is usually combined to meet the desired limits.

The estimation of water content derived from the optimum value that is driven by the maximum dry density since the latter has a significant effect on the final strength (Williams 1986). Table 2.5 shows the typical range of moisture content for different materials which can be adopted for compaction tests.

Finally the amount of cement is governed by strength and/or durability depending on the criteria adopted. The general mix design sequence is demonstrated in Figure 2.5.

Table 2.5: Tentative range of optimum moisture contents for various materials (Shahid 1997)

Material description	Possible range of optimum water content ( percentage by mass of dry aggregate),
Clean gravel sand mixtures	4 - 6
As-dug gravel sand mixtures	5 - 7
Crushed rock aggregate	3.5 5.5
Sand	8 - 10
Silts and clays	plastic limit

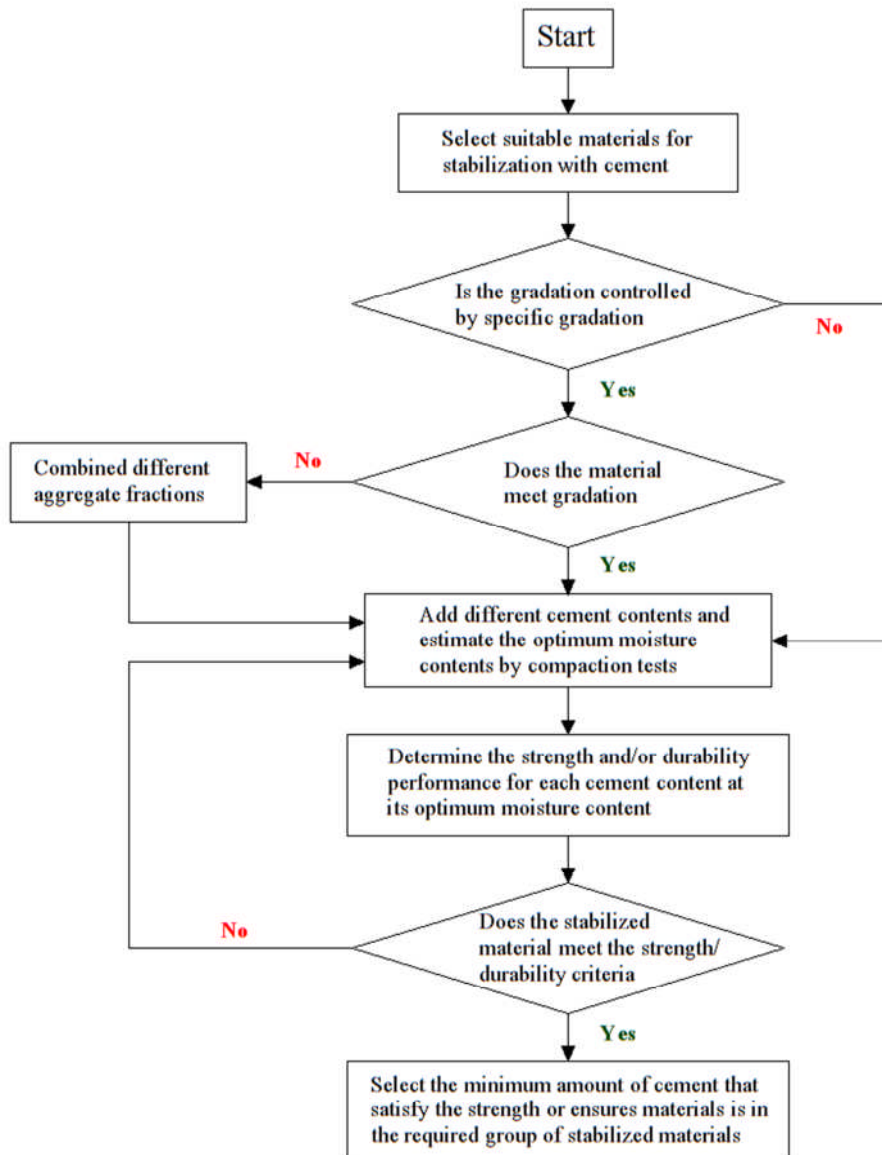


Figure 2.5: Cement-stabilized materials mixture design sequence.

## 2.9 Compaction

Compaction plays a very important role that directly affects the performance of cement-stabilized mixtures. In previous studies, different methods of compaction have been used during the mix design of cemented materials but the majority of them have used Proctor methods. For example, [Gnanendran and Piratheepan \(2008\)](#) and

Gnanendran and Piratheepan (2009) have used the standard Proctor method while other authors (Su et al. 2013; Barišić et al. 2014; Barišić et al. 2015; Nusit et al. 2015; Paul and Gnanendran 2015) utilized the modified Proctor compaction.

In terms of sample fabrication, different authors utilized different methods for samples compaction. Vibrating hammer compaction was used by some researchers (Shahid 1997; Thompson 2001). Sobhan and Krizek (1999) and Paul and Gnanendran (2015) have used the static compression method while Gnanendran and Piratheepan (2009) utilized the gyratory compactor. In their study, Jameson (2010) and Jameson and Howard (2012) have used the laboratory roller-compactor to manufacture slabs which was then sawn as beams.

Zhu et al. (2014) claimed, based on their experimental study, that vibratory compaction is more effective as compared with static compaction. Regarding the difference between compaction methods, White and Gnanendran (2005) performed a study to assess the effect of compaction methods (standard Proctor vs. gyratory compactor) on the strength and stiffness modulus of cementitiously stabilized materials. They drew a conclusion that the compaction method does not show any statistical importance for the investigated properties provided that same density was achieved. Later, Williams (2013) compared between the Proctor and gyratory compactor methods to investigate the possibility of using the latter to manufacture the roller-compacted samples. One of the main his finding is, at lower water contents, similar densities were achieved by the two methods.

At higher moisture content, in contrast, the gyratory method tends to produce higher densities than those achieved by the Proctor method. Based on his findings, the author considered the gyratory compactor as a good alternative compaction method that can be used during the mix design stage. However, he criticized this method as this, due to the higher densities, requires more compaction in the field to achieve the laboratory density.

The author of this research disagrees with the latter criticism. This is because the idea is to take full advantage of the mixtures, and this, can be achieved by increasing their density. This may not be possible if the mixture design relied on a method that may produce a density less than that can be reached in the field. Furthermore, greater field compaction can be justified by the higher densities and hence the higher strengths. In addition, [Amer et al. \(2003\)](#) have reported that the samples manufactured by gyratory compactor showed similar behaviour with those extracted from the field, in terms of mechanical properties.

In the absence of an investigation that compares between all the available compaction methods, it seems that the vibrating hammer compaction method is more suitable for the compaction of cement-stabilized aggregate mixtures as stated in the previous literature ([Drnevich et al. 2007](#); [Chilukwa 2013](#)). However, the gyratory compaction method is an alternative as the above literature has shown. Regarding the laboratory roller compactor, the author of this research believes this may be not suitable for the current study due to unknown rubber distribution which may result in uneven distribution between different samples sawn or cored from the manufactured sample

## **2.10 Curing**

Curing causes strength improvement of the cement-stabilized materials resulting from the cement hydration. This improvement depends, to large extent, on the curing method, duration and temperature. To accelerate the aging of the sample and hence simulate the long term behavior in a short period, the curing temperature is normally increased. However, curing at very high temperature may cause microcracking in the sample (Bullen 1994).

Most previous studies (Sobhan and Krizek 1999; Sobhan and Mashnad 2000; Gnanendran and Piratheepan 2008; Paul 2011) cured the compacted samples in their moulds for 24 or 48 hours and then sealed the samples by wrapping them, after demoulding, with polythene sheets and putting them in a plastic bag. Finally, they were stored in a humid room with temperature of  $20-23 \pm 2^{\circ}\text{C}$  for the required curing period(s).

## **2.11 Characterization of cement-stabilized mixtures and their typical properties**

### **2.11.1 Unconfined compressive strength (UCS)**

Although the UCS test is most widely used to characterize cement-stabilized mixtures because of its simplicity and low cost, as well as its established relationships with other properties (Piratheepan et al. 2009; Jitsangiam and Nikraz 2011). Brown et al. (1993) considered this to be unsuitable to evaluate the performance of these mixtures since it does not simulate the actual behaviour. In addition, it does not characterize material in terms of the input parameter required

for structural design (Jitsangiam and Nikraz 2011). Nevertheless, it is still used even by the UK specification (BS EN 14227-1:2004), through System I. However, the latter specification adopts both tensile strength and compressive elastic modulus through System II for CBGMs evaluation. Moreover, as stated earlier in this chapter, some countries utilize another test such as flexural test for that purpose.

UCS is usually conducted according to BS EN 13286-41. The sample in this test is compressed till failure and the peak load is recorded to compute the UCS. In addition, the UCS test can be used to measure the stiffness modulus from stress-strain relationship in accordance with (BS EN 13286-43:2003). This relationship is obtained by instrumentation of the tested in and by measuring the deformation for each load increment.

### **2.11.2 Tensile strength**

Tensile strength can be measured either directly (BS EN 13286-40) or indirectly (BS EN 13286-42). The direct tensile strength can be considered the most accurate method for measuring tensile properties. However, the difficulties resulting from sample preparation and the test set-up to prevent sample eccentricity may limit the wide-spread use of this method (Carpenter et al. 1992; Thompson 2001). On the other hand, the ease of in sample preparation represents one of the main advantages of the indirect tensile test. In addition, it makes it possible to compare results with those obtained from cored specimens from the field (Thompson 2001).

### 2.11.3 Stiffness modulus

[Khoury and Zaman \(2007\)](#) stated that stiffness modulus test is more appropriate than the unconfined compressive strength to characterize cement stabilized materials and to evaluate their durability. This is because of its role in pavement design. Stiffness modulus can be obtain from the cyclic plate loading test ([Behiry 2013](#)), the cyclic compressive strength test ([Zhang and Li 2009](#)), the cyclic indirect tensile test ([Khattak and Alrashidi 2006](#)) and the cyclic flexural test ([Sobhan 1997](#)).

There are different methods used for design of flexible pavement. Of these, the mechanistic-empirical pavement design method ([Applied Research Associates 2004](#)) is becoming the most popular method preferred on the other method since it is normally not restricted to a specific range of construction materials as compared with other procedures ([Lav and Lav 2014](#)). Pavement responses in terms of stresses and strains resulting from modeling of pavement structure represent the main inputs for the design of pavements using the mechanistic-empirical method. To calculate these responses it is necessary to estimate the elastic modulus of the mixtures that form the pavement layers ([Nusit et al. 2015](#)). The more accurate the pavement layer moduli are estimated, the more accurate the resulting pavement responses.

To accurately estimate this important parameter, different testing methods by various testing mode have been suggested by different organizations. For example, [Austroad \(2010\)](#) utilizes the modulus estimated from the flexural test as a pavement analysis input. Also, this organization recommends using the correlation with UCS in case of flexural test unavailability ([Nusit et al. 2015](#)). In the USA, [NCHRP \(2004\)](#) utilizes

the elastic modulus computed based on [ASTM C469](#). This test is usually performed in compressive mode utilizing either laboratory manufactured samples or those extracted from the field. However, research conducted for PCA by [Scullion et al. \(2008\)](#) indicated the difficulty and impracticality of the test. Based on their results, they did not recommend using this test for modulus characterization of cement-stabilized materials. Moreover, [Nusit et al. \(2015\)](#) criticized the use of this test since it is conducted under monotonic loading while the pavement, in the reality, is under the cyclic loading. Past studies conducted on concrete and cement-stabilized mixtures revealed that the dynamic moduli are higher than those estimated based on monotonic loading. Dynamic moduli in these studies were estimated utilizing either ultrasonic or resonant frequency methods.

From observing different researches conducted previously in different countries, a large diversity was observed regarding the numeric values of the estimated moduli (see Table 2.6 (which summarizes the numeric values of moduli with type of aggregate, percent of cement, density, etc.)). It is not clear whether these differences come from the diversity of testing method and/or due to the type and arrangement of aggregate on mesoscale level. In addition to these sources of differences, there is also another variability which is that between the values achieved in the laboratory and those achieved in field. Several reasons are behind this difference. This might include the difference between the curing condition, distribution of aggregate, difference in achieved densities,...etc. [Shahid \(1997\)](#) pointed out, based on his laboratory and field investigations, that both strength and modulus of elasticity of the cement-stabilized aggregates are about two-thirds those achieved in the field. In

addition, [Scullion et al. \(2008\)](#) indicated that there was a 50% reduction in the modulus value measured in the field as compared with laboratory one.

The use of cement-stabilized mixtures in pavement layer construction is no longer considered as a design option but it becomes an important part of the modern pavement structure subjected to heavy loads ([Nusit et al. 2015](#)). Therefore, the study of cement-stabilized mixtures properties and their characterization becomes an urgent necessity for the most efficient, economic and durable pavement structure. Of these characterizations, the estimation of the stiffness modulus has special importance, as stated earlier.

Table 2.6: Elastic moduli estimated by different methods for different materials and binder contents with their typical values

Author (s)	Testing method	Aggregate type	Cement content	Range of elastic modulus, MPa
Scullion et al. (2008)	Nondestructive - Seismic	Limestone aggregate with 19mm max. aggregate size	3%	14,000-16,000
	Compressive- Dynamic	Limestone aggregate with 19mm max. aggregate size	3%	9,100-11,721
	Compressive- Resilient	Limestone aggregate with 19mm max. aggregate size	3%	7,170-9,308
Sobhan and Mashnad (2003)	Flexural -dynamic	Recycled concrete aggregate	4% cement + 4% fly ash	690-790
Thompson (2001)	Flexural dynamic	Gravel aggregate	4.5% - 8.5%	32,000-40,000
Williams (1986)	-	Gritstone aggregate Limestone aggregate	60-150 Kg/m <sup>3</sup> 90-120 Kg/m <sup>3</sup>	17,700-40,100 30,400-43,100
Shahid (1997)	Compressive Indirect tensile	Gravel aggregate Limestone aggregate	4%-6% 3% - 5%	17,800-38,700 (compressive) 15,500-30,100 (indirect tensile)
Barišić et al. (2015)	Compressive Ultrasonic	Gravel-slag mixtures	2%-4%	963-3,650 9,554-19,997
Mandal et al. (2014)	Nondestructive- ultrasonic	Sand-cement Gravel-cement Clay-cement	6% 3% 12%	17,000-21,000 20,000-41,000 10,000-25,000
Arulrajah et al. (2015)	Flexural-dynamic	Recycled concrete aggregate and recycled glass	3%	9,601-22,600
Disfani et al. (2014)	Flexural-dynamic	Recycled concrete aggregate and crushed brick blends	3%	9,435.3-10,700
Yeo (2011)	Flexural-dynamic	Crushed rock	1%-6%	15,000-25,000

Table 2.6 .....Continued

Author(s)	Testing method	Aggregate type	Cement content	Range of elastic modulus, MPa
BSI (2013)	Compressive Indirect tensile	Any aggregate comply with EN13242	-	2,000-40,000
Yeo (2011)	Flexural-dynamic	Crushed rock	1%-6%	15,000-25,000
Thøgersen et al. (2004)	-	-	-	25,000-45,000
Austrad (2008) as reported by Arnold et al. (2012)	Flexural	Hornfels Siltstone basalt	3% 4% 1.5%-3%	12,490-16,560 6,760-13,350 9,500-11,600
Austrad (2008) as reported by Arnold et al. (2012)	Indirect tensile method	Siltstone Hornfels	4% 3%	17,580-21,760 23,370
Disfani et al. (2014)	Flexural-dynamic	Recycled concrete aggregate and crushed brick blends	3%	9,435.3-10,700
Arulrajah et al. (2015)	Flexural-dynamic	Recycled concrete aggregate and recycled glass	3%	9,601-22,600
Austrad (2008) as reported by Arnold et al. (2012)	Indirect tensile method	Siltstone Hornfels	4% 3%	17,580-21,760 23,370
Austrad (2008) as reported by Arnold et al. (2012)	Flexural	Hornfels Siltstone basalt	3% 4% 1.5%-3%	12,490-16,560 6,760-13,350 9,500-11,600
Thøgersen et al. (2004)	-	-	-	25,000-45,000
BSI (2013)	Compressive Indirect tensile	Any aggregate comply with EN13242		2,000-40,000

Even though different studies have been conducted to estimate the elastic modulus under different testing methods and modes, these were adopted one or two methods /modes for specific set of mixtures. There is no study reported in the literature regarding the evaluation and comparison of different methods and modes. Consequently, this study, in the light of diversity of the investigated mixtures that includes different aggregate composition and degree of cementation/ stabilization, it was intended to study and compare different testing methods and modes in addition to investigating the effect of rubber and cement on the evaluation direction and hence assess the sensitivity of different testing protocols to the change of aggregate composition and/or stabilization degree. The practical implication of this investigation is estimate the elastic modulus reliably, accurately and economically for pavement analysis.

#### **2.11.4 Fatigue performance and damage**

Cement-stabilized pavement layers are normally fatigued due to the effect of repeated traffic loads. These loads generate tensile stresses/strains at the bottom of these layers (Figure 2.6). In general, limited studies have been conducted to investigate the fatigue behaviour of cement-stabilized aggregate. The majority of these studies have reported the fatigue performance in terms of stress ratio–cycles to failure or S-N curves. Table 2.7 summarizes some of the established fatigue equations. The most popular fatigue equation appears to be the one suggested by MEPDG which is

$$\log N_f = \frac{0.972 \beta_{c1} - S}{0.0825 \beta_{c2}} \quad (2.1)$$

where  $N_f$  is the fatigue life,  $S$  is the stress ratio and  $\beta_{c1}$  and  $\beta_{c2}$  are the field calibration coefficients. The necessity for field calibration represents the biggest hurdle for mechanistic-empirical pavement design implementation. Scullion et al. (2008) calibrated Equation 2.1 for two field conditions which are cement-stabilized granular and cemented fine-grained materials. The field calibration factors are presented in Table 2.7.

A very few researches of cement-stabilized aggregate were performed to investigate observe the behaviour during fatigue life. However, (Sobhan and Das 2007; Sobhan et al. 2015) studied the damage accumulation of cemented materials in terms of permanent deformation accumulation in laboratory samples. Gnanendran et al. (2011) conducted a large scale study to estimate the permanent deformation accumulation of cemented materials. In addition, Sobhan and Mashnad (2003) observed the damage of the cemented materials under cyclic flexural loading by characterizing the degradation of the dynamic modulus across the fatigue life.

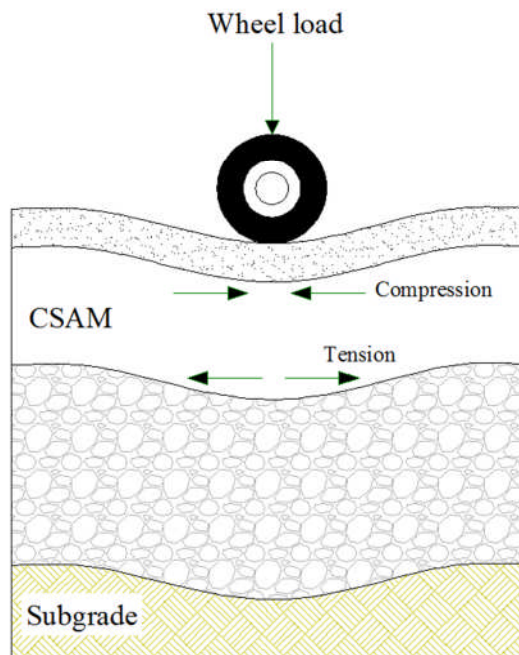


Figure 2.6: Pavement structure containing CSAM base under traffic loading (exaggerated deflection)

Table 2.7: Previous fatigue correlation extracted from the literature.

Equation No.	Model	Mixture	Author(s)
2.2	$S = -0.054 \log N + 0.871$	Cement stabilized Crushed aggregate	Balbo (1997)
2.3	$S = -0.038 \ln N_f + 1.08$	Crushed recycled aggregate	Sobhan and Das (2007)
2.4	$S = -0.038 \ln N_f + 1.047$	Crushed recycled aggregate with HDPE strips	Sobhan and Mashnad (2003)
2.5	$S = -0.098 \ln N_f + 1.126$	Slag-lime stabilized granular materials	Gnanendran and Piratheepan (2009)
2.6	$S = -0.1413 \ln N_f + 1.4121$	Cemented macadam	Ma et al. (2015)
2.7	$S = -0.1197 \ln N_f + 1.4199$	Cemented gravel	Ma et al. (2015)
2.9	$S = -0.0825 \ln N_f + 0.972$	Cement-stabilized materials	Thompson (1986)
The latter equation was calibrated by Scullion et al. (2008)			
$\beta_{c1}=1.0645, \beta_{c2}=0.9003$ ...for the granular S-C and $\beta_{c1}=1.8985, \beta_{c2}=2.5580$ ...for the fine-grained S-C.			
Where: $S = \text{stress ratio} = \frac{\sigma}{MOR}$ , MOR = modulus of rupture and $N_f = \text{fatigue life}$			

### 2.11.5 X-Ray Computed Tomography

X-ray Computed Tomography (X-Ray CT) can be defined as a non-destructive image technique by which an image of a sample's cross-section density distribution is generated (Hassan 2012). It was first designed for medical applications and then used in engineering application to visualize the mixture's internal structure and to obtain the information in digital form with three-dimensional properties and geometry (Tashman et al. 2002). As illustrated in Figure 2.7 the elements of an X-ray CT include source and detector with the test sample between them.

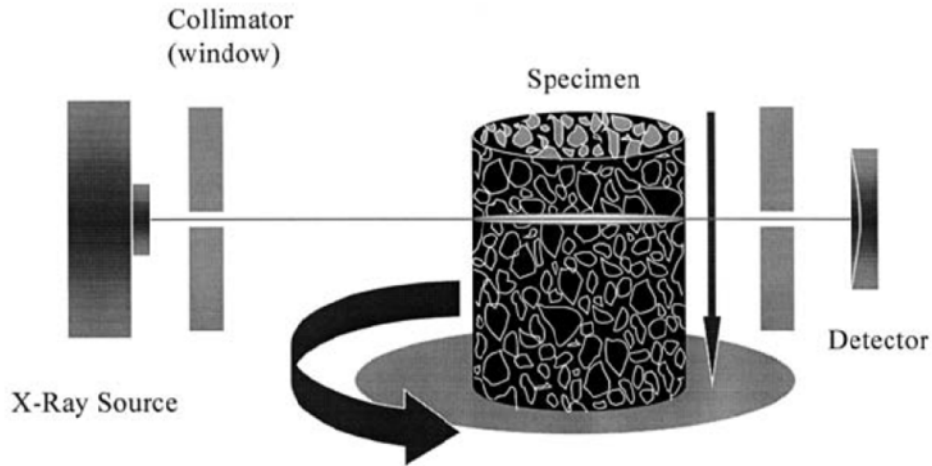


Figure 2.7: Elements of an X-Ray CT set-up (Tashman et al. 2002)

#### 2.11.5.1 Image analysis technique

Image analysis is the process by which an image is converted to a digital form and, by applying various mathematical procedures, significant information can be extracted from it. It involves three stages which are image acquisition, image processing and image interpretation. The first stage utilizes the x-ray to acquire the image while the remaining two stages may be done using commercial software such as Image J and Image Pro-Plus (Khan 2010) to process and quantify the required information.

#### 2.11.5.2 X-ray applications

One of the main advantages of this technique is its non-destructive nature which means that the same scanned sample can be used for other tests. In addition to its ability to fathom the internal structure of the sample, it may provide valuable information to help more completely understand the behaviour of the different

mixtures. However, the thresholding process which is used to discriminate between different materials with different densities represents a challenge facing this tool (Hassan 2012) because it introduces some subjectivity into the analysis. Several studies have been conducted using x-rays to quantitatively characterize the internal structure of different mixtures, with emphasis on asphaltic mixtures. The following applications were conducted:

1. Quantification of air voids and their distribution (Masad et al. 1999; Tashman et al. 2002).
2. Visualizing fibre distribution (Erdem et al. 2011).
3. Orientation and particle size distribution of aggregate (Masad et al. 1999).
4. Study of internal damage of asphaltic mixtures (Khan 2010; Hassan 2012).

Recently, some researchers (Erdem et al. 2012; Najim and Hall 2013) utilized x-ray techniques to study, quantitatively, the distribution of air voids in concrete mixtures. It is worth mentioning that the x-ray technique is used extensively to characterize asphalt concrete mixtures while its application is still limited in concrete mixture evaluation. No studies were identified in the literatures that characterize the internal structure of cement bound granular mixtures by the x-ray technique.

## **2.12 Previous suggested correlations**

To understand the relationship between different parameters and to use them for estimating some parameters-especially the more advanced one from the simple tests-many authors have developed correlations. Table 2.8 illustrates the most popular correlations suggested for different cementitious materials. It will be interesting to

investigate and proof these correlations and also to see what the role has on aggregate composition and degree of cementation their applicability.

Table 2.8: Previous developed correlation extracted from literature.

Author(s)	Correlation	Units	Aggregate type	Remarks
<b>Strengths Vs. strengths</b>				
Piratheepan et al. (2009)	$ITS = 0.1119 * UCS$	-	Sandy gravel	
Wen et al. (2014)	$ITS = 0.86 F_s$	-	Range of materials: clay, silt, sand and gravel	
Wen et al. (2014)	$ITS = 0.12 * UCS$	-	Range of materials: clay, silt, sand and gravel	
Wen et al. (2014)	$F_s = 0.14 * UCS$	-	Range of materials: clay, silt, sand and gravel	
Solanki (2010)	$F_s = 0.41 * UCS$	-	Range of soils, stabilizers and additives	
Solanki (2010)	$ITS = 0.16 * UCS$	-	Range of soils, stabilizers and additives	
<b>Strengths Vs. moduli</b>				
Wen et al. (2014)	$E_{it} = 7980 * ITS$	-	Range of materials: clay, silt, sand and gravel	
Austroad (2004)	$E = 1814 * UCS^{0.88} + 3500$	Both in MPa	Used for highly cemented crushed rock	
Austroad (2004)	$E = 2240 * UCS^{0.88} + 110$	Both in MPa	-used for highly cemented natural gravel	
Arellano and Thompson (1998)	$E = 57,500 * UCS^{0.5}$	Both in psi	High quality cement coarse grain materials	
Arellano and Thompson (1998)	$E_s = 14.4 * UCS^{0.25}$	Both in MPa	-	Used for UCS of more than 7 MPa
Wen et al. (2014)	$E_f = 131.087 * UCS + 62382$	Both in psi	Range of materials: clay, silt, sand and gravel	
CSRA (1986)	$E = 4.16 * UCS^{0.88} + 3484$	E in MPa and UCS in kPa	-	
ACI 318-77	$E = 33 * w^{1.5} * UCS^{0.5}$	Both in psi	-	

Lim and Zollinger (2003)	$E = 4.38 * w^{1.5} * UCS^{0.75}$	E, w and UCS in psi, pcf and pcs , respectively	Crushed limestone	
CSRA (1986)	$E = 8 * F_s + 3500$	E in MPa and F <sub>s</sub> in kPa		
Wen et al. (2014)	$E_f = 936.28 * F_s + 62382$	Both in psi	Range of materials: clay, silt, sand and gravel	
Arnold et al. (2012)	$E_f = K * UCS$ K=1000 to 1250	-	-	
<b>Static vs. Dynamic moduli</b>				
BS 8110 Part 2	$E = 1.2E_d - 19$	Both in MPa	-	
Croney and Croney (1998)	$E_d = 10 + 0.8.E_s$	-	-	-
Williams (1986)	$E_s = 6/7 E_d$	-		
Piratheepan et al. (2009)	$E_d = 1.2661E_s$	-	Sandy gravel	

### 2.13 Concluding remarks

1. Despite its capability and application, X-ray scanning combined with image processing is seldom utilized to study the internal structure of the cement-stabilized materials. Therefore, based on its reviewed applications, this may provide an important technique for understanding the internal structural for the cemented mixtures.
2. There is no widely accepted characterization protocol for the cement-stabilized mixture, especially using more advanced techniques.
3. To understand the behaviour and the failure mechanisms of cement-stabilized mixtures under cyclic loading, there is a need to do more investigation regarding

damage accumulation and degradation of cemented materials across the fatigue life of the mixture.

4. Due to its crucial role in pavement analysis and design, it is necessary to investigate how rubber and cement may affect the measurement methods of stiffness modulus. It will be also beneficial, especially in the light of the large diversity of the stiffness moduli value reported in the literature, to compare between different measurement methods and the typical values obtained from the modified mixtures when measured by different procedures.
5. Evaluation of the fatigue behaviour of the modified mixtures is an important issue in an assessment of any materials due to its direct impact on the pavement analysis and design of the pavement structure subjected to repeated loading.
6. As the rubberized cement-stabilized mixtures will be evaluated for highway application, there is a need to evaluate their performance under cyclic loading. However, such testing procedures are not standardized. There is, therefore, need to develop equipment and suggest testing methodologies to adequately characterize these characteristics of the materials.
7. Large diversity was noticed in the literature regarding the method used to characterize the stiffness modulus for cement-stabilized materials. This diversity also includes the typical values obtained. In addition, no study was found reporting the differences and comparison between these characterization methods.

## 2.14 Reference

Adaska, W. S., D. R. Luhr, C. Petit, I. Al-Qadi and A. Millien (2004). Control of reflective cracking in cement stabilized pavements. Fifth International RILEM Conference on Reflective Cracking in Pavements, RILEM Publications SARL.

Amer, N., N. Delatte and C. Storey (2003). "Using gyratory compaction to investigate density and mechanical properties of roller-compacted concrete." *Transportation Research Record: Journal of the Transportation Research Board* 1834(1): 77-84.

Applied Research Associates, I. (2004). *Guide for Mechanistic-Empirical Design of New and Rehabilitated Pavement Structures*. Illinois.

Arellano, D. and M. R. Thompson (1998). *Stabilized Base Properties (Strength, Modulus, Fatigue) for Mechanistic-Based Airport Pavement Design*, Final Report, Technical Report of Research, Department of Civil Engineering University of Illinois at Urbana-Champaign, Illinois.

Arnold, G., C. Morkel and G. van der Weshuizen (2012). *Development of tensile fatigue criteria for bound materials*, NZ Transport Agency report No. 463, New Zealand Institute of Highway Technology.

Arulrajah, A., M. M. Disfani, H. Haghghi, A. Mohammadinia and S. Horpibulsuk (2015). "Modulus of rupture evaluation of cement stabilized recycled glass/recycled concrete aggregate blends." *Construction and Building Materials* 84: 146-155.

Baghdadi, Z. A. (1982). "Accelerated strength testing of soil-cement."

Balbo, J. T. (1997). *High quality cement treated crushed stones for concrete pavement bases*. Proceedings of the Sixth International Purdue Conference on Concrete Pavement November.

- Barišić, I., S. Dimter and T. Rukavina (2014). "Strength properties of steel slag stabilized mixes." *Composites Part B: Engineering* 58: 386-391.
- Barišić, I., S. Dimter and T. Rukavina (2015). "Elastic properties of cement-stabilised mixes with steel slag." *International Journal of Pavement Engineering*(ahead-of-print): 1-10.
- Behiry, A. E. A. E.-M. (2013). "Utilization of cement treated recycled concrete aggregates as base or subbase layer in Egypt." *Ain Shams Engineering Journal*.
- Brown, A. J., C. D. F. Rogers and N. H. Thom (1993). Field assessment of road foundations. Final report submitted to TRL
- BSI, T. B. S. I. (2013). *Hydraulically Bound Mixtures. Cement Bound granular Mixtures*, BSI. BS EN 14227-1:2013.
- Bullen, F. (1994). "The resilient moduli of cement treated materials." *Road and Transport Research* 3(2).
- Carpenter, S., M. Crovetto, K. Smith, E. Rmeili and T. Wilson (1992). *soil and base stabilization and associated drainage considerations. volume ii: mixture design considerations. final report.*
- Chilukwa, N. N. (2013). *Vibratory hammer compaction of granular materials*, Stellenbosch: Stellenbosch University.
- Choi, Y.-K. and K. D. Hansen (2005). "RCC/Soil-Cement: What's the Difference?" *journal of materials in civil engineering,ASCE* 17: 371-378.
- Crony, D. and P. Crony (1998). *The design and performance of road pavements*, McGraw-Hill, UK.
- CSRA (1986). *Cementitious stabilization in road construction. TRH13. C. o. S. R. Authorities. Pretoria.*

- De Beer, M. (1990). Aspects of the design and behaviour of road structures incorporating lightly cementitious layers. PhD thesis, University of Pretoria.
- Disfani, M. M., A. Arulrajah, H. Haghghi, A. Mohammadinia and S. Horpibulsuk (2014). "Flexural beam fatigue strength evaluation of crushed brick as a supplementary material in cement stabilized recycled concrete aggregates." *Construction and Building Materials* 68: 667-676.
- Drnevich, V. P., A. C. Evans and A. B. Prochaska (2007). "A Study of Effective Soil Compaction Control of Granular Soils."
- Erdem, S., A. R. Dawson and N. H. Thom (2011). "Microstructure-linked strength properties and impact response of conventional and recycled concrete reinforced with steel and synthetic macro fibres." *Construction and Building Materials* 25(10): 4025-4036.
- Erdem, S., A. R. Dawson and N. H. Thom (2012). "Micromechanical Structure-Property Relationships for the Damage Analysis of Impact Loaded Sustainable Concrete." *Journal of Materials in Civil Engineering*.
- Foley, G. (2002). "Mix design for stabilised pavement materials."
- Garber, S., R. O. Rasmussen and D. Harrington (2011). *Guide to Cement-based Integrated Pavement Solutions*.
- Gnanendran, C., J. Piratheepan, J. Ramanujam and A. Arulrajah (2011). "Accelerated laboratory pavement model test on cemented base and clay subgrade." *Geotechnical Testing Journal* 34(4): 1.
- Gnanendran, C. T. and J. Piratheepan (2008). "Characterisation of a lightly stabilised granular material by indirect diametrical tensile testing." *International Journal of Pavement Engineering* 9(6): 445-456.

- Gnanendran, C. T. and J. Piratheepan (2009). "Determination of fatigue life of a granular base material lightly stabilized with slag lime from indirect diametral tensile testing." *Journal of Transportation Engineering* 136(8): 736-745.
- Grilli, A., M. Bocci and A. Tarantino (2013). "Experimental investigation on fibre-reinforced cement-treated materials using reclaimed asphalt." *Construction and Building Materials* 38: 491-496.
- Hassan, N. A. (2012). Microstructural characterization of rubber modified asphalt mixtures PhD thesis, The university of Nottingham.
- Highway England (2009). "Manual of contract documents for highway works, volume 2 notes for guidance on the specification for highway works." Series 800 2.
- Jameson, G. (2010). Towards the revision of Austroads procedures for the design of pavements containing cemented materials.
- Jameson, G. and A. Howard (2012). Preliminary investigation of the influence of micro-cracking on fatigue life of cemented materials.
- Jitsangiam, P. and H. Nikraz (2011). "Mix Design of Cementitious Basecourse."
- Khan, R. (2010). Quantification of microstructural damage in asphalt, University of Nottingham.
- Khattak, M. J. and M. Alrashidi (2006). "Durability and mechanistic characteristics of fiber reinforced soil-cement mixtures." *International Journal of Pavement Engineering* 7(1): 53-62.
- Khoury, N. and M. M. Zaman (2007). "Durability of stabilized base courses subjected to wet-dry cycles." *International Journal of Pavement Engineering* 8(4): 265-276.
- Lav, M. A. and A. H. Lav (2014). "Effects of stabilization on resilient characteristics of fly ash as pavement material." *Construction and Building Materials* 54: 10-16.

Lim, S. and D. G. Zollinger (2003). "Estimation of the compressive strength and modulus of elasticity of cement-treated aggregate base materials." *Transportation Research Record: Journal of the Transportation Research Board* 1837(1): 30-38.

Little, D. N. (1995). *Guidelines for mixture design and thickness design for stabilized bases and subgrades*, The Texas A&M University.

Ma, Y., J. Gu, Y. Li and Y. Li (2015). "The bending fatigue performance of cement-stabilized aggregate reinforced with polypropylene filament fiber." *Construction and Building Materials* 83: 230-236.

Mandal, T., J. M. Tinjum and T. B. Edil (2014). non-destructive testing of cementitiously stabilized materials using ultrasonic pulse velocity test 2. *Transportation Research Board 93rd Annual Meeting*.

Masad, E., B. Muhunthan, N. Shashidhar and T. Harman (1999). "Internal structure characterization of asphalt concrete using image analysis." *Journal of computing in civil engineering* 13(2): 88-95.

Najim, K. B. and M. R. Hall (2013). "Crumb rubber aggregate coatings/pre-treatments and their effects on interfacial bonding, air entrapment and fracture toughness in self-compacting rubberised concrete (SCRC)." *Materials and Structures*.

NCHRP (2004). *Mechanistic-empirical design of new and rehabilitated pavement structures*. National cooperative highway research program. Washington, D. C., National research council. NCHRP project 1-37A report

Nusit, K., P. Jitsangiam, J. Kodikara, H. H. Bui and G. L. M. Leung (2015). "Dynamic Modulus Measurements of Bound Cement-Treated Base Materials." *Geotechnical Testing Journal*, Vol.38, No.3 38(3): 1-15.

O'Flaherty, C. A. (2002). "Highways: The location, design, construction and maintenance of road pavements."

Paul, D. K. (2011). "Characterisation of Lightly Stabilised Granular Materials by Various Laboratory Testing Methods." PhD Thesis, University of New South Wales, Australian.

Paul, D. K. and C. T. Gnanendran (2012). "Effects of curing time on the tensile characteristics of lightly stabilized granular base materials." 4th Conference on Geotechnical and Geophysical Site Characterisation, Porto de Galinhas, Brazil.

Paul, D. K. and C. T. Gnanendran (2015). "Characterization of Lightly Stabilized Granular Base Materials Using Monotonic and Cyclic Load Flexural Testing." Journal of Materials in Civil Engineering: 04015074.

PCA (2005). "soil cement technology for pavement different products for different applications." Portland Concrete Association(illinois).

PIARC (Permanent International Association of Road Congresses,1991). "Semi-Rigid Pavements."

Piratheepan, J., C. Gnanendran and S.-C. Lo (2009). "Characterization of cementitiously stabilized granular materials for pavement design using unconfined compression and IDT testings with internal displacement measurements." Journal of Materials in Civil Engineering 22(5): 495-505.

Scullion, T., J. Uzan, S. Hilbrich and P. Chen (2008). "Thickness Design Systems for Pavements Containing Soil-Cement Bases." PCA R&D Serial(2863).

Scullion, T., J. Uzan, S. Hilbrich and P. Chen (2008). "Thickness design systems for pavements containing soil cement bases." PCA R&D Serial(2863).

Shahid, M. A. (1997). "Improved Cement Bound Base Design for Flexible Composite Pavement." PhD Thesis, University of Nottingham.

Sobhan, K. (1997). "Stabilized fiber reinforced pavement base course with recycled aggregates." PhD Thesis, Northwest University, Evanstone, Illinois.

Sobhan, K. and B. M. Das (2007). "Durability of soil–cements against fatigue fracture." *Journal of Materials in Civil Engineering* 19(1): 26-32.

Sobhan, K., L. Gonzalez and D. Reddy (2015). "Durability of a pavement foundation made from recycled aggregate concrete subjected to cyclic wet–dry exposure and fatigue loading." *Materials and Structures*: 1-14.

Sobhan, K. and R. J. Krizek (1999). "Fatigue behavior of fiber-reinforced recycled aggregate base course." *Journal of materials in civil engineering* 11(2): 124-130.

Sobhan, K. and M. Mashnad (2000). "Fatigue durability of stabilized recycled aggregate base course containing fly ash and waste-plastic strip reinforcement." Final Rep. Submitted to the Recycled Materials Resource Centre, Univ. of New Hampshire.

Sobhan, K. and M. Mashnad (2003). "Fatigue behavior of a pavement foundation with recycled aggregate and waste HDPE strips." *Journal of geotechnical and geoenvironmental engineering* 129(7): 630-638.

Solanki, P. (2010). Characterization of cementitiously stabilized subgrades for mechanistic-empirical pavement design, PhD thesis, The university of Oklahoma

Su, Z., D. Fratta, J. M. Tinjum and T. B. Edil (2013). Cementitiously Stabilized Materials Using Ultrasonic Testing. Transportation Research Board 92nd Annual Meeting.

Sunarjono, S. (2008). "The influence of foamed bitumen characteristics on cold-mix asphalt properties." PhD Thesis, University of Nottingham, Department of Civil Engineering.

Tashman, L., E. Masad, J. D'Angelo, J. Bukowski and T. Harman (2002). "X-ray tomography to characterize air void distribution in superpave gyratory compacted specimens." *International Journal of Pavement Engineering* 3(1): 19-28.

- Theyse, H. L., M. De Beer and F. C. RUST (1996). "Overview of South African Mechanistic Pavement Design Method." *Transportation Research Record: Journal of the Transportation Research Board* Volume 1539
- Thøgersen, F., C. Busch and A. Henrichsen (2004). "Mechanistic Design of Semi-Rigid Pavements - An Incremental Approach." Report 138, Danish Road Institute.
- Thompson, I. (2001). "Use of Steel Fibers to Reinforce Cement Bound Roadbase." PhD Thesis, University of Nottingham.
- Thompson, M. (1986). "mechanistic design concepts for stabilized base pavements." TRL (2003). "Literature review: stabilised sub-bases for heavily trafficked roads."
- Wen , H., B. Muhunthan, J. Wang, X. Li, T. Edil and J. M. Tinjum (2014). *Characterization of Cementitiously Stabilized Layers for Use in Pavement Design and Analysis.*
- White, G. W. and C. T. Gnanendran (2005). "The influence of compaction method and density on the strength and modulus of cementitiously stabilised pavement materials." *International Journal of Pavement Engineering* 6(2): 97-110.
- Williams, R. I. T. (1986). "Cement-treated pavements : materials, design and construction " Elsevier Applied Science.
- Williams, S. (2013). "Comparison of the Superpave Gyrotory and Proctor Compaction Methods for the Design of Roller-Compacted Concrete Pavements." *Transportation Research Record: Journal of the Transportation Research Board*(2342): 106-112.
- Yeo, Y. S. (2011). *characteristics of cement-stabilized treated crushed rock base course for western australian roads.* PhD, Curtin University.

Zhang, P. and Q. Li (2009). "Effect of polypropylene fibre on mechanical and shrinkage properties of cement-stabilised macadam." *International Journal of Pavement Engineering* 10(6): 435-445.

Zhu, J., T. Zhu, Z. Dong and D. Wu (2014). "Effect of rubber particles on cement stabilized gravel system." *Journal of Wuhan University of Technology-Mater. Sci. Ed.* 29(5): 990-995.

### **Specifications**

BS EN 14227-1:2004, Hydraulically bound mixtures- Specification- Part 1: Cement bound granular mixtures, British Standards Institutes, London

BS EN14227-10:2006, Hydraulically bound mixtures- Specification- Part 10: Soil treated by cement, British Standards Institutes, London

BS EN 14227-1:2013, Hydraulically bound mixtures- Specification- Part 1: Cement bound granular mixtures, British Standards Institutes, London

BS EN 13286-41:2003, Hydraulically bound mixtures- Part 41: Test method for determination of the compressive strength of hydraulically bound mixtures, British Standards Institutes, London

BS EN 13286-43:2003, Hydraulically bound mixtures- Part 43: Test method for determination of the modulus of elasticity of hydraulically bound mixtures, British Standards Institutes, London

BS EN 13286-40, Hydraulically bound mixtures- Part 40: Test method for determination of the direct tensile strength of hydraulically bound mixtures, British Standards Institutes, London

BS EN 13286-42, Hydraulically bound mixtures- Part 42: Test method for determination of the indirect tensile strength of hydraulically bound mixtures, British Standards Institutes, London

ASTM C469, Standard test method for static modulus of elasticity and Poisson's ratio of concrete in compression, American Society for Testing Materials

## **Chapter Three**

### **Rubberized cementitious mixtures**

#### **3.1 Introduction**

Being the first study that investigates comprehensively the properties and behaviour of cement-stabilized aggregate mixtures incorporating different amounts of rubber and cement, it was necessary to review the previous studies conducted regarding the rubberized cementitious materials. In this chapter, it was intended to define some terminology related to crumb rubber production. Most importantly, a review of different rubberized cementitious materials in terms of their mechanical characteristics is presented. These materials include mainly concrete as well as some other materials like cemented-stabilized materials and roller compacted concrete.

## 3.2 Waste tires

One of the main environmental issues worldwide is the management of solid waste materials because of increasing amounts of these materials generated each year. It is estimated that about 250 million scrap tires are generated every year in European countries. In addition, for eastern Europe, North America, Latin America, Japan and Middle East, the same figure are produced annually (Oikonomou and Mavridou 2009), while in the United States the amount is about 270 million tires (Siddique and Naik 2004). For the last thirty years, many investigations have been done in order to evaluate the feasibility of utilizing these products in various applications in civil engineering field. The reason behind that can be summarized as follows (Khaloo et al. 2008; Taha et al. 2008; Oikonomou and Mavridou 2009; Pelisser et al. 2011):

1. To reduce the detrimental environmental effects of these materials.
2. To reduce the costs associated with obtaining increasingly unavailable natural resources.
3. To support the development of construction sustainability.
4. Attempts to produce mixtures with special features to overcome the negative attributes of concrete such as brittle behaviour and low loading toughness.
5. To find an efficient method to dispose of these wastes without any side effects.

### 3.2.1 Scrap tire recycling

Recycling is usually applied for passenger car, trucks, and bicycles waste tires. During this process, the rubber is extracted from tires after removing steel and fabric. There are three methods for waste tires recycling (Memon et al. 2012), namely

ambient grinding, cryogenic grinding and aqua-blast methods. However, the first two methods are most widely used.

Ambient recycling is conducted at room temperature to mechanically reduce the size of shred using cracker milling. As a result, rough surfaces and large surface areas are usually obtained by this method. The diagrammatic representation for this method is shown in Figure 3.1. Cryogenic or freezing grinding as it is sometimes called, on the other hand, is performed at low temperature (-87 to -198 C) using liquid nitrogen which makes rubber very brittle and easily fractured ([Rahman 2004](#); [Hassan 2012](#)).

Figure 3.2 illustrates the schematic representation for this method. For some soft materials where it is difficult to grind them into required size at ambient temperature, the cryogenic one is preferable. Although different methods essentially reduce the size of large tire pieces and separate the rubber from the steel, different recycling methods give different surface area which in turn is an important feature of the rubber obtained. Unlike in the ambient grinding technique, the rubber produced by cryogenic method mostly has a lower surface area which in turn may cause less reaction rate with hot bitumen ([Memon et al. 2012](#)).

### **3.2.2 Size based classification**

Waste rubber can be obtained from cars or trucks consumer tires. Basically, rubber particles obtained from the latter source are much stiffer than those produced from the former one which may lead to stronger and stiffer concrete ([Papakonstantinou and Tobolski 2006](#)). However, the rubber from car tires has been much more used in

the previous researches (Ganjian et al. 2009). This is because far more car tires are discarded every year than from trucks.

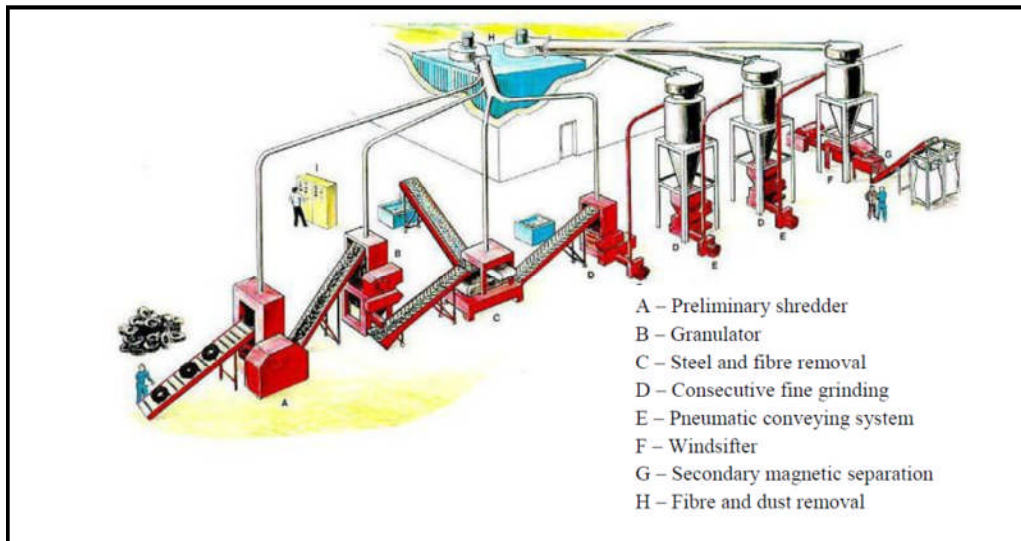


Figure 3.1: Illustration of Ambient granulating for scrap tire recycling system (Hassan 2012)

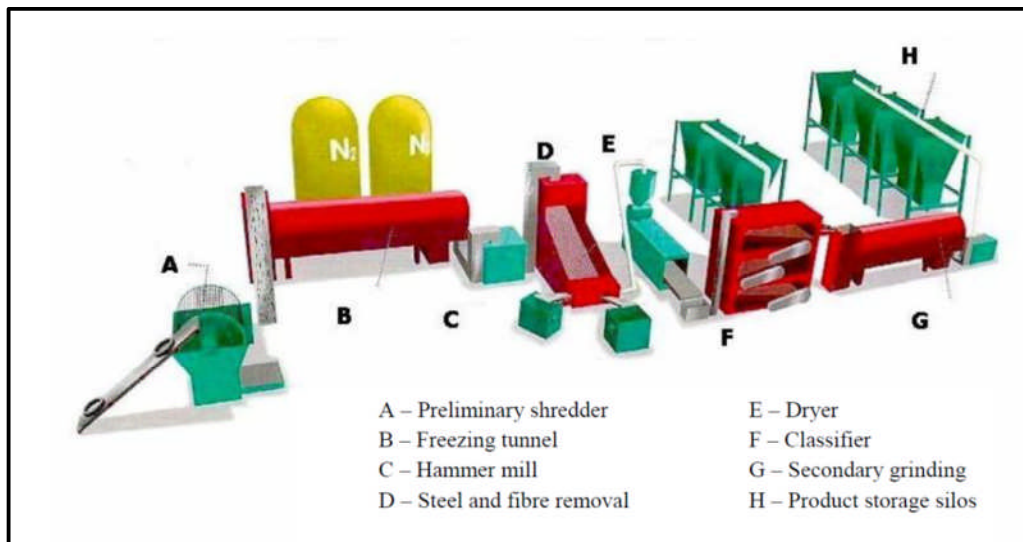


Figure 3.2: Illustration of cryogenic grinding for scrap tire recycling system (Hassan 2012)

All previous authors classified the rubber from waste tires into shredded or chipped, ground and crumb rubber based on its size. However, reviewing previous literature during the course of this study revealed that there is a conflict between the size ranges that define the limits between each rubber class. Authors (Eldin and Senouci 1993; Siddique and Naik 2004; Taha et al. 2008) defined the shredded, ground and crumb rubbers as the particles with size of 13-76 mm, 19-0.15 mm, and 4.75-0.075 mm, respectively. However, Ganjian et al. (2009) classified the crumb size as that take in between 0.425 mm and 4.75 mm while 0.075 - 0.475 mm represents the size of ground rubber. The study conducted by Huang et al. (2004) suggested to use the smaller size of rubber to reduce the potential reduction in the strength of rubber-modified concrete. Figure 3.3 illustrates the appearance of different rubber sizes

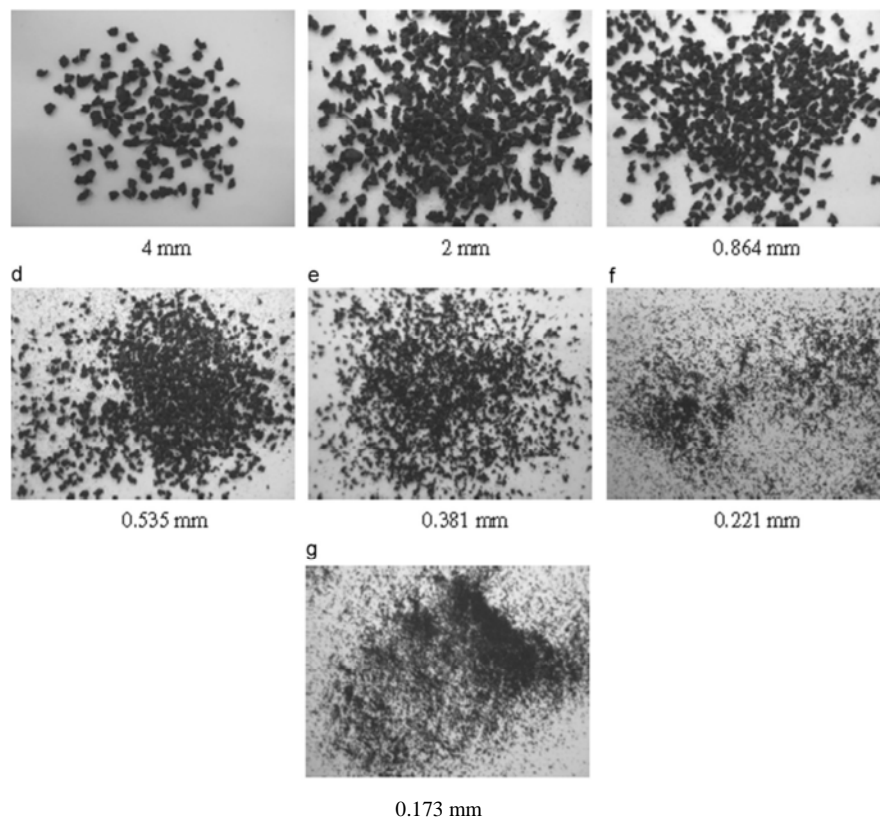


Figure 3.3: Illustration of different sizes of recycled crumb rubber (Thomas and Gupta 2016)

### **3.3 Review of rubberized cementitious mixtures studies**

#### **3.3.1 Rubberized concrete**

In the previous researches, rubber was utilized extensively, as compared with other cementitious materials, in normal concrete and other types of concretes almost as a replacement of fine or coarse aggregate or both. The following subsections presents a review of these findings in terms of mixture density, air-voids, strength, modulus of elasticity, toughness properties and dynamic properties.

##### **3.3.1.1 Air-voids and density**

Recently, [Erdem et al. \(2012\)](#) utilized X-ray technique to investigate the air-voids distribution through different types of aggregate including rubberized concrete sample as shown in Figure 3.4. It is clear, from this figure, that the air-voids content in case of rubberized concrete is higher than those of gravel or brick aggregate. This agreed with previous findings e.g. [Khatib and Bayomy \(1999\)](#) who reported that rubberized concrete contains higher air-voids than does normal concrete. High air content may be due to rough surface of rubber particles which in turn tend to entrap air-voids. In addition, the water repelling tendency of rubber aggregate may attract air which adheres to the rubber ([Khatib and Bayomy 1999](#)). Consequently, the air-voids increase with rubber content increasing. This air, as well as the rubber content, has a direct effect on concrete density. Investigations conducted by [Eldin and Senouci \(1993\)](#), [Goulias and Ali \(1997\)](#), [Khatib and Bayomy \(1999\)](#) and [Li et al. \(2004\)](#) revealed that the density of concrete in which the fine aggregate was replaced by rubber particles decreased with rubber percentage increasing. As illustrated in

Figure 3.5, the maximum decrease in density was between 15% and 23% which happened when all the fine aggregate was replaced.

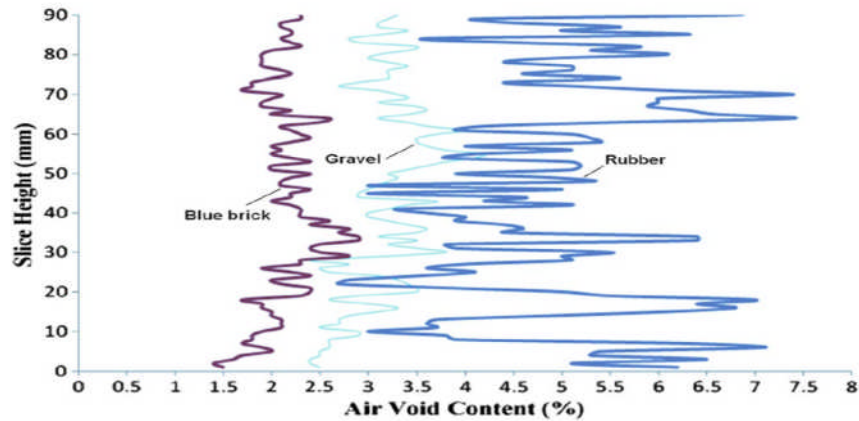


Figure 3.4: Air-voids distribution through concrete samples (Erdem et al. 2012)

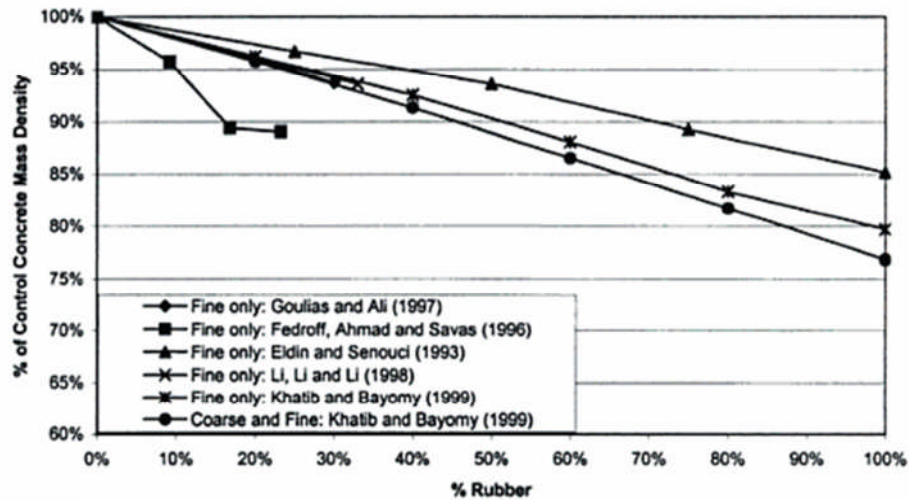


Figure 3.5: Relationship between density and fine rubber percentages (Pierce and Williams 2004)

The same trend was observed by Eldin and Senouci (1993) and Khatib and Bayomy (1999) when they replaced coarse aggregate or both fine and coarse aggregate

together by waste rubber. However, in this case the maximum decrease in concrete density was between 23% and 33% as shown in Figure 3.6. Balaha et al. (2007), Khaloo et al. (2008) and Taha et al. (2008) also observed the reduction in density with rubber content increase. When the rubber content in a concrete mixture is lower than 10-20% of the total aggregate volume, the decrease in the unit weight due solely to the rubber content is negligible (Khatib and Bayomy 1999).

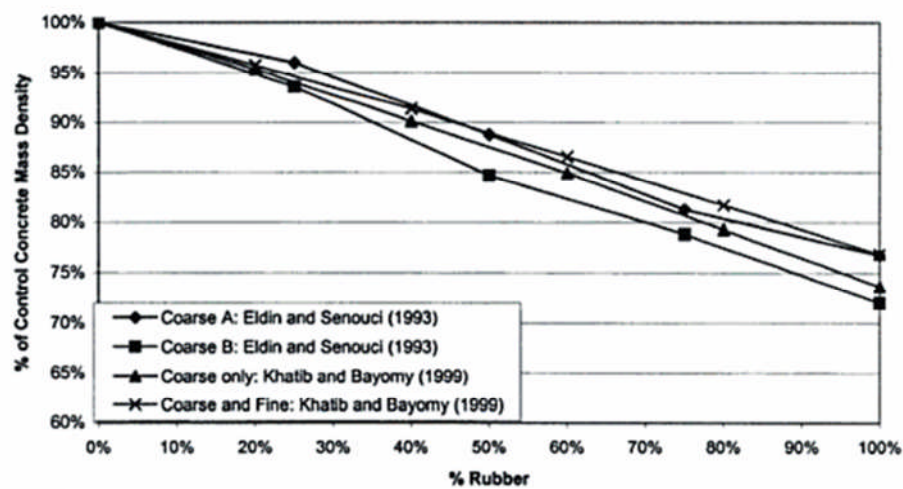


Figure 3.6: Relationship between density and coarse rubber percentages (Pierce and Williams 2004)

### 3.3.1.2 Compressive, flexural and tensile strengths

Investigations (Eldin and Senouci 1993; Topcu 1995; Fattuhi and Clark 1996; Toutanji 1996; Khatib and Bayomy 1999; Güneysi et al. 2004; Khaloo et al. 2008; Taha et al. 2008; Zheng et al. 2008; Atahan and Yücel 2012) have shown that the compressive strength decreased with rubber inclusion in the case of both fine and/or coarse aggregate replacement. Some results are collected and summarized in Figure 3.7 and Figure 3.8 as reported by Pierce and Williams (2004).

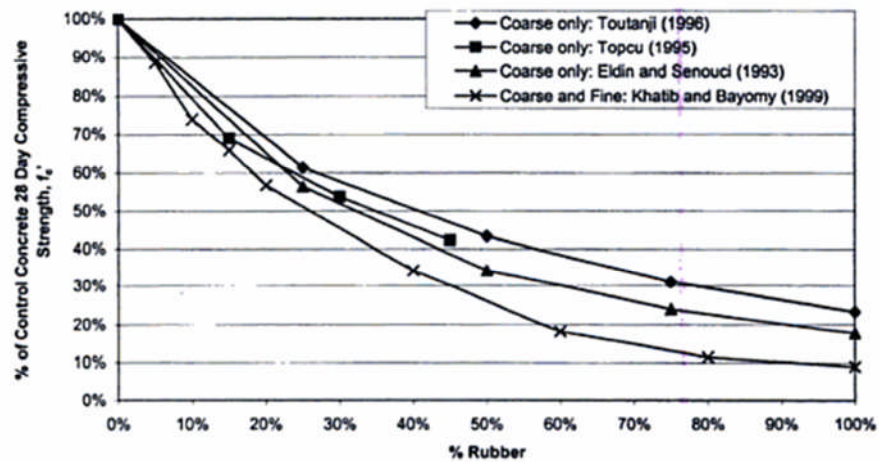


Figure 3.7: Relationship between compressive strength and rubber percentages: coarse aggregate replacement (Pierce and Williams 2004)

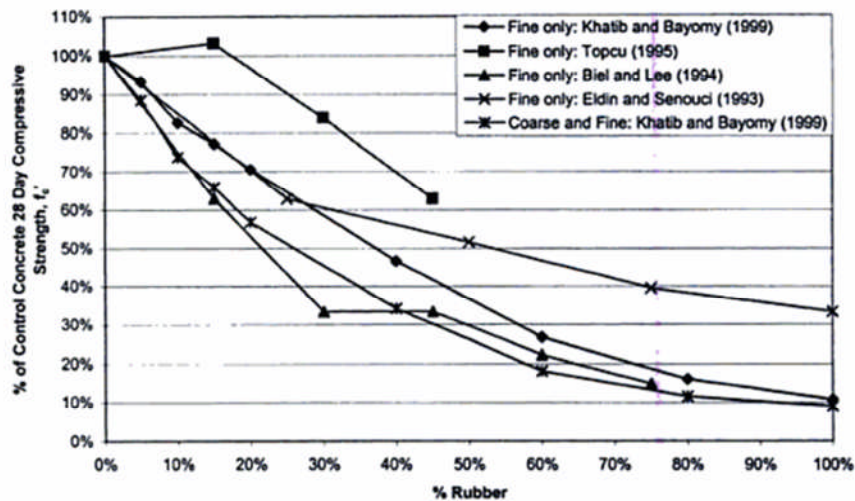


Figure 3.8: Relationship between compressive strength and rubber percentages: fine aggregate replacement (Pierce and Williams 2004)

In accordance with these figures, the compressive strength was reduced by 80-90 % when all the coarse aggregate has been replaced by rubber chips. On the other hand, this figure drops by 65-85 % when the substitution is done only for the entire fine aggregate. Some of above authors have investigated the replacement of the coarse aggregate and fine aggregate separately and compared the two effects. They drew a

conclusion which confirms that the reduction in compressive strength is greater when coarse aggregate is replaced by rubber as compared with fine aggregate replacement. However, others ([Fattuhi and Clark 1996](#)) observed an opposite trend. One possible explanation for that may lie behind the distribution of rubber within the sample. However, the above studies were limited to mechanical properties without any internal structure observations. Consequently, investigation and exploring the internal structure of the rubberized sample may provide valuable information which will reinforce the understanding of material's behaviour.

Two reasons are behind the reduction in compressive strength ([Eldin and Senouci 1993](#); [Khatib and Bayomy 1999](#); [Thomas and Gupta 2016](#)). Firstly, the difference in rigidity between rubber particles and surrounding matrix leads to stress concentrations in the stiffer matrix and enables the cracks to generate around the rubber particles which might contribute to the acceleration of the rate of failure. Secondly, the bad adhesion observed between rubber and matrix may lead to air-voids like behaviour for rubber aggregate which will cause weakness in the concrete.

Although some authors ([Taha et al. 2008](#)) attributed the reduction in strength to the softening effect of rubber particles as a main contributor, it seems logically that both of the reasons mentioned, with the second one as a major contributor, are responsible for strength decrease. This claim can be substantiated by reviewing the studies in which the rubber was treated to enhance its adhesion with the surrounding matrix which finally led to a decrease in the reduction of compressive strength. For example, when [Pelisser et al. \(2011\)](#) treated the rubber with Na OH and used silica fume in rubberized concrete, the reduction in compressive strength was only 14%. This led

them to conclude that the rubber is a good source of aggregate provided that suitable treatment is used. Also, similar behaviour was obtained by [Güneyisi et al. \(2004\)](#). Thus the above emphasize the importance of ensuring good adhesion as this significantly reduces the loss of compressive strength of concrete.

Although many authors have reported the above different reasons, it seems, by critically analysing the properties of materials constituting the rubberized mixture, that there is another important factor which may play a role. This is the uniformity of rubber distribution though the final mixture since the difference in materials' specific gravities may lead to segregation of rubber particles which in turn may create weak areas and cause stress concentrations in the sample which eventually lead to failure. [Jingfu et al. \(2009\)](#) compared, based on the observation of the rubber distribution in the fractured surface, between the distribution of rubber in normal concrete and roller compacted concrete (Figure 3.9). The latter mixture, as revealed from their study, showed homogeneity in the rubber distribution while in the former mix, on the other hand, the floating of light rubber caused an increase in the amount of rubber in the upper part as compared with the lower part. [Turatsinze and Garros \(2008\)](#), when they cut a large rubberized concrete cylinder, drew the same above conclusion. The study of rubber distribution is rarely investigated in the literature especially in the quantitative manner.

In terms of tensile strength, many authors reported reduction in tensile strength as a result of the substitution of fine and/or coarse with rubber particles. However, a recent study ([Grinys et al. 2012](#)) has reported a slight increase in tensile strength when a small amount was used. [Pierce and Williams \(2004\)](#) summarized the previous

findings (Figure 3.10). It can be concluded from Figure 3.10 that the maximum reduction in tensile strength is between 40-70% which occurred at 100% replacement.

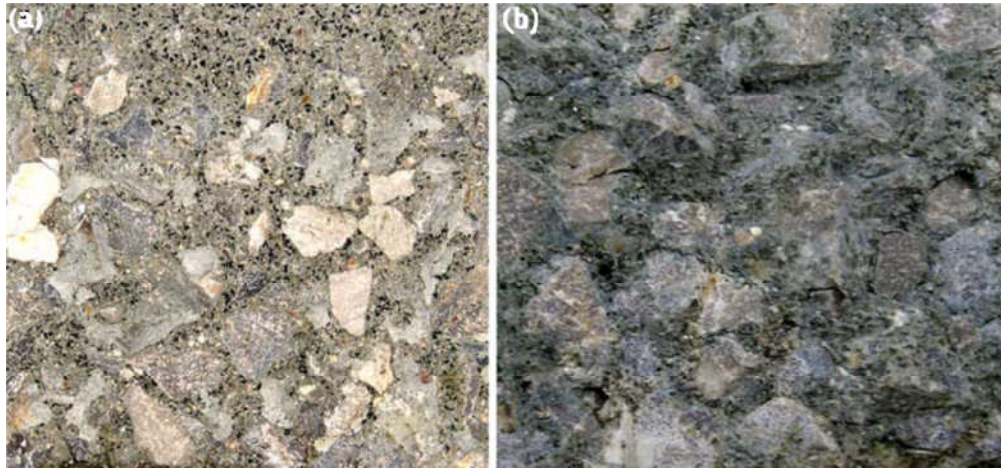


Figure 3.9: Rubber distribution in rubberized concrete (a) and roller-compacted concrete (b) (Jingfu et al. 2009)

By comparing and contrasting the information in Figures 3.7, 3.8 and 3.10, it can be said that the rate of compressive strength reduction is more than that of tensile strength.

Toutanji (1996) studied the effect of incorporating rubber particles on flexural and toughness properties of rubberized concrete. His results showed that the inclusion of rubber particles caused a reduction in flexural strength as illustrated in Figure 3.11. However, the toughness and ductility were increased significantly. In addition, the reduction in flexural strength was half of that for the compressive strength. In another study, Aiello and Leuzzi (2010) stated that replacement of fine aggregate had no effect on the post-cracking behaviour of the modified mixture; whereas substituting coarse aggregate with rubber affected the above behaviour significantly and led to a good residual strength, even after cracking.

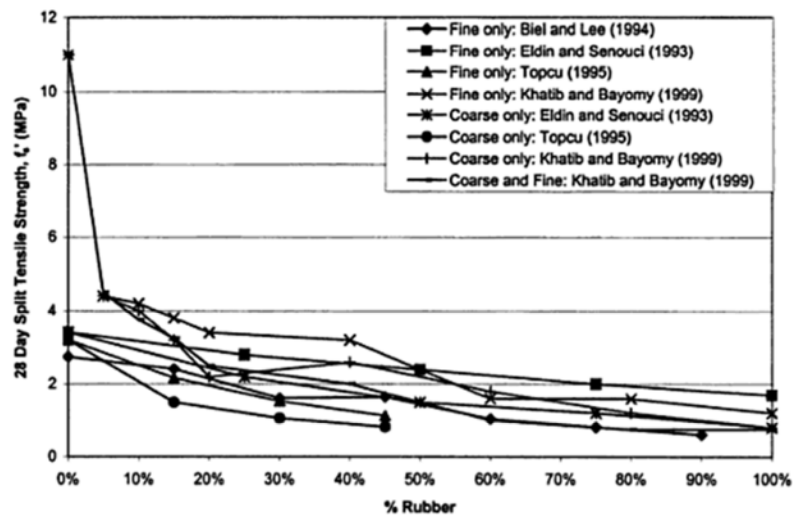


Figure 3.10: Relationship between tensile strength and rubber percentages: fine and coarse aggregate replacement (Pierce and Williams 2004)

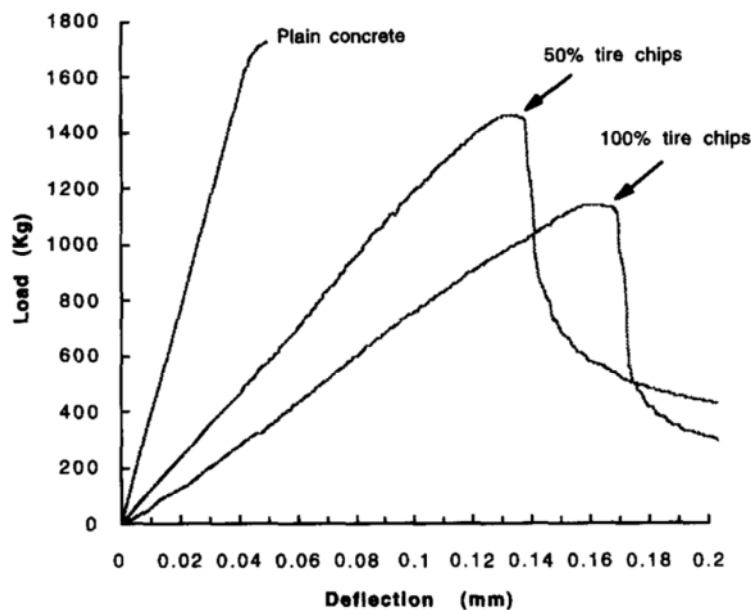


Figure 3.11: Load- Deflection for concrete with different rubber contents (Toutanji 1996)

### 3.3.1.3 Modulus of elasticity, toughness and ductility

Elasticity, toughness and ductility represent other important properties that govern the behaviour of pavement structures in which the modified stabilized mixtures may

serve. Several authors (Goulias and Ali 1997; Topcu and Avcular 1997; Güneyisi et al. 2004; Khaloo et al. 2008; Zheng et al. 2008; Ganjian et al. 2009; Atahan and Yücel 2012) reported a decrease in elastic modulus as a result of rubber addition as shown in Figure 3.12. This is because of the low elastic modulus as compared with those of aggregate particles (Pelisser et al. 2011). This means that the modified concrete has less stiffness and less brittleness which in turn will ensure high deformability and ductility. Furthermore, adding rubber will also increase material toughness (Balaha et al. 2007; Taha et al. 2008). In fact, high toughness leads to higher fracture energy and a greater ability to absorb dynamic loads which lead to a higher cracking resistance and to a higher cracking propagation resistance (Li et al. 2004; Son et al. 2011). Accordingly, Khaloo et al. (2008) observed less width and less propagation velocity for the cracks in rubberized concrete in comparison with plain concrete.

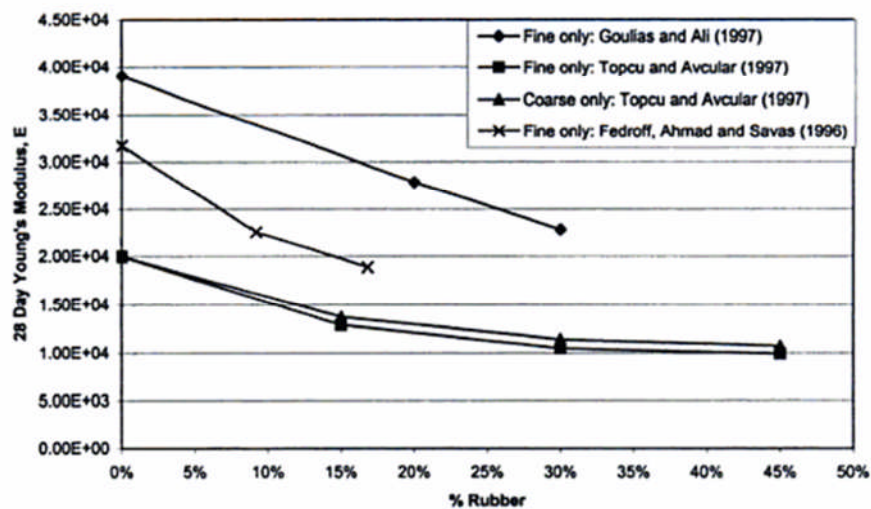


Figure 3.12: Relationship between elastic modulus and rubber percentages: fine and coarse aggregate replacement (Pierce and Williams 2004)

### 3.3.1.4 Rubberized concrete under repeated loading

Since most civil engineering structures are designed to support static loads, the majority of the researches for rubberized concrete were conducted under static or nondestructive testing, the latter mainly in terms of ultrasonic pulse velocity and resonant frequency testing methods.

Regarding the nondestructive characterization, previous studies, performed on rubberized concrete showed a decrease in the speed of the ultrasonic wave through the rubberized samples. This decreased as the amount of rubber increased in the rubber-modified concrete. The dynamic modulus of elasticity measured by the resonant frequency testing also declined as the rubber incorporated in the concrete sample increased.

However, A limited number of studies were performed to evaluate the behaviour of such modified mixtures under cyclic loading (Wang et al. 2010; Liu et al. 2013). However, the recent researches conducted by the latter authors revealed improved fatigue performance after modification with rubber particles as shown in Figure 3.13. In terms of the damage evolution, Liu et al. (2013) observe three transition phases which correspond to the different internal damage development degrees. These occurred during 10%, 10%-90% and the last 10% of the fatigue life. Zheng et al. (2008) conducted a compressive cyclic load on rubberized concrete samples and estimated the brittleness index from the stress-strain hysteresis loop. Their results showed a lower brittleness after rubber inclusion.

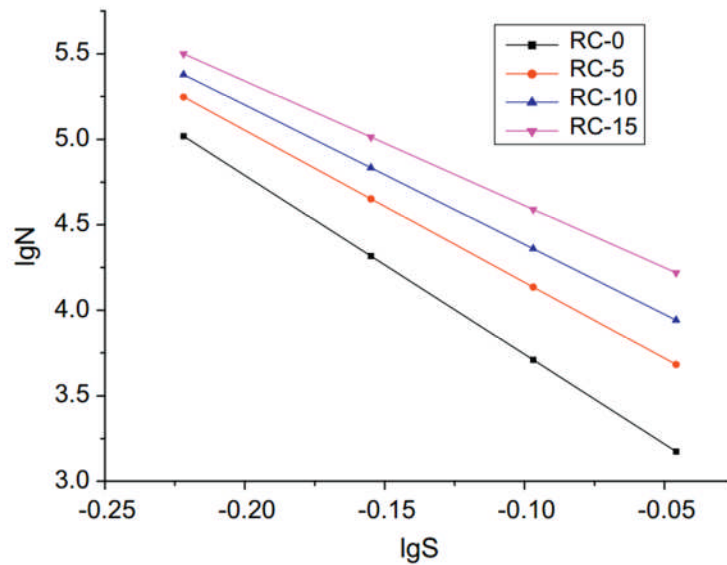


Figure 3.13: Fatigue line for different mixtures reported by (Liu et al. 2013)

### 3.3.2 Cracking and failure patterns

Quantification and observation of cracking mode is important for better understanding of the mechanism of failure and the way by which the stresses and strains distribute inside the materials which, in turn, is necessary to optimize the material's design. Most of previous studies (Eldin and Senouci 1993; Liu 2013), relied on the visual observations of the failed samples to draw a conclusion that rubberized concrete showed gradual and ductile failure as compared with mixtures containing no rubber (see Figure 3.14, for example). In addition, these rubberized samples showed significant displacement without full loss of integrity.

Regarding the mechanism of cracking, most studies relied on a logical hypothesis which unfortunately, usually lacked hard evidence. Eldin and Senouci (1993) considered rubberized concrete, in their theoretical investigation, as a plate and the

rubber particle in it as voids (due to the lower stiffness of rubber as compared with surrounding matrix). Based on mechanics of materials principles, they found the stresses concentrated at the locations of the rubber inclusions. They suggested a failure mechanism for rubberized concrete illustrated in Figure 3.15. Since they proved from their theoretical study that the stresses will concentrate at the rubber edges, this will cause microcracks in the body of the sample. Due to the presence of the rubber particles of elastic nature, they will act like tiny springs that contribute in delaying the crack widening.



Figure 3.14: Failure pattern under static compressive loading for plain (left) and rubberized (right) concretes (Liu 2013)

Further investigation conducted by Duarte et al. (2015), based on the finite element analysis of indirect tensile test simulation of rubber concrete sample, revealed that crack initiation starts in the cement matrix near the rubber particle due to stress concentration at these locations as shown in Figure 3.16.

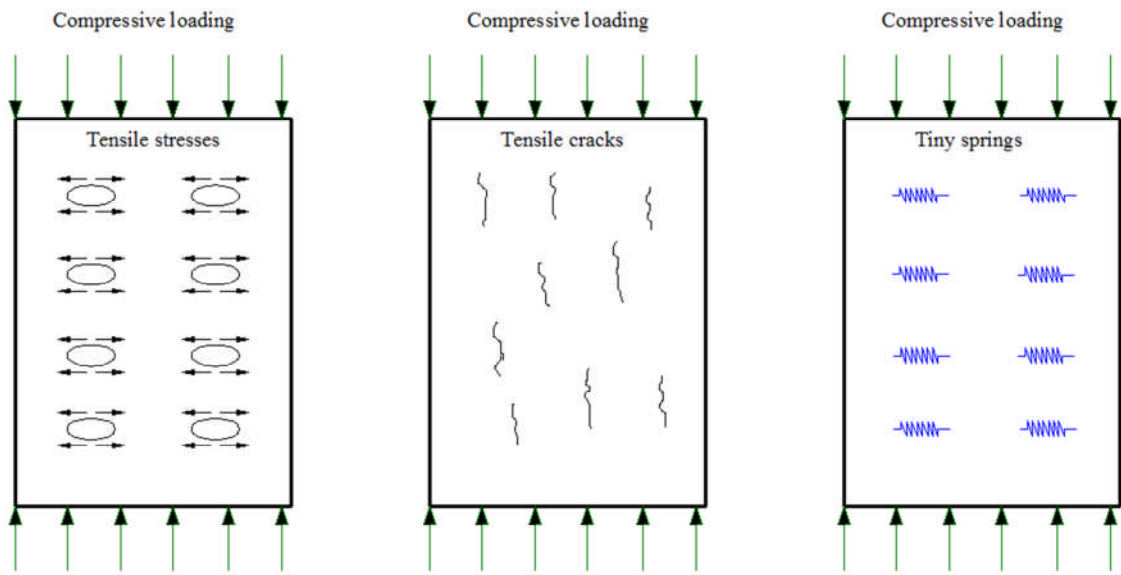


Figure 3.15 Modelling rubberized concrete under compressive loading (Redrawn from (Eldin and Senouci 1993))

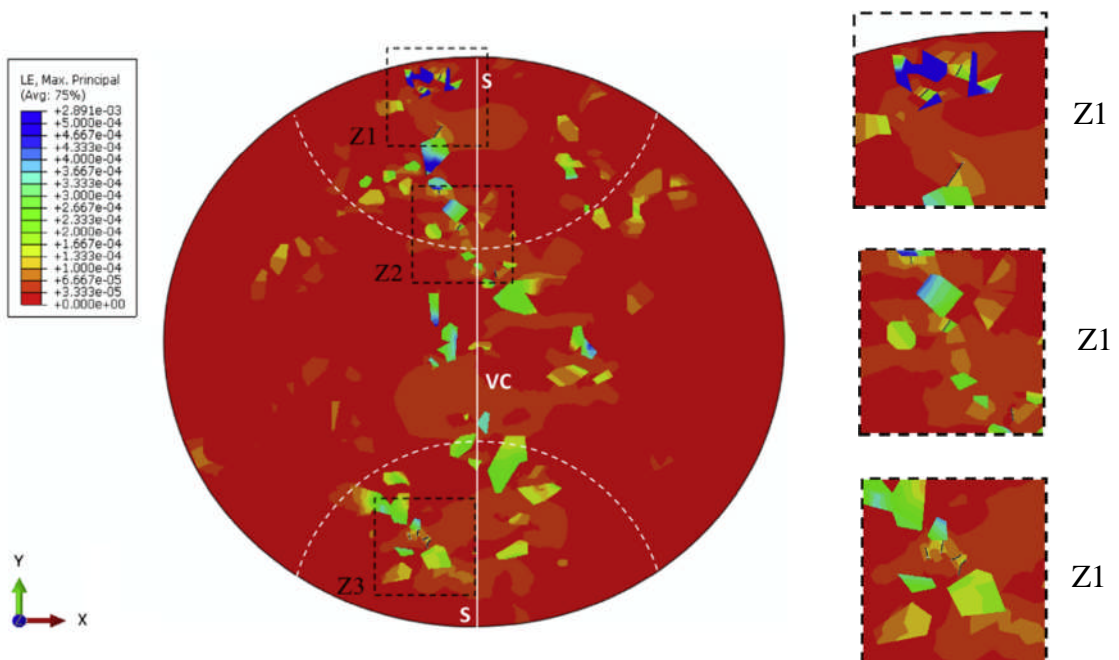


Figure 3.16: Finite element analysis of rubberized concrete samples under indirect tensile testing (Duarte et al. 2015). Blue colour indicates points at which crack initiation is most likely

Eldin and Senouci's assumption that the rubber particles behave as a void seems logical especially in the light of the huge difference of rubber particle and the cement matrix of high cement content. However, cement-stabilized aggregate mixtures normally have low cement contents as compared with those used in concrete mixtures. In addition, unlike conventional concrete, cement-stabilized aggregate, since it is a compacted mixture, will resist the applied load by aggregate interlocking and frictional resistance which may make the aggregate role more significant in such mixtures. Therefore, it will be interesting to investigate the behaviour of rubberized compacted cement-stabilized aggregate mixtures. Furthermore, the effect of cementation level can be expected to influence the performance of such modified mixtures. This will enable an understanding of the effect of relative stiffness between the rubber and the cement matrix on the final performance of the mixture and the failure mechanism of the composite material.

### **3.3.3 Other rubberized cementitious materials**

#### **3.3.3.1 Rubberized cement-stabilized materials**

From a critical inspection of the literature, there seems to be no readily available study about use of the rubber in cement-stabilized mixtures. This was confirmed by [Guo et al. \(2013\)](#). However, he reported just two studies in the Chinese language in one of which Zhang Rong-hui concluded that the inclusion of rubber powder may reduce the tensile stress at the bottom of stabilized layer. In addition, it had a positive effect on mechanical properties and life of pavement. On the other hand, [Qin Feng \(2010\)](#), in another study, showed that the addition of rubber can enhance the shrinkage and erosion resistance of cement stabilized mixtures ([Guo et al. 2013](#)).

[Shahin and Hong \(2010\)](#) investigated the effect of crumb rubber and rubber powder on some mechanical properties of cemented soft clay. Their result revealed a decrease in strength and stiffness modulus of the modified mixtures. However, less detrimental effect was observed in the case of the rubber powder as compared with the crumb one. They attributed that to the larger weak planes created in the soil matrix after crumb rubber addition.

It seems that the uniformity of the rubber distribution may play a certain role. Recently, [Zhu et al. \(2014\)](#) studied some properties of cement-stabilized gravel in which they replaced the gravel aggregate by 0.5%, 1% and 1.5% powdered rubber by volume. Unfortunately, the authors did not mention the cement content used to stabilize these mixtures. Their findings showed a decrease in the compressive strength, where there the decrease was 13% and 19% for the low and high replacement ratios, respectively. In addition, a Mercury Intrusion Porosimetry (MIP) test indicated a wider pore distribution range. They concluded that inclusion of rubber had a positive impact on the durability of the modified mixtures.

[Guleria and Dutta \(2011\)](#) studied the effect on the compressive strength of replacing the fly ash (of fly ash-lime-gypsum mixtures) with tire chips. The replacement levels were 5%, 10% and 15% by the weight of fly ash. They evaluated the effect of curing time (7, 28, 90 and 180 days), curing method (desiccator, burlap and water filled container) and rubber chip treatment method (dry, sodium hydroxide and carbon tetrachloride). Their results revealed that introducing of rubber chips inside the recycled composite cause a decline in the UCS value. In addition, the last mentioned

treatment method proved to be effective in increasing the UCS. Furthermore, the decrease in the UCS was highest when the sample cured in water filled container.

### **3.3.3.2 Rubberized roller-compacted concrete**

Few studies have been conducted to investigate the effect of replacing the fine aggregate by rubber (at between 0 to 120 Kg/m<sup>3</sup>) on the properties of roller-compacted concrete. In their study, [Jingfu et al. \(2009\)](#) examined the mechanical properties in terms of tensile strength (direct and flexural), compressive strength and shrinkage. Their results showed a slight decrease in the compressive strength and stiffness modulus. The flexural and tensile strengths and the elongation at failure, on the other hand, were improved after rubber inclusion. Based on their visual inspection, they observed a uniform rubber distribution and ductile behaviour.

This reported behaviour is not due to rubber particles alone but, rather, to the combined effect of rubber and cement together. The authors intended to keep the same level of the compressive strength of the mixtures after rubber inclusion which made them increased the cement quantity to compensate the reduction resulting from rubber incorporation. Therefore, the effect of rubber inclusion alone is unclear in the mentioned study.

Following [Jingfu et al. \(2009\)](#), [Meddah et al. \(2014\)](#) performed an experimental study to investigate the effect of crumb rubber, by up to 30% of the aggregate volume, on the mechanical properties of roller compacted concrete manufactured from gravel aggregates. The main findings from their study are, firstly, reductions in

compressive, tensile, modulus of elasticity and flexural strength of the mixtures due to rubber inclusion. However, changing the surface roughness conditions of the rubber particles, by treatment with Na OH solution, has increased the mechanical properties. This increase in the compressive strength was about 11 - 28% while the tensile strength was improved by 15-20% after rubber treatment.

In all the above studies, conducted on compacted rubberized mixtures, the studies were limited to a few properties. Also, these studies did not take into account the behaviour of such mixtures under cyclic loading, nor did they investigate mechanisms of failure.

### **3.4 Concluding remarks**

1. There are very few studies that deal with the investigation of cement-stabilized aggregate mixtures incorporating tire crumb rubber intended to be used as a base course in the pavement structure.
2. The internal structure properties, at mesoscale level, in terms of mechanism of failure, crack propagation and rubber distribution, even in the case of rubberized concrete, is not mentioned in the present literature.
3. Few studies, even in the case of rubberized concrete, were conducted to investigate the behaviour of such modified mixtures under cyclic loading.
4. Evaluating the effect of cementation level may improve and broaden the understanding regarding how incorporation of soft rubber particles in cement-

stabilized mixtures of different stiffness may affect their behaviour and failure mechanisms. This is needed since such issues are still unclear even in normal concrete, despite previous extensive studies related to rubberized concrete.

5. For adequate characterization and future improvement of the behaviour of the cement-stabilized aggregate mixtures, it is necessary to identify the mechanism of their failure and support this both quantitatively and qualitatively. One of the candidate approaches is by observing the internal structure utilizing the combination of X-ray CT scans and image processing techniques.
6. Another gap in the literature is the quantitative evaluation of the rubber distribution in the rubberized mixture and the extent to which this distribution may affect the mechanical properties.

### 3.5 Reference

Aiello, M. A. and F. Leuzzi (2010). "Waste tyre rubberized concrete: properties at fresh and hardened state." *Waste Manag* 30(8-9): 1696-1704.

Atahan, A. O. and A. Ö. Yücel (2012). "Crumb rubber in concrete: Static and dynamic evaluation." *Construction and Building Materials* 36: 617-622.

Balaha, M. M., A. A. M. Badawy and M. Hashish (2007). "effect of using ground waste tire rubber on the behavior of concrete mixes." *Indian journal of Engineering and Materials Science* 14: 427-435.

Duarte, A., B. Silva, N. Silvestre, J. de Brito and E. Júlio (2015). "Mechanical characterization of rubberized concrete using an image-processing/XFEM coupled procedure." *Composites Part B: Engineering* 78: 214-226.

Eldin, N. N. and A. B. Senouci (1993). "Rubber-tire particles as concrete aggregate." *Journal of Materials in Civil Engineering* 5(4): 478-496.

Erdem, S., A. R. Dawson and N. H. Thom (2012). "Micromechanical Structure-Property Relationships for the Damage Analysis of Impact Loaded Sustainable Concrete." *Journal of Materials in Civil Engineering*.

Fattuhi, N. and L. Clark (1996). "Cement-based materials containing shredded scrap truck tyre rubber." *Construction and Building Materials* 10(4): 229-236.

Ganjian, E., M. Khorami and A. A. Maghsoudi (2009). "Scrap-tyre-rubber replacement for aggregate and filler in concrete." *Construction and Building Materials* 23(5): 1828-1836.

Goulias, D. G. and A.-H. Ali (1997). Non-destructive evaluation of rubber modified concrete. *Infrastructure Condition Assessment@ sArt, Science, and Practice*, ASCE.

- Grinys, A., H. Sivilevičius and M. Daukšys (2012). "Tyre Rubber Additive Effect on Concrete Mixture Strength." *Journal of Civil Engineering and Management* 18(3): 393-401.
- Guleria, S. and R. Dutta (2011). "Unconfined compressive strength of fly ash–lime–gypsum composite mixed with treated tire chips." *Journal of Materials in Civil Engineering* 23(8): 1255-1263.
- Güneyisi, E., M. Gesoğlu and T. Özturan (2004). "Properties of rubberized concretes containing silica fume." *Cement and Concrete Research* 34(12): 2309-2317.
- Guo, H. M., H. Zhu and Y. Zhou (2013). "The Applied Research of Waste Crumb Rubber in Road Base." *Applied Mechanics and Materials* 253: 317-321.
- Hassan, N. A. (2012). Microstructural characterization of rubber modified asphalt mixtures PhD thesis, The university of Nottingham.
- Huang, B., G. Li, S.-S. Pang and J. Eggers (2004). "Investigation into waste tire rubber-filled concrete." *Journal of Materials in Civil Engineering* 16(3): 187-194.
- Jingfu, K., H. Chuncui and Z. Zhenli (2009). "Strength and shrinkage behaviors of roller-compacted concrete with rubber additives." *Materials and Structures* 42(8): 1117-1124.
- Khaloo, A. R., M. Dehestani and P. Rahmatabadi (2008). "Mechanical properties of concrete containing a high volume of tire-rubber particles." *Waste Management* 28(12): 2472-2482.
- Khatib, Z. K. and F. M. Bayomy (1999). "Rubberized Portland cement concrete." *Journals of Materials in Civil Engineering, ASCE* 11: 206-213.
- Li, G., M. A. Stubblefield, G. Garrick, J. Eggers, C. Abadie and B. Huang (2004). "Development of waste tire modified concrete." *Cement and Concrete Research* 34(12): 2283-2289.

- Liu, F., W. Zheng, L. Li, W. Feng and G. Ning (2013). "Mechanical and fatigue performance of rubber concrete." *Construction and Building Materials* 47: 711-719.
- Liu, R. (2013). *Recycled Tires as Coarse Aggregate in Concrete Pavement Mixtures*.
- Meddah, A., M. Beddar and A. Bali (2014). "Use of shredded rubber tire aggregates for roller compacted concrete pavement." *Journal of Cleaner Production* 72: 187-192.
- Memon, N. A., K. ANSARI and Z. A. ALMANI (2012). "Influence of the Scrap Tyre Processing Techniques on the Physical Properties of the Crumb Rubber."
- Oikonomou, N. and S. Mavridou (2009). "The use of waste tyre rubber in civil engineering works." *Sustainability of construction materials*. WoodHead Publishing Limited, Abington Hall, Cambridge.
- Papakonstantinou, C. G. and M. J. Tobolski (2006). "Use of waste tire steel beads in Portland cement concrete." *Cement and Concrete Research* 36(9): 1686-1691.
- Pelisser, F., N. Zavarise, T. A. Longo and A. M. Bernardin (2011). "Concrete made with recycled tire rubber: Effect of alkaline activation and silica fume addition." *Journal of Cleaner Production* 19(6-7): 757-763.
- Pierce, C. and R. Williams (2004). *Scrap Tire Rubber Modified Concrete: Past, Present, and Future*, Thomas Telford.
- Rahman, M. (2004). "characterisation of dry process crumb rubber modified asphalt mixtures." PhD Thesis, University of Nottingham.
- Shahin, M. A. and L. S. Hong (2010). "Utilization of Shredded Rubber Tires for Cement-Stabilized Soft Clays." *Ground Improvement and Geosynthetics* 207: 181.
- Siddique, R. and T. R. Naik (2004). "Properties of concrete containing scrap-tire rubber--an overview." *Waste Manag* 24(6): 563-569.

- Son, K. S., I. Hajirasouliha and K. Pilakoutas (2011). "Strength and deformability of waste tyre rubber-filled reinforced concrete columns." *Construction and Building Materials* 25(1): 218-226.
- Taha, M. M. R., A. S. El-Dieb, M. A. Abd El-Wahab and M. E. Abdel-Hameed (2008). "Mechanical, Fracture, and Microstructural Investigations of Rubber Concrete." *Journal of Materials in Civil Engineering, ASCE* 20: 640-649.
- Thomas, B. S. and R. C. Gupta (2016). "A comprehensive review on the applications of waste tyre rubber in cement concrete." *Renewable and Sustainable Energy Reviews* 54: 1323-1333.
- Topcu, I. B. (1995). "The properties of rubberized concrete." *Cement and Concrete Research* 25(2): 304-310.
- Topcu, I. B. and N. Avcular (1997). "collision behaviours of rubberized concrete." *Cement and Concrete Research* 27(12): 1893-1898,.
- Toutanji, H. A. (1996). "The Use of Rubber Tire Particles in Concrete to Replace Mineral Aggregates." *Cement & Concrete Composites* 18: 135-139.
- Turatsinze, A. and M. Garros (2008). "On the modulus of elasticity and strain capacity of self-compacting concrete incorporating rubber aggregates." *Resources, conservation and recycling* 52(10): 1209-1215.
- Wang, C., Y. Zhang and A. Ma (2010). "Investigation into the fatigue damage process of rubberized concrete and plain concrete by AE analysis." *Journal of Materials in Civil Engineering* 23(7): 953-960.
- Zheng, L., X. S. Huo and Y. Yuan (2008). "Strength, modulus of elasticity, and brittleness index of rubberized concrete." *Journal of Materials in Civil Engineering* 20(11): 692-699.

Zheng, L., X. Sharon Huo and Y. Yuan (2008). "Strength, Modulus of Elasticity, and Brittleness Index of Rubberized Concrete." *Journal of Civil Engineering* , ASCE.

Zhu, J., T. Zhu, Z. Dong and D. Wu (2014). "Effect of rubber particles on cement stabilized gravel system." *Journal of Wuhan University of Technology-Mater. Sci.* Ed. 29(5): 990-995.

## **Chapter Four**

### **Mixture design and initial investigation**

#### **4.1 Introduction**

Behaviour of composite materials is largely affected by the properties of their components. Therefore, assessment of these components properties will provide vital information to design and optimize the mix for these composites and, at the same time, contributes to the interpretation of the behaviour of the composite mixture. This chapter describes the material selection, characterisation and mixture design methodology adopted for conventional and rubberized mixtures, together with some of their mix design related properties such as density and compacity. The latter is an important property that influences the final performance, which has led some specifications (e.g. [BS EN 14227-1:2013](#)) to impose certain limits upon it. Another purpose of this chapter is to evaluate the possible use of the vacuum saturation method to estimate the compacity of cement stabilized mixtures since the investigated mixtures represent a range of mixes of different composition and cementation level (low, moderate and high). Finally, concluding remarks are presented.

## 4.2 Materials used

### 4.2.1 Aggregates

The aggregate used in this project is a crushed limestone with a nominal maximum size of 20 mm obtained from Dene quarry in Nottinghamshire, UK. This was collected, dried and stored in different stockpiles according to their fractions size which are 20 mm, 14 mm, 10 mm, 6 mm, dust and fillers. Figure 4.1 depicts the different sizes used.

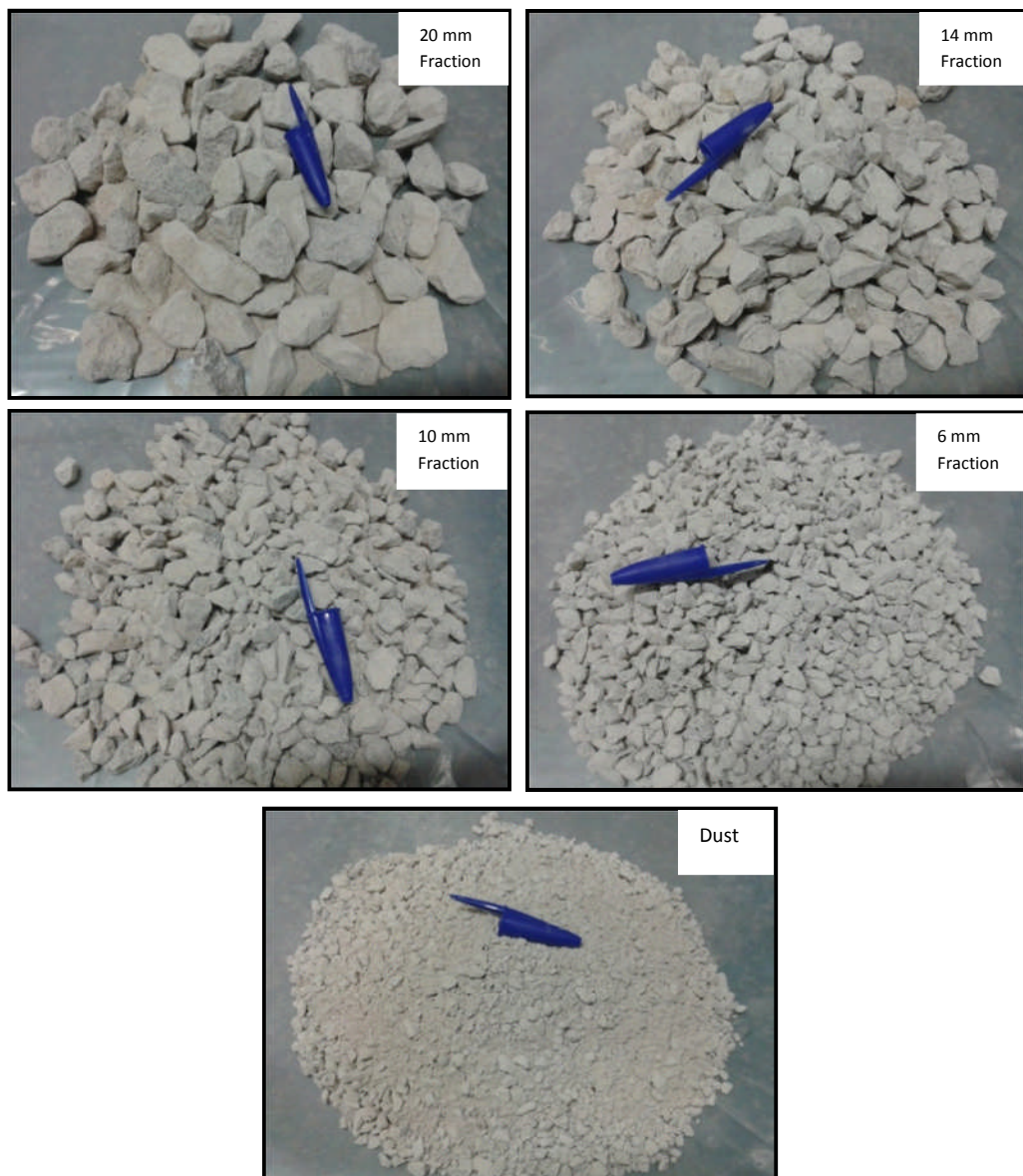


Figure 4.1: Different sizes of aggregate fractions

### 4.2.2 Crumb Rubber

The crumb rubber particles (Figure 4.2) examined in this study was sourced from J Allcock and Sons Ltd. in Manchester. It was manufactured by mechanical shredding of waste tires. It was classified as uniformly graded and angular with size ranging from 2 to 6 mm. Two reasons are behind selecting this size. Firstly, from the economic point of view, this size is cheaper and commonly available as compared with finer ones (Najim 2012). Secondly, initial examination showed that the gradation of this size is similar to that of the 6 mm natural aggregate fraction (Figure 4.1) which would be likely to enable replacement of some of the latter size without a big change in volumetric relationships of the mix. The chemical composition and physical properties of the crumb rubber is summarized in Table 4.1 and Table 4.2, respectively.



Figure 4.2: Crumb rubber appearance

Table 4.1: Chemical composition of crumb rubber (Sukontasukkul 2009)

Composition	Composition % by weight
Natural rubber	23.1
Synthetic rubber	17.9
Carbon black	28
Steel	14.5
Ash content%	5.1
Fabric, fillers, accelerators, etc.	16.5

Table 4.2: Physical properties of crumb rubber (Najim 2012)

Property	Value
Specific gravity	1.12
Apparent density	489 kg/m <sup>3</sup>
Thermal conductivity	0.11 W/k m
Tensile resistance	4.2–15 MPa
Speed of combustion	Very low
Water absorption	0.65 (negligible)
Sunlight effect	Nil
Weak acids/bases effect	Nil

### 4.2.3 Cement

The cement used in this study as a stabilizing agent is an ordinary Portland cement CEM I 52.5 N produced by CEMEX company conforming with BS EN 197-1: 2000. Some of physical and chemical properties as provided by supplier are listed in Table 4.3.

Table 4.3: Physical and chemical properties of cement

Property	Determined as
Specific gravity	3.15
Fineness	420
Oxide	Determined as (%)
SiO <sub>2</sub>	19.6
Al <sub>2</sub> O <sub>3</sub>	4.9
Fe <sub>2</sub> O <sub>3</sub>	3.1
CaO	63.1
MgO	1.2
SO <sub>3</sub>	3.4
LOI	2.7
Chloride as Cl	0.05
Alkalis as (Na <sub>2</sub> O)	0.74

### 4.3 Tests on Aggregates

#### 4.3.1 Particle size distribution

Particle size distribution for natural aggregate and crumb rubber is performed in accordance with [BS EN 933-1:2012](#) by sieve analysis through a set of sieves placed on a mechanical shaker. The gradation of each aggregate fraction is shown on Figure 4.3. It can be clearly seen from figure that, as mentioned earlier, the gradation of 6 mm is the closest size to that of crumb rubber,

#### 4.3.2 Particle specific gravity and water absorption

Specific gravity and water absorption of different aggregate fractions was estimated as outlined in [BS EN 1097-6:2000](#) and [BS EN 1097-7:2008](#) depending on aggregate size. The results are listed in Table 4.4.

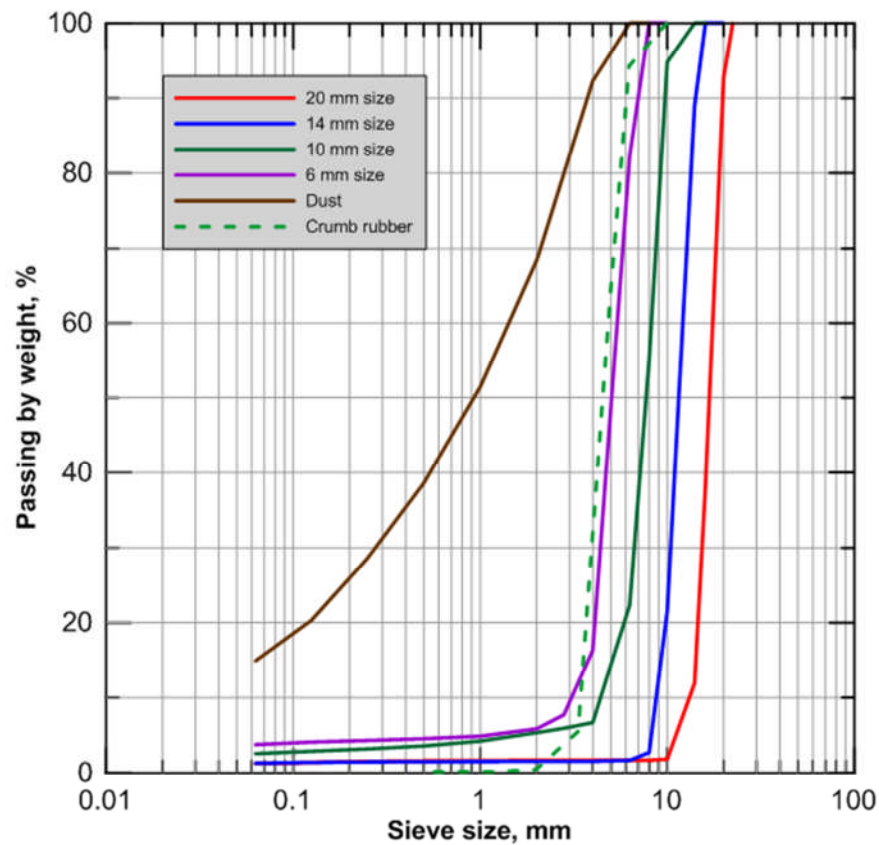


Figure 4.3: Particle size distribution of natural aggregate fractions and crumb rubber

Table 4.4: Properties of aggregate included in this study (Sunarjono 2008)

Fraction size*, mm	20	14	10	6	Dust
Dry specific gravity	2.633	2.067	2.608	2.427	2.668
Saturated surface dry specific gravity	2.653	2.634	2.640	2.526	2.674
Apparent specific gravity	2.685	2.679	2.693	2.696	2.686

- Characterized by largest size.

### 4.3.3 Aggregate surface roughness

Rubber particles were characterized to evaluate whether they possessed the required roughness to provide frictional resistance when compacted with natural aggregate.

The ability to resist applied load in this type of mixture depends to some extent on the

roughness of aggregate particles being used. Rao and Prasad (2002) claimed that the shear strength increases proportionally with increase in surface roughness of the aggregate particles. Grinys et al. (2012) pointed out the rough rubber ensures better binding with the surrounding materials and hence resist stress more effectively. However, Tasong et al. (1998) pointed out this might depend not only on the aggregate roughness alone but also on the structure and strength of aggregate particles itself. In fact, this is also the case for compacted unbound materials. For example, Pan et al. (2006) attributed the improvement in shear strength to the increase in angularity and aggregate roughness which led to better interlocking and frictional resistance. Consequently, characterization of aggregate surface roughness may provide vital information to explain the mixture behaviour and to ensure if replacement of natural aggregate with rubber will affect this property.

To this end, surface roughness of both natural aggregate and rubber was measured using a three-dimensional (3D) non-contact profilometer with laser scanner, Talysurf CLI 1000 (Taylor Hobson) at the University of Nottingham as shown in Figure 4.4. Six samples were selected randomly from the 6 mm natural aggregate and crumb rubbers. These were mounted on equipment holder then they were scanned. Two measurements were taken for each sample. The results of examined materials are summarized in Table 4.5. Results indicate that the roughness of the rubber particles is around 50% greater than that of natural aggregate. This may lead to a conclusion that, in terms of frictional resistance, rubber particles have a positive effect, being even better than natural aggregate, which should ensure good interaction with other particles when compacted. Furthermore, rough particles secure better adhesion with cement paste (fine and cement). Segre and Joekes (2000) reported that the roughness of rubber

particles has a positive effect on the mechanical properties of rubberized concrete mixtures.

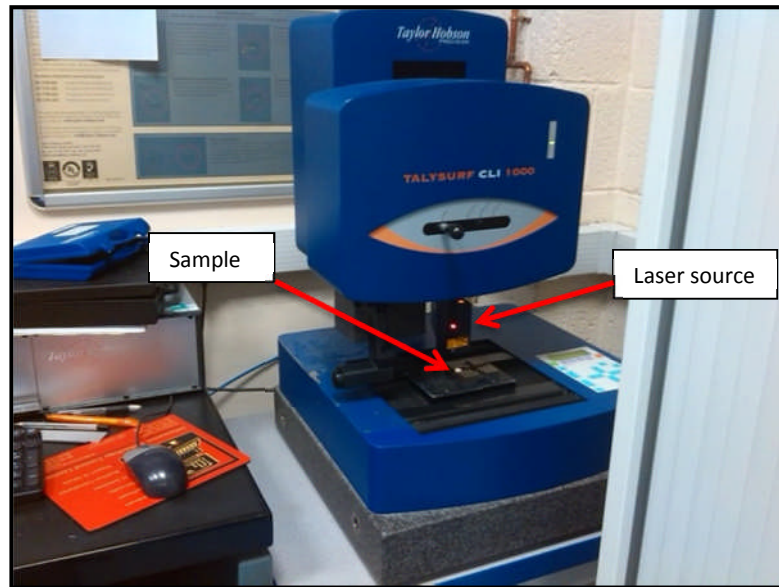


Figure 4.4: Surface roughness apparatus at the University of Nottingham

Table 4.5: Surface roughness characterization results

Particle type	Roughness (mm)						Mean	Std. Dev.	COV, %
	Sample 1		Sample 2		Sample 3				
	1	2	1	2	1	2			
6 mm natural aggregate	0.00709	0.00742	0.0094	0.00583	0.00751	0.00664	0.00816	0.00248	0.3036
Crumb rubber	0.0168	0.0152	0.0123	0.0119	0.0143	0.0234	0.01684	.00497	0.2950

#### 4.3.4 Aggregate strength and stiffness

Since the main properties that will be investigated in this research are strength and stiffness, it was desirable to evaluate the strength and modulus of elasticity of the main components of the mixture (aggregate). This will help understanding of the behaviour and failure mechanisms of the cement-stabilized mixtures. This was done as follows: firstly, large limestone blocks were brought from the same quarry that produce the different aggregate fractions used in this investigation. Then four cylindrical samples with a dimension of 37.24 mm diameter  $\times$  74.08 mm height were cored from these blocks. These were tested for unconfined compressive strength (UCS) using a RDP Stiff Testing Machine (1000 kN capacity). Axial deformation was measured via two Linear Variable Differential Transducers (LVDTs) and the average value was used to calculate strains at each load increment. Figure 4.5 illustrates appearance of aggregate cores and the UCS testing configuration.



Figure 4.5: a. Aggregate cores and b. testing set-up for UCS of aggregate

Figure 4.6 shows the stress-strain relationship of four aggregate samples. As can be seen from the latter figure, elastic moduli of the four samples are similar with marginal differences. However, UCS values had a range of 13%. This, in turn, suggests that differences in the mixtures' strength may be partially explained due to the variability of aggregate particle strength.

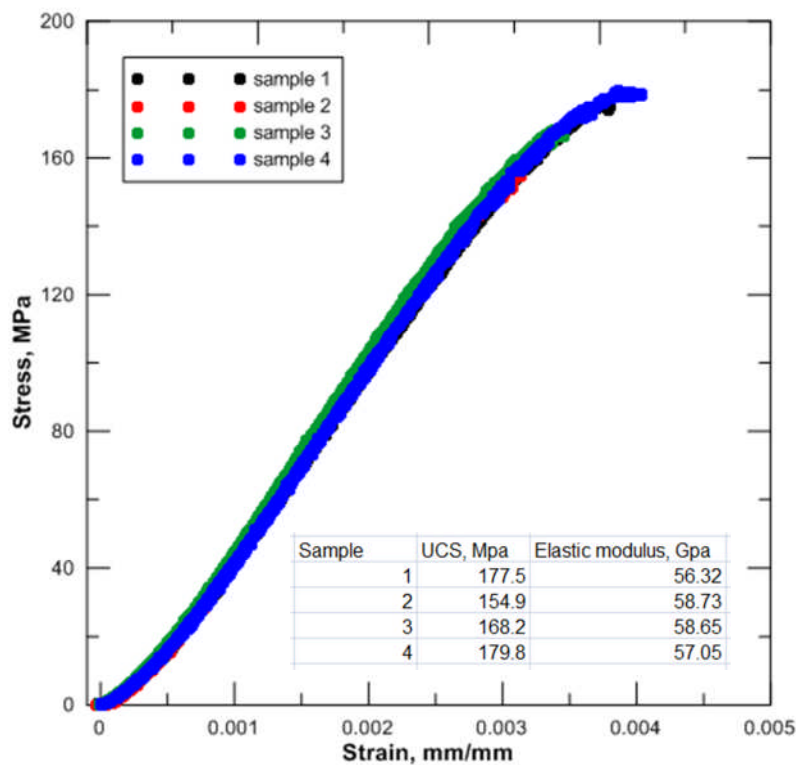


Figure 4.6: Stress-strain relationship for different aggregate samples.

#### 4.4 Mix design methodology

The gradation described in [BS EN 14227-1:2013](#) - [CBGM2-0/20] was adopted as a design gradation in this study. Different aggregate fraction sizes mentioned previously were combined together in different proportions using the trial and error method ([Garber and Hoel 2009](#)). These are 11%, 20%, 11%, 13% and 45% for 20 mm, 14mm,

10mm, 6mm and dust, respectively. The gradation of the combined aggregate in these proportions is shown in Figure 4.7.

Three cement contents were used in this study. These are 3%, 5% and 7% by the dry weight of aggregates. The first two percentages were used and reported by some authors (Shahid 1997; Wu et al. 2011) while the third level was taken to investigate the effect of high cement content.

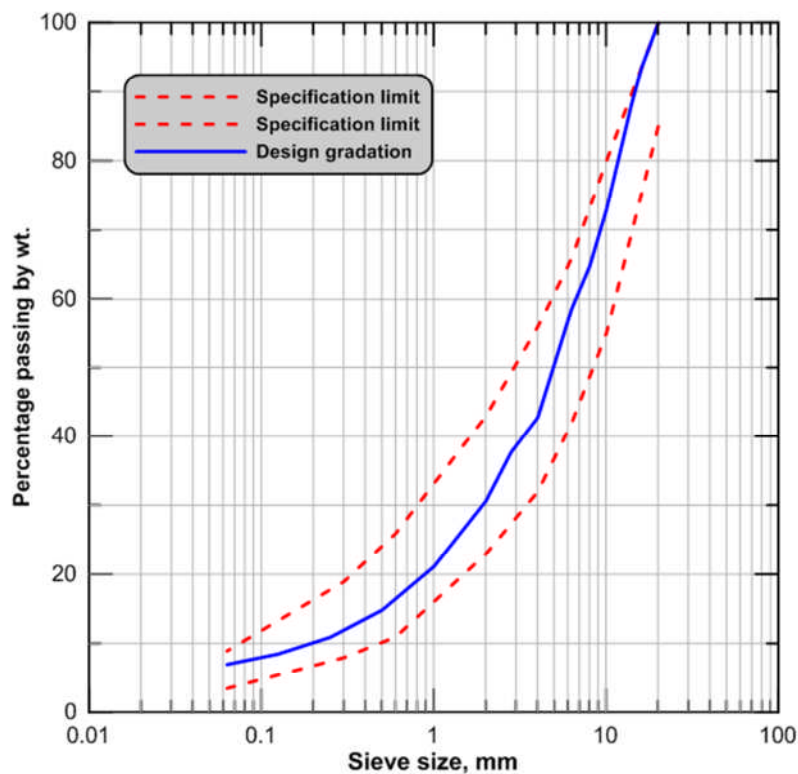


Figure 4.7: Design gradation of cement stabilized mixture used in this study

Regarding compaction method, Drnevich et al. (2007) and Chilukwa (2013) reported that vibratory compaction is the better method that simulates the field compaction which led them to recommend using this method for granular materials compaction. Furthermore, the vibratory compaction represent an effective method for compaction

the granular materials as reported by [Moore et al. \(1970\)](#). Consequently, the estimation of optimum moisture content and maximum dry density for different aggregate-cement mixtures was conducted as described in BS EN 13286-4:2003. The results are illustrated in Table 4.6.

Table 4.6: Optimum moisture contents and maximum dry densities

Cement content, %	Optimum water content, %	Maximum dry density, Kg/m <sup>3</sup>
3	4.5	2392
5	4.6	2396
7	4.7	2403

Due to the fact that aggregate gradation has an important effect on density which in turn highly affects the strength of the CBGMs ([Williams 1986](#); [Sun and Wang 2007](#)), it was decided to keep the same gradation for virgin and rubberized mixtures. This was done by volumetric replacement of the 6 mm fraction size with crumb rubber particles having a similar gradation. This in turn helps to ensure the same packing thereby making possible comparison of behaviour of mixes (as described later in this thesis) only on the basis of change to aggregate characteristics. Three replacement levels with the crumb rubber particles at 5% cement content were used, which are 15%, 30% and 45% by the volume of the 6 mm fraction size, equivalent to 2.1%, 4.2% and 6.2% of the total volume of aggregate, respectively. To produce comparable mixtures, the quantity of water and cement were kept constant for all rubber replacement levels. Maintaining a constant cement content by mass ratio would reduce the weight of cement for each replacement level when some of the aggregate was replaced by rubber of low specific gravity. As the water was computed on the basis of mass of cement plus aggregate, the mass of water would also reduce. Had this approach been adopted,

the rubber content, cement content and water content would all have changed at each replacement level at the same time. Accordingly, for each cement level, the same amount of cement and water was used as for the virgin mixtures. In other words, all volumetric proportions were kept constant for each rubberized mixture for each nominal cement content.

To evaluate the effect of cement content on the properties of rubberized mixtures, the mixture of 30% rubber content was investigated at different cement contents, as listed earlier, and the performance was compared with the same mixtures without rubber.

The investigated mixtures are tabulated in Table 4.7. The different mixtures are designated depending on the cement and rubber contents where C and R denote cement content and rubber content, respectively. For example C5R30 indicates a mixture containing 5% cement content and 30% of the 6 mm aggregate by volume, is rubber.

Table 4.7: Investigated mixtures

Cement content, % by weight of aggregate of reference mix		Rubber replacement percentages, by volume of 6 mm natural aggregate			
		0%	15%	30%	45%
3	C3R0			C3R30	
5	C5R0		C5R15	C5R30	C5R45
7	C7R0			C7R30	

#### 4.5 Samples preparation and curing

To produce comparable mixtures and hence to investigate the effect of rubber and cement only, variability due to changing aggregate gradation between different samples was eliminated by batching samples individually (Figure 4.8a). Regarding mixing sequence, cement and dust were dry-mixed firstly until a uniform color was obtained. The cement-dust mixture was added to the rest of the aggregate and mixed for one minute. After adding the appropriate water quantity, all materials were mixed thoroughly for another two minutes. All mixing was conducted manually. On completion of mixing, the mixture was compacted in three layers inside a lubricated spilt mould, with diameter of 101.6 mm, using a Kango 638 electrical vibrating hammer (Figure 4.8b) with circular tampers of 100 mm and 150 mm for cylindrical samples and a square tamper of 98 mm × 98 mm for prisms. The compaction time was 60 sec. per layer as recommended by [BS EN 13286-51:2004](#).

Past experience with testing-cement stabilized samples confirmed a very low strain level developed during testing and that there was a high sensitivity to small unevenness in the surface of the sample which, therefore, needs accurate instrumentation ([Scullion et al. 2008](#)). From the initial investigations during the course of this study, the impossibility of achieving a smooth and level surface was noticed. This made it difficult to fix the instrumentation or conducting accurate testing. To overcome this problem, it was decided to manufacture the sample to achieve about 115 mm height then trim it down to a 100 mm using a diamond saw.

Three samples were manufactured for each mix. Once the compaction was finished, specimens were left inside their moulds and covered with wet paper and polythene

sheets to prevent moisture loss. On the next day, they were demoulded and wrapped with nylon film and placed in wet polythene bags and closed tightly and left in a humid room for 28 days. Figure 4.9 illustrates the appearance of the manufactured samples.

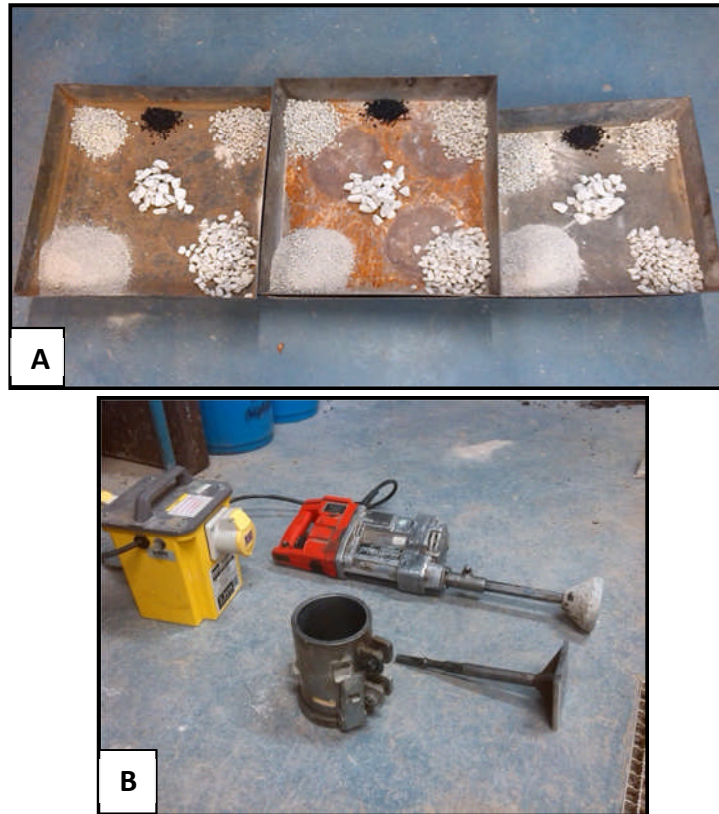


Figure 4.8: Sample preparation: a. batching aggregate for each sample and b. details of moulds and compaction equipment.

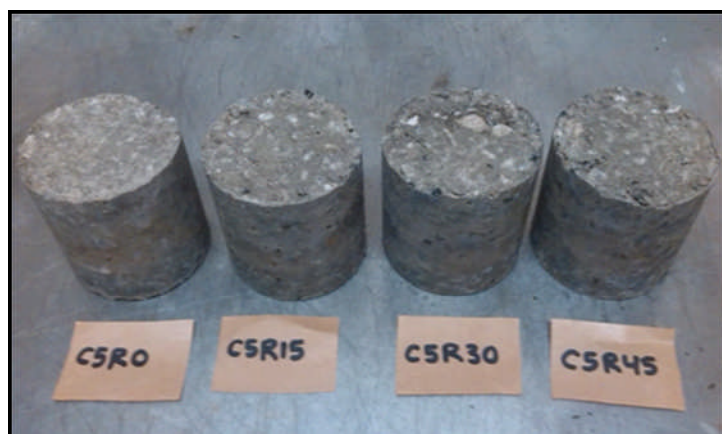


Figure 4.9: Samples appearance for different rubber contents at 5% cement.

## 4.6 Some properties related to mixture design

### 4.6.1 Bulk density determination

Density was estimated, after curing, of small cylinders, big cylinders and prisms using the water displacement method. Three samples per mixture were assessed. The test is widely used in concrete (without foil) and asphalt (with foil) technologies. It simply includes taking the sample weight in air and then in water as shown in Figure 4.10. Then the density was calculated using Equation 4.1

$$\rho_b = \frac{w_a}{w_a - w_w} \cdot 1000 \quad (4.1)$$

where

$\rho_b$ =bulk density (Kg/m<sup>3</sup>)

$w_a$  = weight of specimen in air.

$w_w$ = weight of specimen in water.

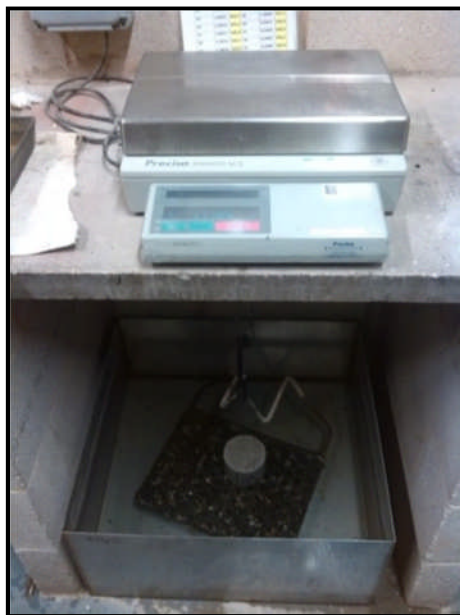


Figure 4.10: Density measurement arrangement

### 4.6.2 Compacity

The density of the compacted mixture, as stated earlier, represents an important parameter that greatly affects the final performance of the resulted mixture. [Williams \(1986\)](#) reported that a 5% decrease in mixture density causes a 40-50% decline in compressive strength of the mixture. Furthermore, [Bhandari \(1979\)](#) as reported by [Adaska et al. \(2004\)](#) claimed that there was a decrease in shrinkage tendency by more than 50% for soils compacted at modified Proctor as compared with those compacted at Proctor method. The efficiency of compaction can be checked in different ways. In asphaltic mixtures, this is done by comparing the achieved density versus the maximum theoretical density and estimating the percentage of air-voids accordingly. Maximum theoretical density can be computed simply from the density of the component materials used in the correct proportions assuming there are no air-voids. The ratio of achieved to the maximum theoretical density is known as the compacity. In soil mechanics, compaction effectiveness is judged by comparing the achieved dry density and the maximum dry density that can be achieved in ideal laboratory conditions and not to the theoretical maximum (i.e., “solid density”).

Referring to William’s conclusion, increasing density slightly will also increase material strength which means taking greater advantage of the compacted material. CSAM as a compacted material are designed and governed by the soil mechanics principles. However, the European specification ([BS EN 14227-1:2004](#)) requires that the ratio between maximum dry density and maximum theoretical dry density should be above 82%.

Two purposes are behind investigating the compacity. Firstly, to assess how the crumb rubber of high elasticity may affect the compaction efficiency and secondly to determine what the role the cements play in this process.

While specifying compacity is a useful control approach, ensuring that the required degree of particle packing has been achieved, one of its weaknesses is that it does not specify the method of laboratory compaction. There are many different suggested laboratory methods including Proctor ([BS EN 13286-2](#)), vibrocompression ([BS EN 13286-3](#)), vibrating hammer ([BS EN 13286-4](#)) and vibrating table ([BS EN 13286-5](#)). Different compaction methods have different compaction effort and may achieve different packing arrangements even when delivering the same density. This means that the compacity criterion may be satisfied for one compaction method and not for another depending on compaction effort. Even when it is achieved the mechanical response may vary depending on the method by which the specification was satisfied. Additionally, from the practical point of view, the compacity concept should be applied to the achieved dry density in the field rather than laboratory maximum dry density. This is because failing to satisfy the above condition in the laboratory does not necessarily mean failing in the field due to difference between field and laboratory compaction.

#### **4.6.2.1 Compacity by mathematical method as per BS EN 14227-1:2013**

Compacity in accordance with [BS EN 14227-1:2013](#) is defined as “the ratio of the absolute volume of the solid to apparent volume of the mixture”. This can be calculated using Equation 4.2 as recommended by the above specification.

$$C = \left( \frac{\gamma_m}{100} \right) \times \left( \frac{a}{\gamma_A} + \frac{b}{\gamma_B} + \frac{c}{\gamma_C} \dots \right) \quad (4.2)$$

where: C is the compacity factor,  $\gamma_m$  is the maximum dry density of the mixture and  $\gamma_A$ ,  $\gamma_B$ ,  $\gamma_C$ , are particle densities of material A, B and C, respectively; a, b, c represent the percentages of material A, B, C in the total mixture.

#### 4.6.2.2 Compacity by experimental method

Due to the very limited number of studies performed to evaluate the compacity of cement-bound mixtures, the applicability of estimating this property experimentally was evaluated in this study. This was done utilizing the vacuum-saturation method which is widely used to evaluate the porosity of concrete mixtures. The compacity can be calculated as (100-porosity), where porosity is expressed as a percentage. The difference between porosity calculation in concrete technology and porosity (or air-voids) in asphaltic mixture technology is that the first relies on the direct measurement of the pores using the volume of water ingressing under vacuum while, in the second, it is based on subtracting the calculated components' volumes from the whole volume of the compacted sample.

In this study, three samples were used for each mix. Specimens were dried at  $100 \pm 5^\circ\text{C}$  until constant weight was achieved then their weight was recorded. To ensure full water saturation, the dried samples were placed in a desiccator and subjected to vacuum for 4 hrs. (Figure 4.11). Then these were kept submerged in water for another 20 hrs. After that, the weights of saturated specimens in water and in air were recorded. Porosity is computed using Equation 4.3.

$$p = \frac{m_s - m_d}{m_s - m_{ss}} \times 100 \quad (4.3)$$

where

$p$  = porosity (%).

$m_s$  = mass of saturated specimen in air.

$m_d$  = mass of oven dried specimen.

$m_{ss}$  = mass of saturated specimen in water.

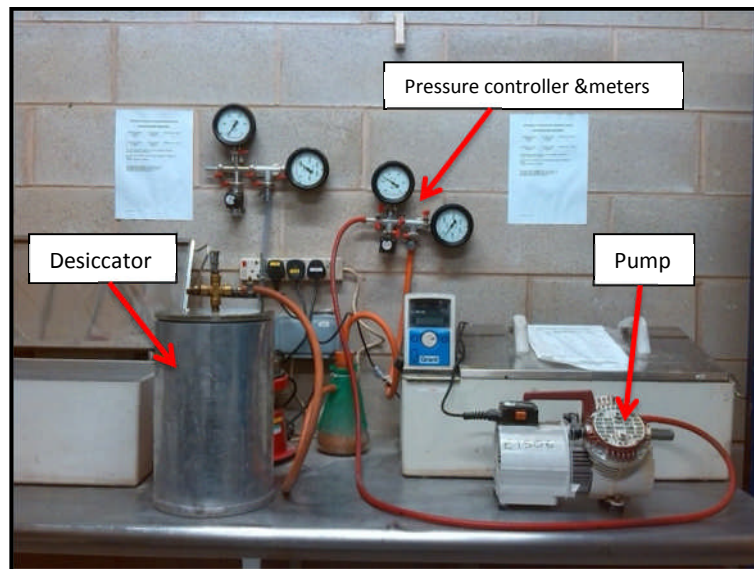


Figure 4.11: Porosity measurement arrangement

## 4.7 Results and discussion

### 4.7.1 Bulk density

Figure 4.12 and Figure 4.13 illustrate the effect of rubber replacement proportion and cement content on the density of CSAMs. Mixture density decreased by 1.097%, 2.35% and 3.885% when the 6 mm natural aggregate was replaced by 15%, 30% and

45% rubber particles, respectively as shown in Figure 4.12. As expected, replacing natural aggregate by crumb rubber caused a decrease in mixture density due to the lower specific gravity of rubber particles as compared with natural ones. On the other hand, increasing the cement content in virgin mixtures from 3% to 5% and 7% has improved the density by 0.49% and 1.11%, respectively while this enhancement is found to be 1.2% and 1.8%, respectively for the rubberized mixtures (containing 30% rubber) as illustrated in Figure 4.13. One important issue regarding using of rubber particle in compacted mixtures is that rubber particles may affect the compaction efficiency detrimentally due to the high elasticity of the rubber (causing immediate decompaction when load is removed) or the damping nature of rubber which make it act as an energy dissipation device. This in turn may be another factor that contributes to density decline.

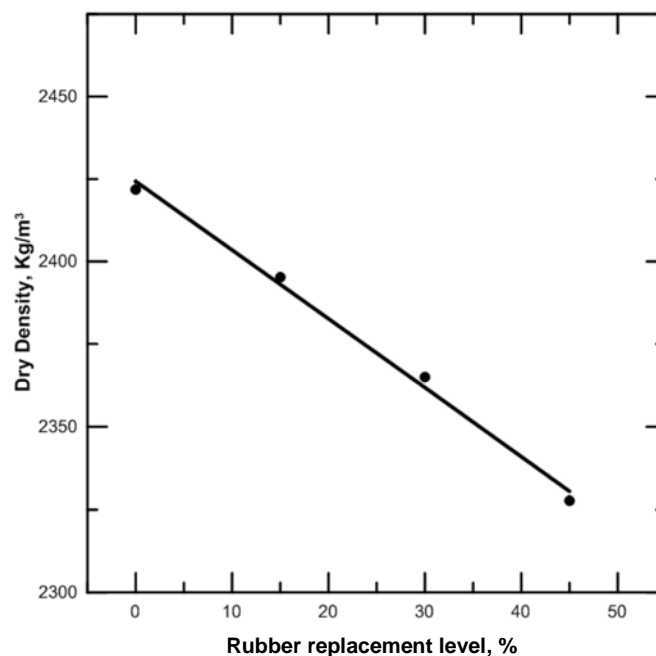


Figure 4.12: Effect of rubber content on dry density.

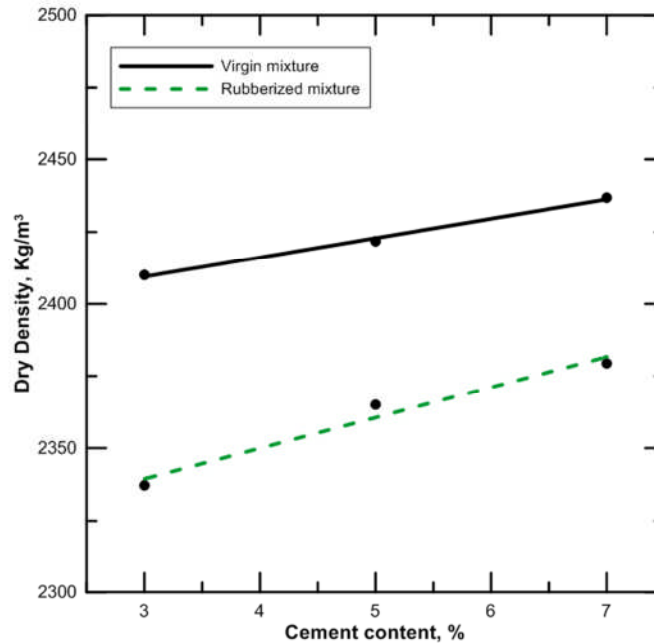


Figure 4.13: Effect of cement content on density of RCSAMs and CSAMs

## 4.7.2 Compacity

### 4.7.2.1 Effect of rubber content on the compacity of CSAMs

As can see from Figure 4.14, the maximum difference in compacity was at rubber replacement of 45% which is 0.92% reduction in the compacity of the mixture which means a decline in density. This can lead, interestingly, to the conclusion that not only the low specific gravity of rubber is responsible for density reduction, but the reduction of compaction efficiency, due to the damping effect or elastic rebound of the rubber particles, is also affecting the density of the mixture negatively. The practical consequence of the latter findings is to avoid rubber replacement with high volumetric ratios.

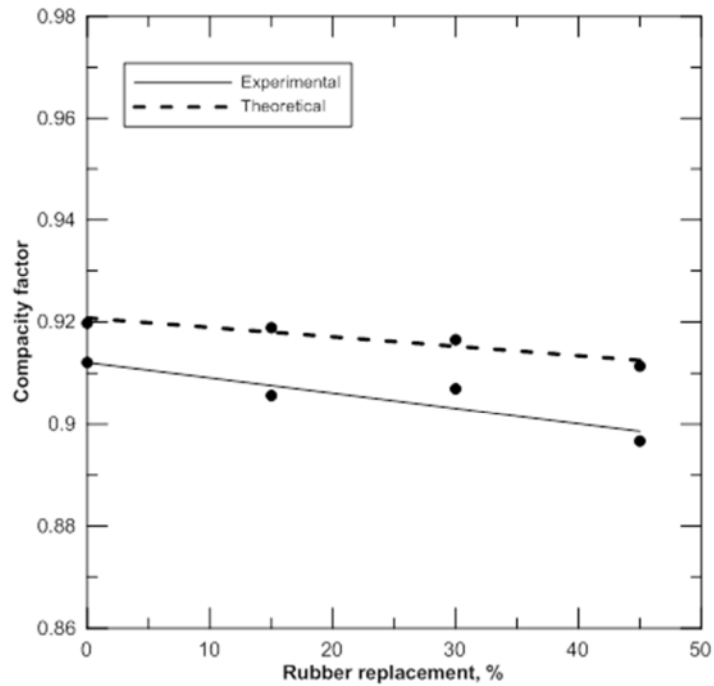


Figure 4.14: Effect of rubber content on compacity value.

#### ***4.7.2.2 Effect of cement content on the compacity of CSAMs and RCSAMs***

Referring to Figure 4.15 we can infer that increasing cement content has improved the compacity of both CSAMs and RCSAMs. However, this enhancement is more obvious in RCSAMs especially in the case of increasing cement from low to medium contents where the compacity was increased by 1.1% versus about 0.5% in the case of virgin mixtures. In other words, the largest drop in compacity due to rubber inclusion was observed at low cement content. This may be because of damping effect of rubber is more active in case of low cement content. After 5% cement content usage, the difference in compacity due to rubber inclusion becomes constant.

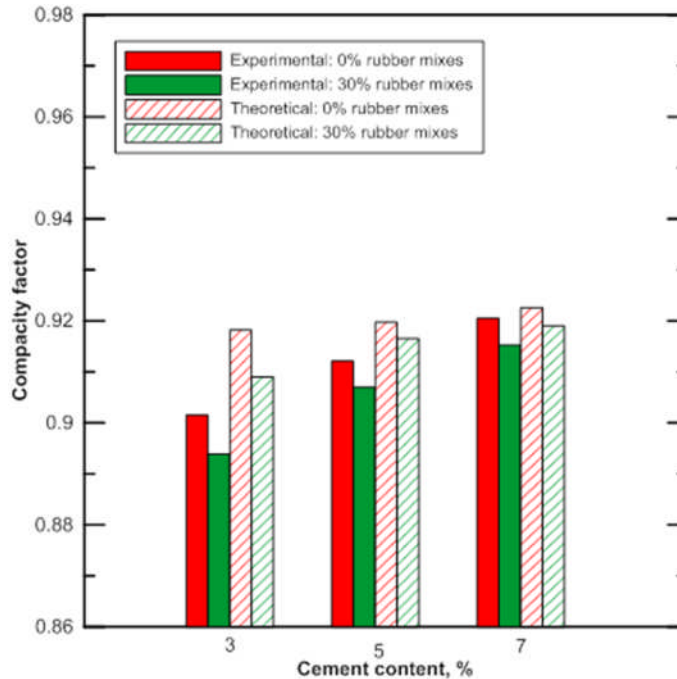


Figure 4.15: Effect of cement content on compacity value of RCSAMs and CSAMs.

#### 4.7.2.3 Comparison between theoretical and experimental procedures

It can be concluded, from the latter two figures that at low cement contents, there is a difference between theoretical and experimental procedures. Compacity, calculated experimentally based on porosity, includes the inter-particles voids, voids in cement paste (fines plus cement) and voids in aggregate particles themselves. In spite of allowing for occluded voids in the aggregate by using apparent specific gravities to calculate aggregate volume, some differences are still exist. This is because the volume of water-accessible voids during the porosity procedure is greater than that estimated based on particle density test, since the former was conducted under vacuum while the latter is normally performed under immersion. This makes more water volume penetrate inside the aggregate particle under vacuum which means a greater estimate of volume of accessible voids. The latter voids will make that difference especially for

aggregate of high porosity (e.g. many recycled aggregates). The compacity, from a technical point of view, represents the inter-particles voids which describe the compaction efficiency as it is impossible to eliminate aggregate voids.

At high cement levels, on the other hand, the calculated compacity approaches the one estimated experimentally. The reason behind this can be explained as follows: when aggregate, cement and water are mixed together and compacted by vibrating hammer, the water and the fine particles (including cement) will penetrate and make a film around the aggregate particles. This contributes in making the aggregate particles less affected by the water during the vacuum saturation process. The above mechanism is illustrated in Figure 4.16. Another possible factor that may have a positive role in preventing water to ingress into aggregate particles is the features of the matrix surrounding the aggregate particles, which may have less porosity due to its high cement content. Based on the above results and their analysis, it can be said that the vacuum saturation is unsuitable to estimate compacity of the mixtures at low and moderate cement contents.

The author believes that the experimental vacuum porosity procedure can be used indirectly to evaluate the bond strength between aggregate particles and surrounded matrix. This is because the existence of enough cement content to penetrate open voids in aggregate particles and to form a film around the aggregate particle will reduce (or may prevent) water ingress during vacuuming and at the same time will secure a good bond strength. This hypothesis will be examined in the following chapters.

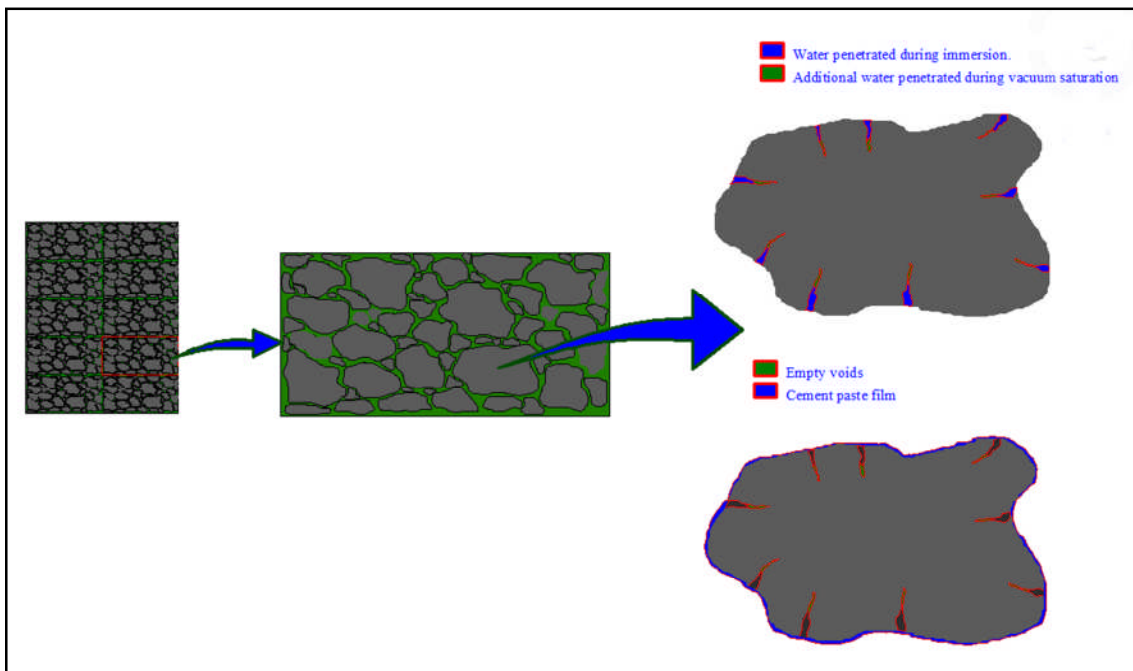


Figure 4.16: Mechanism of water penetration and cement paste film coating

#### 4.8 Concluding remarks

1. High roughness of rubber as compared with natural aggregate may ensure good interaction and adhesion with cement matrix. Consequently, replacement with rubber will not affect the frictional resistance of the compacted mixtures.
2. It is observed, in the range of tested aggregate cores, that some variability in the strength of the aggregate mineral may justify the difference in mixture strength. However, little variability was obtained in the modulus of elasticity of aggregate cores.
3. Adopting weight proportioning in the mixtures containing light particles like rubber is a misleading approach which can cause change in all the mixture component proportions at the same time. Accordingly, it is recommended to

replace on a volumetric basis when replacing materials with different specific gravities.

4. The reduction in density of RCSAMs is partly due to the low specific gravity of rubber and partly due to reduction in the compaction efficiency due to rebound and damping effects of crumb rubber particles.
5. In the range of investigated mixtures, estimation of compacity based on vacuum-saturation procedure adopted in concrete mixtures is found to be unsuitable for the mixtures containing low cement contents due to penetration of water inside aggregate particles during vacuuming. This could overestimate the porosity and hence the compacity of the mixtures. However, this overestimation degree reduced in the mixture with high cement content since these will have a film around aggregate particles as well as having a dense cement matrix.
6. Cement has a positive effect on compacity of the mixtures which indicates that the cement strengthening mechanism comes from an increase in binding materials and at the same time from the density improvements by the pore filling effect.

## 4.9 References

- Adaska, W. S., D. R. Luhr, C. Petit, I. Al-Qadi and A. Millien (2004). Control of reflective cracking in cement stabilized pavements. Fifth International RILEM Conference on Reflective Cracking in Pavements, RILEM Publications SARL.
- Chilukwa, N. N. (2013). Vibratory hammer compaction of granular materials, Stellenbosch: Stellenbosch University.
- Drnevich, V. P., A. C. Evans and A. B. Prochaska (2007). "A Study of Effective Soil Compaction Control of Granular Soils."
- Garber, N. J. and L. A. Hoel (2009). Traffic & highway engineering, Cengage Learning.
- Grinys, A., H. Sivilevičius and M. Daukšys (2012). "Tyre rubber additive effect on concrete mixture strength." *Journal of Civil Engineering and Management* 18(3): 393-401.
- Moore, R. K., T. W. Kennedy and W. R. Hudson (1970). "Factors affecting the tensile strength of cement-treated materials." *Highway Research Record*(315).
- Najim, K. B. (2012). Determination and enhancement of mechanical and thermo-physical behaviour of crumb rubber-modified structural concrete. PhD thesis, The University of Nottingham.
- Pan, T., E. Tutumluer and J. Anochie-Boateng (2006). "Aggregate morphology affecting resilient behavior of unbound granular materials." *Transportation Research Record: Journal of the Transportation Research Board* 1952(1): 12-20.
- Rao, G. A. and B. R. Prasad (2002). "Influence of the roughness of aggregate surface on the interface bond strength." *Cement and Concrete Research* 32(2): 253-257.
- Scullion, T., J. Uzan, S. Hilbrich and P. Chen (2008). "Thickness Design Systems for Pavements Containing Soil-Cement Bases." *PCA R&D Serial*(2863).

Segre, N. and I. Joekes (2000). "Use of tire rubber particles as addition to cement paste." *Cement and Concrete Research* 30: 1421±1425.

Shahid, M. A. (1997). "Improved Cement Bound Base Design for Flexible Composite Pavement." PhD Thesis, University of Nottingham.

Sukontasukkul, P. (2009). "Use of crumb rubber to improve thermal and sound properties of pre-cast concrete panel." *Construction and Building Materials* 23(2): 1084-1092.

Sun, R.-s. and S.-y. Wang (2007). "Research on Fatigue Performance of the Different Gradation of Cement Stabilized Crushed Stone [J]." *Journal of Highway and Transportation Research and Development* 6: 013.

Sunarjono, S. (2008). "the influence of foamed bitumen characteristics on cold-mix asphalt properties." PhD Thesis, University of Nottingham, Department of Civil Engineering.

Tasong, W., C. Lynsdale and J. Cripps (1998). "Aggregate-cement paste interface. II: Influence of aggregate physical properties." *Cement and Concrete Research* 28(10): 1453-1465.

Williams, R. I. T. (1986). "Cement-treated pavements : materials, design and construction " Elsevier Applied Science.

Wu, P., A. Molenaar and I. L. Houben (2011). Cement-bound road base materials, Report 7-11-218.

## **Specifications**

BS EN 197-1: 2000, Cement- Part 1: Composition, specifications and conformity criteria for common cement, British Standards Institute

BS EN 933-1:2012, Tests for geometrical properties of aggregate- Part 1: Determination of particle size distribution-Sieving method

BS EN 1097-6:2000, Tests for mechanical and physical properties of aggregates- Part 6: Determination of particle density and water absorption

BS EN 1097-7:2008: Tests for mechanical and physical properties of aggregates- Part 7: Determination of particle density of filler

BS EN 14227-1:2013, Hydraulically bound mixtures-specification, Part 1: cement bound granular mixtures, British Standards Institution, London

BS EN 13286-51:2004, Unbound and hydraulically bound mixtures- Part 51: Methods for the manufacture of test specimens of hydraulically bound mixtures using vibrating hammer compaction

BS EN 13286-2:2004, Unbound and hydraulically bound mixtures- Part 2: Methods for the determination of the laboratory reference density and water content-Proctor compaction

BS EN 13286-3:2003, Unbound and hydraulically bound mixtures- Part 3: Methods for Laboratory reference density and water content-Vibrocompression with controlled parameters

BS EN 13286-4, Unbound and hydraulically bound mixtures- Part 3: Methods for Laboratory reference density and water content-Vibrating hammer.

BS EN 13286-5, Unbound and hydraulically bound mixtures- Part 3: Methods for Laboratory reference density and water content-Vibrating table.

## **Chapter Five**

### **Behaviour under unconfined compressive and indirect tensile testing**

#### **5.1 Introduction**

Even though highway pavement layers are subjected to dynamic loads, investigating the properties in terms of static testing still represents an important approach which indeed helps to predict mixtures' behaviour under dynamic loads. From the point of view of equipment availability and their cost, the machines used for static testing are normally available and relatively cheap as compared with those used for dynamic testing. The latter testing is basically complicated and needs a professional person to

conduct the test and interpret the results which in turn means more time and cost; something that may be not available due to project size or limited funds. That is why the mechanistic-empirical pavement design guide (MEPDG) uses a three-level approach for material properties necessary for pavement analysis and design (Applied Research Associates 2004). In that guide, Input Level 3 uses default values for these properties. Input Level 2, on the other hand, utilizes the relationship between complicated properties and the most available and simple test such as UCS. Finally, at Level 1 the input properties can be measured experimentally and used for design purpose directly.

The main focus of this chapter is to perform a laboratory study to evaluate the mechanical properties of mixtures containing different rubber and cement contents under monotonic loading and to identify to what extent the aggregate composition and degree of stabilization affect the relationship between different parameters. This was performed in terms of unconfined compressive strength (UCS), indirect tensile strength (ITS), indirect tensile static modulus ( $E_{it}$ ), and toughness from indirect tensile load-deformation curves. In addition, the dynamic properties were also investigated under cyclic indirect tensile testing. This approach is important since it enables comparison with the properties of other cementitious materials such as rubberized concrete mixtures since the latter is normally evaluated by some of the above methods. Finally, due to the fact that CSAMs containing different rubber and cement contents would represent a range of aggregate composition and cementation levels, the established correlation would, in turn, cover a wide range of material combinations and permit estimation of different parameters from simple tests.

## 5.2 Materials, mixture design and samples preparation

Materials, mix design and all preparation steps were kept as previously discussed in Chapter 4. However, another set of samples was manufactured to evaluate the compressive stress-strain relationship using standard split moulds of 150 mm diameter and 300 mm height. All mixing was conducted using a Pancrete mixer of 0.1 m<sup>3</sup> capacity. Compaction was conducted utilizing a vibratory compactor attached to a 150 mm diameter tamper. As stated in Chapter 4, initial investigation showed the impossibility of achieving a level surface to ensure accurate testing. Therefore, a removable mould extension was fabricated and used to ensure achieving more than 300 mm height which was then sawn down to a height of 300 mm using a diamond saw. Three samples were manufactured for each mix. Once the compaction was finished, specimens were left inside their moulds and covered with wet paper and polythene sheets to prevent moisture loss. On the next day, these were demoulded and wrapped with nylon film and placed in wet polythene bags and closed tightly and left in a humid room for 28 days. Figure 5.1 shows the manufactured samples and their curing. In addition, small prisms were also manufactured as discussed later in Chapter 6.



Figure 5.1: Large cylinders (> 300 mm height); b. samples curing.

### 5.3 Experimental Procedures

#### 5.3.1 Unconfined Compressive Strength (UCS) Testing

[BS EN 13286-41:2003](#) was adopted throughout this project to assess unconfined compressive strength (UCS). A 2500 kN testing machine was used as shown in Figure 5.2. Three cylindrical samples with dimension of 100 mm dia. x 100 mm height were manufactured in accordance with [BS EN 14227-1:2013](#) for each mixture and the average value was recorded as an UCS. When any reading differed from the average by 20%, this reading was discarded and the average of other two was adopted ([BS EN 14227-1:2013](#)). The UCS values were computed from the following equation:

$$\text{UCS} = \frac{P}{A} \quad (5.1)$$

Where

P= ultimate compressive failure load, N

A= cross sectional area of the sample, mm<sup>2</sup>

#### 5.3.2 Compressive stress-strain relationship

This test was conducted on large cylinders of 150 mm diameter x 300 mm height in accordance with [BS EN 14227-1:2013](#). Regarding the axial deformation measurement, this was conducted firstly using four linear displacement Potentiometers (LDPs) and secondly using four LVDTs. These were fixed to studs glued on the surface of the sample. This gluing was preceded by a preparatory step to ensure the verticality and horizontality of these instruments. Test setups and preparation steps are shown in Figure 5.3. In spite of the great care taken in test setup

preparation, large differences were obtained from the four LDPs and LVDTs readings. This may be attributed to the cracking underneath the LVDT studs which caused detachment of the LVDTs which in turn caused a difference in reading especially in this type of material where the developed strain is small.



Figure 5.2: UCS testing machine used in this study.

To overcome this problem, it was decided to use a non-contact method to measure the axial deformation along the sample. To this end, a video gauge camera manufactured by Imetrum<sup>®</sup> Company limited was used for that purpose. This technique relies on an image processing principle by tracking specific points, previously defined, using the machine software, on the specially prepared surface. With this measurement technique it was decided to use prismatic samples since tracking the target on a flat surface is more accurate and easier than on the curved surface of a cylinder. The testing was conducted as follows: Firstly, the samples were prepared by painting the surface to be monitored with a white paint; then a little

spray with black paint was performed. So, the final face comprised black dots on a white background. This facilitates tracking during the test. Then, the sample was placed and aligned between testing platens and a lamp was placed in front of the sample to ensure a bright surface. Afterward, the camera was fixed in front of the prepared surface in such a way that ensures display of the prepared face. An Instron machine 8500 with a capacity of 2000 kN was used to test the samples. To investigate the post-peak behaviour, the test was performed in deformation control mode at a rate of 0.5 mm/min. Figure 5.4 shows the test setup and the different preparation steps.

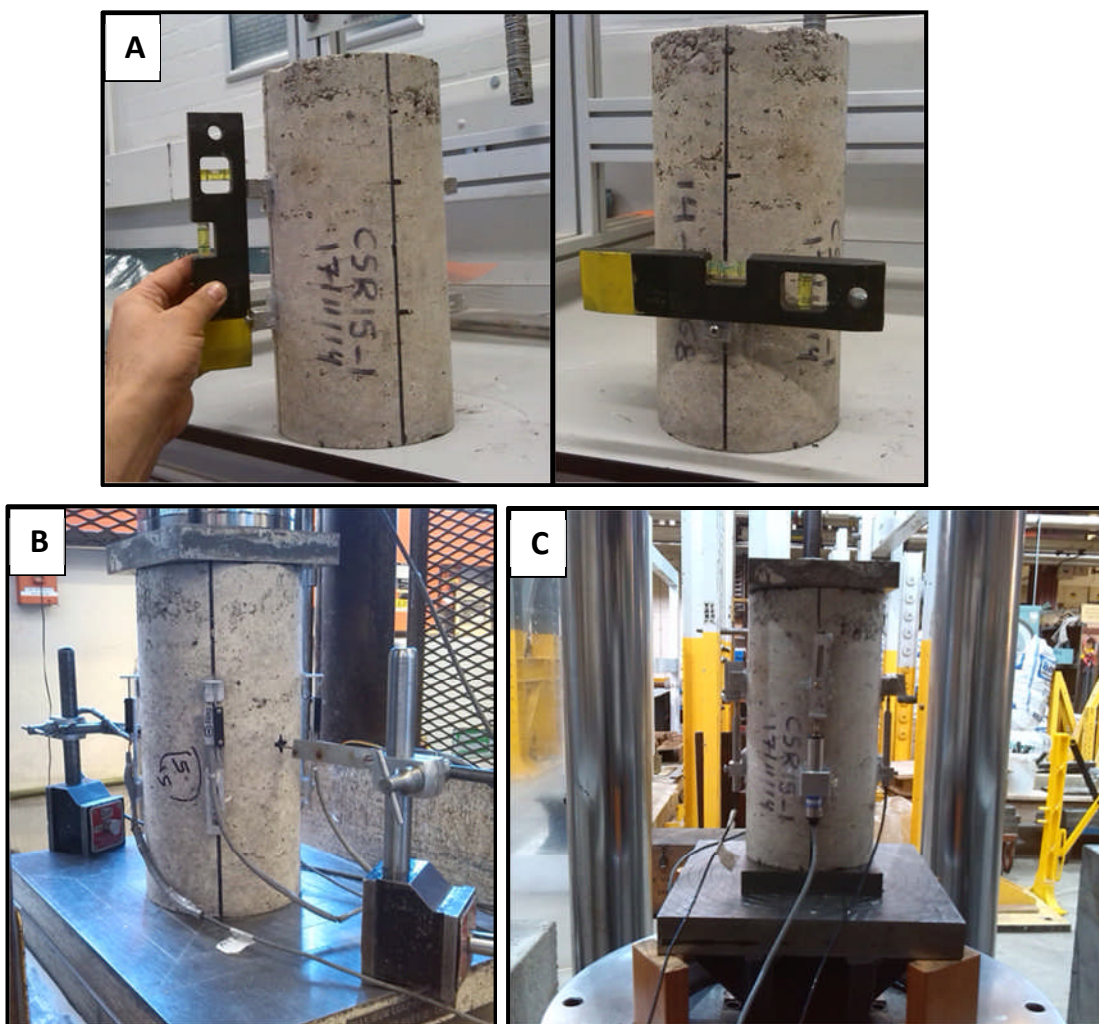


Figure 5.3: Sample preparation and instrumentation setup: a. checking instrumentation alignment; b. LDPs setup and c. LVDTs setup

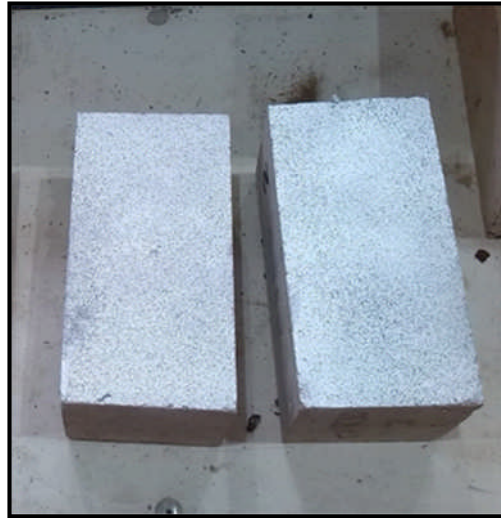


Figure 5.4a: Preparations for test face of samples for video gauge testing.

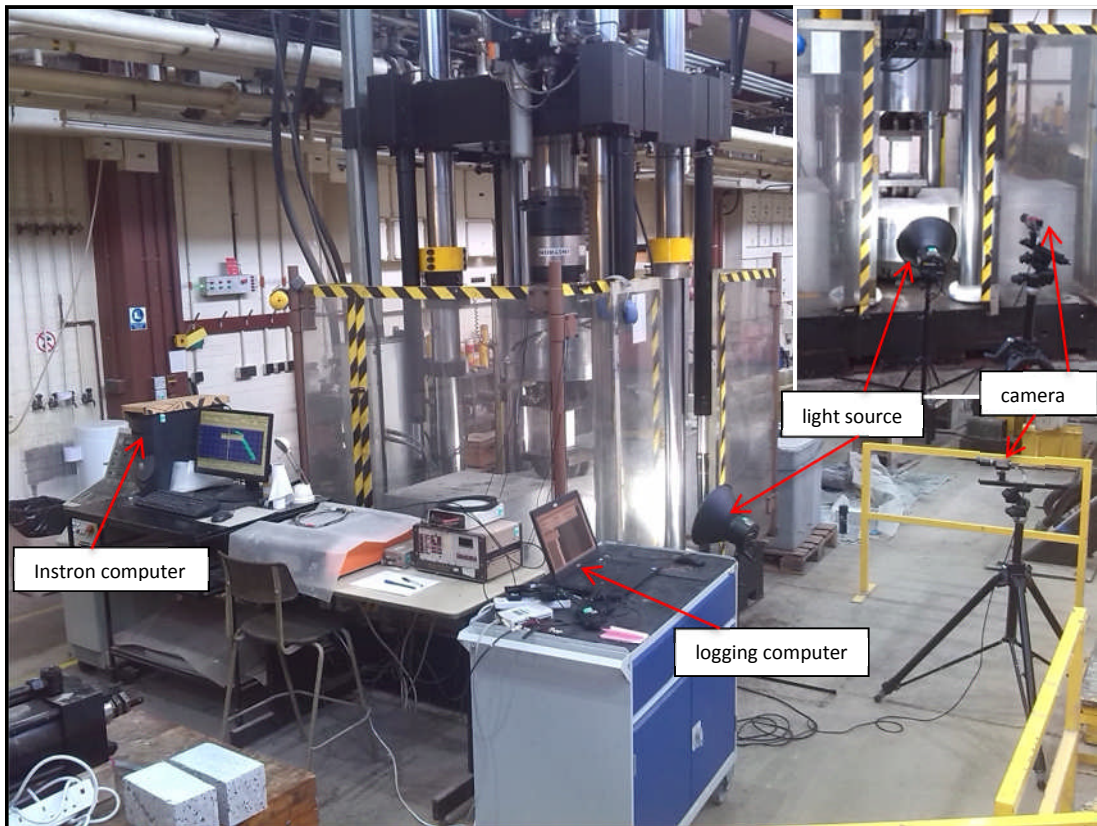


Figure 5.4b: Instron machine and test configuration used for compressive test with video gauge

### 5.3.3 Static indirect tensile testing

BS EN 13286-42:2003 was adopted for indirect tensile strength (ITS) assessment by applying compressive load diametrically to the test cylinders. A 200 kN Instron testing machine was used. The testing machine and the test arrangement is depicted in Figure 5.5. Three cylindrical samples with dimensions of 100 mm dia. x 100 mm height were manufactured in accordance with BS EN 14227-1:2013 for each mixture and the average value was recorded as an ITS. When any reading differed from the average by 20%, this reading was discarded and the average of the other two was adopted (BS EN 14227-1:2013). The indirect tensile strength (ITS) was calculated using the following equation:

$$\text{ITS} = \frac{2P}{\pi hd} \quad (5.2)$$

Where

P= failure load, N

h= thickness of specimen, mm

d= diameter of specimen, mm



Figure 5.5: Instron machine and configuration used for indirect tensile testing.

### 5.3.3.1 Indirect tensile static modulus

Modulus is normally measured jointly with the ITS value to classify a cement-bound mixture as specified in [BS EN 14227-1:2013](#). This was performed in parallel with the ITS test in accordance with [BS EN 13286-43:2003](#) by measuring the lateral deformation of the samples for each load application. In the latter specification, the static modulus of elasticity should be computed based on 30% of ultimate indirect tensile load and its corresponding lateral deformation. However, estimating modulus of elasticity utilizing the formula provided in the latter specification would give inaccurate results since this formula is derived and used for a specific LVDTs arrangement in which both LVDTs are mounted diametrically opposite to each other (i.e., gauge distance equal to diameter of sample). Accordingly the following formula was used as provided by [Solanki and Zaman \(2013\)](#)

$$E_{it} = \frac{2P}{\pi \cdot d \cdot t \cdot \Delta H_T (D^2 + D_g^2)} \left\{ (3 + \nu) D^2 \cdot D_g + (1 - \nu) \left[ D_g^3 - 2D(D^2 + D_g^2) \tan^{-1} \left( \frac{D_g}{D} \right) \right] \right\} \quad (5.3)$$

Where  $P$  = load;  $d$  = diameter of sample;  $t$  = sample thickness;  $\Delta H_T$  = lateral deformation;  $D_g$  = LVDTs gauge distance and  $\nu$  = Poisson's ratio

#### 5.3.3.1.1 Deformation measurement setup development

The LVDTs used in this study are DC type energized by two transducer indicator E309 units manufactured by RDP Electronics Ltd. These instruments were connected to the internal data logger of the testing machine to log data at a frequency of 10 Hz.

Past experience with testing of cement-stabilized samples has revealed a very low strain level developing during testing and high sensitivity to the small unevenness which needs accurate instrumentation ([Scullion et al. 2008](#)). Accordingly, two methods were attempted to measure the lateral deformation of the sample. The first method is by fixing two LVDTs diametrically using external magnetic stands as shown in Figure 5.6. This method gave inconsistent results due to sliding of the LVDT's tips which resulted from the rocking of the specimen during the test. Therefore, a new measurement setup method was developed during the course of this study to accurately measure the lateral deformation. This was done by gluing two LVDTs on both surfaces of the sample through two aluminium holders manufactured for that purpose. Another problem affecting the accuracy of measurement is the difficulty in aligning the four LVDT holders on the sample faces. This problem was also raised by [Wen Haifang \(2014\)](#) in [NCHRP report 789](#). To overcome this problem, they recommended using a gluing jig to ensure parallelism and precise alignment of the LVDTs' blocks. In this study, a gluing jig was manufactured as shown in Figure 5.7. This consists of two wooden plates to be placed at the sample's top and bottom with a circular groove at the plate centre to accommodate the sample ends. At the centre of each groove, a rectangular hole of width equal to the width of the LVDT holder was drilled. To ensure parallelism of these two holes at the top and bottom of the sample, another four circular holes were drilled in each plate in such a way as to ensure the four holes of the top plate coincide with those of the bottom one and, thus, the two rectangular holes. On mounting the sample on the bottom plate, the top plate was placed and the four long screws were tightened with the ends at the eight circular holes (Figure 5.7 and Figure 5.8). After that a gluing gun was used to glue the LVDT blocks to the surfaces of the sample.

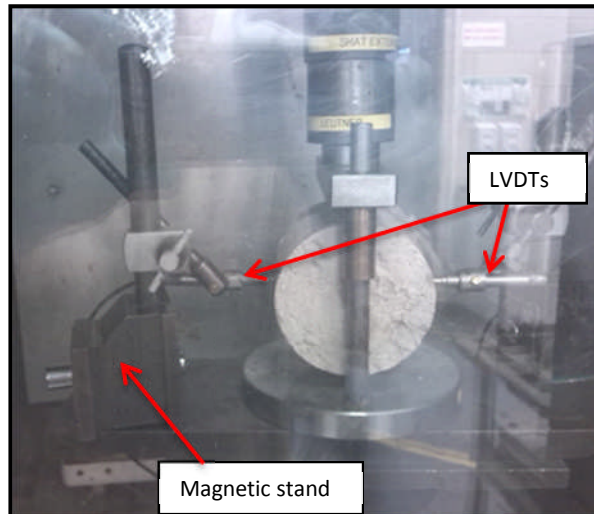


Figure 5.6: Trial arrangement for lateral deformation measurement.

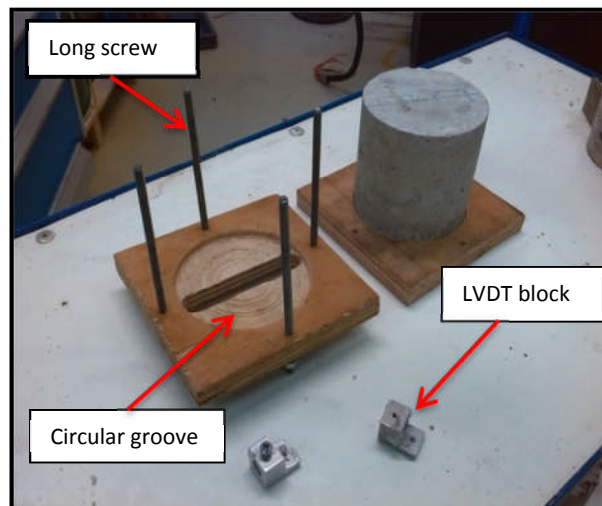


Figure 5.7: Manufactured gluing jig parts

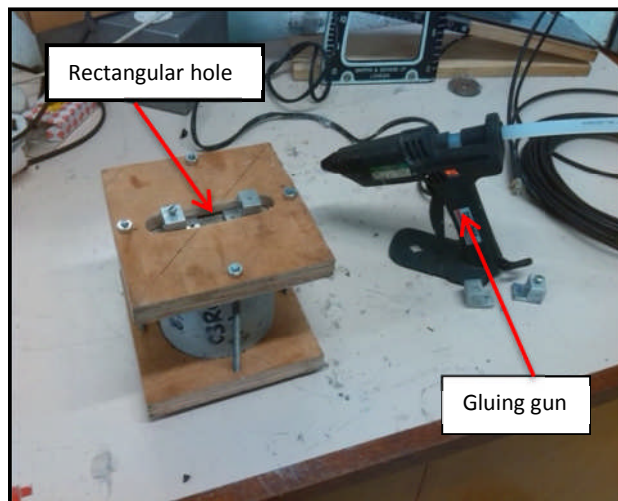


Figure 5.8: Fixing LVDTs holders through the new instrumentation setup

### 5.3.3.2 Toughness based on indirect tensile testing

Toughness is an important material property. This is because it relates to the energy absorbency which reflects the material's ability to resist fracture under monotonic, cyclic or impact loading (Shahid 1997; Liu 2013). To obtain the post-peak load-deflection behaviour and hence quantify toughness of the material, the ITS test was performed at a deformation rate of 0.5 mm/min. The corresponding deflection was measured as mentioned earlier. To evaluate the post-peak loading bearing capacity enhancement, the area under the load-deformation curve can be used to compute the toughness or energy absorption capacity of the material. The estimation of toughness in this manner may include the improvement in strength and ductility due to rubber incorporation as stated by Sobhan and Mashnad (2000). However, due to the reduction in the strength of the mixture as a result of rubber inclusion, it is necessary to normalize the load to its ultimate value to evaluate the enhancement in terms of ductility only. This is also logical since in mechanistic pavement design the stress is usually normalized with respect to the strength and the stress ratio is normally used.

The methodology used by Huang et al. (2005) and Modarres (2013) was adopted to calculate toughness indices from the indirect tensile normalized load-deformation curves as follows

$$\text{Toughness index} = \frac{A_D - A_p}{D - D_p} \quad (5.4)$$

where  $A_D$  and  $A_p$  are the areas under the normalized load-deformation curve up to a specific deformation ( $D$ ) and deformation at peak load ( $D_p$ ), respectively. The former deformation is larger than the latter. For comparable results, toughness indices for all

mixtures were calculated at the same deformation (Huang et al. 2005). This was 1.2 mm which was selected on the basis that all mixtures reached this deformation value after their failure and hence this permits comparison between load-carrying capacities after failure. However, the C7R0 showed very slight deformation after ultimate load i.e., much less than 1.2 mm, which made it incomparable with the other mixtures and it is therefore a brittle mixture. Even though this mixture could have been tested at a lower loading rate which would probably increase its apparent toughness, this would also affect its indirect tensile strength value. Moreover, to make a meaningful comparison between different mixtures, it is necessary to test all of them at the same loading rate.

### **5.3.3.3 Quantification of damage through fractal analysis**

To provide a better understanding of the mechanism of failure for this type of mixture, the failure cracking pattern was characterized quantitatively using fractal analysis. This technique has been extensively used in normal concrete to quantify cracking patterns (Erdem et al. 2012; Farhidzadeh et al. 2014) and fractured surfaces (Issa and Hammad 1994; Carpinteri et al. 1999; Guo et al. 2007). However, no published study was found in the literature regarding the quantification of surface cracks of cement-stabilized mixtures using fractal analysis. In this study, the fractal analysis was performed in terms of the fractal dimension. In addition, the cracking density was also estimated to evaluate the crack separation.

### 5.3.3.3.1 Fractal dimension

In the current study, fractal dimension was estimated using the box-counting method (Mihashi et al. 2006; Erdem and Blankson 2013). An initial investigation performed to extract topological information concerning the cracked area using image processing software, ImageJ, had difficulty in differentiating between the cracks and the rubber particles utilizing a grey thresholding process. For this reason it was decided to digitize the crack network using the following procedure: Images of failed samples were firstly captured using a high resolution camera. These images were inserted into a computer aided design (AutoCAD) software and scaled up to reflect the actual dimensions. The cracks were digitized after that using the software tools. Then, these were covered by imaginary meshes with rectangular grid sizes decreasing step-wise linearly. Then the number of grid squares required to cover the cracks was counted at each step. Finally, the fractal dimension was computed from the slope of the line joining the logarithm of the number of grid squares encountered by the crack and the logarithm of the grid square dimension. Figure 5.9 illustrates fractal dimension estimation methodology alongside with failure patterns of the mixtures containing different rubber contents while Figure 5.10 shows the typical determination of the value of fractal dimension.

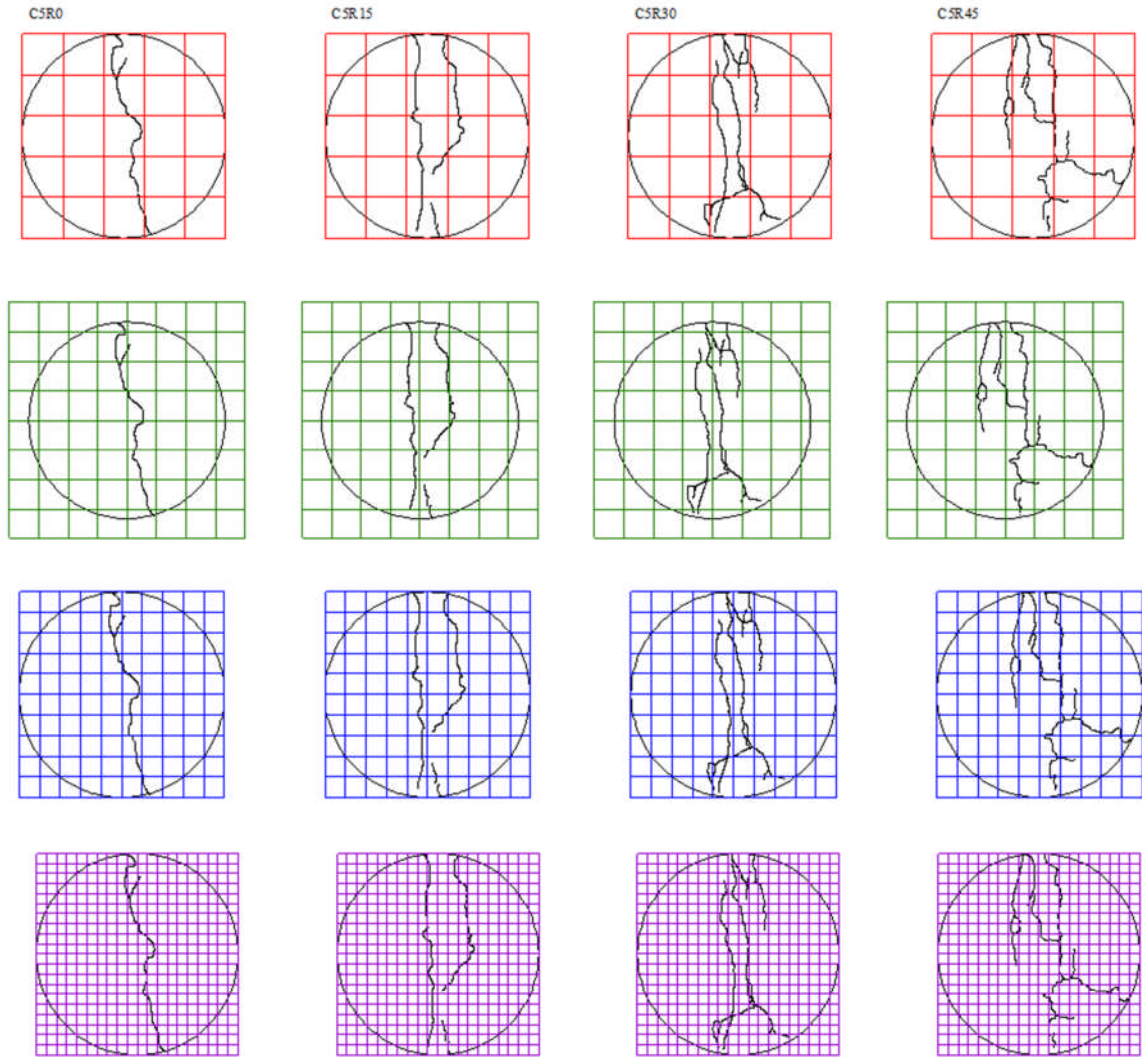


Figure 5.9: Sample cracking pattern traced from failed samples showing application of box counting methodology

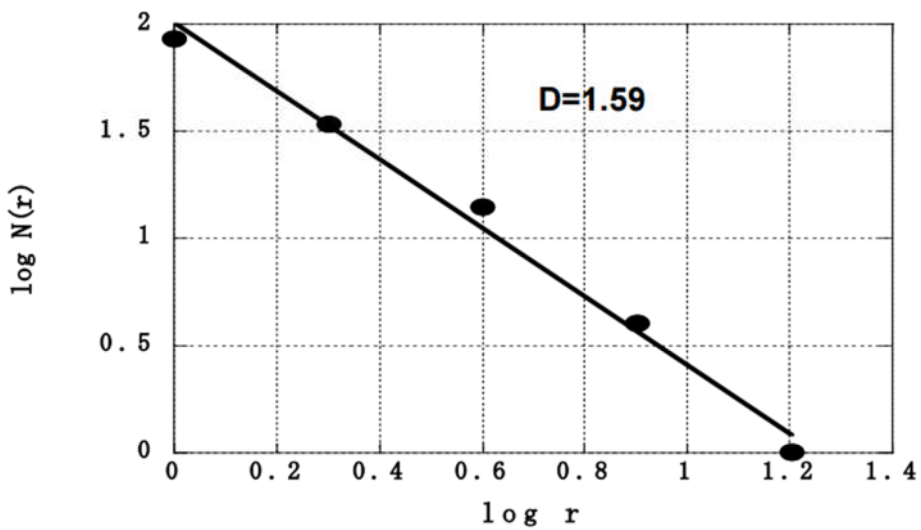


Figure 5.10: A plot of log of box size versus the log of box count (Mihashi et al. 2006)

Cracking density can be estimated by dividing the total length of the cracks by the cross-sectional area of the sample as shown in equation below (Hassan 2012) :

$$\text{Crack density} = \frac{\sum_{i=1}^N l_i}{A} \quad (5.5)$$

Where:  $\sum_{i=1}^N l_i$  = total length of the cracks and  $A$  = total area of the sample cross-section. The total cracks length was measured using computer aided-design software (AutoCAD) tools. In this study, the average of three samples was used for each mixture.

#### **5.3.3.3.2 Fracture energy and fracture toughness based on fractal analysis**

Even though the fracture energy and fracture toughness can be estimated from the macro mechanical testing, some researchers have proposed methods to estimate these parameters based entirely on the fractal analysis of the cracking pattern or depending on both fractal analysis and mechanical testing as shown below.

#### **Williford (1989) formula**

Williford as cited by Pramanik et al. (2012) and Erdem and Blankson (2013) in his patents has suggested a method and, accordingly, formulae to estimate the fracture energy ( $J_{IC}$ ) based on the fractal dimension of the cracks and the material properties as follows:

$$J_{IC} = CL^{(D_s-2)} \quad (5.6)$$

where

$C = \frac{\pi S_y^2}{E}$ ;  $J_{IC}$  =fracture energy;  $L$  = scale of observation;  $S_y$  = ultimate strength;  $E$ = modulus of elasticity and  $D_s$ =fractal dimension. The toughness of the material ( $K_{IC}$ ) can then be calculated from the estimated fracture energy from:

$$K_{IC} = \sqrt{J_{IC}E} \quad (5.7)$$

In this research, since the purpose is to evaluate the effect of rubber and/or cement on the ductility of the materials and not to evaluate their effect on strength, it was decided to normalize the load to its ultimate strength and hence evaluate the effect of rubber on the materials' ductility only.

#### **Guo et al. (2007) formula**

Guo et al. (2007) proposed a formula to compute the fracture energy based entirely on the surface macro-crack as follows

$$\frac{W_s}{G_f} = a \left( \frac{\delta_o}{a} \right)^{1-D_{1-d}} \quad (5.8)$$

where  $W_s$  is the energy dissipated at the surface of the crack,  $G_f$  is the fracture energy at the observation scale  $\delta_o$ ,  $a$  is the Euclidean length (equal to the diameter of the sample) and  $D_{1-d}$  is the fractal dimension that should be computed as explained previously (Section 5.3.3.3.1).

### 5.3.4 Cyclic indirect tensile testing

In spite of adopting the static modulus of elasticity to characterise cement-stabilized materials as presented, for example, in [BS EN 178866-12](#), using the cyclic testing as reported by [Nusit et al. \(2015\)](#) is necessary for mechanistic pavement design since it is representative of what actually happens in the field. As is well-known, no standardization has been issued yet regarding estimation of dynamic stiffness modulus using the repeated load indirect tensile test ([Marradi and Lancieri 2008](#)). Many authors ([Gaspard et al. 2003](#); [Khattak and Alrashidi 2006](#); [Gnanendran and Piratheepan 2008](#)) have estimated the indirect tensile resilient modulus. However, all the above authors developed their own test assumptions and arrangements which, in turn, make this test difficult to perform since test set-up, instrumentation and interpretation of results needs time as well as a professional operator. This may make this test restricted primarily to the research field.

In the asphaltic mixtures industry, the Nottingham Asphalt Tester (NAT) machine is customarily used in the UK and elsewhere mainly for dynamic stiffness modulus estimation or fatigue estimation in an indirect tensile mode as discussed in [BS EN 12697-26-2012](#). Using the NAT machine to characterize the cement-stabilized mixtures is an attractive option especially from the economic and uniformity points of view. This is because this usage will ensure the convenience of using the same equipment for testing both bituminous and cement stabilized mixtures. In addition, utilizing a standardized testing system may ensure uniformity in assessment of pavement mixtures and save effort in terms of testing set up and results analysis by utilizing accompanied software. Due to the limitation of the latter machine, [Nunes](#)

(1997) fabricated a loading rig allowing NAT-like loading in a universal testing machine at much greater load capacity than the 4.3 kN limit usually available. This was to allow effective testing of cement-stabilized materials of high stiffness. The purpose of this section is to study the performance of different mixtures under repeated indirect tensile load. This, in turn, will ensure at the same time a second advantage by evaluating the feasibility of utilizing the current Nottingham Asphalt Tester (NAT-NU14) of capacity 14 kN (not available to Nunes in 1997) to estimate dynamic indirect tensile stiffness modulus for cement-stabilized mixtures. Finally, suggestion a test procedures and protocol to estimate stiffness using the NAT machine.

The testing was conducted as follows: Firstly, the specimens were manufactured, cured and prepared as discussed in Section 4.3.2. However, each sample was manufactured to ensure a height of  $85 \pm 5$  mm which was then trimmed to 70 mm (except for C7R0 where 60 mm is the final sample height to fit with the capacity of the machine). Then, BS EN 12697-26-2012 was adopted to conduct the resilient modulus testing. However, since the load control testing mode is preferred for cemented materials (Nunes 1997), it was adopted rather than the deformation control mode specified in the specification. This is because targeting the horizontal deformation as 3-7  $\mu\text{m}$ , as specified in the latter specification, was suggested depending on the past experience with asphaltic mixtures testing. However, this, in fact, may not necessarily ensure that the cemented materials will remain in the elastic range. Therefore, from the point of view of the author, for cemented materials or any new material other than hot mix asphalt, it is necessary to conduct the indirect tensile strength (ITS) first (either instrumented with LVDTs if a resilient modulus test needs

to be conducted in deformation control mode or simple ITS if it is intended to evaluate the modulus in load control mode). This is to ensure applying stress/strain within the elastic range. Austroad (2008) as reported by Arnold et al. (2012) recommended using less than 40 % of the material strength for conducting the resilient modulus test. Furthermore, the British specification mentioned earlier recommended 30 % for estimation static modulus. To keep the material within the elastic range and to stay within the machine limit, the maximum applied stress was selected to ensure a stress ratio (applied stress/indirect tensile strength) of 30%. After mounting the sample on the testing sub-frame and setting up the instrumentation yoke supplied with machine, the NAT-NU14 was used for sample testing. Figure 5.11 illustrates the testing arrangement using the NAT machine. Five pulses (Marradi and Lancieri 2008) were applied to estimate the resilient modulus by averaging the modulus values computed from each pulse. These five pulses were preceded by five conditioning pulses.

Figure 5.12 depicts the applied load pulses and the resulting deformation. As can be seen from the latter figure, both load and corresponding lateral deformation are in a good synchronization which means no phase angle (i.e. no viscoelastic behaviour or frictional) exists. The resilient modulus for each pulse was calculated using the following formula

$$E_r = \frac{P(v + 0.27)}{z \cdot h} \quad (5.9)$$

where:  $E_r$  is the resilient modulus (MPa),  $h$  is mean thickness of the sample (mm),  $P$  is the peak value of applied load (N),  $\nu$  and  $z$  are Poisson's ratio and horizontal deformation amplitude, respectively. Poisson's ratio was assumed as 0.25 (Barišić et al. 2015).

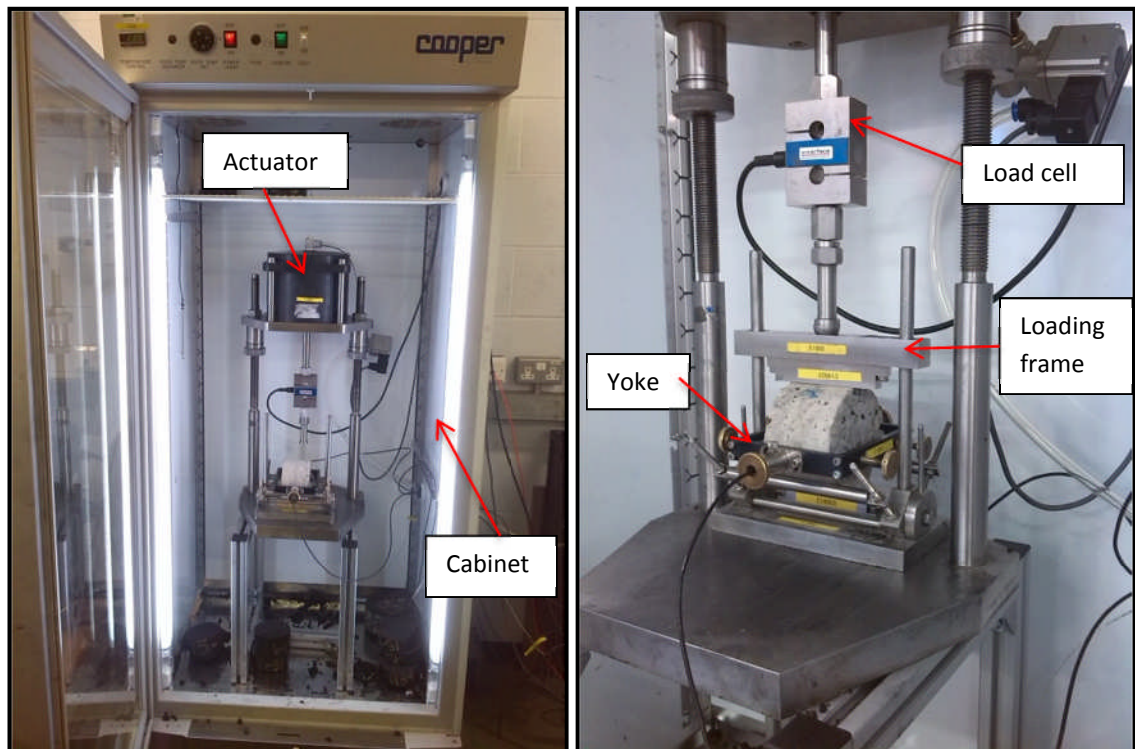


Figure 5.11: Cyclic indirect tensile testing NAT machine with close-up view of test configuration.

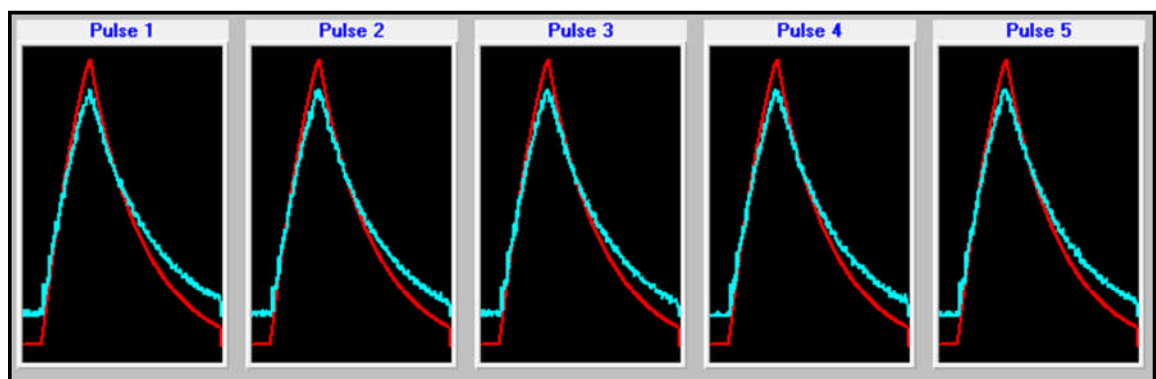


Figure 5.12: Cyclic load wave applied by NAT machine and corresponding deformation

### 5.3.5 Mesostructural investigation

To better understand the failure mechanism and to observe how the cracks propagated, failed specimens were scanned using an X-ray CT machine (Figure 5.13). This includes two systems located in the same cabinet. The first one is the mini focus system of a 300 kV X-ray source and a linear detector. The second system is a micro focus having a 225 kV source with an area detector. To ensure sufficient power of X-ray for penetration through stabilized mixtures, the first system was used in this investigation. Two scans were done for each sample at the top and bottom of the middle third of sample. The resolution of the reported scan is 0.065 mm/pixel. Image J was used to manipulate the CT scan by extracting, enhancement and filtration. The scanned images using the X-ray CT technique depend on the properties of each component inside the sample being scanned. low density component is usually appeared as the darker one while, on the other hand, the brighter object corresponds the denser component.

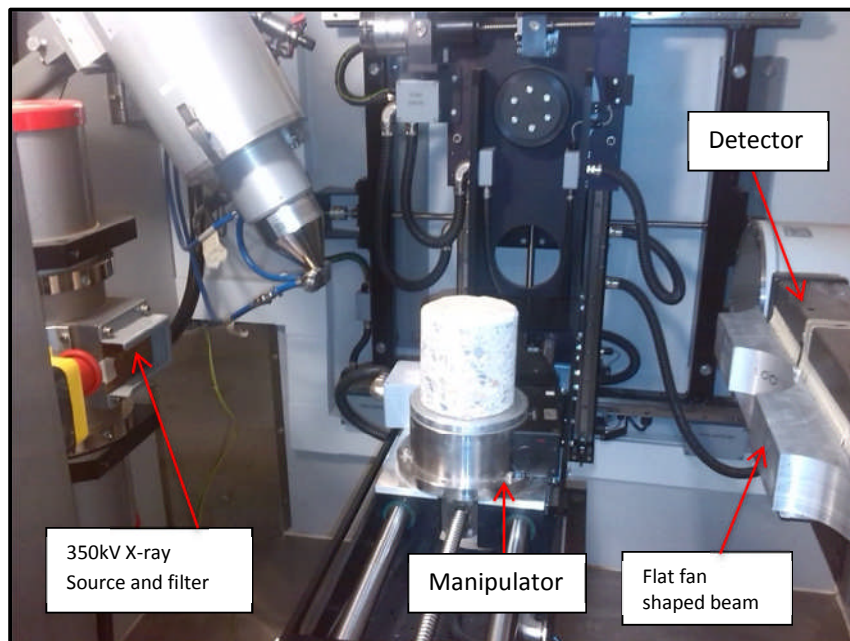


Figure 5.13: X-Ray CT machine parts and alignment of sample.

## 5.4 Results and discussion

### 5.4.1 Unconfined Compressive Strength (UCS) Test

#### 5.4.1.1 *Effect of rubber content on UCS*

The effect of rubber content on UCS of cement-stabilized mixtures is shown in Figure 5.14 at curing ages of 7, 28 and 365 days. As is shown from that figure, incorporating crumb rubber particles in place of the natural aggregate resulted in a compressive strength decline for the mixtures where the UCS, at 28 day age, was dropped by 12.35%, 29.35% and 37.7% when the 6 mm natural aggregate was replaced by 15%, 30%, and 45% rubber, respectively. This is expected since the natural aggregate of high strength and stiffness (as shown in Chapter 4) is replaced by the rubber particles of low strength and stiffness ([Grinys et al. 2012](#)). The low strength of the rubber particle is also expected to reduce the efficiency of aggregate-to-aggregate load transmission through these particles. Furthermore, incorporating the rubber particles has reduced the density due to their low specific gravity and their negative impact on the compaction efficiency (as discussed in Chapter 4) which resulted in a drop in the mixture strength. Regarding the curing period, there is an increase in the UCS as the curing age increases which is fundamentally due to increase in the hydration products that increase the strength of the cement mortar as well as the bond strength between aggregate particles. It is worth mentioning that the increasing cement content (within the range of investigated cement contents) has a beneficial impact on the material density and strength as demonstrated previously.

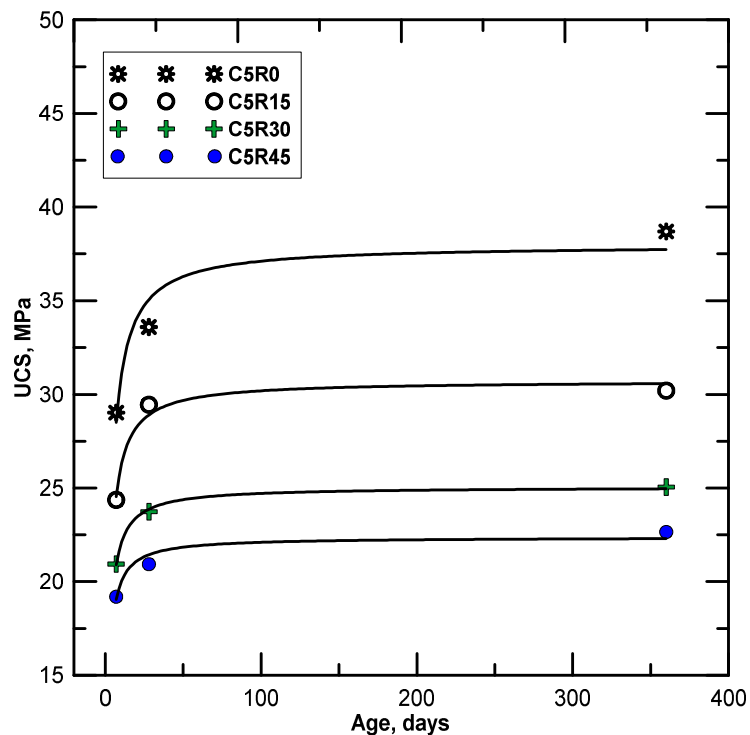


Figure 5.14: Effect of rubber content on UCS at 7, 28 and 365 days

#### 5.4.1.2 Combined effect of rubber and cement contents on UCS

Figure 5.15 illustrates the effect of cement content and curing period on the UCS of both control and rubberized mixtures containing a rubber particle content equal to 30% of the 6 mm fraction. As can be seen from that figure, the general trend is an increase in UCS value as cement content increases since cement will increase the strength of a material's matrix and the bond between particles. In addition, there was an improvement in this parameter with curing time, since hydration is a time-dependent process. The development rate of UCS, in general, is proportional to the amount of cement because the more cement in the mixture the more the hydration products (Barišić et al. 2015) and hence the more the strengthening and binding effect.

Regarding the combined effect of cement and rubber on the UCS, it was observed from the same figure that the UCS declined due to the partial replacement of natural aggregate with crumb rubber at all cementation levels. Furthermore, interestingly, the decline in the UCS value due to rubber incorporation increased as cement content increased, although the increase was less marked as the cement content increased from 5% to 7%. The latter behaviour can be explained as follows: the aggregates in a compacted cement aggregate mixture are interlocked and bonded by the cement matrix to each other which makes them resist the applied loading like an indeterminate structure, i.e. the structure carries the applied load in such a way that each element in the structural system carries part of that load in proportion to its relative stiffness. This means that as cement content increases the difference in the stiffness between rubber particles and surrounding materials will also increase. This, in turn, means that, stresses will be shed from the compliant rubber particles toward the stiffer surrounding materials which will thus absorb more load than the rubber particles. This will result in greater stress concentrations in that material since the rubber will increasingly behave like a void. On the other hand, in the case of low cement content this stiffness difference is lower, which will maximize the role of rubber particles in this structural system. Thus the void-like behaviour depends, to a large extent, on the relative stiffness between rubber particles and surrounding matrix.

Figure 5.16 illustrates the relationship between the UCS at 28 days and UCS at both 7 days and 360 days for all different investigated mixtures (of different rubber and cement contents). This is also compared with both concrete and cement-stabilized aggregate mixtures relationships as reported by [American Concrete Institute \(ACI\)](#) and [Lim and Zollinger \(2003\)](#), respectively. It can be inferred from the latter figure

that at late ages (i.e. 365 days) the current results are in a good agreement with these authors. This, in turn, means the neither rubber nor cement have an effect on the relationship between the UCS at different curing periods. In addition, both of them agree with the ACI reported results. However, at early ages the ACI model gives a conservative prediction for the stabilized materials' strength. The most important conclusion herein is that the development of strength is largely governed by the cement content of the mixtures and percentage of rubber in the mixture.

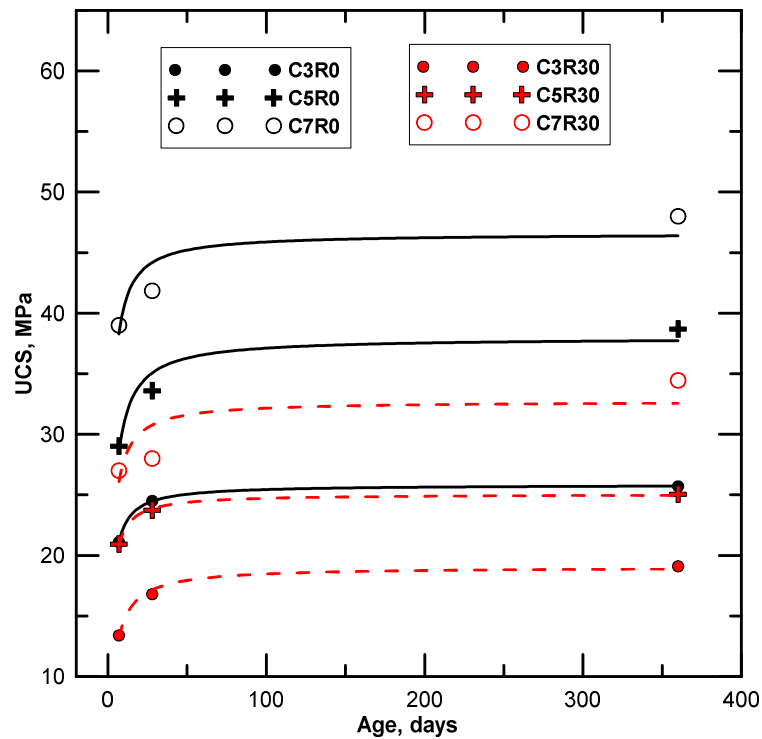


Figure 5.15: Effect of cement content on UCS of control and rubberized mixtures at 7, 28 and 365 days

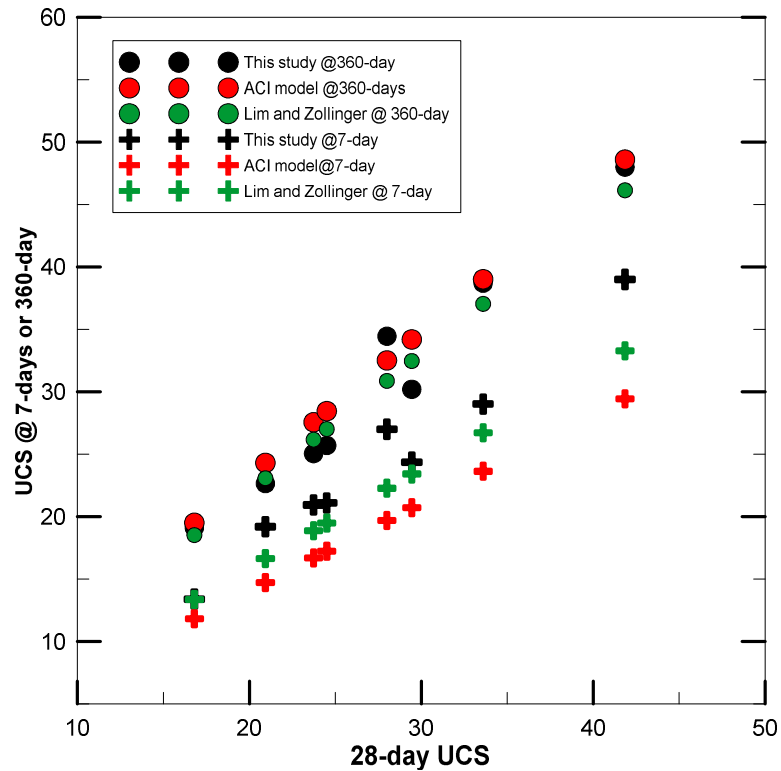


Figure 5.16: Variation of UCS at 28 days with UCS at 7 and 360 days

#### 5.4.2 Compressive stress-strain relationship

The problem of testing cement-stabilized aggregate mixtures was discussed in a report prepared for the [Portland Concrete Association \(PCA\)](#) by [Scullion et al. \(2008\)](#). These authors concluded that the compressive stiffness modulus is a very difficult test to conduct and not recommended for routine testing. They attributed that to the low strain levels normally developed which make it difficult to obtain consistent and accurate results. In addition, these low strains are highly sensitive to any change in the sample geometry, resulting in large differences between the measurements even in the case of small unevenness in the testing surface.

In this study, in spite of the great care in sample preparation and testing, many samples' results were unsuccessful because they were non-reasonable or showed

large variability even after introducing rubber particles. Therefore, it is not advised to conduct this test due to the difficulties associated with sample preparation and instrumentation for accurate data acquisition. However, from the limited results, Figure 5.17 shows the compressive stress-strain behaviour for cemented mixtures containing 5% cement content and different amounts of crumb rubber. It can be seen, qualitatively, that the post-peak behaviour and the ductility of the mixtures proportionally increase as the rubber content of the mixture increases.

Since the cement-stabilized base course within the pavement structure is normally subjected to tensile stress/strains at its bottom, the tensile testing modes are more simulative of the likely in-situ failure mode and will be adopted to characterize and understand the mechanical behaviour and the failure mechanism of these types of mixtures.

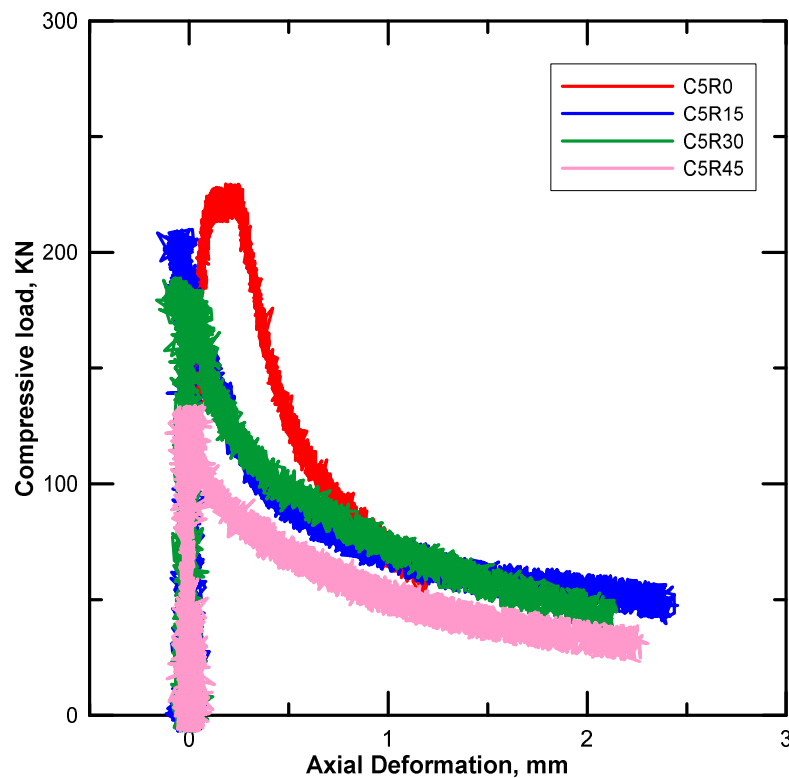


Figure 5.17: Load-axial deformation relationship for different mixtures.

### **5.4.3 Indirect tensile strength (ITS)**

#### ***5.4.3.1 Effect of rubber content on ITS***

It is generally accepted that all cementitious materials (including concretes) are weak in tension and exhibit brittle behaviour (Khelifi et al. 2015). It was found that replacement of natural aggregate by crumb rubber has a negative effect on the indirect tensile strength (ITS) as shown in Figure 5.18. ITS decreased by 3% for each 1% of rubber replacement. This can be attributed, in addition to the lower modulus of elasticity, to the decrease in the number of contacts points between natural aggregate particles as a result of compacity drop. This will lead to a reduction in the efficiency of aggregate interlock and, hence, to an accelerated mixture deterioration since interlock is one of the main mechanisms for sustaining loads. Similar to UCS, ITS also increased with increase in curing period for the same reasons. The same decrease in ITS was observed at both 7 and 28 days for all mixes except C5R45 where there was no further reduction in this parameter, perhaps because of a specific rubber distribution.

#### ***5.4.3.2 Combined effect of rubber and cement contents on ITS***

In terms of indirect tensile strength, it was observed, as shown in Figure 5.19, that the ITS value increased proportionally with higher amounts of cement and/or long curing periods. Similar to the UCS, the reduction in ITS is more obvious at higher cement level than at low contents for the same reasons as stated above.

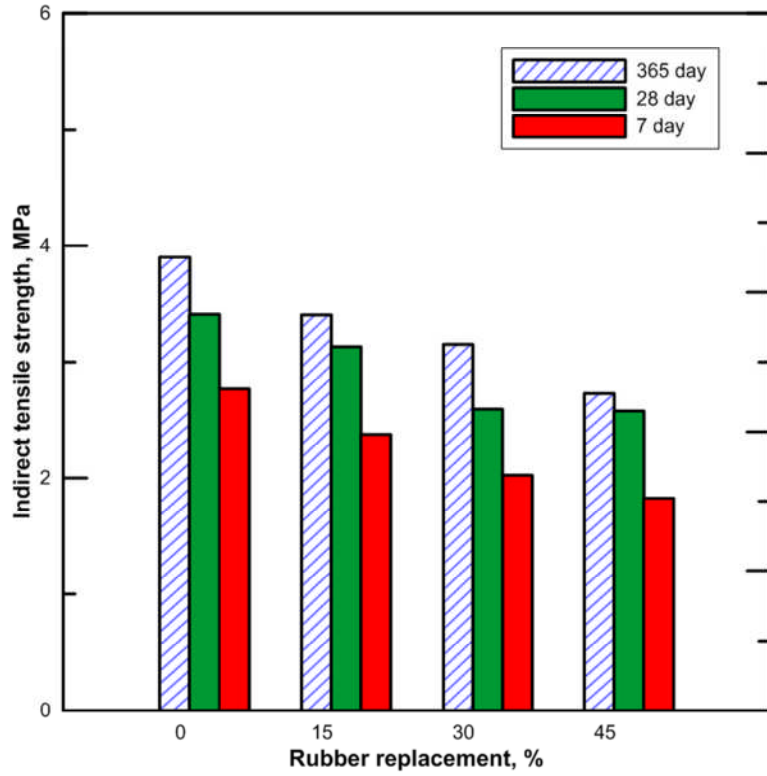


Figure 5.18: Effect of rubber content on ITS at 7, 28 and 365 days

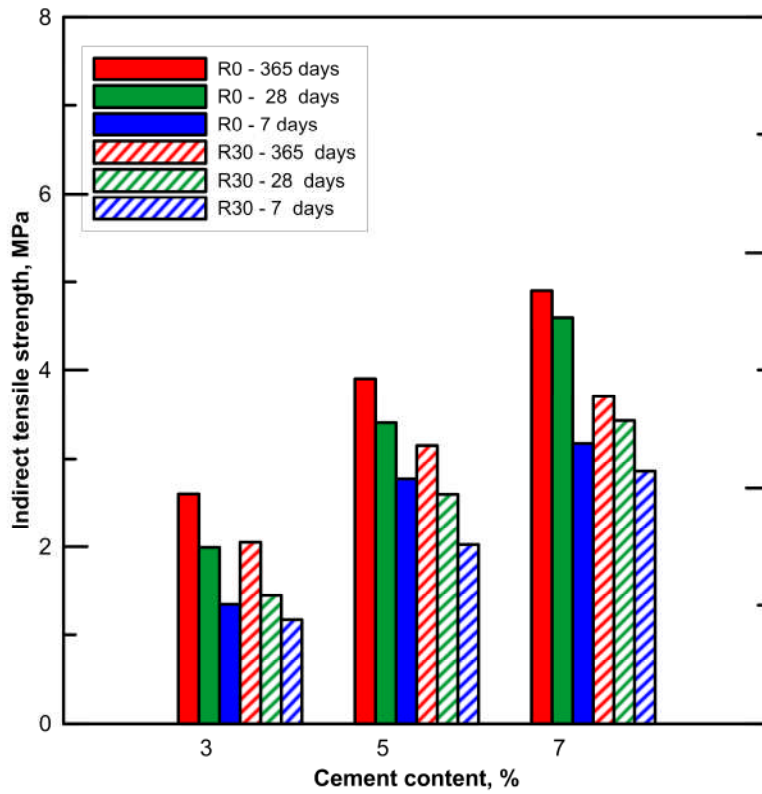


Figure 5.19: Effect of cement content on ITS at 7, 28 and 365 days

Figure 5.20 shows the relationship between UCS and ITS values for different mixtures at different ages. From this figure, it can be inferred that the ITS value is around 10% of the UCS applicable for all investigated mixtures at all curing ages. This means that the relationship between UCS and ITS is a unique relation regardless of mixture composition (aggregate type, degree of cementation and curing period). Ji et al. (2015) in their study for different natural aggregate/recycled asphalt pavement aggregate (RAP)/recycled cement base aggregate blends stabilized with different cement contents concluded that there was a linear relationship in which the  $UCS = 9.786 \times ITS$ . Arellano and Thompson (1998) reported a ratio of between 10% - 15%. Thus the current results confirm these earlier findings.

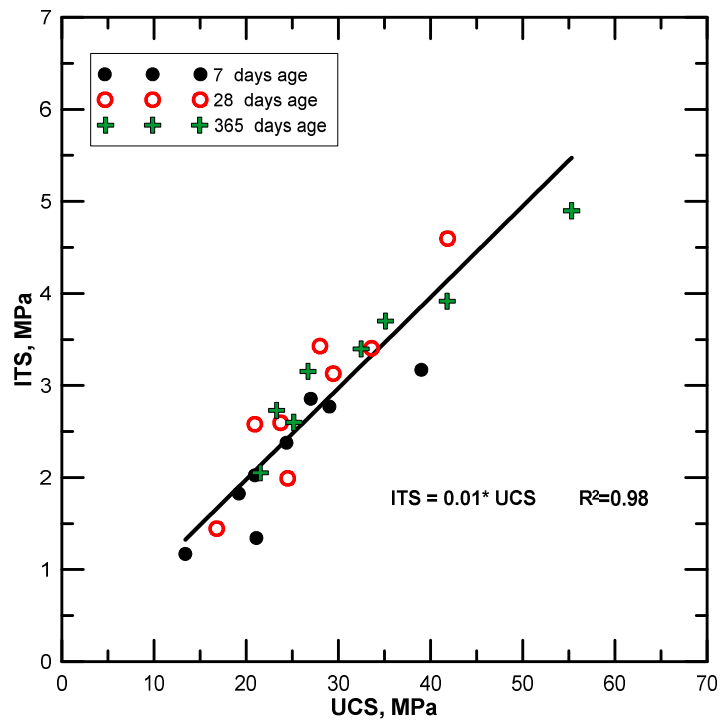


Figure 5.20: Variation of UCS with ITS for different ages, cement and rubber contents.

### ***5.4.3.3 Failure patterns***

In terms of failure mode during indirect tensile testing, the reference mixtures tend to fail in a brittle way resulting in a complete separation of sample halves. This was more obvious at high cement content. In contrast, the mixtures modified with crumb rubber at all cement contents did not experience such a failure mode. Instead, the samples look intact with narrow crack openings. Figure 5.21 and Figure 5.22 illustrate the failure patterns under indirect tensile testing for cement-stabilized mixtures having different rubber contents and cement contents, respectively. This, in turn, confirms the ductile behaviour of such mixtures due to rubber incorporation as stated by [Duarte et al. \(2015\)](#). For UCS samples (Figure 5.23 and Figure 5.24), the same behaviour was observed where the mixtures with no rubber failed by crushing of large pieces from the sample while the rubberized mixtures showed longitudinal cracks without complete failure. This also confirms a ductile behaviour and improvement in energy absorbency. Thus, when rubberized mixtures are used as a base course in the pavement structures, such failure behaviour may have a positive impact on the asphaltic surface course since the narrow crack in these modified layers should contribute to maintaining low tensile strains in overlying asphalt courses. This is because a wide crack in a base course imposes a high tensile strain on the asphaltic course above it. [Solanki \(2010\)](#) stated that reduced crack size have a positive effect on a pavement structure by minimizing reflection cracking.

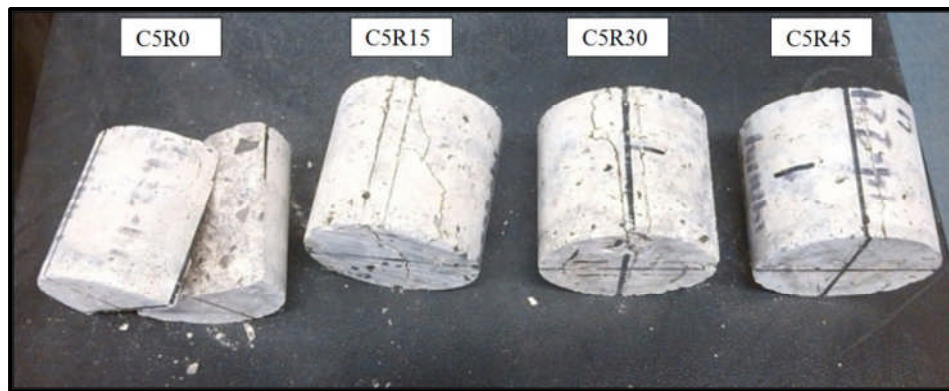


Figure 5.21: Failure pattern of ITS samples containing different rubber contents and 5% cement. .



Figure 5.22: Failure patterns of ITS samples containing different combinations of rubber and cement contents.



Figure 5.23: Failure patterns of UCS samples containing different rubber contents and 5% cement.

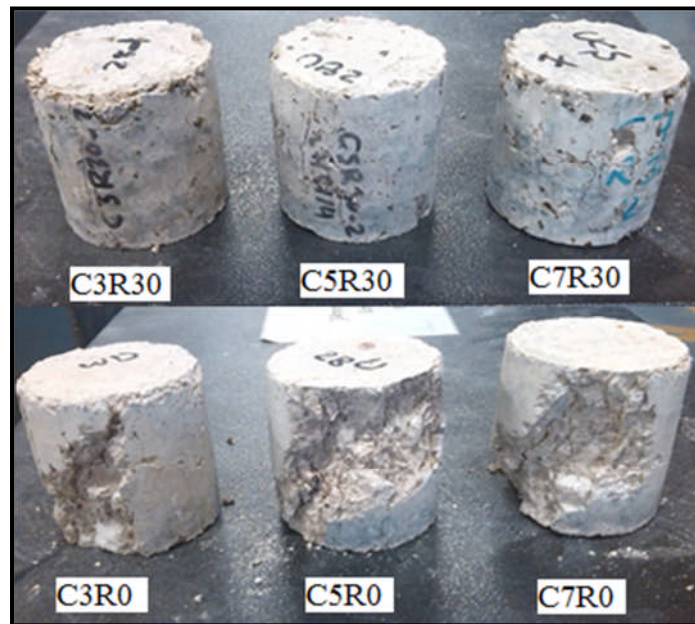


Figure 5.24: Failure patterns of UCS samples containing different combinations of rubber and cement contents.

#### 5.4.4 Load-deformation curves and toughness

##### 5.4.4.1 Effect of rubber content on load-deformation curves and toughness

The load-deformation relationships for different mixtures are illustrated in Figure 5.25 through Figure 5.28. As can be seen from these figures, post-peak load carrying capacity increased with rubber content. From these curves, toughness index was calculated quantitatively as presented in Figure 5.29. It is clearly shown that at all replacement levels there was an improvement in the energy absorption capacity of the mixtures. This improvement was around 27%. However, the differences between the toughness amongst rubberized mixtures can be attributed to the local distribution of the rubber inside the sample which resulted in different crack propagation and hence different toughness indices. Despite the differences between toughnesses of the rubberized mixtures, all of these mixtures have greater toughness than the control

ones. The implication is that the rubber provides energy absorbency to the mixture which may then provide better performance under cyclic or fatigue loading (Modarres and Hosseini 2014).

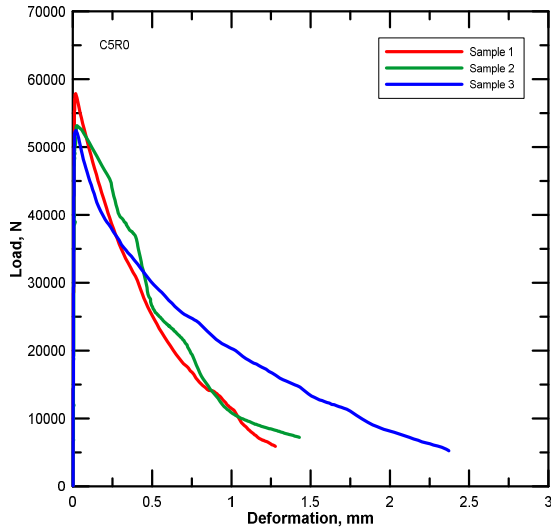


Figure 5.25: load-deformation curve for C5R0

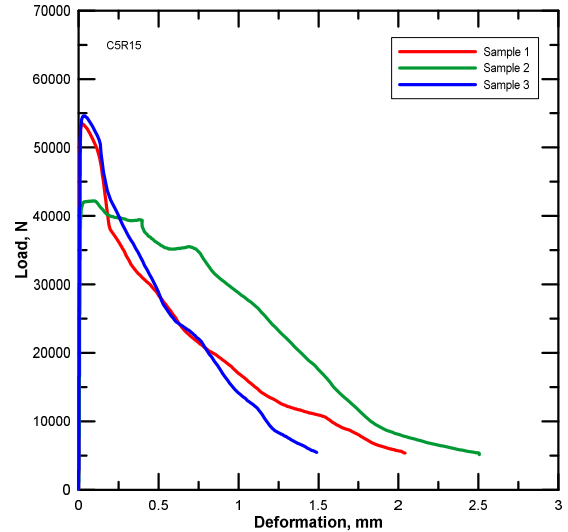


Figure 5.26: load-deformation curve for C5R15

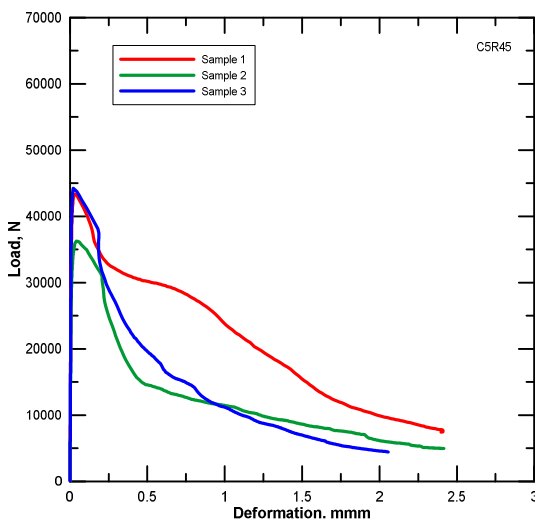


Figure 5.27: load-deformation curve for C5R30

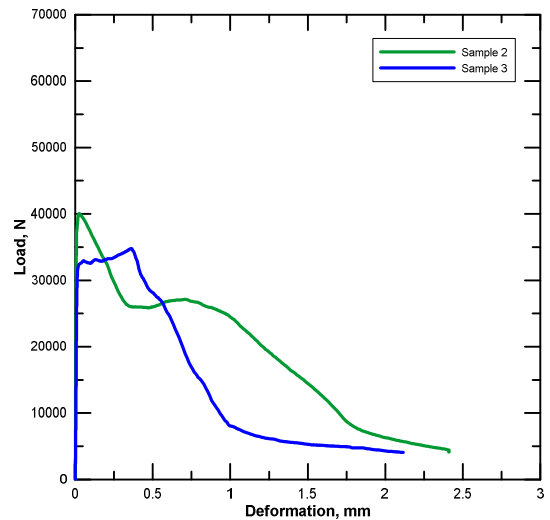


Figure 5.28: load-deformation curve for C5R45

Although many researchers reported similar behaviour when they investigated the effect of rubber on toughness of normal concrete, no clear reasons were reported to

explain this behaviour. However, [Chiaia et al. \(1998\)](#) claimed that the ductility improvement when using weak aggregates is due to a change in the mechanism of microcracking.

The reasons behind ductility improvement due to rubber addition in cement-stabilized materials might be:

- a) Partly because the crumb rubber particles helped to delay crack propagation by relieving some induced local stresses
- b) and partly due to embedding of weak particles inside stiff media lengthening the crack path since the crack path tends to propagate through these weak points.

In addition, since the cracks tend to be propagating as a main crack and branches rather than one main crack, especially for rubber rich mixtures (Figure 5.29), this would cause more energy dissipation as described by [Shah et al. \(1995\)](#) and [Erdem \(2012\)](#). This is evidenced as presented later (Section 5.4.6).

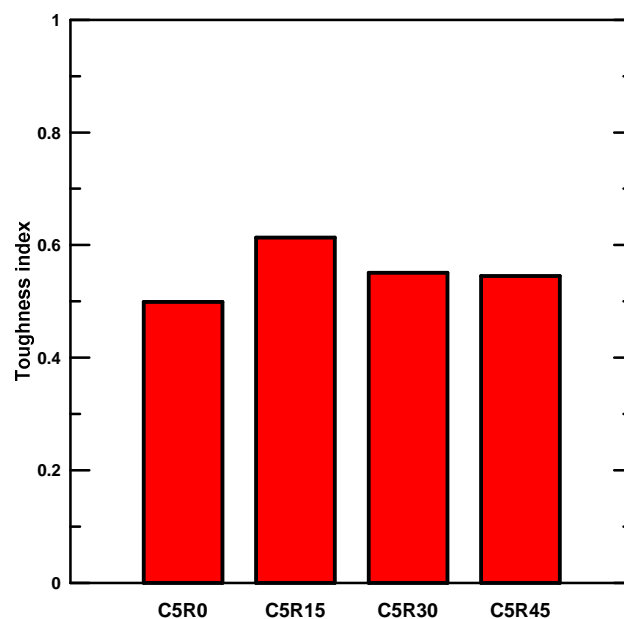


Figure 5.29: Effect of rubber content on toughness indices

To clarify the mechanism of failure and to elucidate the above hypotheses, X-ray CT was utilized to investigate the internal structure of failed samples at mesoscale level. Part (b) of the suggested mechanism is evidenced in Figure 5.30 to Figure 5.32 which show how the cracks propagated for different mixtures containing different rubber contents. Examining these scans clearly supports the suggested failure mechanism as the cracks can be seen to connect rubber particles as indicated by the red arrows in the same figure and tend to avoid areas without rubber (as predicted by reason (b) above). On the other hand, evidencing the explanation (a) can be performed by critically examining the load-deformation relationships. Comparing and contrasting these relationships with the mechanism of fracture process in concrete proposed by [Löfgren \(2005\)](#) (Figure 5.33) reveals, interestingly, a delay in both micro and macro cracking for the RCSAMs during the fracture process where both micro and macro cracking growth zone in rubberized mixtures is greater than those of the control mixture. The latter evidence clearly supports the crack growth delay hypothesis presented above. This was also supported by the tortuous and complex crack patterns as highlighted in fractal analysis. No doubt the applicability of this proposed mechanism depends, to some extent, on the distribution of the rubber particles. The more uniform the rubber distribution, the more uniform the stress/strain distribution can be anticipated to be inside the mixture.

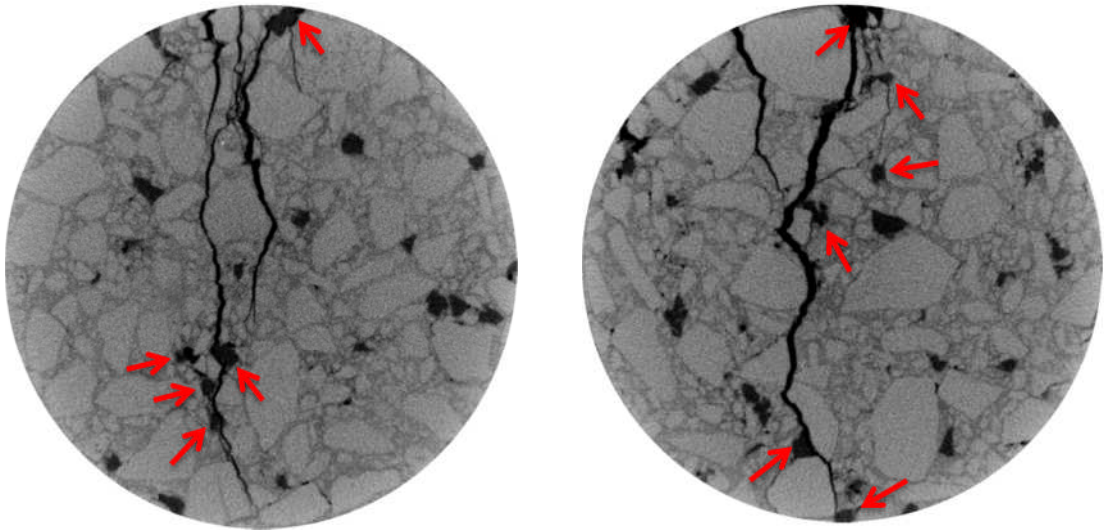


Figure 5.30: Cracks propagation mechanism for C5R15

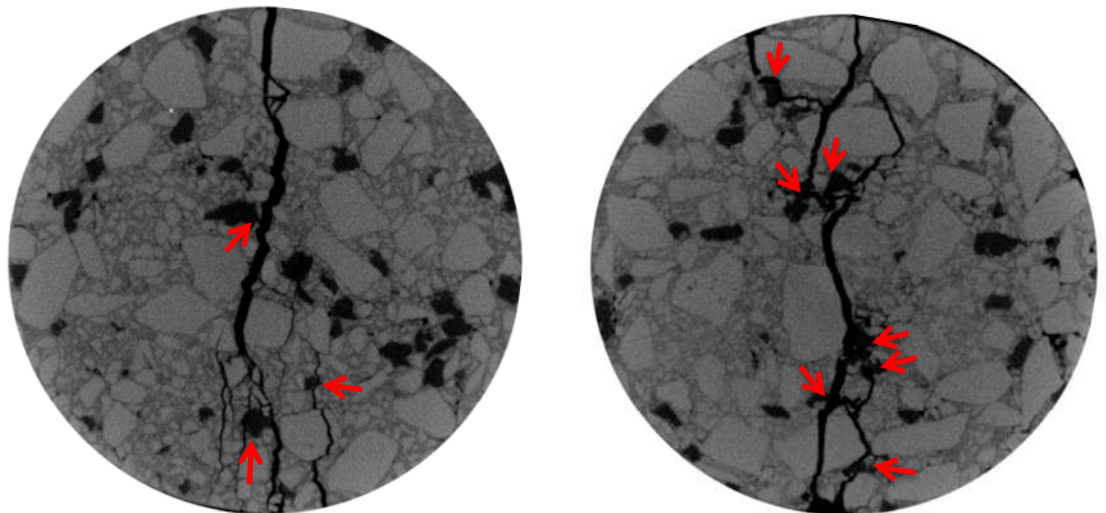


Figure 5.31: Cracks propagation mechanism for C5R30

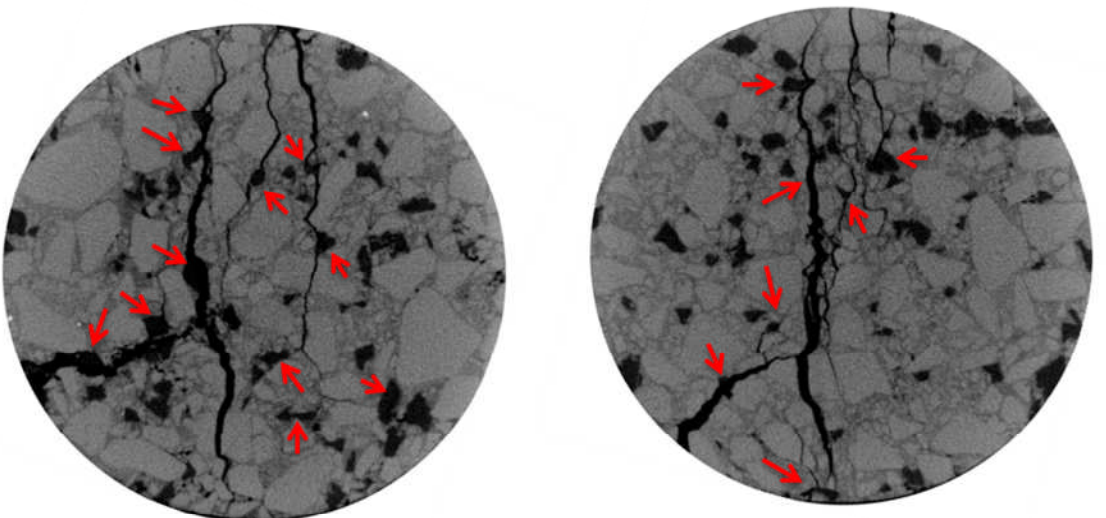


Figure 5.32: Cracks propagation mechanism for C5R45

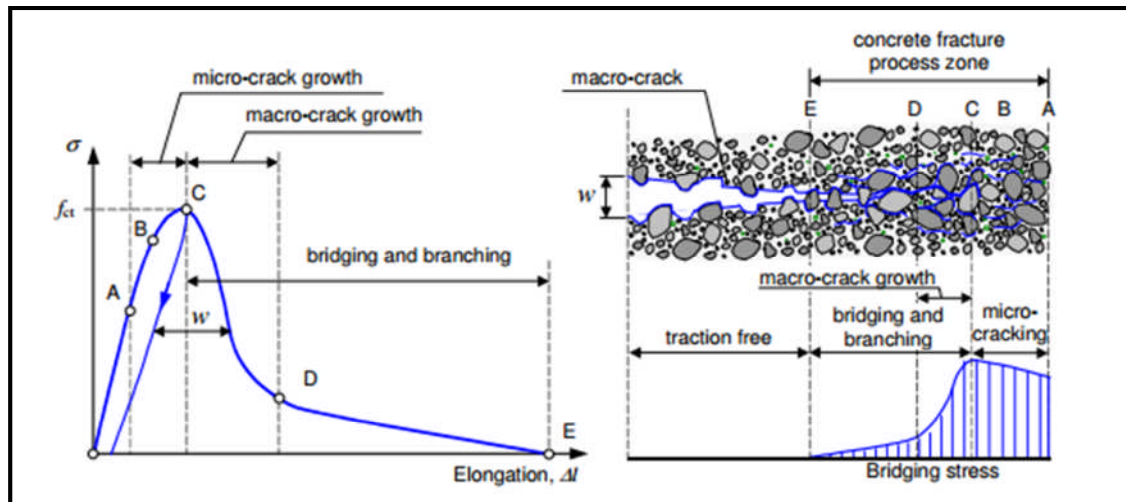


Figure 5.33: Schematic illustration of fracture process (Löfgren 2005)

#### 5.4.4.2 Combined effect of rubber and cement contents on load-deformation relationships and toughness

Figure 5.34 through Figure 5.37 demonstrate the load-deformation relationships for some investigated mixtures of different cement contents. From these curves, toughness indices were estimated (Section 5.3.3). It can be clearly seen from Figure 5.38 that inclusion of more cement caused a reduction in the toughness or energy absorption capacity of the mixture. However, an improvement occurred in the toughness value after modification with crumb rubber at all cement levels. Greater toughness was observed at higher cement contents. This leads to the conclusion that as far as the toughness of the materials is concerned, incorporating rubber in the cemented mixture at high cement content will be beneficial for improving the energy absorption capacity of the material. However, in spite of this, both conventional and rubberized mixtures of low cement content are still tougher than those with high cement contents. Nevertheless, increasing toughness of the material of high strength

(as compared with materials of low cement content) will ensure less pavement thickness with improved fatigue behaviour.

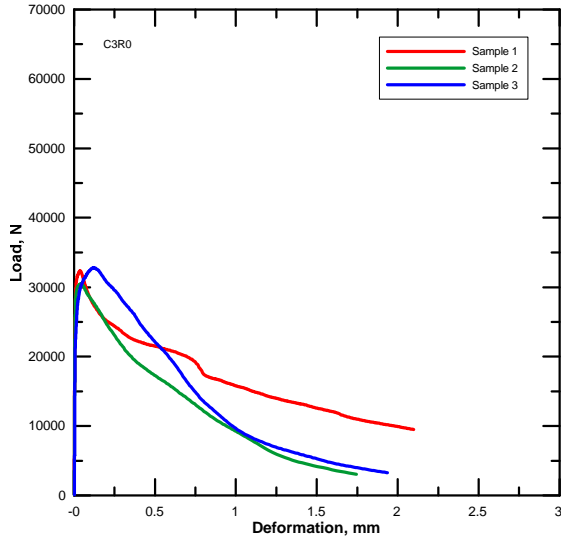


Figure 5.34: load-deformation curve for C3R0

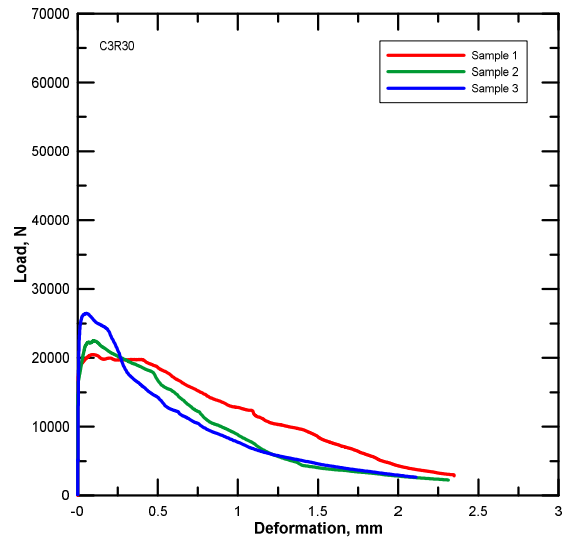


Figure 5.35: load-deformation curve for C3R30

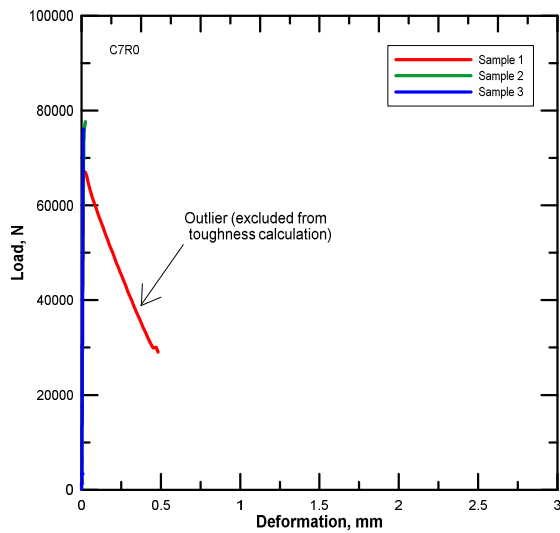


Figure 5.36: load-deformation curve for C7R0

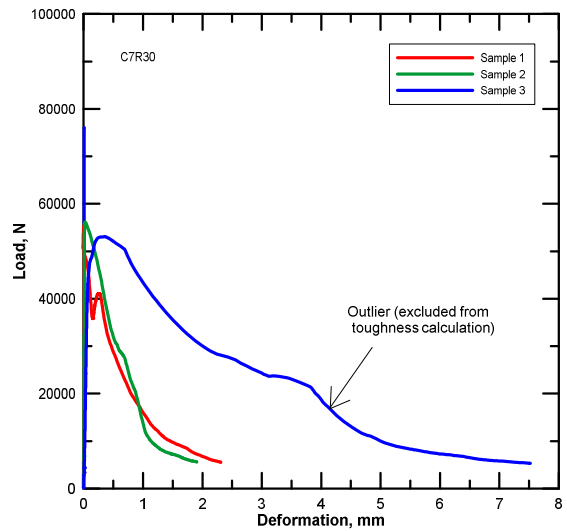


Figure 5.37: load-deformation curve for C7R30

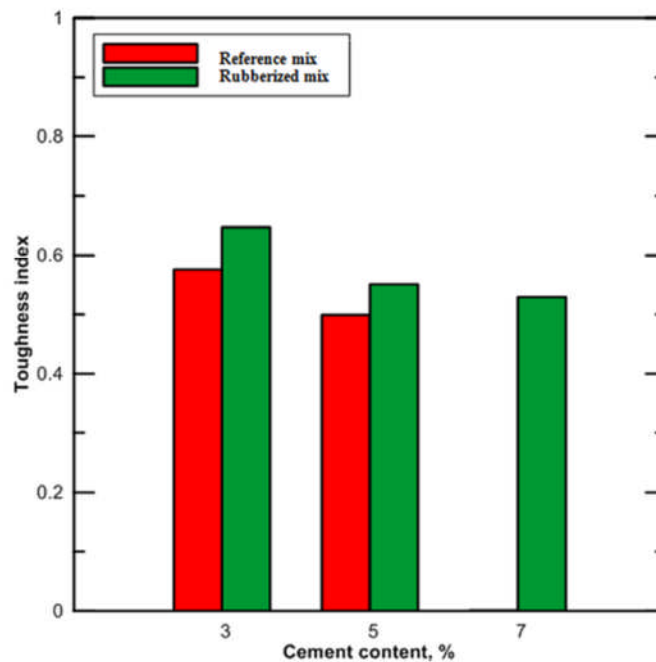
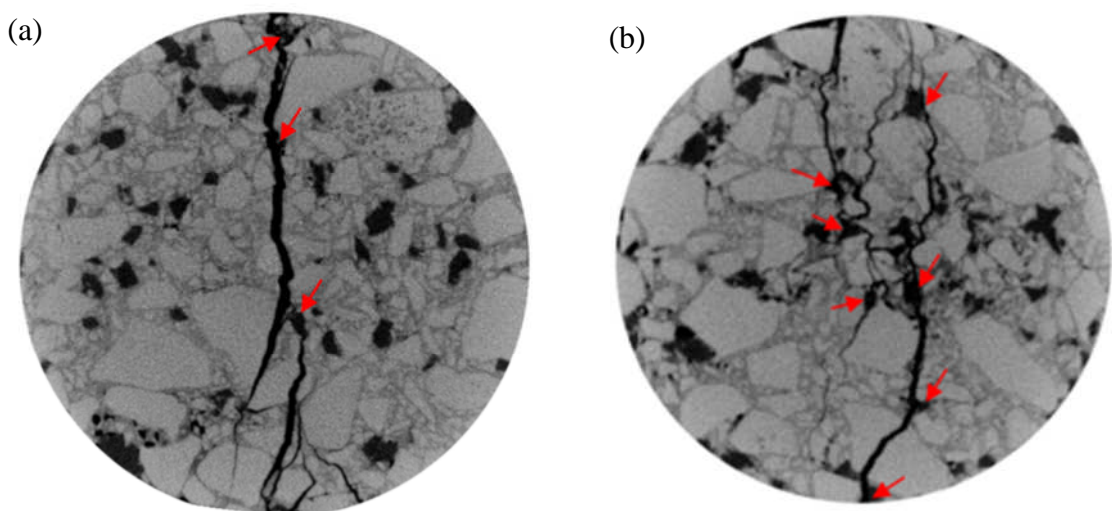


Figure 5.38: Effect of cement content on toughness indices.

It is suggested that the mechanism of toughness improvement is by lengthening the crack propagation path for both reference and rubberized mixtures. This action might decrease the crack growth rate at both micro and macro levels. If an assumption is made that the crack always propagates through the weak points, then this may explain the toughness changes. At low cementation levels, the bond between the aggregate particles and cement mortar (fines and cement) is probably the weakest element in the internal structure of the mixture. Propagation through weak points (primarily around the aggregate particles) will lengthen the crack path and increase the toughness of the mixture. At high cementation degree, on the other hand, there is no contributor to delay the crack propagation due to the better bond between the aggregate and surrounding materials and the dense cement mortar. This will accelerate the crack growth and propagation which in turn decreases the toughness of the materials.

The above hypothesis can be proved by inspection of the load-deformation curves for different mixtures and interpreting the fracturing process in the way proposed by Löfgren (2005). Comparing Figures 5.34 and Figure 5.36 in the light of the fracturing mechanism suggested in Figure 5.33 implies that the zones of micro and macro crack growth are greater in the case of low cement content than that of high cement content. However, when the rubber was incorporated in the poor cement mixture, no big change occurred in the latter zones (compare between Figure 5.34 and Figure 5.35). On the other hand, at 7% cement content, a greater improvement in cracking zones is implied, as a result of rubber inclusion (compare Figure 5.36 and Figure 5.37). The above evidence therefore strongly supports the assumption mentioned above.

Figure 5.39 illustrates the X-ray CT scans of the internal structure of the mixtures having different cement contents. It can be seen from that figure that the crack appears to preferentially propagate through the rubber particles, regardless of the cement content.



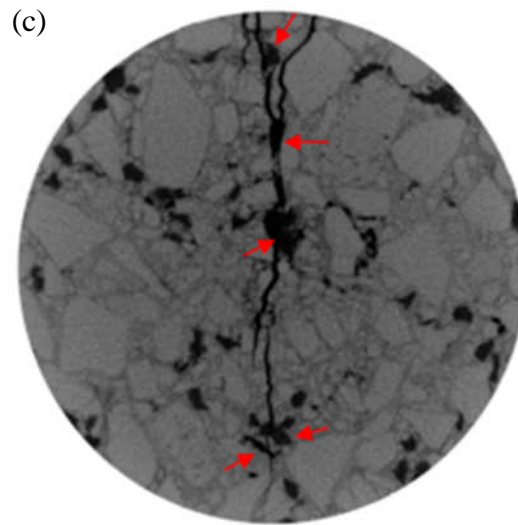


Figure 5.39: Crack propagation mechanism of rubberized mixtures of different cement contents: a. C3R30; b. C5R30 and c. C7R30

#### 5.4.5 Indirect tensile elastic modulus of elasticity ( $E_{it}$ )

##### 5.4.5.1 Effect of rubber content on static modulus of elasticity

As the stiffness of the mixture depends, to a large extent, on the stiffnesses of its constituents, replacement of stiffer natural aggregate having a modulus of elasticity of 57 GPa by softer crumb rubber particles caused a drop in the stiffness of the modified mixture. Figure 5.40 shows the effect of different rubber replacement level on the modulus of elasticity of the stabilized mixture containing 5% cement content. The reasons for the increase in the stiffness of C5R45 relative to C5R30 is not known although it might be because of the less uniform distribution of rubber particles in the mixture. Perhaps an accumulation of rubber particles caused a stress concentration and resulted in premature failure of the sample without large deformation. However, regardless of the individual behaviour, adding rubber can generally be seen to cause a reduction in material stiffness.

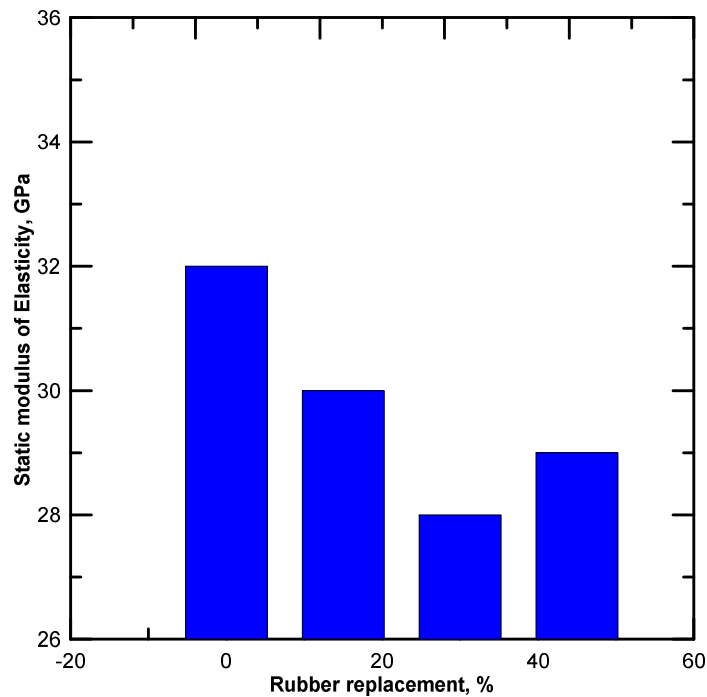


Figure 5.40: Effect of rubber content on indirect tensile static modulus

#### *5.4.5.2 Combined effect of rubber and cement contents on static elasticity modulus*

The effect of cement content on the static modulus of elasticity of reference and rubberized cement-stabilized mixtures is illustrated in Figure 5.41. It can be said, based on the results depicted in the latter figure, that the greater the cement content the greater the stiffness of the mixture. It can be inferred that, for control mixtures, because the stiffness of aggregate is the same for all mixtures having different cement contents as measured in Chapter 4, the stiffness of mixtures is controlled, to large extent, by the stiffness of the matrix (fines plus cement) and its bond with aggregate particles. Thus, increasing the binder in the mixture will produce a matrix with less deformability which means a higher stiffness of the overall mixture. On the other hand, a drop of the stiffness was observed at all cementation levels due to rubber inclusion which is more obvious in the mixture of low cement content than in

that of high cement content. This can be attributed to the relative stiffness of the rubber particles with respect to the surrounding materials which maximizes their role in both load carrying capacity and deformability of the mixture (as discussed in section 5.4.1)

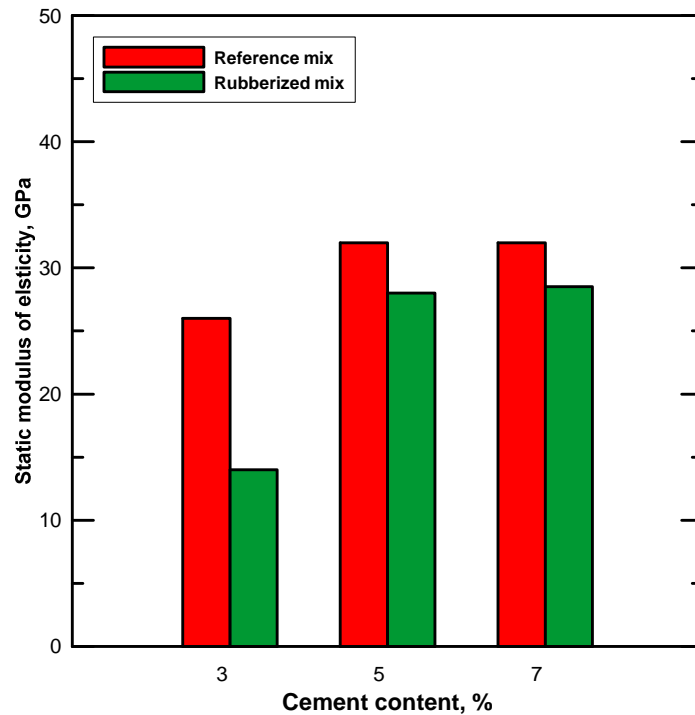


Figure 5.41: Effect of cement content on indirect tensile static modulus

Due to the difficulties associated with measurement of the stiffness modulus in terms of equipment and skilled staff, it is desirable to correlate this property with simple tests like ITS or UCS. Figure 5.42 and Figure 5.43 show the relationship between static modulus of elasticity and ITS and UCS, respectively. As can be seen from these figures the stiffness modulus is related to the ITS ( $R^2 = 0.69$ ) and UCS ( $R^2 = 0.82$ ) linearly which permits the estimation of the stiffness modulus reasonably from these simple tests. Few correlations were reported in literature regarding the relationship between ITS and indirect tensile stiffness modulus. However,

Gnanendran and Piratheepan (2008) reported a linear relationship between these parameters. Comparing and contrasting the current findings with previous studies reveals a good agreement between them and less sensitivity of these relationships to the change in either aggregate composition or degree of cementation.

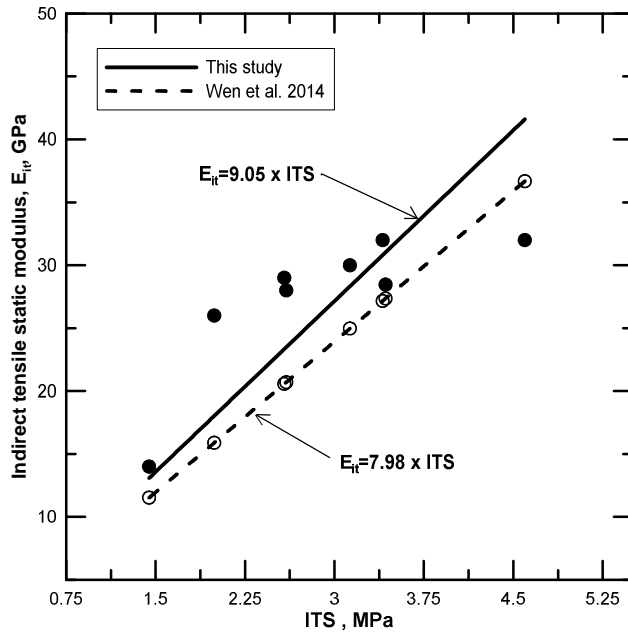


Figure 5.42: Variation of indirect tensile static stiffness modulus versus ITS

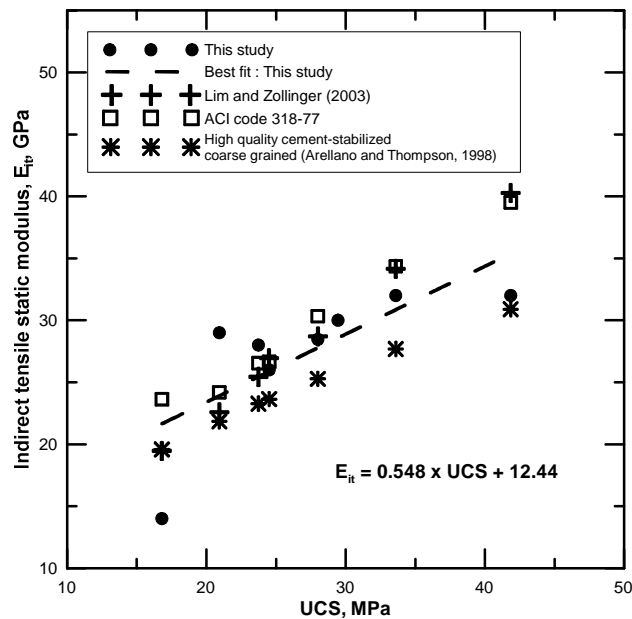


Figure 5.43: Variation of indirect tensile static stiffness modulus versus UCS

### 5.4.6 Damage quantification

Figure 5.44 demonstrates the determination of the fractal dimension according to the methodology presented in Section 5.3.3.3 where the slopes of these lines represent the fractal dimension for the mixtures containing 5% cement and different rubber contents. Fractal dimensions and fracture energies (calculated accordingly using Equations 5.6 and 5.8) for different rubber replacement levels are tabulated in Table 5.1. Generally, higher fractal dimensionality and fracture energy are observed as rubber replacement level increases. This means that as rubber content increases, more energy will be dissipated during fracture of the sample as suggested by [Guo et al. \(2007\)](#) and [Erdem \(2012\)](#). The possible explanation for this phenomenon is that when the cracks developed they propagated through the weak points (i.e., rubber particles), as noted previously. Before the crack propagation, the rubber particles are able to absorb some of the energy developed at the crack tip as the tip reaches them, especially at the microcracking level. This is due to rubber's extensibility and tensile strength. In addition, more energy will disperse since the cracks more easily propagate as branches rather than as one main crack, which agrees with [Yan et al. \(2003\)](#) who attributed this to the disordered crack growth characteristics found in a mixture's internal structure during load application. Together, these explanations determine why more energy was absorbed by the mixture before failure.

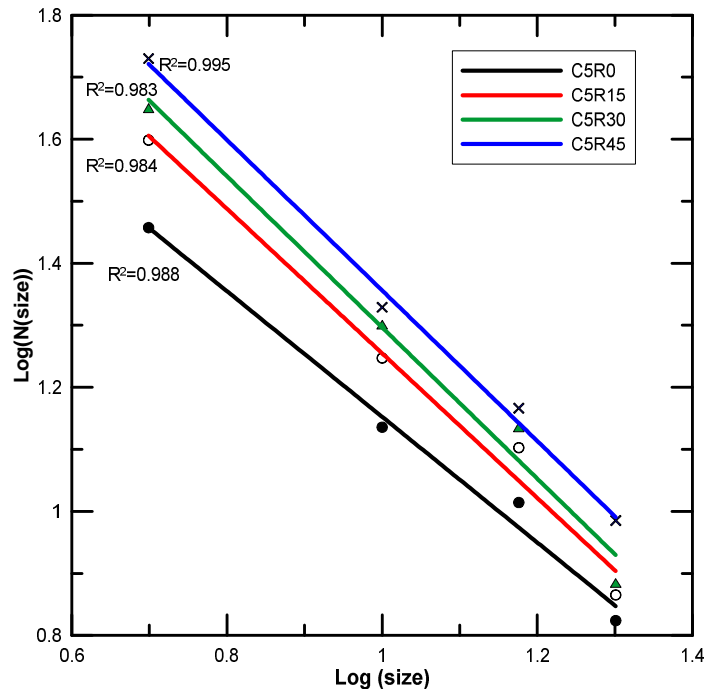


Figure 5.44: A graph of log of box count against the log of box size for mixtures of different rubber contents

The dissipated energy at the surface macro-crack as derived based on fractal analysis, seems related to the toughness of the mixture calculated from the load-deformation responses where both increased after rubber incorporation. This supports the above explanation and confirms that a strong relationship exists between the cracking pattern, represented by the fractal dimension, and the toughness, a finding which is consistent with [Yan et al. \(2002\)](#) and [Tang and Wang \(2012\)](#). It is also in line with energy dissipation capacity improvement reported by [Atahan and Yücel \(2012\)](#) when they investigated the effect of rubber on the fracture energy of normal concrete during impact tests.

On the other hand, the fractal dimensions and corresponding fracture energies for different cement contents for both reference and rubberized mixtures are shown in Figure 5.45 and Table 5.1. It can be clearly seen that the use of rubber has increased the fractal dimension and accordingly the fracture energy for all cement contents with maximum improvement occurring at moderate cement content (5%). The reason for the large increase in fractal dimension and fracture energy due to rubber inclusion at 5% cement content is unclear. Regarding the cracking density, Table 5.1 confirms the increase in the cracking density as the rubber content increases. This, in turn, indicates that the cracks were propagated and separated over a large area as reported by Hassan (2012). In other words, this wide separation indicates that the crack propagated through rubber particles which, in turn, supports the previous hypotheses reported in the current investigation (Section 5.4.4).

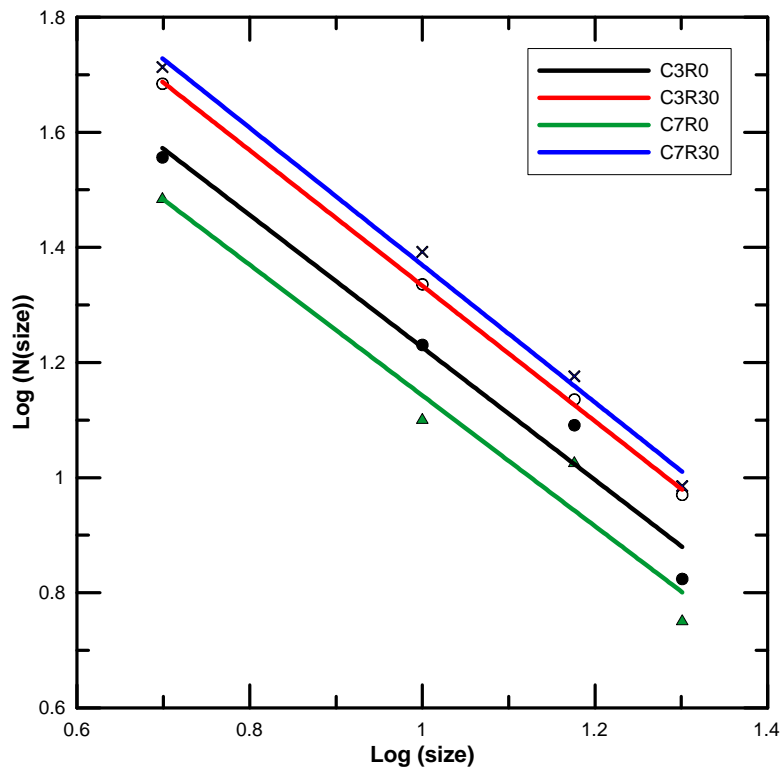


Figure 5.45: A graph of log of box count against the log of box size for reference and rubberized mixtures of different cement contents

### 5.4.7 Comparison fracture energy

Comparison between different methods for fracture energy and toughness estimation reveals that, regardless of the numeric values, these approaches give the same picture regarding the improvement in toughness and fracture energy after rubber inclusion at each investigated cement contents. Inspection of Table 5.1 indicates that at 5% cement content for example, the toughness and fracture energy improved after inclusion of 15%, 30% and 45% rubber content. On the other hand, toughness and fracture energy were also enhanced for C3R0 and C7R0 when modified with 30% of crumb rubber. This leads to the conclusion that the estimation of toughness or fracture energy can provide a quick and simple method to judge the effect of changes in mix parameters.

Table 5.1: Fracture energies and toughness indices based on fractal analysis and experimental procedures

Mix	Crack density	Fractal dimension	Fracture energy		Toughness	
			Fracture energy Williford (1998)	Ws/Gf	Williford (1998)	Experimental
C5R0	0.0175	1.013	0.02004	103.99	0.801	0.500
C5R15	0.0247	1.166	0.02734	164.40	0.906	0.613
C5R30	0.0319	1.219	0.03190	192.70	0.945	0.550
C5R45	0.0329	1.214	0.03056	189.67	0.941	0.545
C3R0	0.0230	1.151	0.03080	157.06	0.895	0.575
C3R30	0.0321	1.177	0.05964	169.88	0.914	0.647
C7R0	0.0205	1.135	0.02439	149.93	0.883	0.001
C7R30	0.0334	1.193	0.03006	178.06	0.926	0.530

#### 5.4.8 Overall discussion of failure mechanism

Duarte et al. (2015) based on their finite element simulation of the ITS test, concluded that the initiation of cracks starts in the cement matrix near the rubber particle. In addition, they revealed that the damage and cracking is more concentrated in the concrete mixtures containing no rubber but this is not the case for the rubberized concrete where the damage is more dispersed. Examining the failure pattern and observing the internal structure of the failed specimens revealed that, regardless of the cement content, the cracks tend to propagate through the rubber particles which is also shown from the fractal analysis where the cracks are more dispersed in rubberized mixtures. However, it seems that this tendency depends to some extent on the degree of cementation by the cement paste, where greater tendency was observed when the cement content was higher. It is believed that this behaviour is strongly interrelated with the void-like behaviour (mentioned earlier) of these rubber particles. Rubber particles embedded inside a stiff matrix behave like a void which attracts the crack. When this happen, the crack will reach the rubber and the latter will try to absorb and relieve the stress on the crack tip. For this reason, the rubber particles will delay the crack growth at microcracking stage and propagation at the macroscale level. This explanation is supported by the load-deflection curves. For this reason, more toughness was observed in rubberized mixtures of high cement content. Similarly, at moderate cement level, the toughness was also improved due to the reasons above. However, comparing and contrasting the reference and rubberized mixtures' behaviour at high and moderate cement contents revealed that the degree of toughness improvement is higher at high cement content whereas this is not the case for 5% cement. In the latter mixture, less improvement was observed due to rubber inclusion. This is because, for the reference mixture of 5% cement content,

the less dense matrix structures may have micro-voids that delay the crack propagation since these micro cracks consume part of the energy due to the micro-crack shielding phenomenon defined by [Shah et al. \(1995\)](#) as cited in [Erdem \(2012\)](#). Consequently, for this reason, this mixture exhibited certain toughness. Per contra, reference mixtures stabilized with 7% cement might have a dense matrix and better bond with the aggregate particles which reduces, or may eliminate, the toughness of these mixtures. When rubber is introduced into these mixtures, propagating cracks through the rubber particles and hence lengthening the crack path, combined with delaying crack growth, are the reasons for greater improvement in the mixtures with high cement contents.

#### **5.4.9 Cyclic indirect tensile testing**

The indirect tensile stiffness modulus under cyclic loading follows the same trend as the static indirect tensile modulus as shown in Figure 5.46 and Figure 5.47 where a drop occurred in this parameter due to rubber incorporation as discussed in Section 5.4.2. However, comparing stiffness modulus value under cyclic load (Figure 5.46 and Figure 5.47) with those under static load (Figure 5.40 and Figure 5.41) reveals that stiffness under cyclic loading is always greater than the static stiffness modulus (Figure 5.50). Similar behaviour was observed by [Gnanendran and Piratheepan \(2008\)](#). This might be attributed to the rate at which the load was applied. The greater the loading rate the more the stiffness modulus.

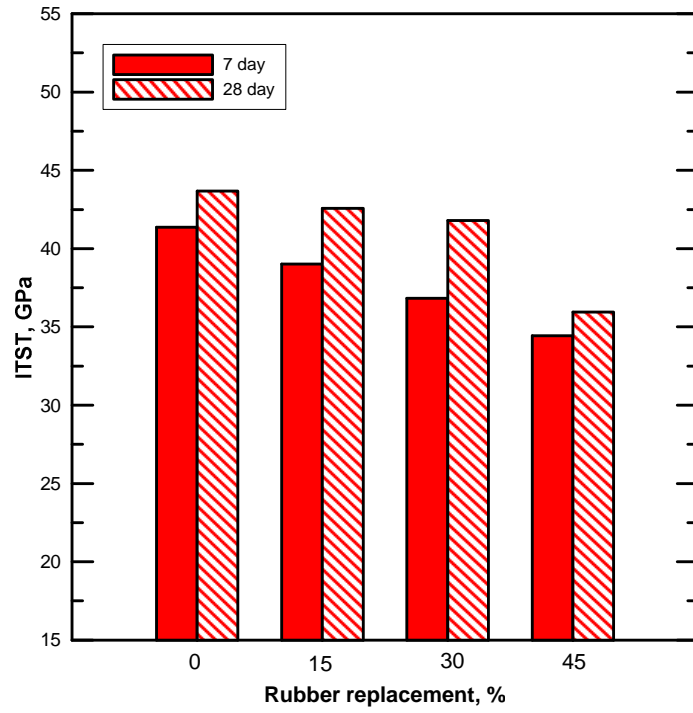


Figure 5.46: Effect of different rubber contents on indirect tensile resilient modulus

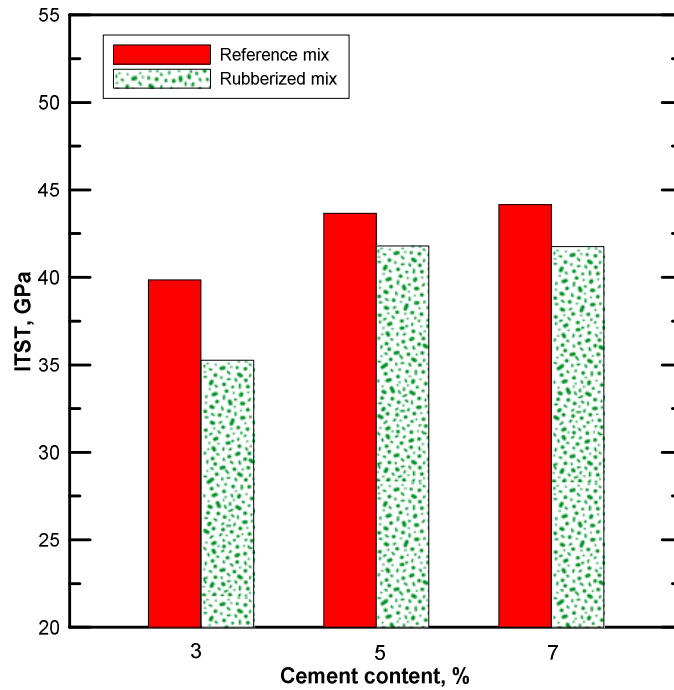


Figure 5.47: Effect of cement content on indirect tensile resilient modulus

Similarly to the static case (Figure 5.41), both reference and rubberized mixtures clearly showed the same trend in the stiffness value with the greater stiffness loss when rubber is added at low cementation level (Figure 5.47). Therefore it is possible to conclude that the NAT machine is an appropriate device to estimate the stiffness modulus under dynamic loading. In addition, it is possible to estimate this dynamic stiffness modulus from the testing under monotonic loading or vice versa, as there is a linear relationship between these two parameters as illustrated in Figure 5.48 with a high degree of correlation ( $R^2=0.98$ ).

Since this correlation covers a range of cementitious mixtures (cement and rubber contents), it can be inferred that a unique relationship exist between these parameters regardless of degree of stabilization and aggregate composition. Figure 5.49 and Figure 5.50 demonstrates the linear relationship between ITS and UCS and dynamic stiffness modulus, respectively, which also shows a fairly high degree of correlation although there are clear outliers (Figure 5.48). All these relationships are in a good agreement with those reported by [Gnanendran and Piratheepan \(2008\)](#). These authors have reported that the simple relationships between UCS or ITS and the more advanced tests can be considered as an important tool for estimating pavement design inputs especially in the absence of sophisticated equipment and/or professionals.

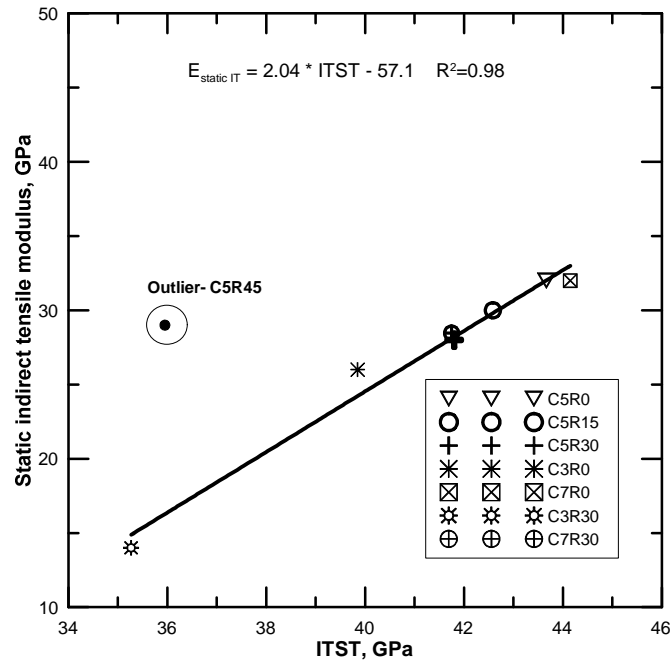


Figure 5.48: Correlation of indirect tensile moduli under static and cyclic loading

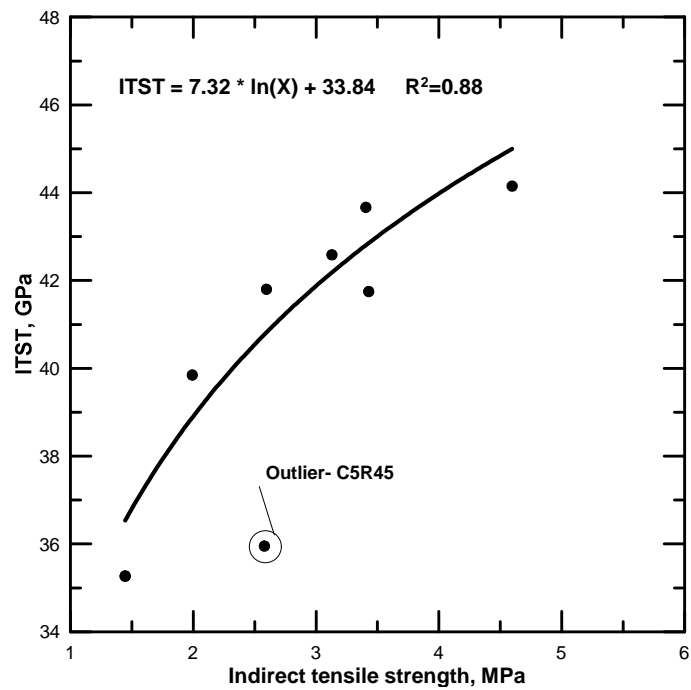


Figure 5.49: Variation of ITST versus ITS

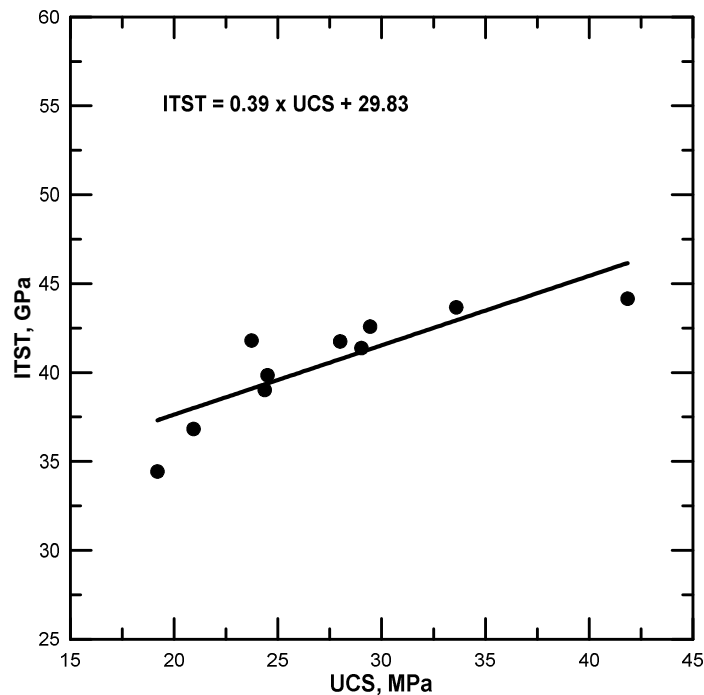


Figure 5.50: Variation of ITST versus UCS

### 5.5 Concluding Remarks

Based on the experimental program and the analysis of results discussed in this chapter:

1. There was a drop in both UCS and ITS for the mixtures in which the natural aggregate was replaced by the crumb rubber at all investigated cementation levels. This can be attributed to the lower stiffness and strength of the rubber particles as compared with the natural aggregates. Another contributory factor to this decline is the damping effect of the rubber particles which affects the compaction negatively.
2. Both ITS and UCS improved when mixtures contained more cement for both CSAMs and RCSAMs. In addition, both of these strength parameters increase as

curing period increase. This is due to the relative improvement in compactibility of the mixtures and due to the increase in the hydration products as a result of increase in cement content and/or curing period. This latter increase is responsible for the enhancement of both the matrix strength and the bond between this matrix and the aggregate particles.

3. Failure patterns of both ITS and UCS samples confirm a ductile behaviour once rubber is added. The higher integrity and narrower cracking of the rubberized mixtures as compared with those containing no rubber is beneficial for overlying pavement surface courses since it may contribute to mitigating reflection cracking from the base course (where rubber modified mixtures would be used) cracking.
4. Behaviour of cemented rubberized mixtures containing different cement contents is governed by the relative stiffness of rubber particles and surrounding materials. At low cementation levels, the relative stiffness is low which permits more even stress/strain distribution across the sample and hence less stress concentration near the rubber particles. In the mixtures with high cement content, on the other hand, the stiffness mismatch between rubber and matrix is high which causes more stress concentrations around the rubber particles since the surrounding matrix absorbs more energy proportional to its stiffness. In other words, at high cementation level the rubber particles might behave like a void, with the degree of this void-like behaviour dependent on the cement content. This behaviour caused a greater decrease in the material's strength when rubber particles were introduced in rich cement mixtures compared to less reduction in more poorly cemented mixtures.

5. Characterization of the stress-strain relationship in compression is extremely difficult even in rubber rich concrete mixtures. Recorded strain values are usually heavily dependent on sample preparation and instrumentation for accurate measurement because of a very low deformation at failure.
6. It was observed that the ITS is around 10% of the corresponding UCS. The relationship between ITS and UCS is independent of aggregate composition and degree of cementation.
7. An improvement in the mixtures' toughness occurred due to rubber incorporation. This improvement is thought to be due to both delaying the crack propagation at micro and macro levels by relieving the stress induced at the crack tip and due to lengthening the crack path when cracks propagate through rubber particles. In this study both of these mechanisms were evidenced. On the other hand, a drop in the material toughness was observed when more cement was used with greater reduction at high cement content. In contrast, the greater improvement in toughness occurred at high cement content after rubber modification of the mixture. Nevertheless, the toughness improved after introducing rubber particles at all cement contents.
8. Inclusion of rubber inside cement-stabilized mixtures reduced the material stiffness which can be attributed to the softness of the rubber particles as compared to the natural aggregate. For all cement contents less stiff mixtures were produced when the rubber was used with the most significant reduction observed at low cementation degree.

9. Results were compared with previous studies conducted by other authors .This gives more validity to the previously proposed correlations since the current research was conducted on various aggregate compositions and cement contents. At the same time, it defines on how cement and rubber may affect the relationship between different mechanical properties. Moreover, the greater confidence in these property relationships permits estimation by simple and available testing methods of the properties that would otherwise require advanced tests.
10. Fractal analysis reveals a higher fractility of the mixtures with increasing rubber which indicates more energy is dissipated during the fracture process. This can be considered a positive sign regarding the fatigue performance.
11. As compared with experimental or experimental-fractal analysis methods, estimation of the toughness and/or fracture energy can be conducted, with some degree of reliability, based on the analysis of surface cracks utilizing the fractal analysis alone.
12. As compared with difficulties encountered in terms of preparation of testing setup, accuracy of instrumentation and interpretation of results, using the NAT machine to characterize cementitious stabilized materials can be considered an excellent option to evaluate the behaviour of these mixtures under dynamic loading. However, adopting the procedure used normally for evaluating asphaltic mixtures in this machine would be likely to deliver misleading and inaccurate results for cementitious materials. This is because the standard procedure does not ensure that these stiff materials are tested within their elastic range.

## 5.6 References

- Applied Research Associates, I. (2004). Guide for Mechanistic-Empirical Design of New and Rehabilitated Pavement Structures. Illinois.
- Arellano, D. and M. R. Thompson (1998). Stabilized Base Properties (Strength, Modulus, Fatigue) for Mechanistic-Based Airport Pavement Design, Final Report, Technical Report of Research, Department of Civil Engineering University of Illinois at Urbana-Champaign, Illinois.
- Arnold, G., C. Morkel and G. van der Weshuizen (2012). Development of tensile fatigue criteria for bound materials, NZ Transport Agency report No. 463, New Zealand Institute of Highway Technology.
- Atahan, A. O. and A. Ö. Yücel (2012). "Crumb rubber in concrete: Static and dynamic evaluation." *Construction and Building Materials* 36: 617-622.
- Barišić, I., T. Dokšanović and H. Draganić (2015). "Characterization of hydraulically bound base materials through digital image correlation." *Construction and Building Materials* 83: 299-307.
- Carpinteri, A., B. Chiaia and S. Invernizzi (1999). "Three-dimensional fractal analysis of concrete fracture at the meso-level." *Theoretical and Applied Fracture Mechanics* 31(3): 163-172.
- Chiaia, B., J. Van Mier and A. Vervuurt (1998). "Crack growth mechanisms in four different concretes: microscopic observations and fractal analysis." *Cement and Concrete Research* 28(1): 103-114.
- Duarte, A., B. Silva, N. Silvestre, J. de Brito and E. Júlio (2015). "Mechanical characterization of rubberized concrete using an image-processing/XFEM coupled procedure." *Composites Part B: Engineering* 78: 214-226.

- Erdem, S. (2012). Impact load-induced microstructural damage of concrete made with unconventional aggregates. PhD thesis, University of Nottingham.
- Erdem, S. and M. A. Blankson (2013). "Fractal–fracture analysis and characterization of impact-fractured surfaces in different types of concrete using digital image analysis and 3D nanomap laser profilometry." *Construction and Building Materials* 40: 70-76.
- Erdem, S., A. R. Dawson and N. H. Thom (2012). "Impact load-induced microstructural damage and micro-structure associated mechanical response of concrete made with different surface roughness and porosity aggregates." *Cement and Concrete Research* 42(2): 291-305.
- Farhidzadeh, A., E. Dehghan-Niri and S. Salamone (2014). "Crack pattern quantification of concrete structures based on fractal analysis." *Safety, Reliability, Risk and Life-Cycle Performance of Structures and Infrastructures*: 361.
- Gaspard, K., L. Mohammad and Z. Wu (2003). Laboratory Mechanistic Evaluation of soil cement mixtures with fibrillated-polypropylene-fibers. Proceeding of the 82nd Transportation Research Board Annual Meeting.
- Gnanendran, C. T. and J. Piratheepan (2008). "Characterisation of a lightly stabilised granular material by indirect diametrical tensile testing." *International Journal of Pavement Engineering* 9(6): 445-456.
- Grinys, A., H. Sivilevičius and M. Daukšys (2012). "Tyre rubber additive effect on concrete mixture strength." *Journal of Civil Engineering and Management* 18(3): 393-401.
- Guo, L.-P., W. Sun, K.-R. Zheng, H.-J. Chen and B. Liu (2007). "Study on the flexural fatigue performance and fractal mechanism of concrete with high

proportions of ground granulated blast-furnace slag." *Cement and Concrete Research* 37(2): 242-250.

Hassan, N. A. (2012). *Microstructural characterization of rubber modified asphalt mixtures* PhD thesis, The university of Nottingham.

Huang, B., X. Shu and G. Li (2005). "Laboratory investigation of portland cement concrete containing recycled asphalt pavements." *Cement and Concrete Research* 35(10): 2008-2013.

Issa, M. and A. Hammad (1994). "Assessment and evaluation of fractal dimension of concrete fracture surface digitized images." *Cement and Concrete Research* 24(2): 325-334.

Ji, X., Y. Jiang and Y. Liu (2015). "Evaluation of the mechanical behaviors of cement-stabilized cold recycled mixtures produced by vertical vibration compaction method." *Materials and Structures*: 1-14.

Khattak, M. J. and M. Alrashidi (2006). "Durability and mechanistic characteristics of fiber reinforced soil–cement mixtures." *International Journal of Pavement Engineering* 7(1): 53-62.

Khelifi, H., T. Lecompte, A. Perrot and G. Ausias (2015). "Mechanical enhancement of cement-stabilized soil by flax fibre reinforcement and extrusion processing." *Materials and Structures*: 1-14.

Liu, R. (2013). *Recycled Tires as Coarse Aggregate in Concrete Pavement Mixtures*.

Löfgren, I. (2005). *Fibre-reinforced Concrete for Industrial Construction--a fracture mechanics approach to material testing and structural analysis*, PhD thesis, Chalmers University of Technology.

- Marradi, A. and F. Lancieri (2008). Performance of cement stabilized recycled crushed concrete. First International Conference on Transport Infrastructure ICTI, Beijing, China.
- Mihashi, H., S. Ahmed, T. Mizukami and T. Nishiwaki (2006). "Quantification of crack formation using image analysis and its relationship with permeability."
- Modarres, A. (2013). "Investigating the toughness and fatigue behavior of conventional and SBS modified asphalt mixes." *Construction and Building Materials* 47: 218-222.
- Modarres, A. and Z. Hosseini (2014). "Mechanical properties of roller compacted concrete containing rice husk ash with original and recycled asphalt pavement material." *Materials & Design* 64: 227-236.
- Nunes, M. C. M. (1997). Enabling the use of alternative materials in road construction, PhD thesis, University of Nottingham.
- Nusit, K., P. Jitsangiam, J. Kodikara, H. H. Bui and G. L. M. Leung (2015). "Dynamic Modulus Measurements of Bound Cement-Treated Base Materials." *Geotechnical Testing Journal*, Vol.38, No.3 38(3): 1-15.
- Pramanik, B., T. Tadepalli and P. R. Mantena (2012). "Surface fractal analysis for estimating the fracture energy absorption of nanoparticle reinforced composites." *Materials* 5(5): 922-936.
- Scullion, T., J. Uzan, S. Hilbrich and P. Chen (2008). "Thickness Design Systems for Pavements Containing Soil-Cement Bases." *PCA R&D Serial*(2863).
- Shah, S. P., S. E. Swartz and C. Ouyang (1995). "Fracture mechanics of concrete." John Willy & Sons Inc, New York.
- Shahid, M. A. (1997). "Improved Cement Bound Base Design for Flexible Composite Pavement." PhD Thesis, University of Nottingham.

Sobhan, K. and M. Mashnad (2000). "Fatigue durability of stabilized recycled aggregate base course containing fly ash and waste-plastic strip reinforcement." Final Rep. Submitted to the Recycled Materials Resource Centre, Univ. of New Hampshire.

Solanki, P. (2010). Characterization of cementitiously stabilized subgrades for mechanistic-empirical pavement design, PhD thesis, The university of Oklahoma

Solanki, P. and M. Zaman (2013). "Behavior of Stabilized Subgrade Soils under Indirect Tension and Flexure." *Journal of Materials in Civil Engineering* 26(5): 833-844.

Tang, W. and Y. Wang (2012). "Fractal characterization of impact fracture surface of steel." *Applied Surface Science* 258(10): 4777-4781.

Wen Haifang, M. B., Wang Jingan, Li Xiaojun, Edil Tuncer, Tinjum James (2014). Characterization of Cementitious Stabilized Layers for Use in Pavement Design and Analysis. Washington, DC, National cooperative highway research program

Yan, A., K.-R. Wu, D. Zhang and W. Yao (2003). "Influence of concrete composition on the characterization of fracture surface." *Cement and Concrete Composites* 25(1): 153-157.

Yan, A., K. Wu and X. Zhang (2002). "A quantitative study on the surface crack pattern of concrete with high content of steel fiber." *Cement and Concrete Research* 32(9): 1371-1375.

### **Specifications**

BS EN 13286-41:2003, Hydraulically bound mixtures- Part 41: Test method for determination of the compressive strength of hydraulically bound mixtures, British Standards Institutes, London

BS EN 14227-1:2013, Hydraulically bound mixtures- Specification- Part 1: Cement bound granular mixtures, British Standards Institutes, London

BS EN 13286-42, Hydraulically bound mixtures- Part 42: Test method for determination of the indirect tensile strength of hydraulically bound mixtures, British Standards Institutes, London

BS EN 13286-43:2003, Hydraulically bound mixtures- Part 43: Test method for determination of the modulus of elasticity of hydraulically bound mixtures, British Standards Institutes, London

## **Chapter Six**

### **Flexural Characterization and understanding**

#### **6.1 Introduction**

Many authors (Arellano and Thompson 1998; Disfani et al. 2014; Arulrajah et al. 2015) confirm that cementitiously stabilized pavement layers, in realistic conditions, are subjected to bending action. Therefore, they stated that the flexural test is the most simulative to what is actually experienced in reality. Consequently, the flexural test as reported by Disfani et al. (2014) is considered the preferred method to characterize cementitiously stabilized materials as compared with other methods. In addition, unlike the direct and indirect tensile testing methods, flexural testing

produces a uniform tensile stress at the bottom of sample and does not need special gripping or alignment arrangements, respectively. Notwithstanding, the indirect tensile testing mode is still an important alternative due to the difficulties in preparing and handling the prisms (Solanki 2010) or in case of weakly cemented samples which may be damaged during installation in the flexural test arrangement. However, this test is criticized since it considers only the uniaxial stress state (Triches 2009). Even though the characterization of a pavement under dynamic load application is more realistic because of its simulative nature, it is necessary to evaluate the behaviour under monotonic loading to estimate the stress ratios required to evaluate the behaviour under dynamic loading. These important flexural characteristics include strength, toughness, modulus and fatigue.

The objective of this chapter is to provide a comprehensive evaluation of the flexural properties of RCBGMs containing different percentages of crumb rubber. At the same time the effect of cement content on the properties of RCSAMs is compared with those of CSAMs. It is worth mentioning that some of the latter properties are prerequisites for the fatigue performance evaluation which will be presented in Chapter 9.

To understand the performance of the different mixtures under flexural loading and their failure mechanism, a part of this chapter is directed to study the fractured surfaces at mesoscale level. This includes firstly the characterization of these fractured surfaces and, secondly, quantitative evaluation and comparison. The purpose is to investigate the potential relationship between crumb rubber particles and the type of cracking and the effect of these soft rubber particles on the crack

propagation during flexural loading. Since the distribution of crumb rubber inside a cement-stabilized mixture is likely to play an important role in stress and strain distribution across the different types of specimens, it was decided to assess, quantitatively, this distribution and to evaluate the probable segregation of these particles.

## **6.2 Materials, mixture design and samples preparation**

The same materials and mixture design were used as discussed in Chapter 4. All mixing was conducted in a pan mixer with a capacity of 0.1 m<sup>3</sup>. In terms of mixing sequence, the cement and dust were firstly mixed together until a uniform colour was achieved then this was added to the rest of aggregate and mixed thoroughly for one minute. After that, mixing for another two minutes was done after adding the required quantity of water. To provide a meaningful comparison and correlations and to overcome any source of variability due to the change in rubber content or gradation ..., etc., it was decided to conduct two steps: firstly, to use the same compaction method used previously and, secondly, to batch, mix and compact each prism individually. Standard 100 mm x 100 mm x 500 mm steel moulds were used for manufacturing prisms. In order to achieve a uniform density, regular dimensions and a smooth surface for accurate testing, a mould extension was fabricated to fit on top of the mould and used so that more than a 100 mm height was achieved. The specimen was then sawn down to 100 mm height using a diamond saw. After placement in the mould, the mixture was compacted in three layers using a Kango 368 vibrating hammer fitted with a 100 mm x 100 mm square tamper. Figure 6.1 illustrates the manufacturing process steps.

Due to the fact that the compacted mixtures are sensitive to the density of the mixture, manufacturing uniform samples will permit comparison between different modified mixtures. Furthermore, it will eliminate the most of the variability that result due to differences in fabrication. To this end, the following methodology was used for prism manufacture. After mixing and placing the fresh materials into mould, the mix was compacted slightly and then a plywood plate of dimension to fit into the steel mould was used to fit above the fresh mix. Afterwards, compaction was applied in such a way as to ensure applying the same compaction effort for each part of the prism. The adopted compaction methodology is shown in Figure 6.1c. The compaction time was 60 second per layer at each position and each was scarified prior to compaction of the next layer. Triplicate samples were manufactured for each mix. All manufactured samples were left inside their moulds and covered with wet paper and polythene sheets to prevent moisture loss. After 24 hours, they were demoulded and wrapped with nylon film and placed in wet polythene bags and closed tightly. Then, they were moved to the humid room and kept for 28 days. After 28 days curing, samples were demoulded, then the samples were trimmed-off as shown in Figure 6.2. After that, the measurement of density was conducted using the water displacement method.

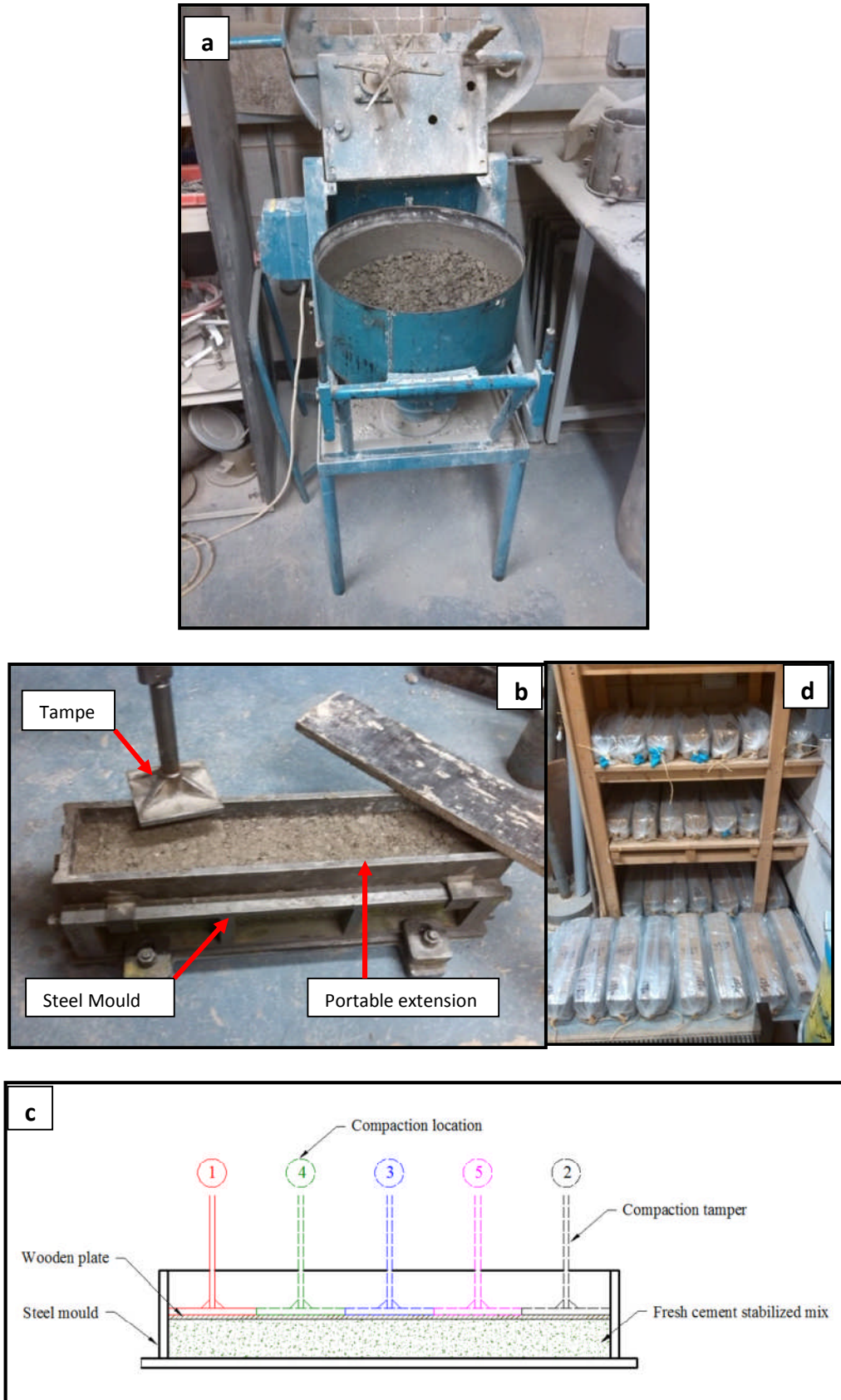


Figure 6.1: Sample preparation: a. mixing of materials; b. Sample moulds and moulding; c. compaction procedure and d. samples curing

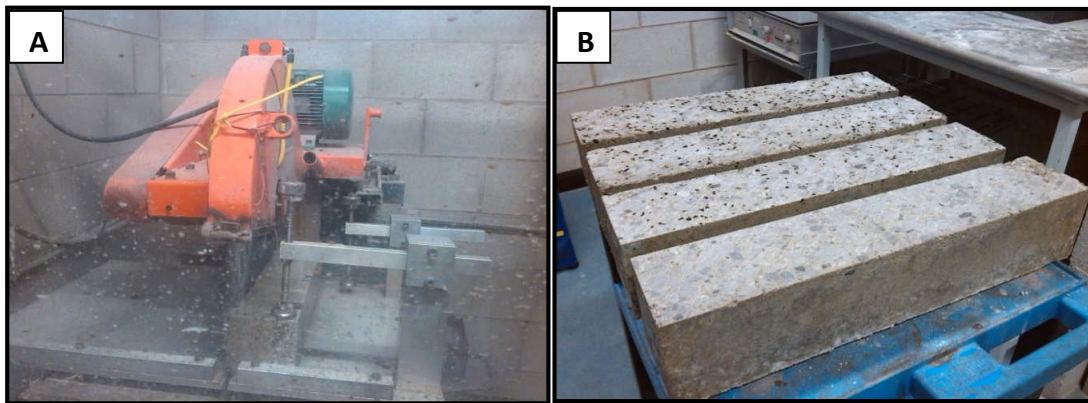


Figure 6.2: Sample preparations (a) sawing prismatic samples. (b) Sawn specimens

### 6.3 Testing equipment and procedure

Flexural testing was conducted in accordance with [BS 188: Part 118:1983](#). A 200 kN capacity closed loop deflection controlled Zwick 1484 universal testing machine was used for the static flexural testing program. The four-point bending test configuration was used for prismatic specimens spanning 300 mm. To obtain the post-peak load-deflection behaviour, the test was conducted under deformation control at a stroke rate of 0.05 mm/min and the corresponding deflection was measured at mid-span using two linear variable differential transducers (LVDTs). These were mounted utilizing the Japanese yoke arrangement. The average value from these two LVDTs was used as the measure of deflection at each load application. Figure 6.3 illustrates the flexural testing configuration.

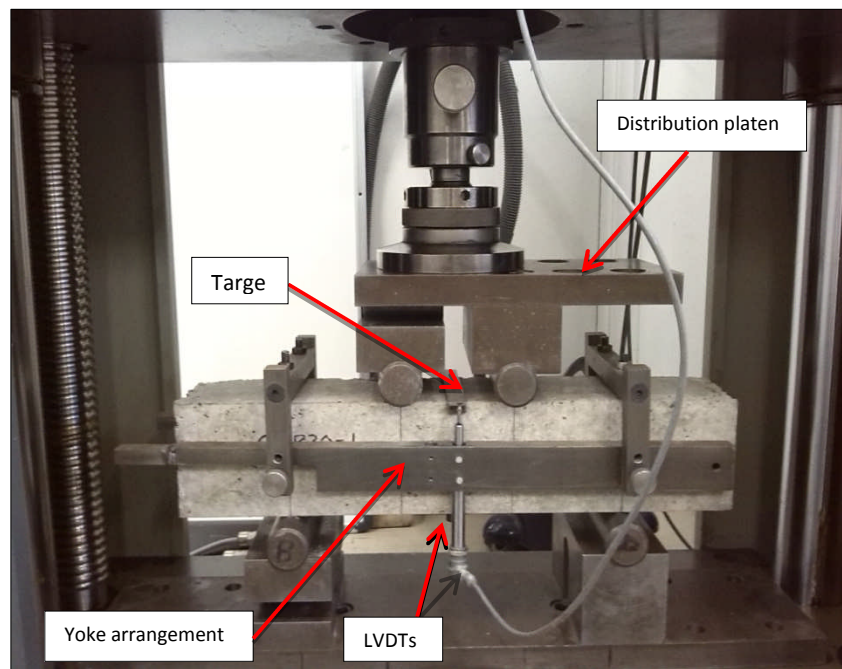


Figure 6.3: Static flexural testing configuration.

## 6.4 Methods of analysis

### 6.4.1 Flexural strength and static flexural modulus

Tests were conducted at 28-day age and the average of triplicate specimens was used to represent each mix. The flexural strength was computed utilizing the following formula

$$F_s = \frac{PL}{bh^2} \quad (6.1)$$

where  $F_s$ ,  $L$ ,  $P$ ,  $b$ ,  $h$  are the flexural strength in MPa, beam span in mm, ultimate load in N, width of the prism in mm and height of the prism in mm, respectively. Static flexural modulus of elasticity can be estimated from the linear part of the load-deflection curve based on 30% of the ultimate load and its corresponding deflection

(Arnold et al. 2012). Based on elastic theory, flexural stiffness modulus,  $E_f$ , can be computed using the following equation

$$E_f = \frac{Pa(3L^2 - 4a^2)}{4bh^3\delta} \quad (6.2)$$

If  $a = \frac{L}{3}$  is substituted in equation 6.2, then this becomes,

$$E_f = \frac{23PL^2}{108bh^3\delta} \quad (6.3)$$

where:  $a$  = span between load application points in mm and  $\delta$  = deflection at mid-span in mm. It should be noted that in this study the shear deformation was neglected. This is because the square of the ratio between beam height and span i.e.,  $(h/L)^2$  is much less than unity (Jitareekul 2009).

#### 6.4.2 Flexural toughness

Toughness can be considered as an indication of the ability of a material to absorb energy (Erdem 2012) or, in other words, it is an expression of the energy required to fully fail the specimen. In terms of normal concrete, a limited amount of research has been conducted to quantify the toughening effect due to rubber replacement (Najim and Hall 2012). Flexural toughness was estimated from the area under the load-deflection curves as standardized in the ASTM C 1018 method which is most widely used. This specification defines the toughness in terms of three indices ( $I_5$ ,  $I_{10}$  and  $I_{20}$ ) which were calculated by dividing the area under the load-deflection curve at

deflections of 3, 5.5 or 10 times the first crack deflection, respectively, by the area under the curve up to the deflection when the first crack was observed. Figure 6.4 illustrates the methodology of the toughness estimation procedure.

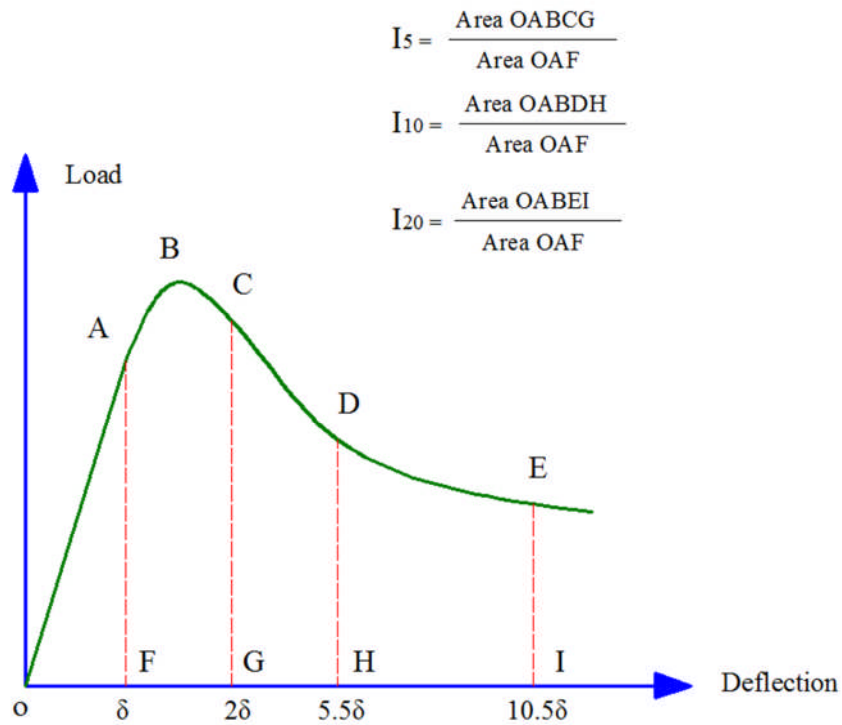


Figure 6.4: Toughness determination methodology. Redrawn from (Erdem 2012).

## 6.5 Flexural testing results and discussion

### 6.5.1 Flexural strength

Figure 6.5 illustrates the effect of rubber replacement on flexural strength. A clear reduction in strength is seen as the amount of rubber replacement increases. It seems that the introduction of rubber has an adverse effect on the aggregate interlocking, which can be considered, in this type of mixture, as the main factor for frictional resistance development. The latter is the mechanism by which the compacted mixtures resist applied traffic loading. In addition, the reduction in flexural strength

can be attributed also to the drop in both tensile and compressive strengths due to replacement of natural aggregate of high strength by the softer rubber particles.

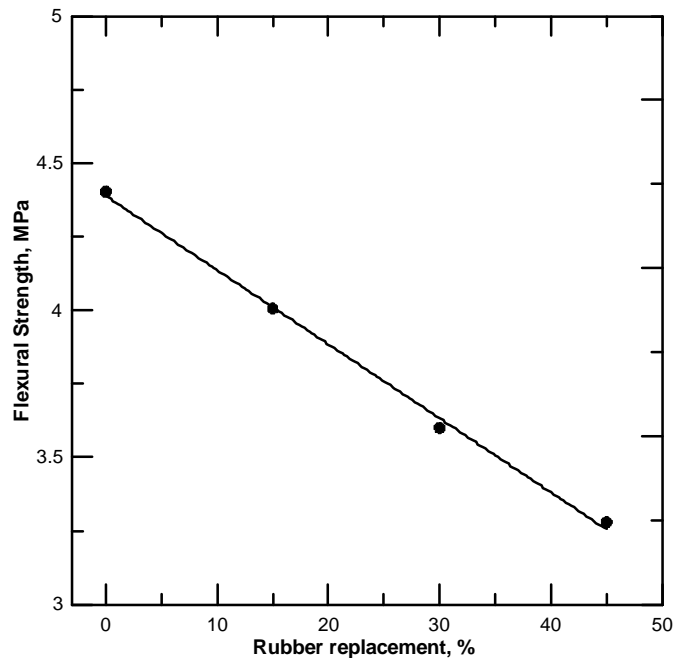


Figure 6.5: Effect of rubber replacement on flexural strength

Regarding the effect of cement, it can be seen from Figure 6.6 that increasing the amount of cement resulted in an increase in flexural strength of the material for both reference and rubberized mixtures due, no doubt, to increase in hydration products that enhanced bonding of aggregate with surrounding materials. Also, this is associated with an increase in both tensile and compressive strengths. The same figure also shows that the decrease in the material strength due to rubber inclusion is more pronounced in heavily stabilized materials than those lightly cemented. This behaviour is consistent with the trend observed in the indirect tensile testing program presented in Chapter 5. Therefore, it will be more feasible, from the strength point of view, to use rubber as an aggregate replacement in weakly cemented mixes. This is because in the stronger mixtures, the cost may increase due to using more cement

and causing more reduction in the material's strength. However, such a decision is not easy to take at this stage since the pavement structural design not only depends on strength but on other parameters such as stiffness and fatigue behaviour.

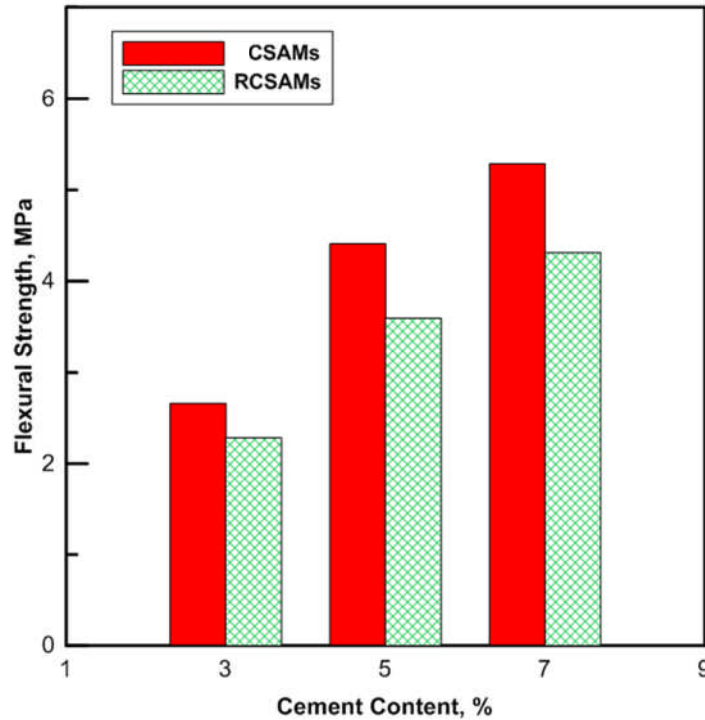


Figure 6.6: Effect of cement content on flexural strength

Figure 6.7 and Figure 6.8 depict the relationships between flexural strength and UCS and ITS, respectively. As can see from Figure 6.8, the tensile strength obtained from the indirect tensile method is less than the value estimated based on flexural testing. This is because the elastic behaviour assumed previously (Equation 6.3) does not occur up to failure (Williams 1986; Arellano and Thompson 1998). On the other hand, Figure 6.7 shows that there is a strong relationship between flexural strength and the UCS ( $R^2 = 0.99$ ). This means that the former value can be computed from the latter parameter. The developed correlation as presented on the figures is highly consistent with the suggested correlation in Wen et al. (2014). This suggests that the

correlation between the latter two parameters is a unique relation regardless of the aggregate composition and the degree of stabilization.

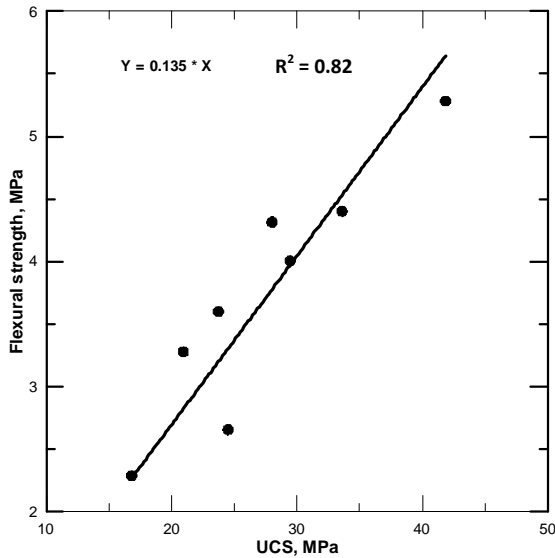


Figure 6.7: Flexural strength and UCS relationship.

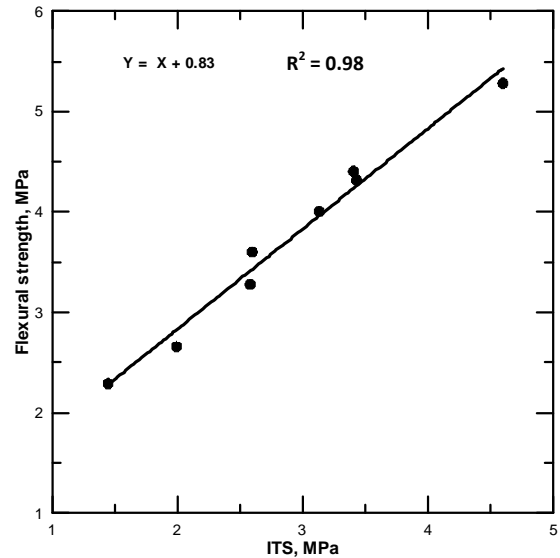


Figure 6.8: Flexural strength and ITS relationship.

### 6.5.2 Load-deformation relationships and flexural toughness

Figure 6.9 through Figure 6.16 show the load-deformation relationships for different investigated mixtures. From these, the toughness values were computed in accordance with the procedure discussed in Section 6.4.2. The conclusion that can be drawn from Figure 6.17 is that the replacement of natural aggregate by rubber enhances the toughness of the resulted mixtures. This can be attributed to the same reasons as discussed in Chapter 5 (Section 5.4.4).

These findings are very consistent with the behaviour observed under indirect tensile testing as presented in the previous chapter. Furthermore, many authors (Toutanji 1996; Aiello and Leuzzi 2010; Guleria and Dutta 2011; Najim 2012) have reported

similar improvement in flexural toughness due to the inclusion of rubber in concrete mixtures. In addition, this means improvement in deformability of the material and, hence, the formation of a more ductile material (Topcu 1995). In fact, this may ensure a mixture with less sensitivity to fatigue cracking which is, as reported by Brown (2012), the main mode of failure in bound base courses of pavement structures. This will be checked later in Chapter 9.

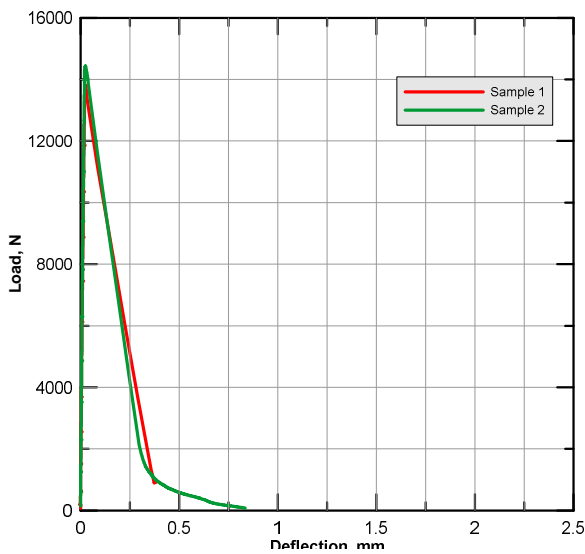


Figure 6.9: Load-deformation curves for C5R0

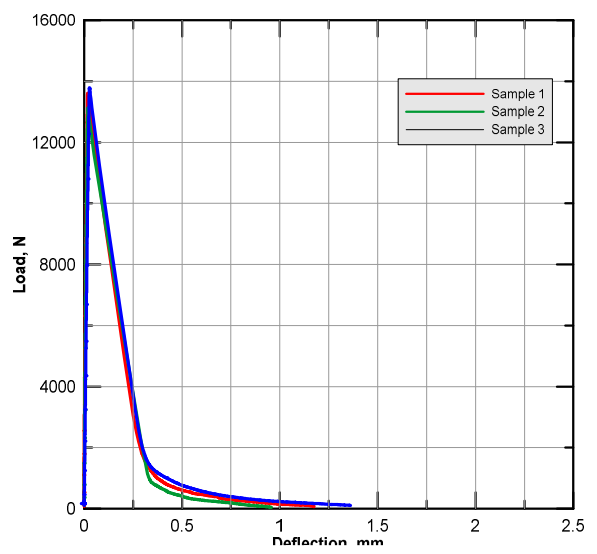


Figure 6.10: Load-deformation curves for C5R15

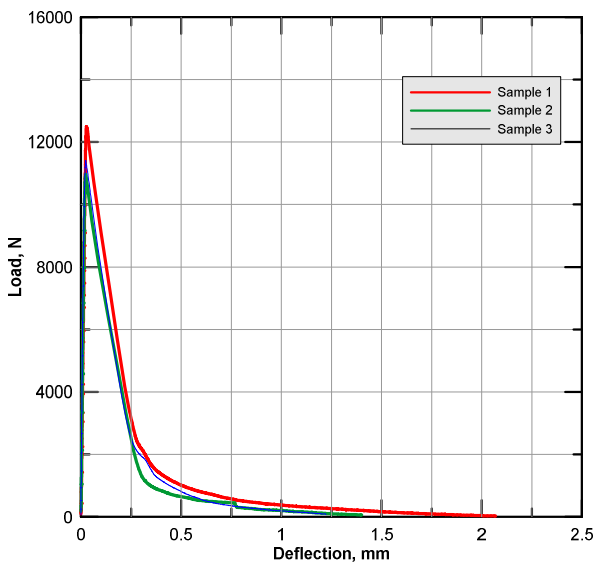


Figure 6.11: Load-deformation curves for C5R30

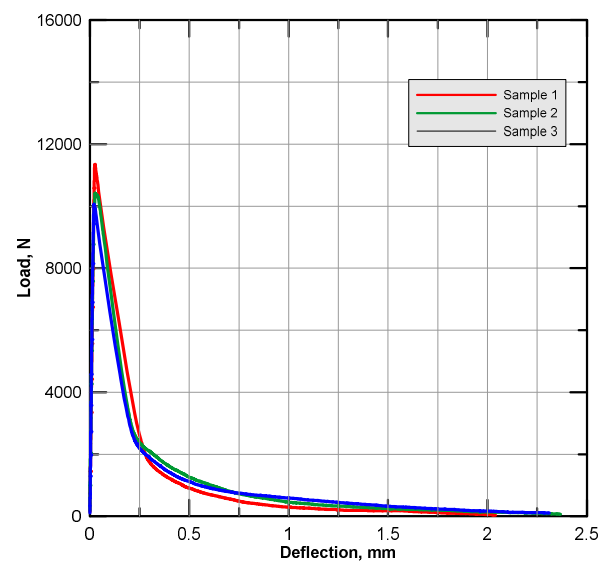


Figure 6.12: Load-deformation curves for C5R45

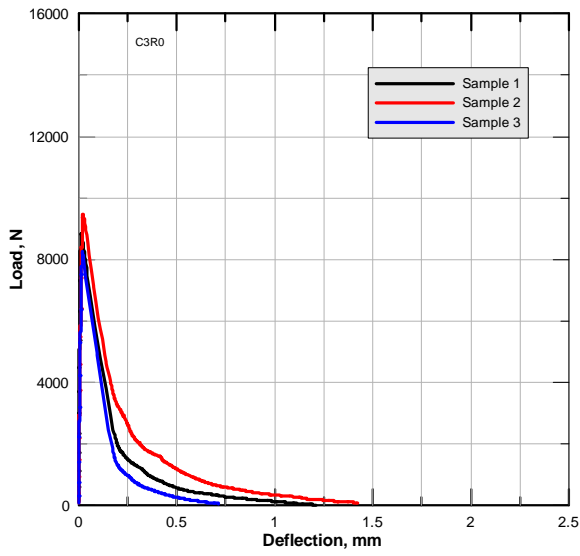


Figure 6.13: Load-deformation curves for C3R0

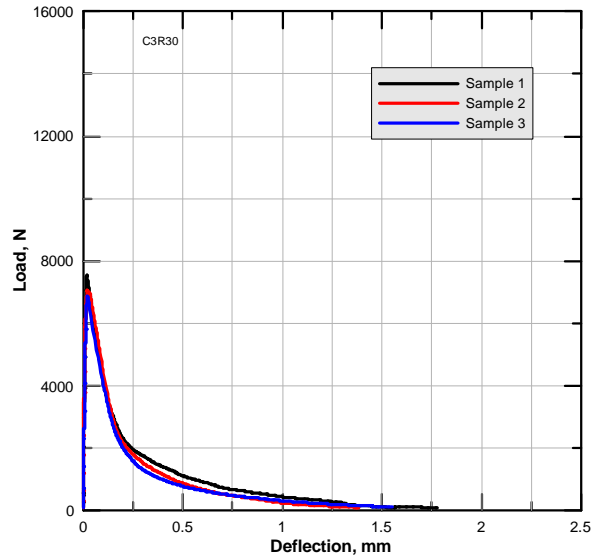


Figure 6.14: Load-deformation curves for C3R30

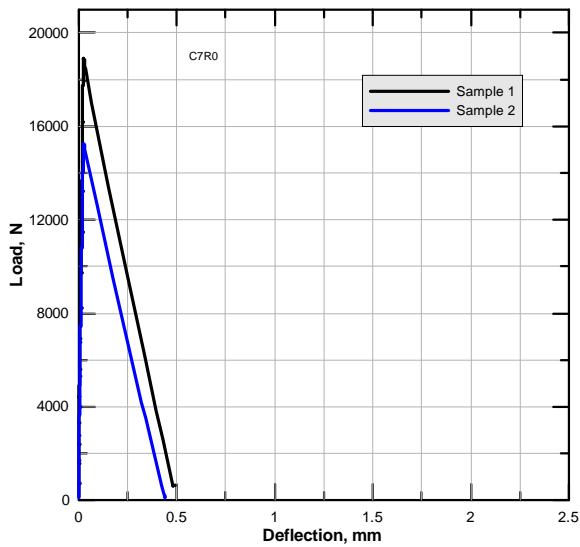


Figure 6.15: Load-deformation curves for C7R0

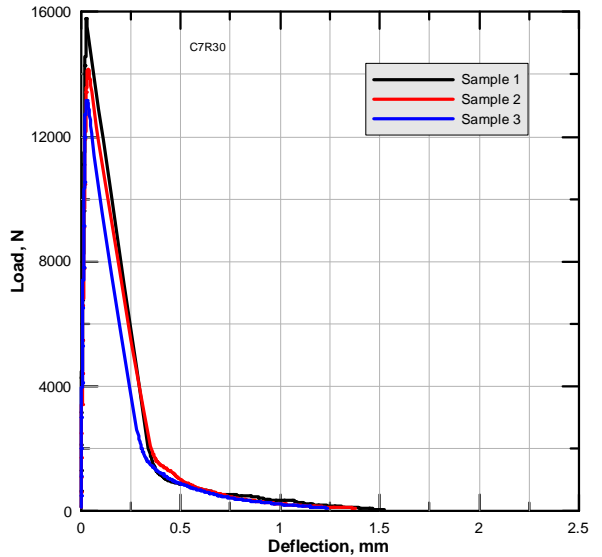


Figure 6.16: Load-deformation curves for C7R30

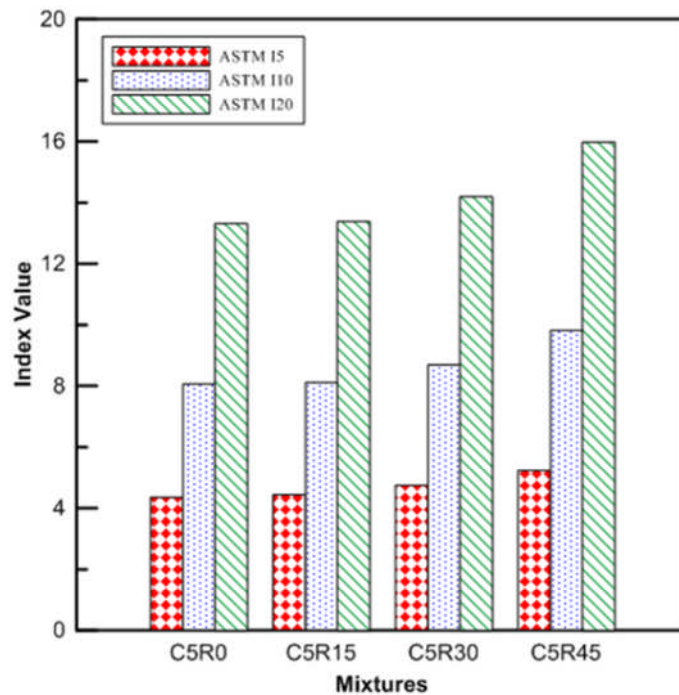


Figure 6.17: Toughness indices for CSAMs containing different amounts of rubber and 5% cement

In spite of the improvement in the material toughness due to the replacement of natural aggregate with rubber, the addition of more cement has no obvious effect on the toughness value of the rubberized mixtures. The toughness indices  $I_5$ ,  $I_{10}$ ,  $I_{20}$  for the CSAM and RCSAM show (Figure 6.18) the same behaviour at different cement contents. However, the toughness was improved due to rubber inclusion at all cement contents as is clear from the same figure. This supports the interpretation that the mechanism of a slight increase in toughness due to rubber addition may depend on the delaying (when the crack reaches the rubber particles) and lengthening (since the crack propagates through the rubber particles) of the crack propagation. If it were a crack bridging effect, we would expect to see increased toughness with increased cement content because of the better bond between rubber and adjacent material.

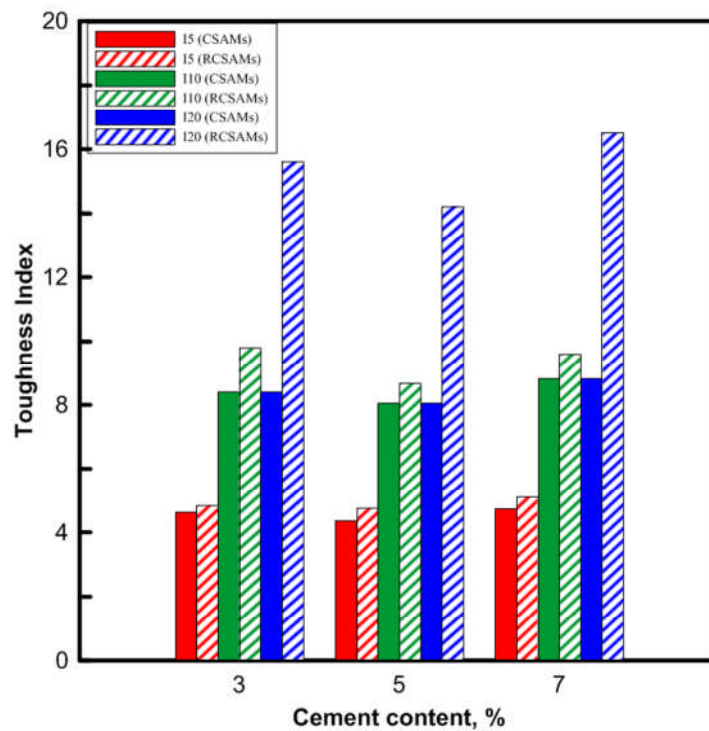


Figure 6.18: Toughness indices for CSAMs containing different amounts of cement and 30% rubber

### 6.5.3 Static flexural modulus of elasticity

Figure 6.19 clearly shows that there was a reduction in the stiffness of mixtures due to replacement with rubber particles. This, in fact, confirms the same behaviour presented previously (Chapter 5) and is in good agreement with previous findings conducted for concrete mixtures (Turatsinze and Garros 2008; Najim and Hall 2012).

By comparing and contrasting the CSAMs and RCSAMs (Figure 6.20), it seems that the increase in cement content has increased the materials' stiffnesses for both types with the same rate of change. However, there was a pronounced increase in the stiffness of the mixtures when cement content increased from 3% to 5% and little further benefit when the cement was increased to 7%. This may suggest, in terms of

stress attractiveness, that the use of higher than 5% cement to stabilize the mixture may not improve the ability of the mixtures to attract stress in pavement since the latter depends largely on the stiffness of that layer in which these mixtures will be used. In many circumstances a reduced stiffness without significant strength loss would be desirable, reducing brittleness and attraction of load. Nevertheless, increasing the latter by using stiffer cement-stabilized materials may be beneficial especially in cases that require designing the stabilized layer as the main structural layer of a pavement.

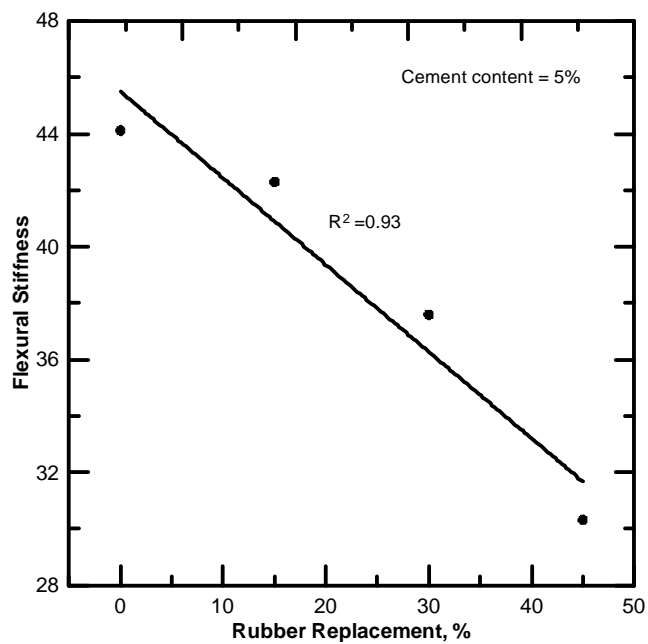


Figure 6.19: Effect of rubber replacement on static flexural stiffness

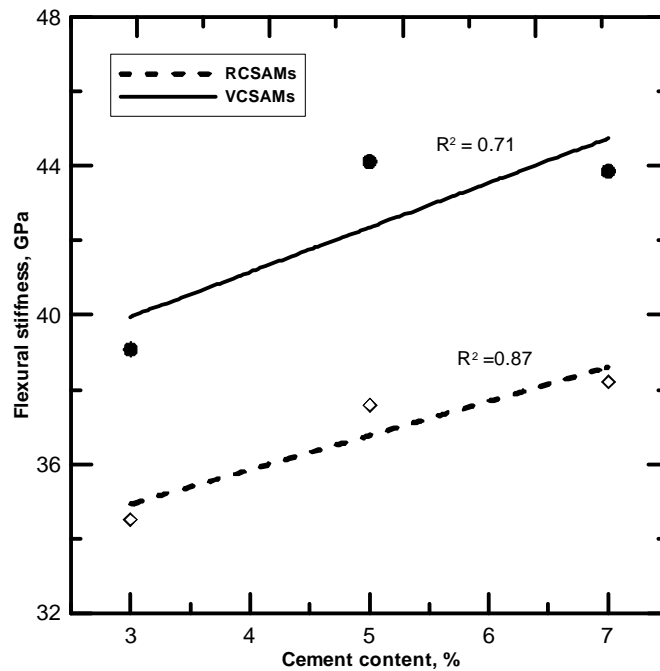


Figure 6.20: Effect of cement content on static flexural stiffness

Figures 6.21, 6.22 and 6.23 illustrate the relationships between static modulus of elasticity and UCS, ITS and flexural strength, respectively. From these, it can be concluded that there was a good relationship between these latter parameters. However, it seems that the UCS is better correlated with flexural modulus as compared with the other two. These correlations can be used to estimate, reliably, the flexural modulus from the simple parameters in case of the unavailability of advanced tests or skilled testing staff, as recommended by the Mechanistic-Empirical Pavement Design Guide under Input Level 2.

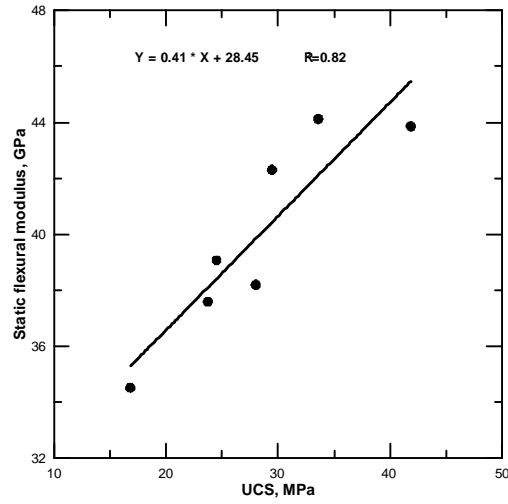


Figure 6.21: Static flexural modulus and UCS relationship

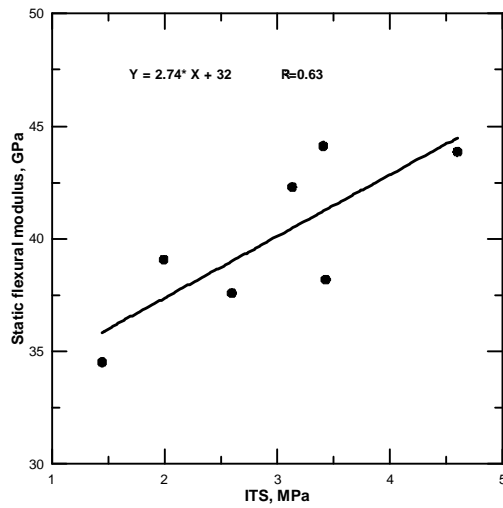


Figure 6.22: Static flexural modulus and ITS relationship

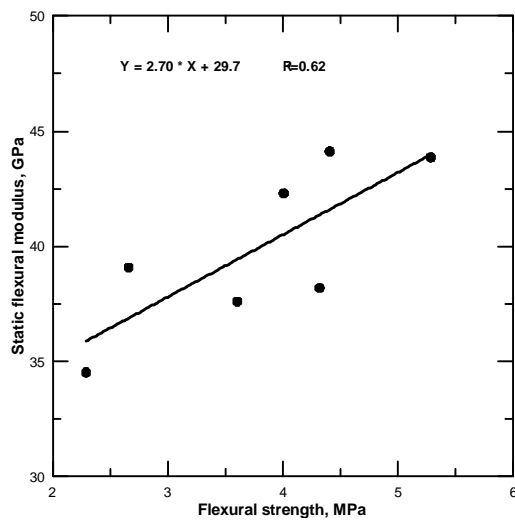


Figure 6.23: Flexural strength and modulus relationship

### 6.5.4 Failure patterns

Observing fractured surfaces of failed samples reveals that, at low cement contents (3%), the dislocation of the aggregate particles is the predominant failure mode. In samples contained 5% cement content, the cracks were propagated through the aggregate particles (aggregate fracture) and around the aggregate (aggregate dislocation). Finally, in highly cemented mixtures, the majority of aggregate particles were fractured. Figure 6.24 illustrates the three different failure patterns.

The reason behind these three failure patterns may be because of the different bond strengths between aggregate particles and the aggregate-cement matrix interface. This is largely controlled by the presence and penetration of the water-cement slurry under compaction pressure and because of the density of the cement matrix (fines plus cement) giving reasonable strength around the aggregate particles. The latter observations and explanation support the hypothesis proposed in Chapter4 (Section 4.3.1) regarding the performance obtained during vacuum-saturation testing.

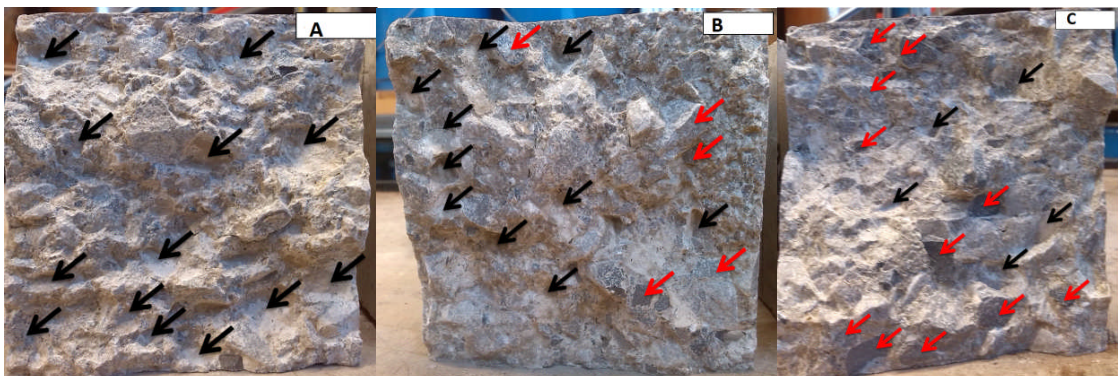


Figure 6.24: Failure pattern of CSAMs at different binding degrees: A.3% cement, B. 5% cement and C.7% cement (Red and black arrows indicate failure through and around aggregate, respectively)

## 6.6 Quantification of the flexural induced fractured surfaces

To provide more understanding regarding the effect of rubber on the behaviour of CSAMs and the mechanism of their failure, a quantitative evaluation of the flexural induced fractured surfaces was performed in terms of 3D tortuosity, volumetric surface texture ratio (VSTR) and roughness number (Ra).

### 6.6.1 Quantification parameters

#### 6.6.1.1 Volumetric Surface Texture Ratio (VSTR)

This was suggested by [Vandenbossche \(1999\)](#). The volumetric surface texture ratio (VSTR) is the texture volume above and below the mean plane (Figure 6.25) divided by the total projected area. VSTR can be calculated from predetermined segments on the surface using the following equation ([Chupanit and Roesler 2008](#)):

$$\text{VSTR} = \frac{\sum |R_i \cdot A_i| + \sum |S_j \cdot A_j|}{\sum (A_i + A_j)} \quad (6.4)$$

where

$R_i$ =distance above mean plan.

$S_j$ =distance below mean plane.

$A_i$  and  $A_j$ = projected area of each grid (1 mm<sup>2</sup>).

To estimate these surface parameters, it is necessary to acquire the fractured surface in terms of xyz coordinates.. This was done utilizing a photogrammetry procedure.

One application of the VSTR is its use to calculate volumetric surface texture (VST) which is used for calculation of joint load transfer and joint shear stiffness in analysis of cracked flexible pavements (Vandenbossche 1999; Chupanit and Roesler 2008; Vandenbossche et al. 2014). The surface area was calculated according to the methodology presented in Chupanit and Roesler (2008).

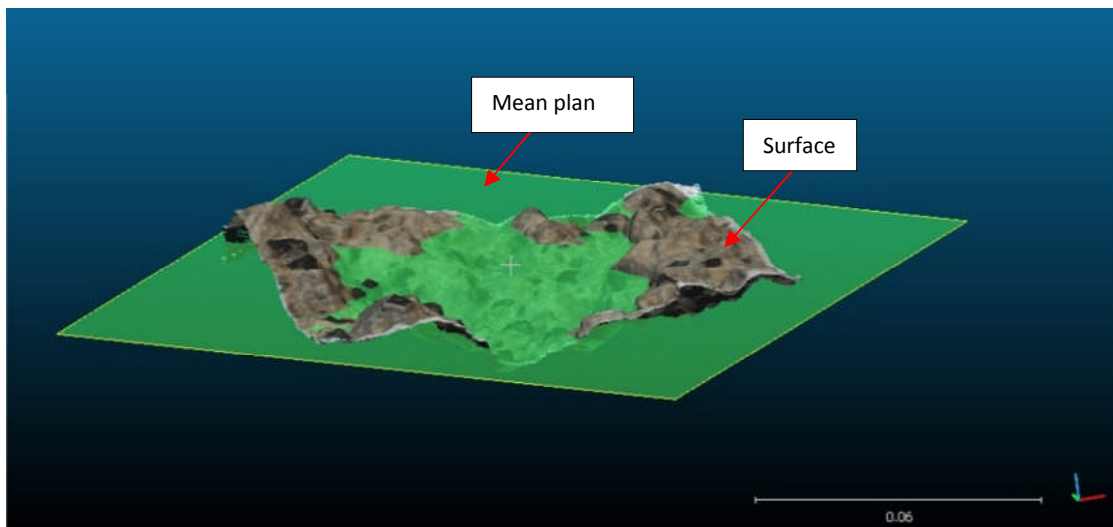


Figure 6.25: Illustration of fractured surface and the plane surface.

#### 6.6.1.2 3D tortuosity

Tortuosity can be defined as the ratio between the actual crack length and the projection of that crack (Hassan 2012). In this research, the earlier definition was extended to evaluate the 3D tortuosity as the ratio of the surface area of the fractured surface to the projection of that surface. The surface area of the fractured surface was estimated according to the methodology presented in Chupanit and Roesler (2008) as the summation of all small triangles (formed by connecting the xyz data) which form that surface (Figure 6.26) using the following equations:

$$\text{Area} = \sqrt{S(S - a)(S - b)(S - c)} \quad (6.5)$$

$$S = \frac{a + b + c}{2} \quad (6.6)$$

$$a = \sqrt{(x_1 - x_2)^2 + (y_1 - y_2)^2 + (z_1 - z_2)^2} \quad (6.7)$$

$$b = \sqrt{(x_2 - x_3)^2 + (y_2 - y_3)^2 + (z_2 - z_3)^2} \quad (6.8)$$

$$c = \sqrt{(x_3 - x_1)^2 + (y_3 - y_1)^2 + (z_3 - z_1)^2} \quad (6.9)$$

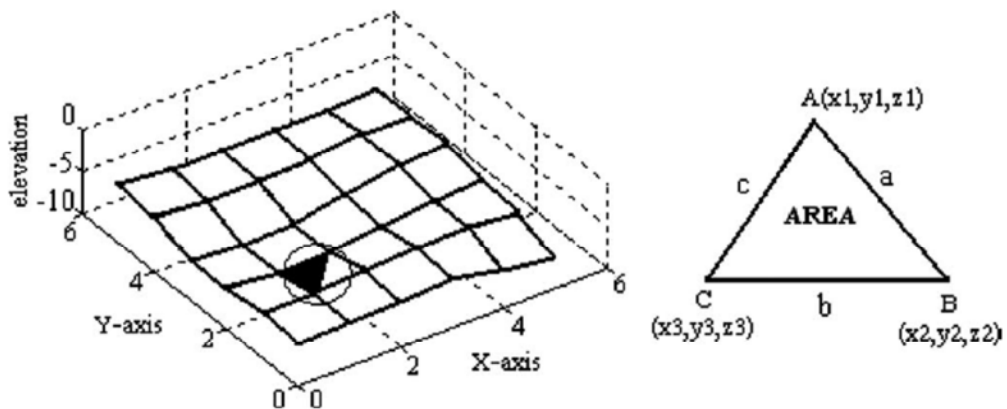


Figure 6.26: Surface area estimation methodology (Chupanit and Roesler 2008)

### 6.6.1.3 Arithmetic mean roughness ( $R_a$ )

This is another measure to describe the fractured surface either on a two (fracture profile) or a three (fractured surface) dimensional basis. This can be estimated using the following formula (Padilla 2008):

$$R_a = \frac{1}{mn} \sum_{i=0}^{m-1} \sum_{j=0}^{n-1} |Z(x_i, y_j) - Z_{av}| \quad (6.10)$$

Where

$m, n$  = number of points in  $x$  and  $y$  directions, respectively.

$Z(x_i, y_j)$  = topographical data of the surface.

$Z_{av}$  = average surface height which can be calculated as follows:

$$Z_{av} = \frac{1}{mn} \sum_{i=0}^{m-1} \sum_{j=0}^{n-1} Z(x_i, y_j) \quad (6.11)$$

### 6.6.2 Fractured surfaces characterization methods

To estimate the previous surface parameters, it is necessary to acquire the topographical information for these fractured surfaces in digital form of xyz data. Several methods were used in the past for acquisition of the fractured surfaces of concrete and rock samples. These include vertical scanning interferometer (Erdem and Blankson 2013), laser scanning (Carpinteri et al. 1999; Chupanit and Roesler 2008), 3D scanner (Hong et al. 2006; Werner et al. 2013), dyed water tank (Issa and Hammad 1994; Issa et al. 2003), probes method (Vandenbossche 1999; Vandenbossche et al. 2014) and photogrammetric methods (Lee and Ahn 2004). In this research, due to unavailability of the above techniques, it was intended to use the photogrammetric procedure for fractured surface topographical data acquisition. Even though the laser scanning by profilometry utilized in Chapter 4 (Section 4.3.3) can be used, in theory, to characterize the fracture surfaces, the limitation associated

with the available version of machine (maximum difference between surface points is 10 mm) has prevented its use in this part of the study.

### **6.6.3 Photogrammetric method**

Surface characterization using a photogrammetric procedure provides many advantages especially in terms of its fast applicability and medium cost. In addition, the generated 3D model can be improved by adding more images. However, this may be time consuming since the processing demands more time (Santos and Júlio 2013). There are two main approaches that can be used to process digital images to generate 3D surfaces using either algorithms from photogrammetry or from the motion (SfM) technique which has been largely developed by the computer vision community. Using close-range photogrammetry, it is possible to reach an estimated accuracy of better than 1mm with non-metric cameras (Remondino and Fraser 2006). There are a number of commercial photogrammetric software packages able to give accurate 3D surface measurements. In SfM, however, often the visualisation and automation of the 3D model is more important than the accuracy. Similar to stereo-photogrammetry, SfM can use a set of images acquired with a consumer grade camera to generate a 3D surface. The main difference compared to photogrammetry is that image acquisition can be more flexible in relative position and attitude of the images. The procedures that both photogrammetry and SfM share are: camera calibration, image matching, and inverse triangulation with bundle adjustment for 3D point cloud generation. Figure 6.27 shows this sequence of adopted activities.

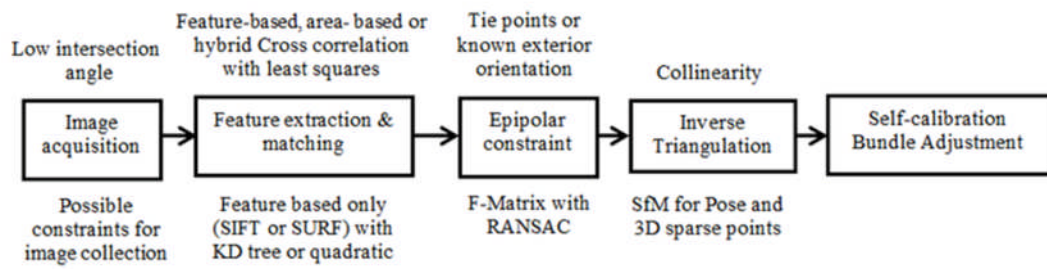


Figure 6.27: A flow diagram of the photogrammetric and structure from motion processes (Farhan et al. 2015).

The photogrammetric and SfM processes were used to generate the 3D surface modelling of fractured cement-stabilized aggregate samples in terms of a cloud of X, Y, Z coordinated points. Firstly, the fractured surfaces were carefully trimmed, from the rest of the fractured halves, to avoid any damage that may affect them. Two samples were used for each mixture. To minimize the processing time and to help extraction of the coordinates defining the fractured surface, the sides of each sample were painted white and placed on a white background. This helped the process of removing unwanted point as it is easier to differentiate points on the fractured surface from those on the white surfaces. Then, several images from different angles and positions were captured, after control point fixing, using a Canon 5D Mark II high resolution camera. A datum is required to define the coordinate system and four specially designed markers of 50 x 50mm which were placed on each of the samples as shown in Figure 6.28b and surveyed using a reflectorless total station (LeicaTPS 1200) in order to produce coordinates so they could be used as control points in the image orientation process, see Figure 6.27. The experimental procedure is illustrated in Figure 6.28.

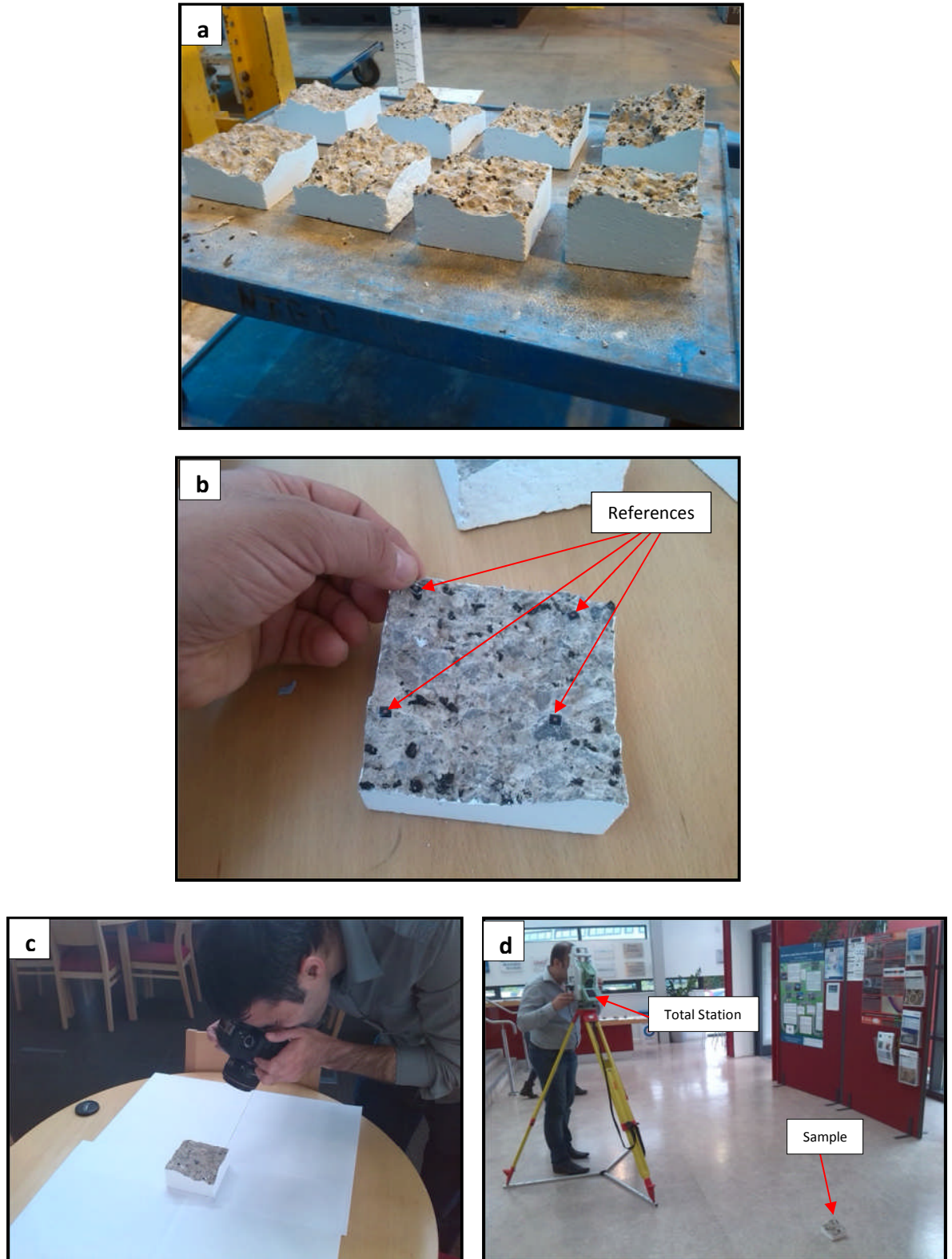


Figure 6.28: Photogrammetric procedure preparation steps: a. painted fractured samples; b. fixing references; c. image capturing from different angles and d. surveying references coordinates on fractured surfaces

Eight fractured samples were modelled and transformed to their ‘total station’ coordinate system utilizing the aligning tool in Cloud Compare software (CloudCompare 2013). Cloud Compare provides details of the transformation process such as the transformation matrix, Root Mean Square Error (RMSE) of the transformation and the recovered scale. With four control points on each sample the RMSE values of the residuals give a quality estimate when transforming each sample to a local ‘total station’ coordinate system. This gives an indication of the estimated quality of the coordinates defining the surface. RMSE values for different scanning are tabulated in Table 6.1. As can be seen from the latter table, significant differences among RMSE values exist between different samples of the same mixture especially for C5R0 and C5R15. This can be attributed to the process of surveying and measuring targets or the difference in the angle of image capturing during image acquisition process (Santos and Júlio 2013), where the RMSE value is a scanning-dependent parameter. However, as can be seen from Table 6.1 all the RMSE values are well below 1mm with an average RMSE value of 0.64mm. This was considered acceptable for the purposes of these experiments. Based on the work by Beshr and Abo Elnaga (2011), RMSE values of less than 0.2mm are achievable for the coordinates of the marks based on a range of less than 2m, and an inclination of less than 45°, so there appears to be the possibility of further improving the technique in the future.

Table 6.1: RMSE of the residuals at the control points on the fractured surface (Farhan et al. 2015)

Sample ID	C5R0-1	C5R0-2	C5R15-1	C5R15-2	C5R30-1	C5R30-2	C5R45-1	C5R45-2
RMSE (mm)	0.54	0.20	0.68	0.44	0.84	0.82	0.88	0.73

#### 6.6.4 Fractured surface quantification findings

Based on the above procedure, the 3D digital fractured surfaces were constructed from the xyz coordinates for each surface as shown in Figure 6.29 through Figure 6.36. From these surfaces, the tortuosity, roughness and VSTR were estimated from the procedures mentioned above. Figures 6.37, 6.38 and 6.39 reveal that the inclusion of rubber causes greater tortuosity, roughness and VSTR, respectively, for all replacement levels. This can be explained as follows. An increase in the embedded rubber particles increases the number of weak points because of the large differences between moduli of rubber and adjacent particles. This, in turn, may causes cracks to divert via these weak points, hence changing (and maybe lengthening) the crack path so that it becomes more tortuous. However, amongst the rubberized mixtures, the smaller differences between the values of tortuosity, roughness and VSTR might be because of the local distribution of the crumb rubber inside the sample. In addition, each surface parameter gave different rankings where C5R15 has, for example, the larger VSTR while C5R30 has the larger tortuosity. [Chupanit and Roesler \(2008\)](#) have reported the same behaviour and they attributed that to unavoidable differences in the scale and resolution when scanning to assess both surface parameters.

Based on these results it can be concluded that the great benefit from the rubber inclusion, in terms of the load transfer efficiency, can be achieved up to 30% rubber replacement. After that the crack may propagate in such a way that produce less tortuosity since the density of rubber distribution inside the mixtures may make a crack propagates straightforward through these rubber particles. This, in fact, confirms the same conclusion presented in Chapter 4 regarding avoidance of higher replacement levels.

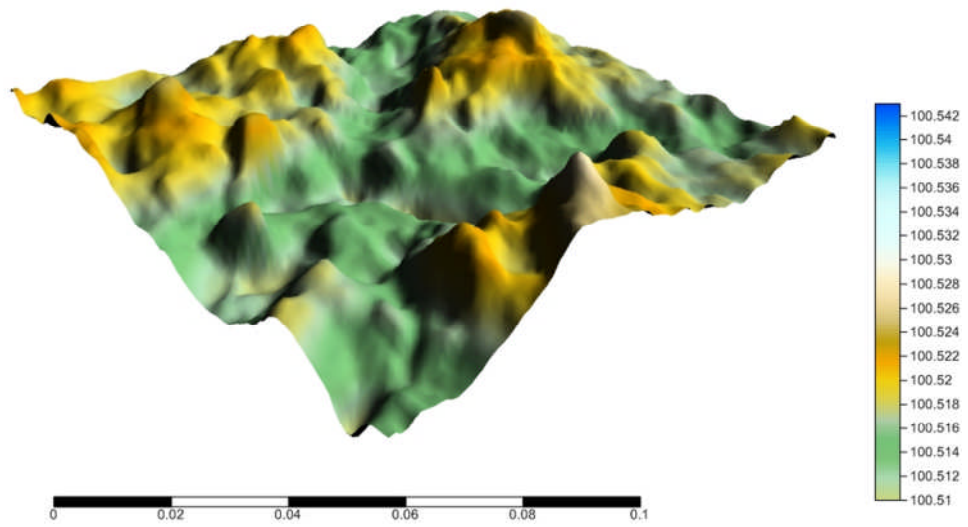


Figure 6.29: Samples of fractured surface scan of C5R0-1

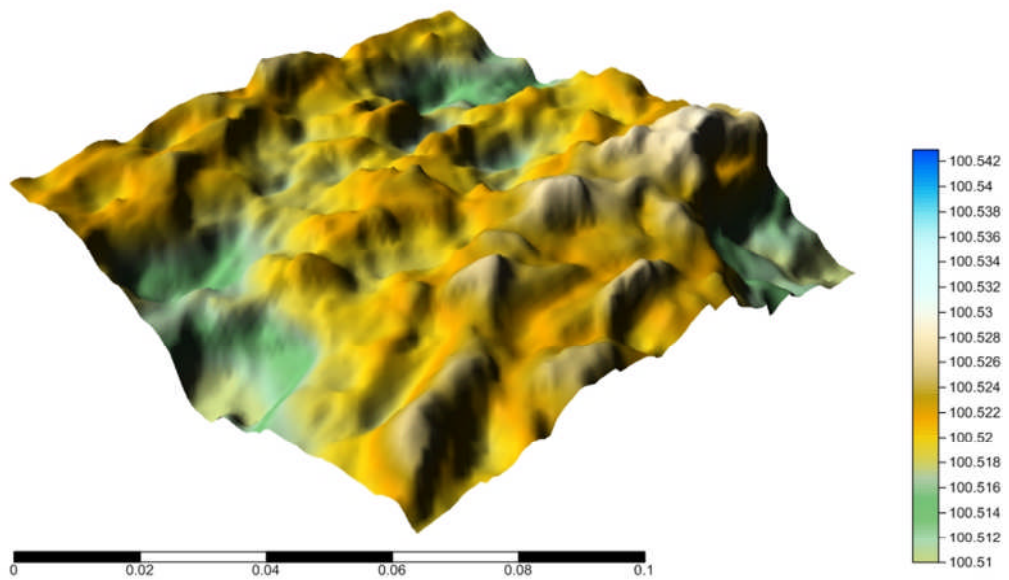


Figure 6.30: Samples of fractured surface scan of C5R0-2

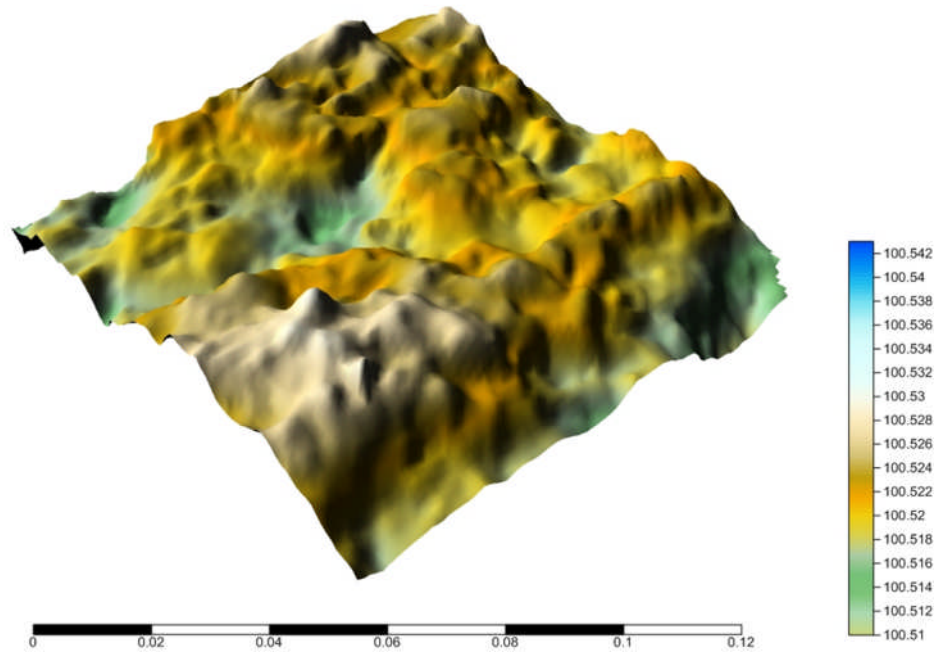


Figure 6.31: Samples of fractured surface scan of C5R15-1

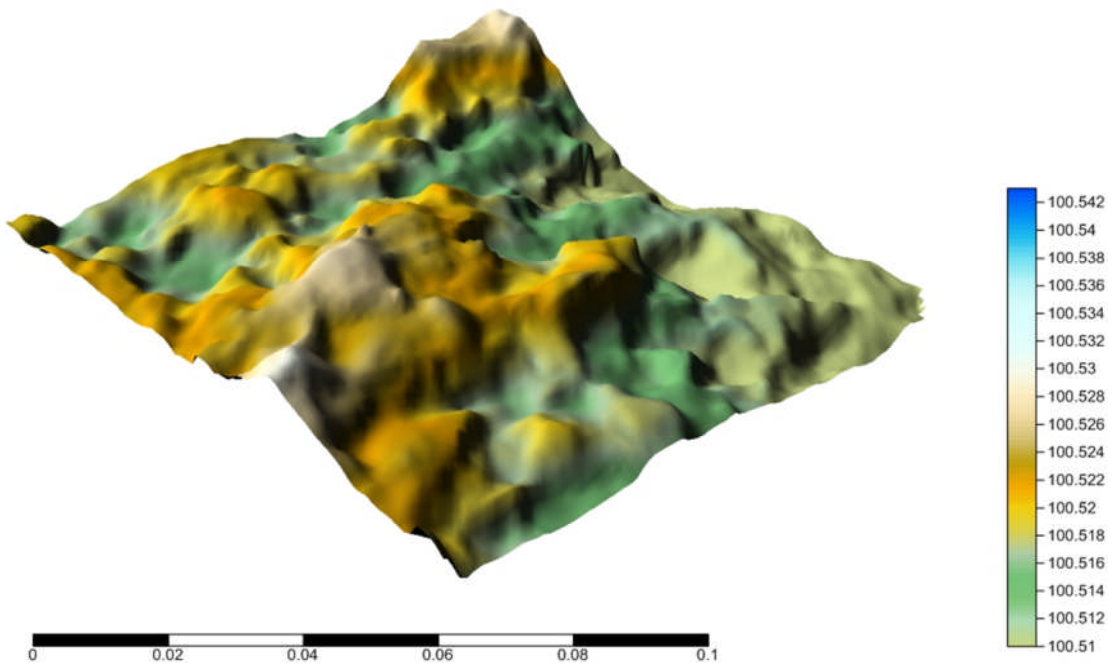


Figure 6.32: Samples of fractured surface scan of C5R15-2

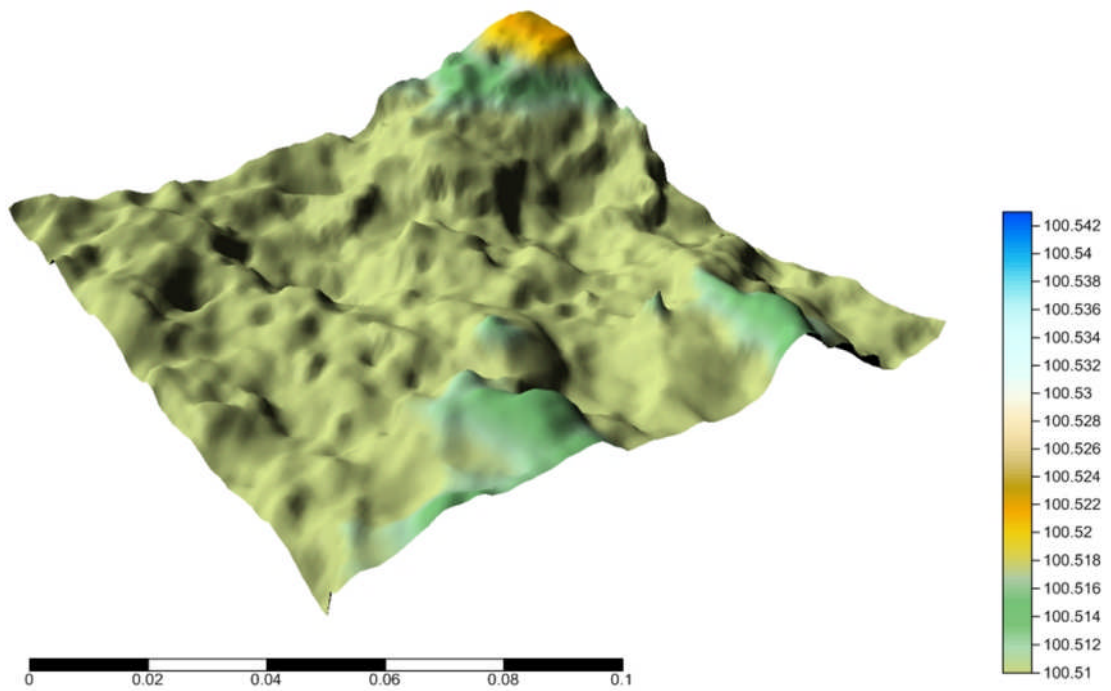


Figure 6.33: Samples of fractured surface scan of C5R30-1

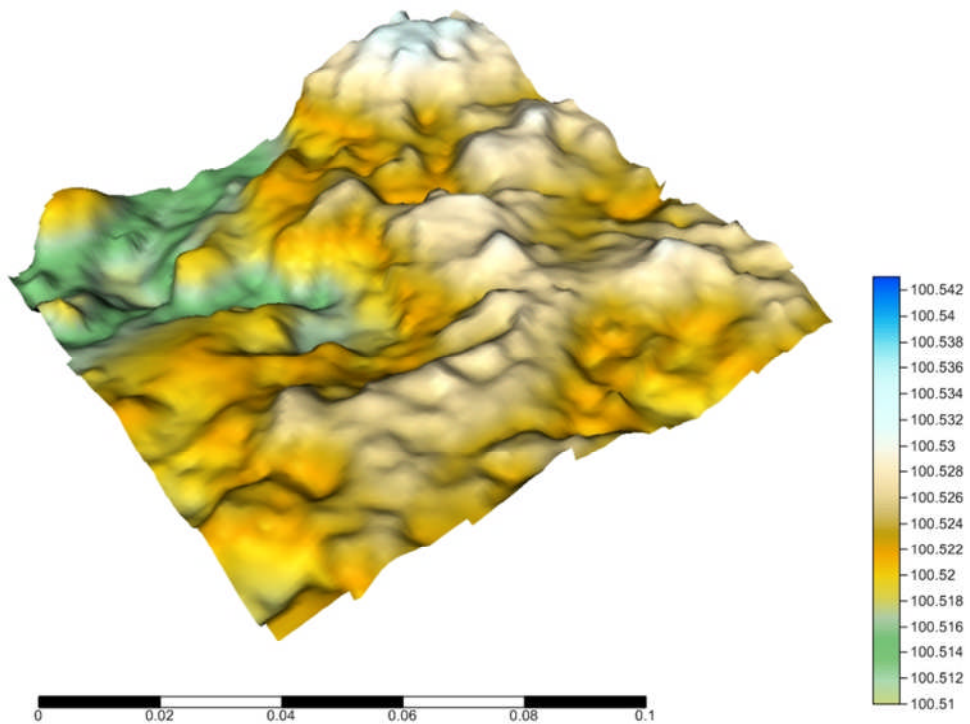


Figure 6.34: Samples of fractured surface scan of C5R30-2

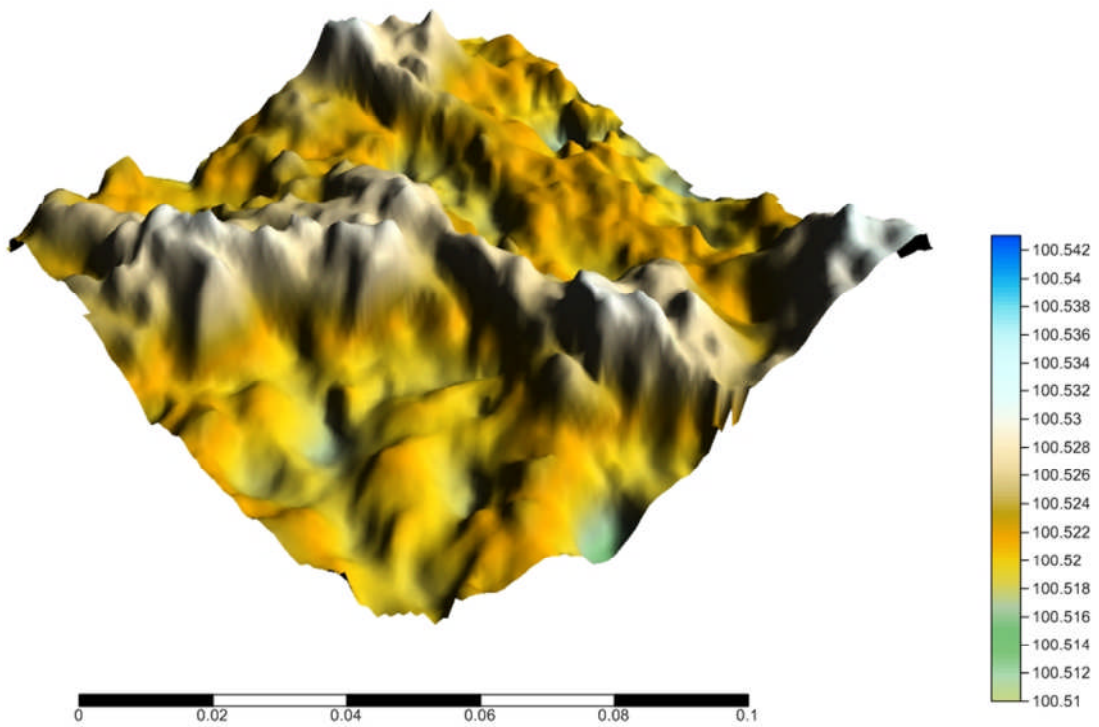


Figure 6.35: Samples of fractured surface scan of C45R0-1

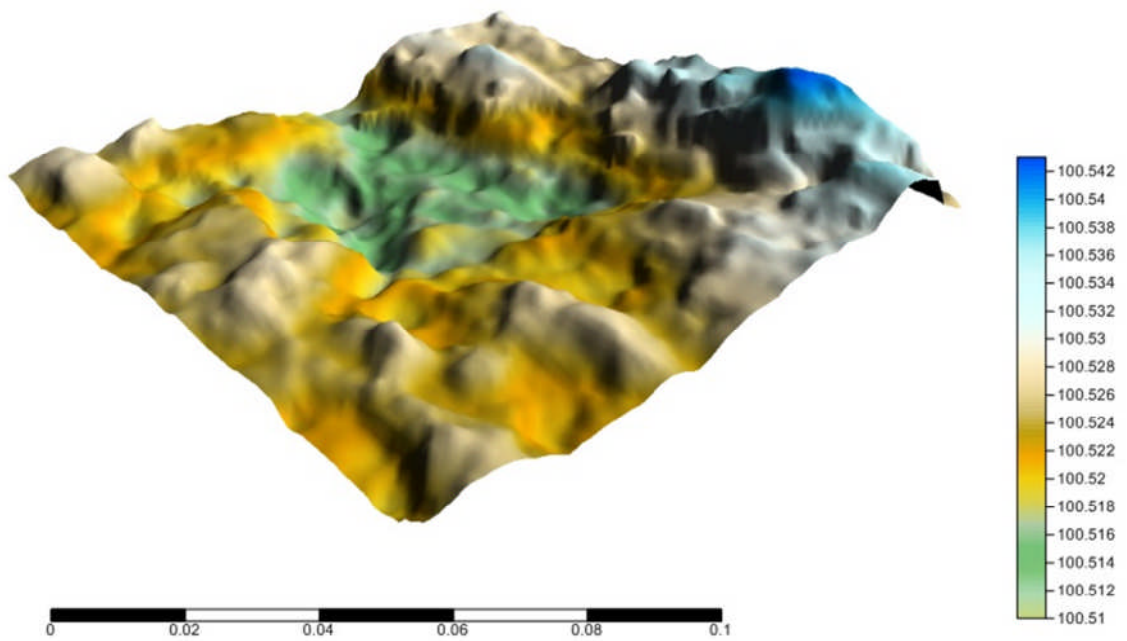


Figure 6.36: Samples of fractured surface scan of C45R0-2

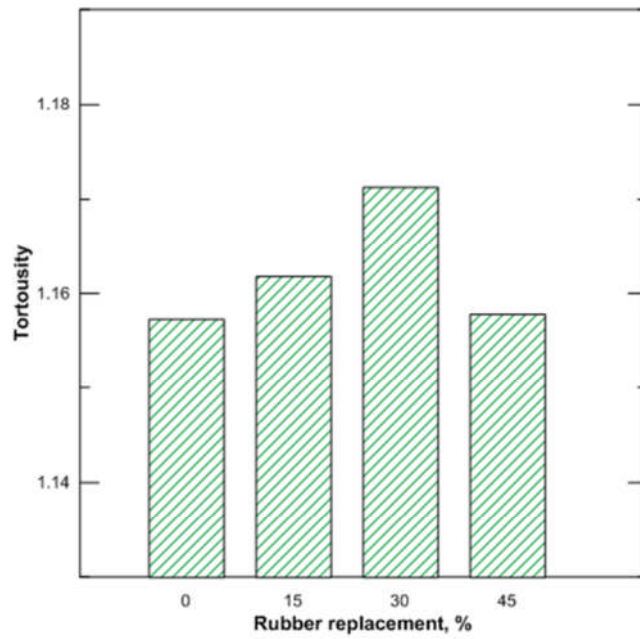


Figure 6.37: Effect of rubber content on 3D tortuosity

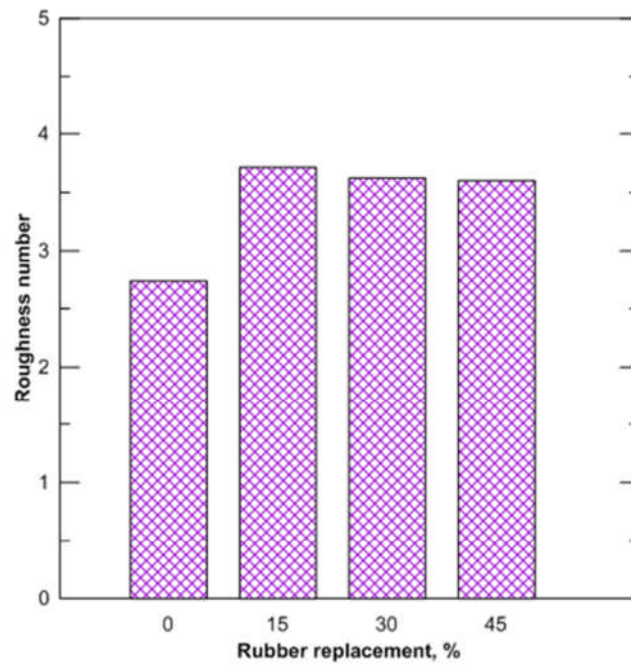


Figure 6.38: Effect of rubber content on roughness number.

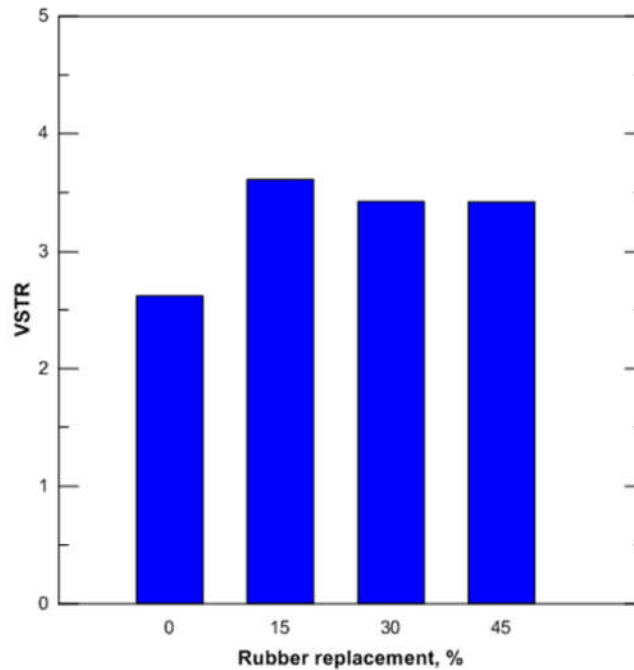


Figure 6.39: Effect of rubber content on VSTR.

### 6.6.5 Implications of fractured surface study

The practical implication of tortuosity increase is production of tougher and less brittle materials as observed by [Guo et al. \(2007\)](#) who introduced a brittleness parameter as the inverse of the tortuosity value (brittleness parameter =  $A/A_s$ , where  $A_s$  and  $A$  represent the surface area of the fracture surface and the projection of that surface, respectively). In addition, these findings also support the previous ones reported in this Chapter and Chapter 5 in terms of toughness and fractal analysis.

Unlike dowelled rigid pavements, aggregate interlock represents the only means for load transfer between blocks after cracking. A rougher crack is likely to ensure good load transfer efficiency across the crack after its formation ([Vandenbossche 1999](#); [Vandenbossche et al. 2014](#)) from which greater material toughness results. This, in turn, may reduce the risk of reflective cracking and increase the shear stiffness of the joint.

### **6.7 Failure mechanism**

In support of the previously mentioned hypothesis that the rubber deflects the crack route through the mixture, the amount of rubber per perpendicular unit length across the fractured surface was determined by an image processing technique utilizing the ImageJ software. Firstly, the fracture surfaces images were captured using a high resolution camera. Then these were converted from RGB mode to an 8 bit greyscale. ImageJ tools were then utilized to conduct thresholding (Figure 6.40) and, eventually, to estimate the rubber content across this surface. The resulting measurement was compared with the quantity used which was known from the mix design. It was found, as shown in Figure 6.41, that the proportion of rubber visible on the crack surface is more than that used. Furthermore, this difference increases as rubber content increases. The above results confirm that the cracks propagate around rubber particles which supports the conjecture of longer crack paths. This, in fact, explains clearly the increased flexural toughness reported in this chapter. Findings of the investigation conducted for flexure-induced cracking of the prismatic samples seem quite consistent with the previous findings conducted for the cylindrical specimens failed under indirect tensile testing. This, in turn, suggests that there is a unique failure mechanism of the cemented aggregate as previously explained, regardless of the method of characterization.

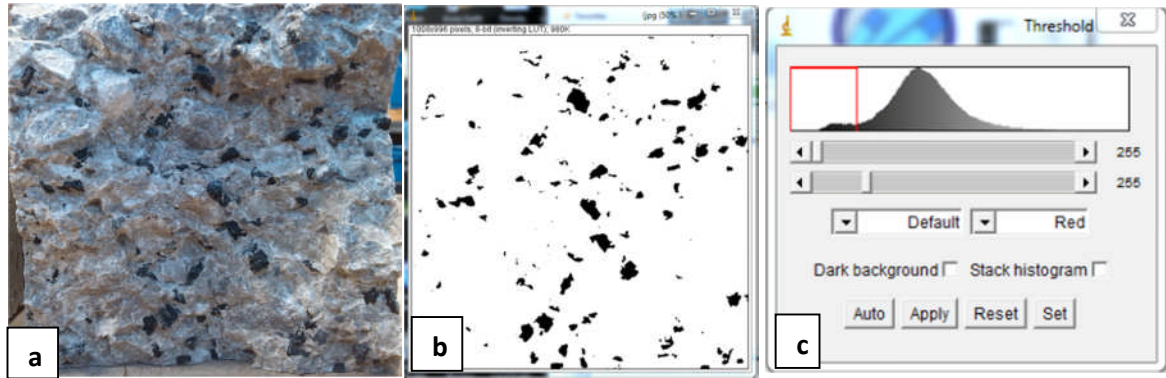


Figure 6.40: Analysis of rubber quantity through fractures surface: a. captured image, b. thresholded image and c. thresholding process.

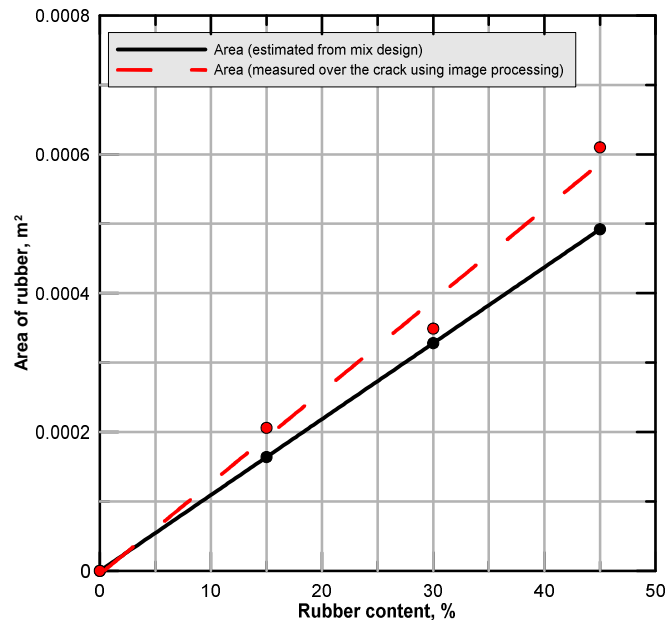


Figure 6.41: Effect of replacement level on amount of rubber across the fractured surfaces.

## 6.8 Rubber distribution study

Rubber particles have an important effect on the cracking and crack propagation mechanism as evidenced in this chapter and in Chapter 5 where it was observed that the cracks propagate through these particles. Therefore, rubber distribution inside the

mixture has an important effect on the stress/strain distribution and hence the crack initiation and propagation. Consequently, to provide a comprehensive understanding about the mixtures in which some rubber particles were incorporated, it is necessary to investigate the internal structure at mesoscale level to quantify the rubber distribution inside rubberized samples. This is believed to be the first time that the quantitative rubber distribution for cementitious materials (not just cement-stabilized mixtures) containing different amounts of rubber has been attempted. This is also to ascertain if a non-uniform rubber distribution would cause asymmetrical stress distribution and hence reduce the load carrying capacity of the samples. To this end, rubber distribution will be quantitatively examined both vertically and radially and the segregation will also be evaluated.

### **6.8.1 Experimental procedure and image analysis**

Cylindrical and prismatic samples, manufactured as previously described were used in this investigation. Three mixtures were used in this study: C5R15, C5R30 and C5R45. The X-ray machine at The University of Nottingham was used.. Image cropping, scaling, filtration and thresholding were conducted using ImageJ software.

Initial investigations showed that there were two cases with images having a high degree of disruption. These occurred in the case of wet or hot samples.. For this reason, and before scanning, the samples were dried for 24 hours at 105° C. After that, these were left for 4 hours to cool down. Samples were mounted in the X-ray machine and some "Blue tack" was placed underneath the sample to avoid any rocking during the sample scanning.

### **6.8.1.1 Interval of X-ray scanning**

It is generally accepted that the less the scanning interval, the less information is lost. However, from initial scanning trials, it was observed that the scanning requires about 8 minutes per slice which means around 26.7 hours (plus setup time) is required to scan a sample of 100 mm diameter at 0.5 mm intervals. Since the objective of this study is to quantify the rubber distribution of particle sizes ranging from 2 to 6 mm, it will be adequate to do x-ray scanning at an interval of 1 mm. The X-ray machine described in Chapter 5 was used for X-ray scanning to produce a hundred 2D images at 1 mm slice interval for each sample. These were converted to 8-bit format for more processing and analysis.

### **6.8.1.2 Filtration and thresholding**

Due to insufficient illumination, the scanned images may contain some noise. For better and accurate data acquisition from these images, it is necessary to remove this noise through filtering of the images. This can be conducted through a smoothing process which is considered as the simplest method of filtering. This process proved to be effective in the case of small noise problems.

Image thresholding is a process to separate and extract the desired objects of the image from the background of that image based on the pixel's density. Images are normally produced with a grey scale ranging from 0 (the darker pixels) to the 255 (the lighter pixels). Thresholding is normally conducted by choosing a value on the grey scale to define a region of interest. The result of this process is the conversion of the grey scale image to a binary image (black/white image) where the pixels having a

value below the threshold value are converted to black while those above will be converted to white.

### **6.8.1.3 Image analysis methodology**

It was observed during the initial investigation that the grey level of the rubber particles and of the air-voids is quite similar which makes it extremely difficult to discriminate between these two components. Therefore, the following methodology was suggested and implemented for thresholding. Firstly, the threshold value was selected based on visual observation. Then the analysis was conducted and the amount of rubber in the rubberized samples was estimated from image analysis. The latter was compared with the actual amount of rubber used in the mixture based on the mix design. If these were equal then the initial value could be considered as the design threshold. Otherwise, another threshold value was attempted until the amount of rubber calculated based on image analysis and from mix design were equal.

Initial inspection of the scanned images revealed some rubber clusters in the horizontal plane (Figure 6.42). For better assessment of rubber distribution in cemented mixtures, it is necessary to evaluate the distribution both vertically and radially. Vertical distribution can be computed by studying the change in rubber percentage from one image to the next above or below.

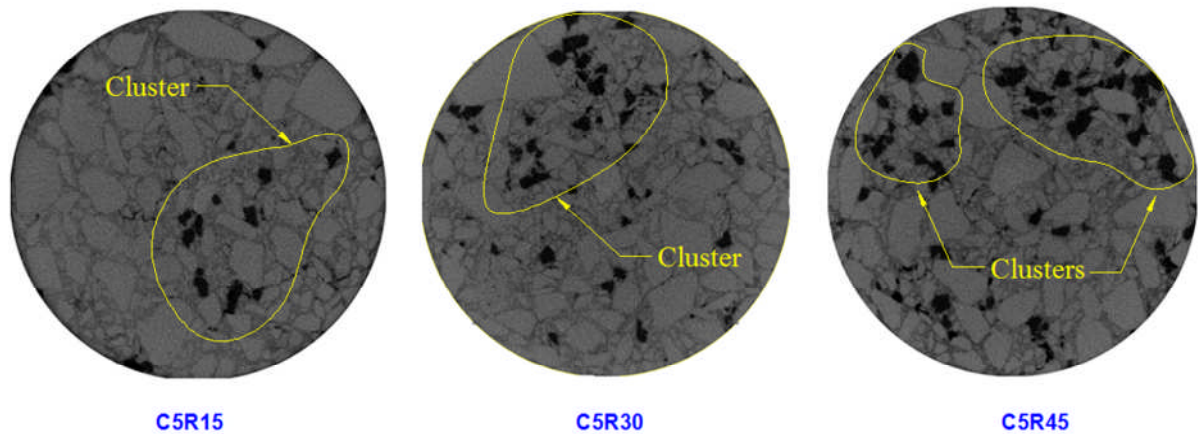


Figure 6.42: Samples x-ray images showing the rubber clustering in cemented mixtures

To this end, the radial distributions were evaluated along with the rubber segregation methodology by evaluating the rubber contents and distribution in the internal core and external ring of equal cross-sectional areas. The details are presented in the next section.

#### 6.8.1.4 Segregation analysis

The rubber segregation was evaluated based on image analysis using ImageJ software and the methodology presented in Erdem (2014) was adopted. Erdem's methodology assesses the aggregate segregation, quantitatively, in concrete samples both horizontally and vertically. After capture, images were filtered and thresholded as previously discussed. The binary images along the sample height were used to estimate the volume of total rubber in the upper and lower halves and this was expressed as a ratio of the total rubber volume in the whole samples (Figure 6.43a) using Equations 6.4 and 6.5.

$$R_{Vu} = \sum_{i=i1}^{in} V_{vu} \div V_{af} \quad (6.12)$$

$$R_{Vl} = \sum_{j=j1}^{jn} V_{vl} \div V_{af} \quad (6.13)$$

where  $R_{vu}$ ,  $V_{vu}$  and  $V_{af}$  represent volumetric ratio of rubber in upper half, volume of aggregate in upper half and volume of aggregate in whole sample, respectively. Similarly,  $R_{vl}$ ,  $V_{vl}$  and  $V_{af}$  are for the lower half. In terms of horizontal segregation, Erdem's methodology was adjusted in this research since his was suggested to evaluate the horizontal segregation in cubical specimens. Therefore, instead of the lower and upper parts in horizontal direction used by the latter author, internal and external parts were used in this research (Figure 6.43b). Then the volumetric ratios in external ( $R_{ve}$ ) and internal ( $R_{vi}$ ) parts were calculated as follows:

$$R_{Ve} = \sum_{i=i1}^{in} V_{ve} \div V_{af} \quad (6.14)$$

$$R_{Vi} = \sum_{j=j1}^{jn} V_{vi} \div V_{af} \quad (6.15)$$

To assess the segregation quantitatively, Erdem (2014) stated that he used the following criteria:

$$R_{vu}=R_{vl}=1 \text{ and } R_{re}=R_{ri}=1$$

No segregation

$1.0 > R_{vu} \geq 0.85$  or  $1.0 > R_{vl} \geq 1.15$  Moderate segregation

$1.0 > R_{re} \geq 0.85$  or  $1.0 > R_{ri} \geq 1.15$

$R_{vu} < 0.85$  or  $R_{vl} > 1.15$  High segregation

$R_{ri} < 0.85$  or  $R_{re} > 1.15$

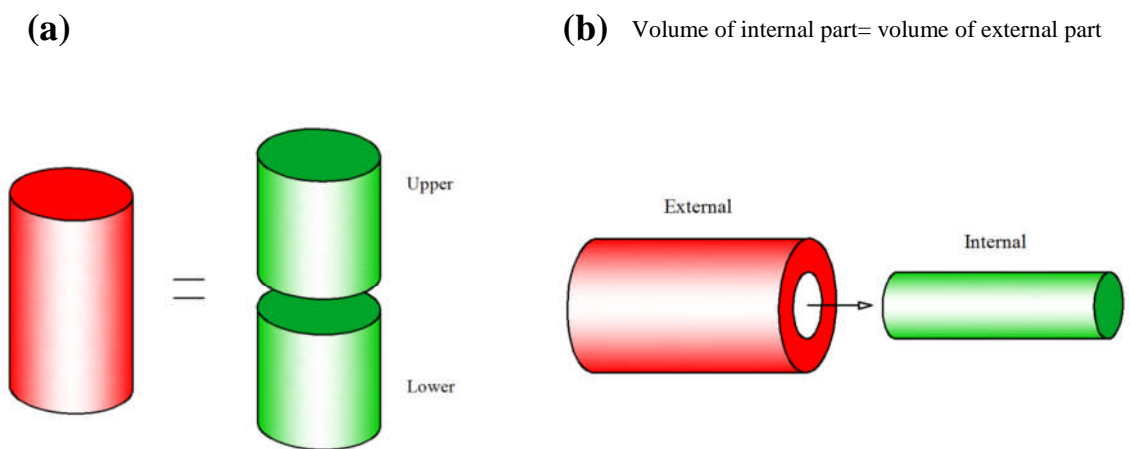


Figure 6.43: Methodology for radial (a) and vertical (b) segregation evaluation

[Erdem \(2014\)](#) used these criteria to describe the segregation of aggregate in a concrete mixture. These are on the basis of  $\pm 15\%$  deviation from uniform distribution (i.e., 50:50). Unfortunately, this author provided an incorrect formalization for the percentages in the upper, lower, internal and external zones. Inspection of the criteria and the formalized equation in their present forms reveals that the resulting proportion will never be more than 100%. Therefore, the expressions given above (Equations 6.12, 6.13, 6.14 and 6.15) have been modified to make them consistent with the provided criteria. This was conducted by adjusting the dominator of the latter equation to become 50% of  $V_{af}$ .

## 6.8.2 Rubber distribution and segregation results and discussion

### 6.8.2.1 Vertical and radial rubber distribution

Figure 6.44 illustrates the rubber distribution along the sample height for different rubberized mixtures. This figure shows that the rubber distribution is fairly uniform for C5R15 and C5R30 where the standard error was estimated as 7.9% and 7.6% for the latter two mixtures, respectively. The C5R45 showed the larger variability (standard error of 14.8%) as compared with the other two replacement levels. This, in fact, confirms the assumption made in Chapter 5 (Section 5.2.2) regarding the non-uniform rubber distribution.

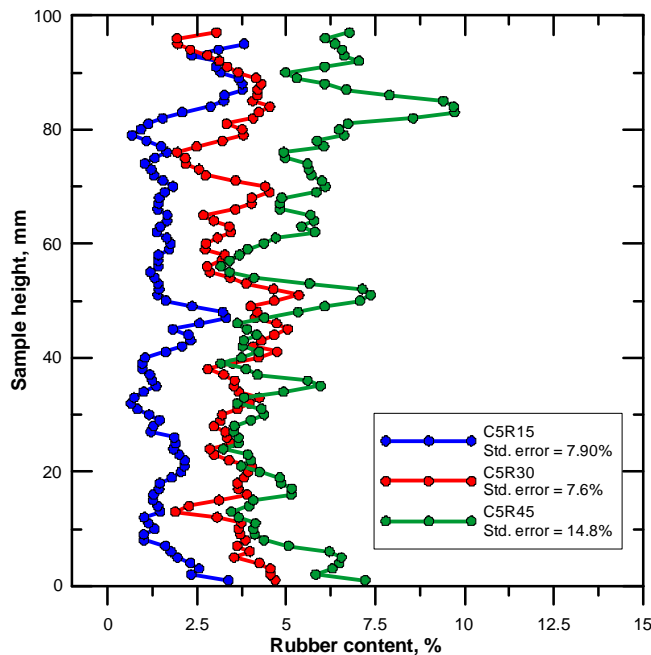


Figure 6.44: Vertical rubber distribution for different RCSAMs

Regarding the radial distribution, Figure 6.45, Figure 6.46 and Figure 6.47 show the rubber distribution in the internal core and external ring for investigated rubberized mixtures. There is a uniform rubber distribution throughout the sample height in both

internal and external parts of the C5R15 sample as is clear from Figure 6.45. The standard error of the mean in these parts is 3.7% and 6.25%, respectively.

In the sample of C5R30, the same previous distribution was observed. However, 4.7% and 5.3% are the standard error of the vertical rubber distribution in the internal and external parts, respectively. Finally, the C5R45 sample demonstrated a large variability where the standard error of the rubber distribution across the sample height was estimated as 10.4% and 9.1%, respectively, for internal and external sample parts.

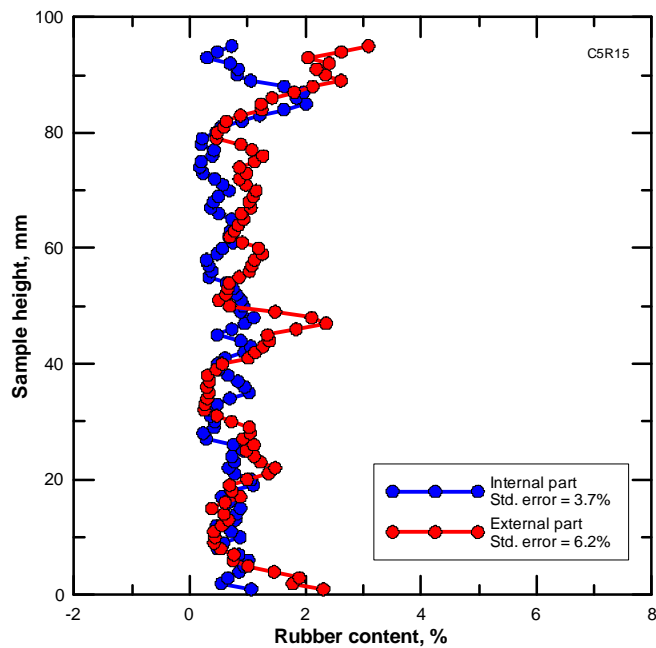


Figure 6.45: Radial rubber distribution in external and internal parts of C5R15 sample

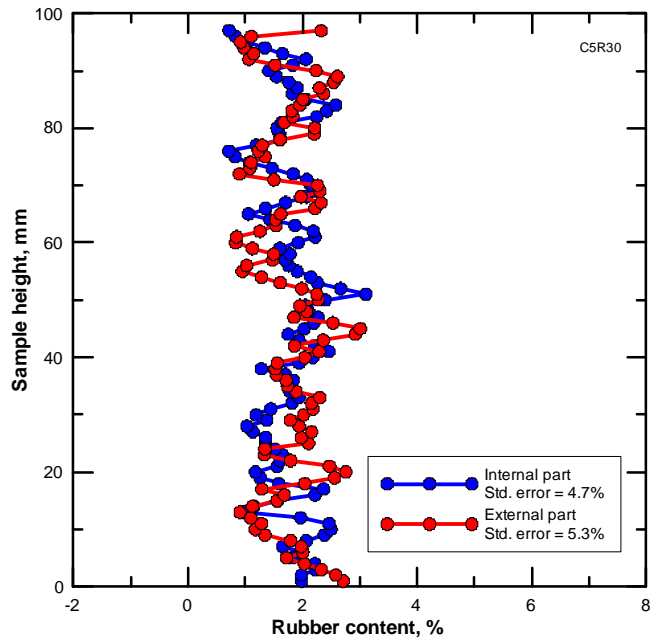


Figure 6.46: Radial rubber distribution in external and internal parts of C5R30 sample

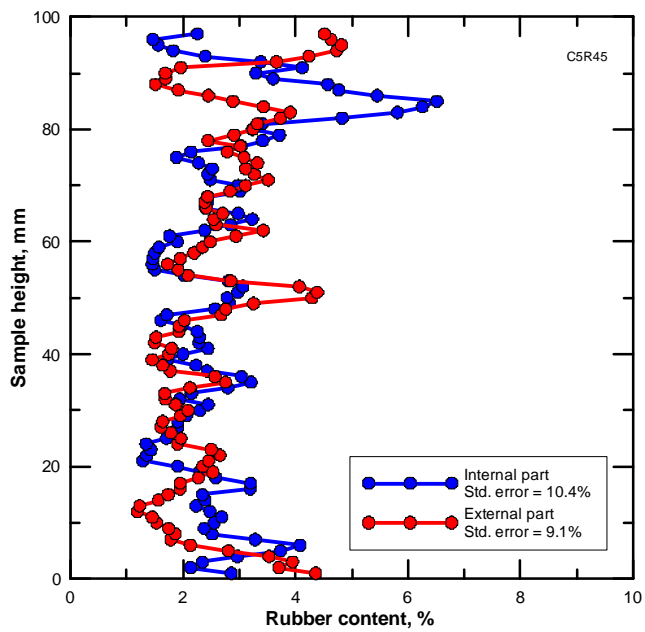


Figure 6.47: Radial rubber distribution in external and internal parts of C5R45 sample

### 6.8.2.2 Rubber segregation analysis

Rubber segregation deals with the quantity of rubber in the different parts (upper, lower, internal and external) of the rubberized sample. Table 6.2 shows rubber

segregation analysis for cement-stabilized aggregate mixtures containing different rubber replacement levels. In terms of the uniformity of rubber distribution, as can be seen from this table, C5R30 showed the least variation both vertically and radially where these are 1% and 0.3%, respectively. The 3D representation of the rubber in the latter mixture sample is illustrated in Figure 9.48. However, the maximum variation was less than 20% which can lead to a conclusion that there was a reasonable uniformity in the rubber distribution across the cylindrical samples. This, in turn, is expected to mean that the particular distribution of the rubber particles inside the cemented mixtures has little effect on the strength reduction of the modified mixture. Due to the scope of this research and the expensive cost of the scan, one sample was X-rayed for each mixture.

Table 6.2: Rubber segregation analysis for RCSAMs containing different amount of rubber

Mixture	Vertical distribution			Radial distribution			Segregation Degree
	$R_{vu}$ ( $R_{vu}/0.5$ )	$R_{vi}$ ( $R_{vi}/0.5$ )	Difference	$R_{re}$ ( $R_{re}/0.5$ )	$R_{ri}$ ( $R_{ri}/0.5$ )	Difference	
C5R15	56.32% (112.6%)	44.57% (89.1%)	11.64%	59.9% (80.2%)	40.11% (119.8%)	19.8%	<b>High</b>
C5R30	49.89% (99.77%)	50.10% (101.8%)	1%	50.15% (99.7%)	49.85% (100.3%)	0.3%	<b>moderate</b>
C5R45	57.66% (115.3%)	41.68% (83.4%)	16.1%	49.10% (101.8%)	50.90% (98.2%)	1.8%	<b>High</b>

$R_{vu}+R_{vi}$  should be sum to 100%;  $R_{re}+R_{ri}$  should be sum to 100%.

Small errors are observed due to the discretization of the X-ray CT scans

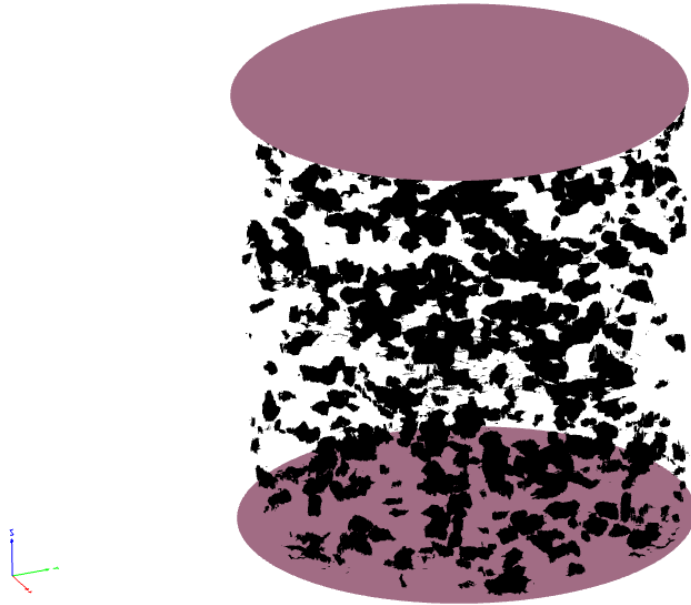


Figure 6.48: Sample of 3D distribution for RCSAMs containing 30% rubber replacement

To answer an interesting question regarding the uniformity of rubber distribution in prismatic samples, a simple qualitative study was conducted. Firstly, three samples were manufactured by the same procedure as described earlier and cured for 28-days. Afterwards, these were sliced longitudinally at top third, middle third and bottom third. A sample of rubber distribution is depicted in Figure 6.49 and Figure 6.50. From these figures, the uniformity of the rubber distribution across different samples containing different amounts of rubber can be seen qualitatively (Farhan et al. 2015).

Based on the rubber distribution investigation, it can be concluded that there is no significant non-uniformity in the rubber distribution in the investigated mixtures. However, from observing the rubber distribution at 45% replacement level, there is some indication that higher replacement ratios might be prone to larger variations.

This confirms the effectiveness of the mixing method in producing reasonably uniform distribution. In addition, it is possible for future studies (to avoid the heavy duty work and speed up the manufacturing process) to core samples from the manufactured slabs since this will not affect the results due to uncertainty of rubber distribution.

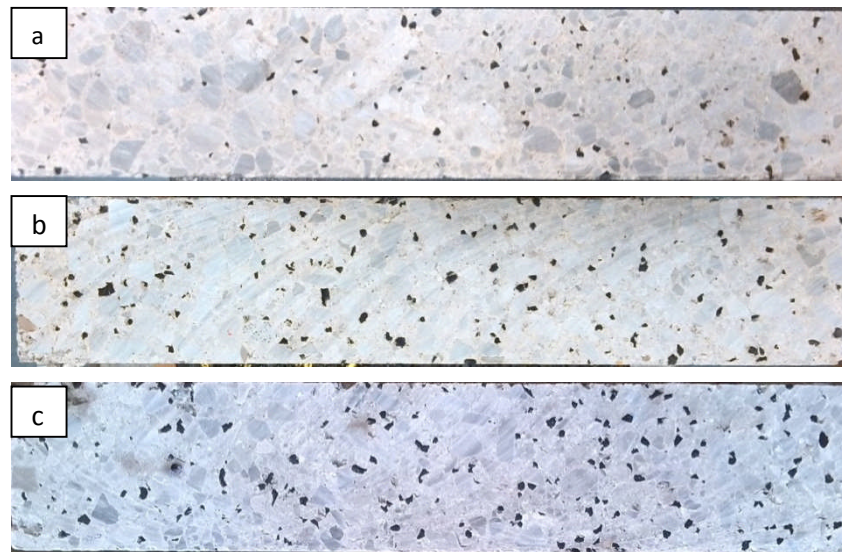


Figure 6.49: Samples of rubber distribution in the middle of prismatic specimens containing (a) 15%, (b) 30% and (d) 45%

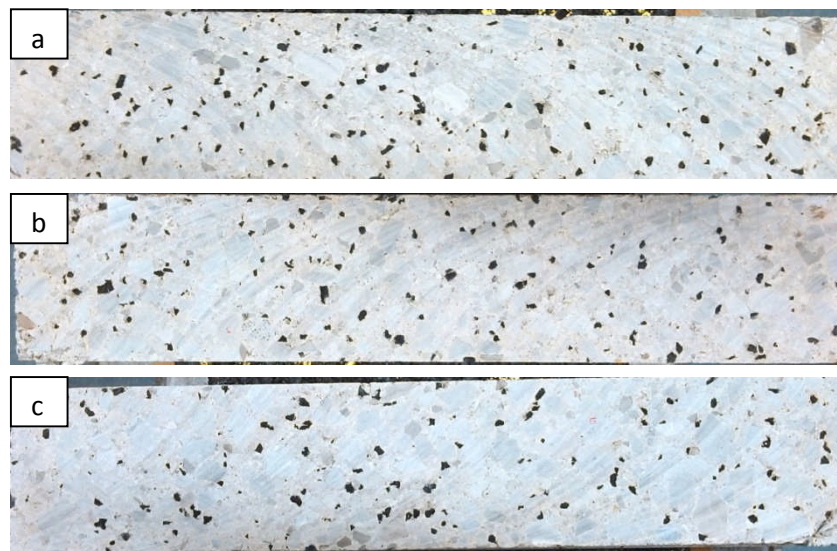


Figure 6.50: Samples of rubber distribution in prismatic specimen containing 30% rubber replacement at (a) top, (b) middle and (d) bottom

## 6.9 Concluding remarks

### *Conclusions regarding the flexural properties*

1. A reduction occurred in the flexural strength of the cemented mixtures upon rubber incorporation. This increased as rubber replacement increased. On the other hand, increasing cement content improves the flexural strength. However, the reduction in flexural strength due to rubber inclusion seems to be larger in the case of heavily stabilized mixtures than in lightly cemented mixtures.
2. Static flexural modulus was reduced as a result of using the soft rubber particles. Increasing stabilizer content increases the stiffness of both rubberized and reference mixtures. Stiffnesses of both rubberized and reference mixtures are sensitive to the addition of stabilizer up to about 5% cement content. Further addition of cement will probably not be beneficial since the cost of more cement may not lead to a noticeable improvement in stiffness.
3. Replacement of natural aggregate with crumb rubber has a positive impact on producing tougher pavement mixtures. Furthermore, this finding is observed at all cement contents. However, cement content does not have a clear effect on the flexural toughness of either the reference or the rubberized mixtures.
4. Good bond was achieved at higher cement contents. Observing the fractured surfaces of highly cemented samples reveals that majority of the cracks were propagated through aggregate.
5. The following correlations presented in Table 6.3 below are concluded:

Table 6.3: Flexural properties correlations

No.	Correlation	Parameters and units	Figure No.	R <sup>2</sup>
1	$F_s = 1.262 * ITS$	$F_s$ = flexural strength, MPa $ITS$ =indirect tensile strength, MPa	6.8	0.62
2	$F_s = 0.135 * UCS$	$F_s$ = flexural strength, MPa $ITS$ =unconfined compressive strength, MPa	6.7	0.99
3	$E_f = 2.74 * ITS + 32$	$E_f$ = static flexural modulus, GPa $ITS$ =indirect tensile strength, MPa	6.22	0.63
4	$E_f = 0.41 * UCS + 28.45$	$E_f$ = static flexural modulus, GPa $ITS$ =indirect tensile strength, MPa	6.21	0.82
5	$E_f = 2.7 * F_s + 29.7$	$E_f$ = static flexural modulus, GPa $F_s$ = flexural strength, MPa	6.23	0.62

***Conclusions regarding the characterization of flexural-induced fractured surfaces***

1. The photogrammetry method was found to be an effective method to characterize the fractured surfaces of the failed samples.
2. Inclusion of rubber in cement-stabilized aggregate mixtures resulted in a tortuous, larger VSTR and rougher cracking patterns as compared with the reference mixture. This, in turn, should ensure improvement in the load transfer across the cracks. The variability in improvement with different rubber contents can be attributed to the local rubber distribution and scanning resolution dependency of these characterization measures.

3. Quantification of the rubber quantity across the fractured surfaces revealed larger amounts of rubber which indicates the flexure-induced cracks were preferentially propagated through these particles.
4. The findings from the fractured surface characterizations are consistent with the fractal analysis (presented in Chapter 5) and internal structural observations performed for the samples failed under indirect tensile testing. This provides support for the proposed failure mechanism of rubberized cement-stabilized aggregate mixtures which assumes that the cracks are propagating through the rubber particles embedded inside the mixture.
5. Studying the fractured surfaces of the failed specimens, at mesoscale level, provides important information regarding the failure mechanism and nature of the mixtures (brittle vs. ductile).

*Conclusions regarding the mesoscale characterization of internal structures*

1. Quantitative analysis of the rubber distribution revealed a uniform vertical rubber distribution at 15% and 30% replacement levels. However, greater non-uniformity in this distribution appeared at 45%.
2. The radial rubber distribution revealed that the vertical distribution in the internal core and external ring (of the same cross-sectional area) is fairly uniform especially in C5R15 and C5R30 mixtures.
3. Segregation analysis revealed that the least segregation occurred in the mixture containing 30% rubber replacement.

4. Qualitative observations conducted for prismatic samples showed and confirmed the fairly uniform rubber distributions seen in the cylindrical specimens.

## 6.10 References

- Aiello, M. A. and F. Leuzzi (2010). "Waste tyre rubberized concrete: properties at fresh and hardened state." *Waste Manag* 30(8-9): 1696-1704.
- Arellano, D. and M. R. Thompson (1998). *Stabilized Base Properties (Strength, Modulus, Fatigue) for Mechanistic-Based Airport Pavement Design*, Final Report, Technical Report of Research, Department of Civil Engineering University of Illinois at Urbana-Champaign, Illinois.
- Arnold, G., C. Morkel and G. van der Weshuizen (2012). *Development of tensile fatigue criteria for bound materials*, NZ Transport Agency report No. 463, New Zealand Institute of Highway Technology.
- Arulrajah, A., M. M. Disfani, H. Haghghi, A. Mohammadinia and S. Horpibulsuk (2015). "Modulus of rupture evaluation of cement stabilized recycled glass/recycled concrete aggregate blends." *Construction and Building Materials* 84: 146-155.
- Beshr, A. A. A. and I. M. Abo Elnaga (2011). "Investigating the accuracy of digital levels and reflectorless total stations for purposes of geodetic engineering." *Alexandria Engineering Journal* 50(4): 399-405.
- Brown, S. F. (2012). "An introduction to asphalt pavement design in the UK." *Proceedings of the ICE-Transport* 166(4): 189-202.
- Carpinteri, A., B. Chiaia and S. Invernizzi (1999). "Three-dimensional fractal analysis of concrete fracture at the meso-level." *Theoretical and Applied Fracture Mechanics* 31(3): 163-172.
- Chupanit, P. and J. R. Roesler (2008). "Fracture energy approach to characterize concrete crack surface roughness and shear stiffness." *Journal of Materials in Civil Engineering* 20(4): 275-282.
- CloudCompare (2013). *3D point cloud and mesh processing software*

Open Source Project, EDF.

Disfani, M. M., A. Arulrajah, H. Haghghi, A. Mohammadinia and S. Horpibulsuk (2014). "Flexural beam fatigue strength evaluation of crushed brick as a supplementary material in cement stabilized recycled concrete aggregates." *Construction and Building Materials* 68: 667-676.

Erdem, S. (2012). Impact load-induced microstructural damage of concrete made with unconventional aggregates. PhD thesis, University of Nottingham.

Erdem, S. (2014). "X-ray computed tomography and fractal analysis for the evaluation of segregation resistance, strength response and accelerated corrosion behaviour of self-compacting lightweight concrete." *Construction and Building Materials* 61: 10-17.

Erdem, S. and M. A. Blankson (2013). "Fractal–fracture analysis and characterization of impact-fractured surfaces in different types of concrete using digital image analysis and 3D nanomap laser profilometry." *Construction and Building Materials* 40: 70-76.

Farhan, A. H., A. R. Dawson, N. H. Thom, S. Adam and M. J. Smith (2015). "Flexural characteristics of rubberized cement-stabilized crushed aggregate for pavement structure." *Materials & Design* 88: 897-905.

Guleria, S. and R. Dutta (2011). "Unconfined compressive strength of fly ash–lime–gypsum composite mixed with treated tire chips." *Journal of Materials in Civil Engineering* 23(8): 1255-1263.

Guo, L.-P., W. Sun, K.-R. Zheng, H.-J. Chen and B. Liu (2007). "Study on the flexural fatigue performance and fractal mechanism of concrete with high proportions of ground granulated blast-furnace slag." *Cement and Concrete Research* 37(2): 242-250.

Hassan, N. A. (2012). Microstructural characterization of rubber modified asphalt mixtures PhD thesis, The university of Nottingham.

Hong, E., I. Lee and J. Lee (2006). "Measurement of rock joint roughness by 3D scanner." *Geotechnical Testing Journal* 29(6): 482.

Issa, M. and A. Hammad (1994). "Assessment and evaluation of fractal dimension of concrete fracture surface digitized images." *Cement and Concrete Research* 24(2): 325-334.

Issa, M. A., M. A. Issa, M. S. Islam and A. Chudnovsky (2003). "Fractal dimension—a measure of fracture roughness and toughness of concrete." *Engineering Fracture Mechanics* 70(1): 125-137.

Jitarekul, P. (2009). An Investigation into Cold In-Place Recycling of Asphalt Pavements, PhD Thesis ,University of Nottingham, Department of Civil Engineering.

Lee, H.-S. and K.-W. Ahn (2004). "A prototype of digital photogrammetric algorithm for estimating roughness of rock surface." *Geosciences Journal* 8(3): 333-341.

Najim, K. B. (2012). Determination and enhancement of mechanical and thermo-physical behaviour of crumb rubber-modified structural concrete. PhD thesis, The University of Nottingham.

Najim, K. B. and M. R. Hall (2012). "Mechanical and dynamic properties of self-compacting crumb rubber modified concrete." *Construction and Building Materials* 27(1): 521-530.

Padilla, S. (2008). Mathematical models for perceived roughness of three-dimensional surface textures, Heriot-Watt University.

Remondino, F. and C. Fraser (2006). "Digital camera calibration methods: considerations and comparisons." *International Archives of Photogrammetry, Remote Sensing and Spatial Information Sciences* 36(5): 266-272.

Santos, P. M. and E. N. Júlio (2013). "A state-of-the-art review on roughness quantification methods for concrete surfaces." *Construction and Building Materials* 38: 912-923.

Solanki, P. (2010). Characterization of cementitiously stabilized subgrades for mechanistic-empirical pavement design, PhD thesis, The university of Oklahoma

Topcu, I. B. (1995). "The properties of rubberized concrete." *Cement and Concrete Research* 25(2): 304-310.

Toutanji, H. A. (1996). "The Use of Rubber Tire Particles in Concrete to Replace Mineral Aggregates." *Cement & Concrete Composkes* 18: 135-139.

Triches, G. (2009). The fatigue behavior of rolled compacted cobcrete for composite pavements. 2nd workshop on four-point bending, University of Minho, Recored No. 276.

Turatsinze, A. and M. Garros (2008). "On the modulus of elasticity and strain capacity of self-compacting concrete incorporating rubber aggregates." *Resources, conservation and recycling* 52(10): 1209-1215.

Vandenbossche, J. M. (1999). "Estimating potential aggregate interlock load transfer based on measurements of volumetric surface texture of fracture plane." *Transportation Research Record: Journal of the Transportation Research Board* 1673(1): 59-63.

Vandenbossche, J. M., M. Barman and J. N. Kremm (2014). "Using Surface Texture Measurements of a Crack Surface to Establish a Joint Spring Stiffness Representing

the Shear Transfer Capacity." *Transportation Research Record: Journal of the Transportation Research Board*.

Wen , H., B. Muhunthan, J. Wang, X. Li, T. Edil and J. M. Tinjum (2014). *Characterization of Cementitiously Stabilized Layers for Use in Pavement Design and Analysis*.

Werner, S., I. Neumann, K.-C. Thienel and O. Heunecke (2013). "A fractal-based approach for the determination of concrete surfaces using laser scanning techniques: a comparison of two different measuring systems." *Materials and Structures* 46(1-2): 245-254.

Williams, R. I. T. (1986). "Cement-treated pavements : materials, design and construction " Elsevier Applied Science.

## **Chapter Seven**

### **Non-destructive evaluation and their correlations**

#### **7.1 Introduction**

Non-destructive methods, namely ultrasonic and resonant frequency testing, have been used extensively over the last forty years to investigate the properties of different types of concrete. These studies resulted in a standardization of these testing in [ASTM C597-09](#), [ASTM D2845-95](#) and [ASTM C1018](#) for concrete and rock. However, a limited number of investigations was reported in the literature regarding the application of this type of testing to characterize cemented materials ([Su et al. 2013](#); [Mandal et al. 2014](#)).

Therefore, the main focus of this chapter is to evaluate, firstly, the properties of cement-stabilized aggregate mixtures containing different amounts of rubber particles under different cementation levels. This will help to determine to what extent the rubber and its interaction with cement may affect the properties. This may help to reveal the sensitivity of these characterization methods to the small change in aggregate composition and degree of cementation and hence this will lead, at the same time, to the evaluation of the feasibility and suitability of non-destructive testing to characterize cementitiously-stabilized mixtures in general. Since the investigated mixtures include different aggregate compositions or degrees of compaction bonded at different cement contents, the correlation of their response under non-destructive testing with other advanced or destructive tests will provide an important tool to estimate the advanced properties at less cost and effort. It should be noted that the correlations between different tests represent the second input level methodology for pavement analysis and design as recommended by mechanistic-empirical pavement design guide ([Applied Research Associates 2004](#)). This is also a quick and cheap method for assessment of the materials in the field as reported by [Su et al. \(2013\)](#). Finally, a new application was proposed in this research for non-destructive testing as a useful tool to accurately assess the mixtures' behaviour under cyclic loading. This latter methodology will be used in this research for further characterization of CSAMs.

## **7.2 Importance of the non-destructive testing for pavement design**

The mechanistic-empirical pavement design guide ([Applied Research Associates 2004](#)) recommends that one of three input levels (1-3) is to be used in pavement

analysis and design to characterize pavement mixtures (Hilbrich and Scullion 2007). Firstly, Input Level 1 represents the highest level of reliability by measuring the material's fundamental properties directly from the materials to be used in pavement construction. Secondly, due to the fact that the advanced testing methods almost always require well-trained staff and a sophisticated laboratory which may be not always available, the guide introduced Input Level 2. In this level, simple, economic and available testing is conducted and the fundamental properties are then estimated from correlations with these test results. Finally, Input Level 3 relies totally on the default values for these properties. Despite adopting the resonant frequency as a design input by some authors (Nunn 2004; Lav et al. 2006), non-destructive testing provides valuable information to develop correlations with the results of the most advanced tests and these, in turn, provide the required inputs for pavement analysis and design with less time, effort and cost. These laboratory-based correlations along with the direct measurement in this field can be used for quality control purposes by estimating the in situ strength and stiffness.

### **7.3 Materials, mixture design and samples preparation**

Materials, mix design and all sample preparation steps were kept as previously discussed in Chapter 4. In this chapter, the measurement of non-destructive properties was conducted for all different samples' shapes. The reasons behind this are, firstly, to ensure measuring both destructive and non-destructive performance for the same samples and hence obtaining an accurate correlation and the possibility of estimation of different parameters from non-destructive testing. In addition, it is to investigate the effect of sample size on the final property.

## 7.4 Experimental Procedures

### 7.4.1 Ultrasonic Pulse Velocity (UPV)

Ultrasonic pulse velocity test is a rapid test that can be used to assess a material's properties both in laboratory and in the field. This test was conducted to estimate the pulse velocity and the dynamic modulus of elasticity non-destructively in accordance with [ASTM C597](#). The ultrasonic longitudinal propagation stress wave speed was measured by PUNDIT-Plus (Portable Ultrasonic Non-destructive Digital Indicating Tester) manufactured by CNS Farnell, UK. This consists of three parts which include transducer, receiver and electronic control part as shown in Figure 7.1. The direct transmission method was used to measure pulse velocity and dynamic modulus and for both beams (prisms) and cylinders by fully contacting both transducer and receiver to the sample ends via coupling gel. To ensure reliability of results, the apparatus was first calibrated using the calibration bar.

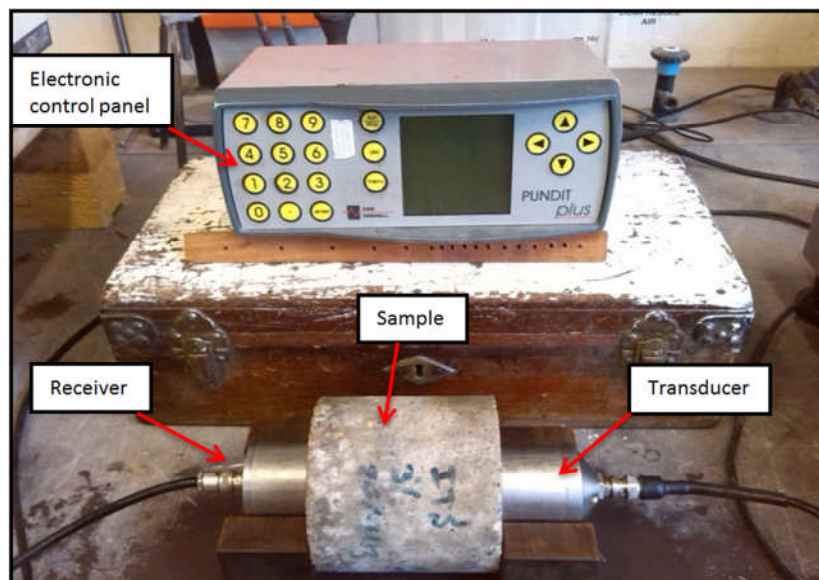


Figure 7.1: PUNDIT-Plus Apparatus and measuring arrangement

### 7.4.2 Resonant-frequency testing

Resonant-frequency is used alternatively to the UPV method to characterize the dynamic properties non-destructively. It was originally developed in United States by Powers in 1938 (Popovics 1998). Unlike the UPV testing, where it is possible to test different sizes and types of samples both in laboratory or in situ, resonant–frequency is used in laboratory for specific sizes of prisms and cylinders (Hassan and Jones 2012). A vibration generator excites the sample. Vibrations are induced at a specific frequency bands until a standing resonant wave is produced. This occurs when both the exciting and sample natural frequencies match. As is well known, the natural frequency of the material is governed by the properties of the material such as modulus of elasticity and Poisson’s ratio. Therefore, this test is used to find these properties non-destructively based on the principle explained above (Lav et al. 2006). In this study, this test was conducted in order to estimate dynamic modulus of elasticity and dynamic shear modulus. These parameters can be used for pavement analysis and design (Nunn 2004; Lav et al. 2006). From these two moduli, dynamic Poisson’s ratio can also be calculated.

Dynamic modulus of elasticity was measured non-destructively using resonant frequency testing by the ERUDITE tester in accordance with the equipment manual and ASTM C215-02. In this test (Figure 7.2), the sample was supported at its centre on the equipment bench and clamped into correct position. The driver and pick up parts were placed in different locations depending on whether dynamic modulus of elasticity (longitudinal mode) or dynamic shear modulus (torsional modulus) was being estimated. Using the recommended frequency range for the specific mode of

test and starting from a low frequency, the frequency was increased gradually until the output meter showed the maximum value which indicates the fundamental resonant frequency of the material. These were used to calculate the dynamic modulus of elasticity and dynamic shear modulus using Eq. 7.1 and Eq. 7.2, respectively. From these two variables, the dynamic Poisson's ratio was calculated from Eq. 7.3 as provided in [ASTM C1018](#).

$$E_{dr} = D. M. (n')^2 \quad (7.1)$$

$$G_d = B. M. (n'')^2 \quad (7.2)$$

$$\nu_d = \left( \frac{E_{dr}}{G_d} - 1 \right) \quad (7.3)$$

where

$$D = 5.093. \left( \frac{L}{d^2} \right) \quad \dots \dots \dots \text{for cylinders}$$

$$D = 4. \left( \frac{L}{b. h} \right) \quad \dots \dots \dots \text{for prisms}$$

$$B = \left( \frac{4. L. R}{A} \right)$$

$n'$  = fundamental longitudinal frequency, Hz

$n''$  = fundamental torsional frequency, Hz

M = mass of sample, kg.

L = length of the sample, m

d = diameter of the cylindrical sample

$A$  = Area of specimen cross-section,  $m^2$

$h, b$  = cross-section dimensions of the prismatic sample,  $m$

$R$  = shape factor = 1 for cylindrical sample; = 1.183 for prismatic sample with square cross-section

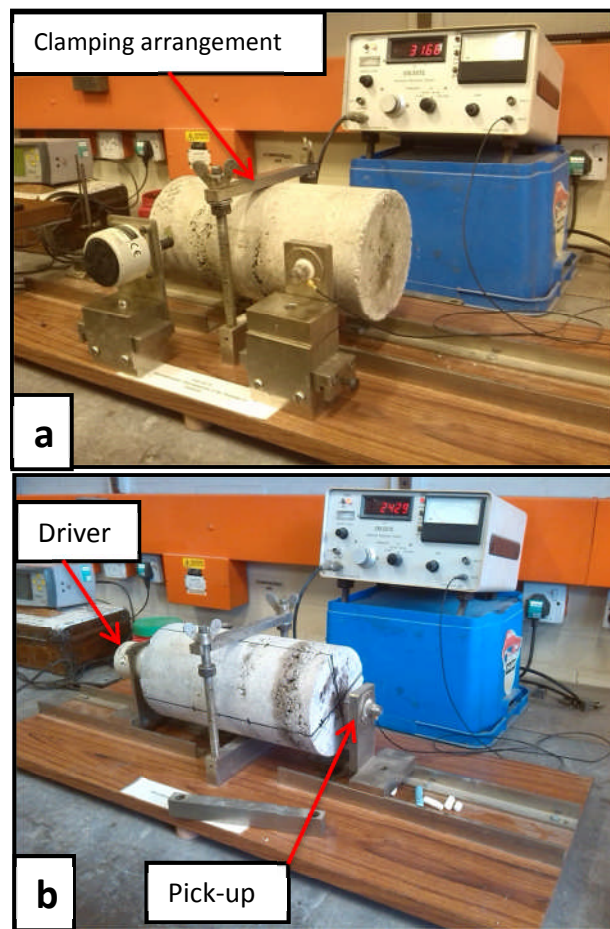


Figure 7.2: Resonant frequency test configuration: a. Torsional mode arrangement; b. longitudinal mode arrangement

## 7.5 Results and discussion

### 7.5.1 Uniformity of different samples densities

One of the important issues that should be taken into consideration when comparing the behaviour under different testing mode or when correlating different parameters

resulting from different tests, especially for these compacted mixtures, is the uniformity of densities of the samples used in these testing. In this section, a comparison between the densities of different samples (small cylinders, large cylinders and prisms) was conducted to ensure comparable results between testing performed on different samples sizes and shapes. Figure 7.3 summarizes the densities of the manufactured samples containing increasing amounts of crumb rubber. It is obvious that, as previously concluded the incorporation of more rubber decreases the density and this trend is valid for different types of samples. Furthermore, the variation in density across the various specimen types at each investigated rubber content, is negligible with a calculated coefficient of variation of less than 1%.

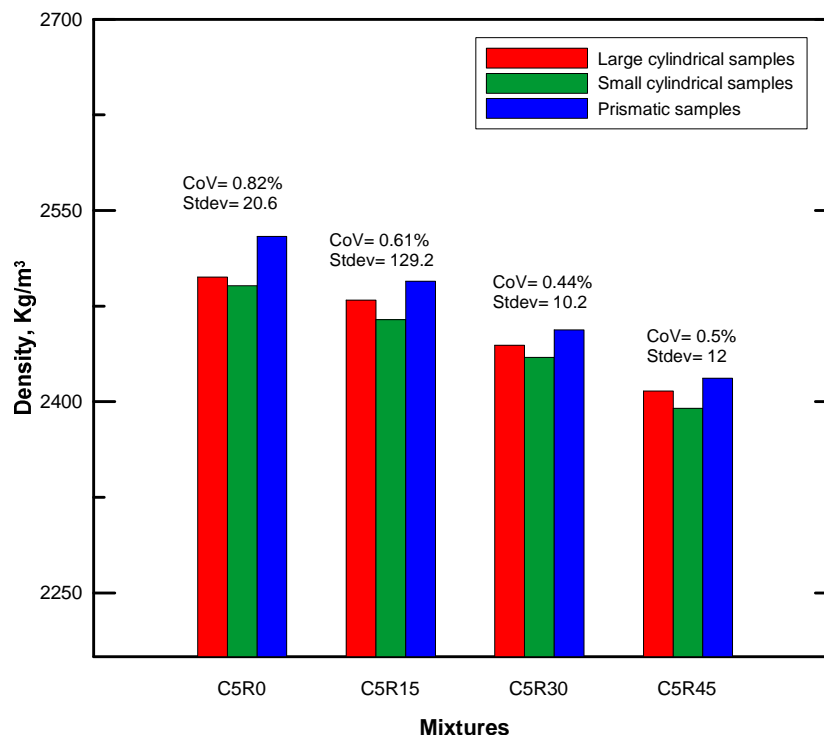


Figure 7.3: Effect of rubber content on densities of different samples types

On the other hand, the same trend as observed previously (Chapter 4) is valid for all other specimens' types where the addition of cement slightly improves the density of

the sample. In addition, the uniformity of densities across all the manufactured samples' types is obvious as shown in Figure 7.4. Coefficient of variation for reference mixtures is than 1% for all cementation levels while for rubberized mixtures it is also less than 1% except at low cement content. From these findings it can be conclude that there is uniformity in the manufacturing process and, most importantly, the comparison and correlation between different tests (even using different types of samples) is valid and accurate.

Even though there is only a small variability between different samples' densities, as mentioned above, it can be seen from both figures (Figure 7.3 and Figure 7.4) that the prisms had slightly higher densities than the large cylinders and the latter presented larger densities than the small cylinders. This can be attributed to the side friction at the mould face which is high in small cylinders and less and even less in large cylinders and prismatic samples, respectively.

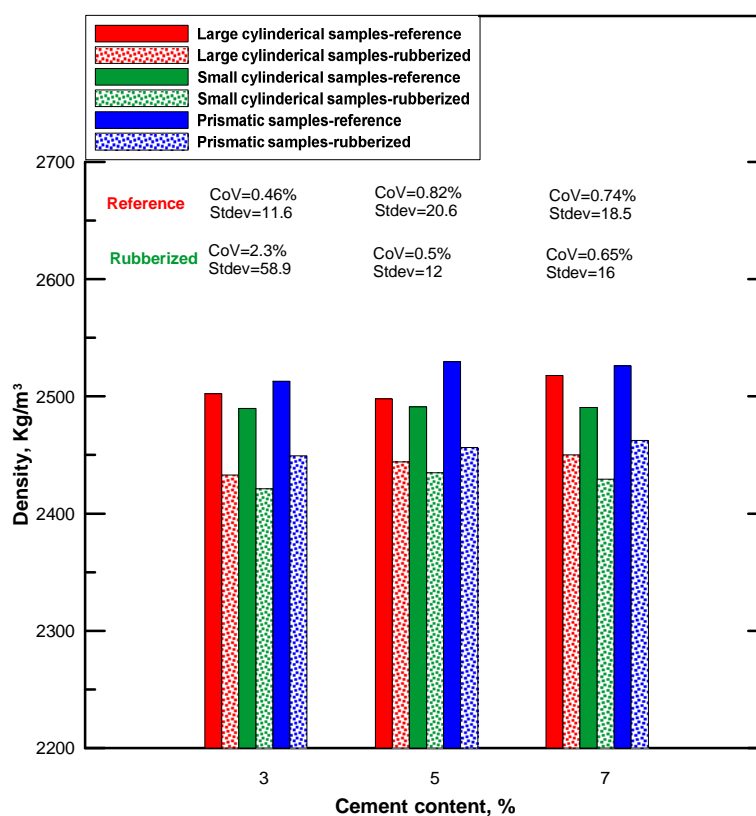


Figure 7.4: Effect of cement content on densities of different samples types

### 7.5.2 Ultrasonic pulse velocity (UPV)

Figure 7.5 shows the effect of various rubber replacement levels on the UPV values. A decline in UPV value occurred as result of partial replacement of natural aggregate by the crumb rubber. Zheng et al. (2008) claimed that a lower modulus of elasticity of rubber particles is responsible for the reduction in wave velocity. This decrease in the UPV value can be attributed to the decrease in aggregate interlocking and hence contact efficiency due to rubber incorporation. The rubber probably caused a decrease in the contacts points between the stiffer natural aggregate particles which, in turn, would affect the transmission of ultrasonic wave. Furthermore, some of the wave energy might be absorbed by the rubber particles of higher elasticity.

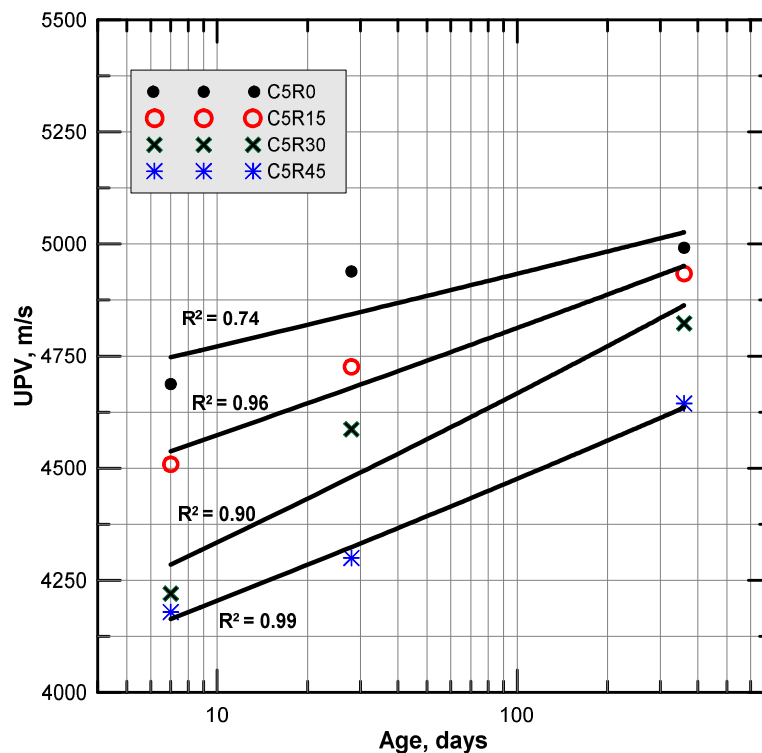


Figure 7.5: Effect of age and rubber content on the UPVs

The same figure also illustrates the effect of curing age on the UPV. Similar to UCS and ITS, UPV improved with length of curing which might be due partly to the improvement of cement mortar and particles' bond which contributes in accelerating the wave transmission through these contacts points. Due to the fact that the wave transmission speed through medium or high voids is less than that of low voids, another possible reason for this increase is probably the reduction in the mixtures voids due to the increase in the hydration products (Bogas et al. 2013). A similar trend was observed by Mohammad (2011) and Su et al. (2013). In general, the improvement in the UPV occurred during the early ages where (except for C5R45) the increase in UPV between 7 and 28 days age is more pronounced than that which occurred between 28 days and 365 days. These results are consistent with Su et al. (2013) who reported that a greater development in the UPV occurred between 1 day and 7 days. Soil-lime mixtures investigated by Yesiller et al. (2001) was confirmed the same behaviour with longer curing ages.

To overcome the heterogeneity of cementitious mixtures and to provide accurate correlation between different tests (utilizing different sample shapes and dimensions), the non-destructive measurements were conducted for each type of sample i.e., every destructive measurement was preceded by a non-destructive measurement hence ensuring measurements for matching samples.

Figure 7.6 demonstrates the effect of rubber content on the UPVs of different samples types. It can be clearly seen from this figure that the decrease in the UPVs is observed for each sample shape with some variation between these shapes. The coefficient of variation is estimated as 2.9%, 2.7%, 3.9% and 4.2% for 0, 15%, 30%

and 45% rubber replacement levels, respectively. On the other hand, the general trend regarding the effect of cement on the UPVs is improvement in this property as cement content increases as shown in Figure 7.7. Again, slight variations were observed in the UPVs values. Even though there was slight variation in the measurement across different samples' shapes, the greater variation was observed in the rubberized mixture as compared with the reference ones for all cement contents. This might be because of the slight variation in the rubber distribution as presented in Chapter 6. However, the non-destructive testing is still insensitive to the rubber distribution as compared with the destructive testing.

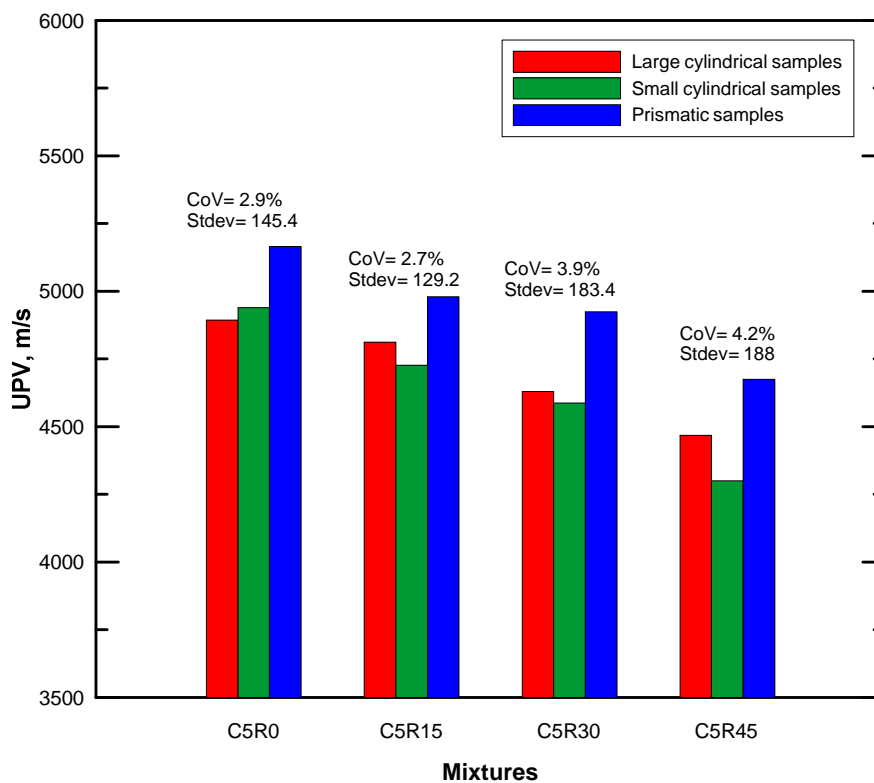


Figure 7.6: Effect of rubber content on UPVs of different samples

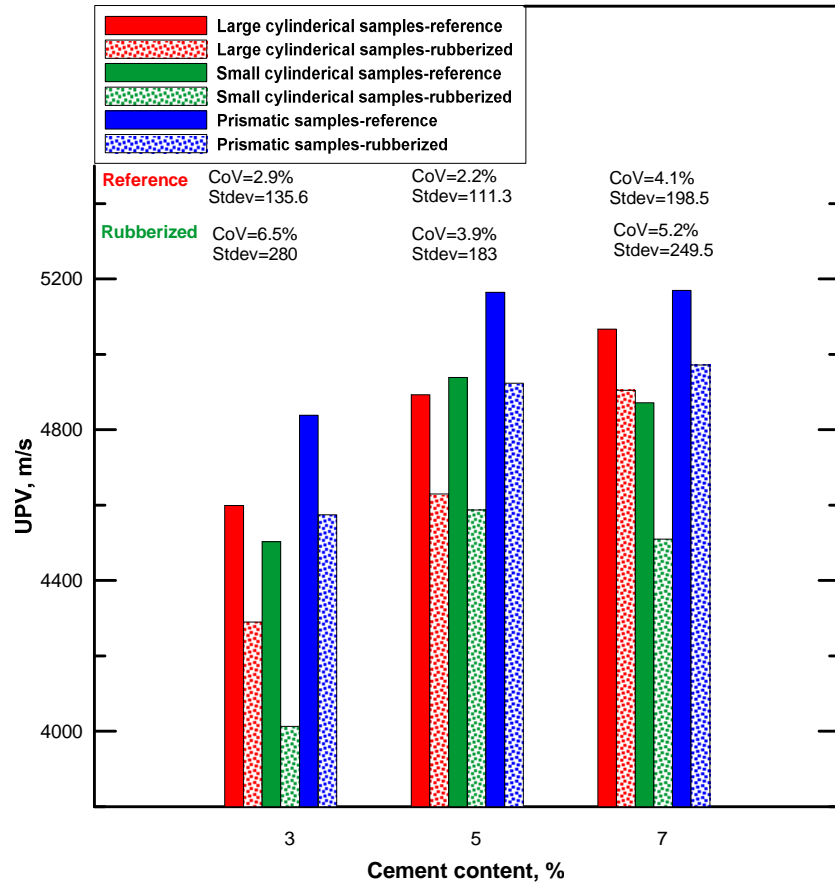


Figure 7.7: Effect of cement content on UPVs of different samples

### 7.5.2.1 Effect of combined effect of cement and rubber on UPV

Regarding the effect of cement content on UPVs of rubberized and reference mixtures, it can be seen from Figures 7.8 that increasing cement content causes an improvement in the UPVs of the mixtures. Furthermore, increasing curing time has a positive impact on the transmission ability of the ultrasonic wave through the sample. However, for both control and rubberized mixtures, it seems that the increase ultrasonic wave velocity is more pronounced when cement content increase from 3% to 5% as compared with that between 5% and 7%. These findings are consistent with the other findings reported in Chapter 6 and Chapter 5.

It worth mentioning that, in the concrete industry, it possible to classify the quality of these mixtures based on their UPVs as reported by Solis-Carcaño and Moreno (2008). Comparing these criteria with the current UPV results at 28 days reveals that C5R0 and C5R15 can be classified as excellent quality while the quality of C5R30 and C5R45 is good. For control mixtures of different cementation levels, the mixtures having 5% cement or higher can be classified as excellent quality mixtures while those below 5% are classified as of good quality. For rubberized mixtures in which 30% of the 6mm fraction size was replaced by an equivalent volume of rubber, despite the differences between the UPVs, all mixtures classified as good quality, regardless of cement content.

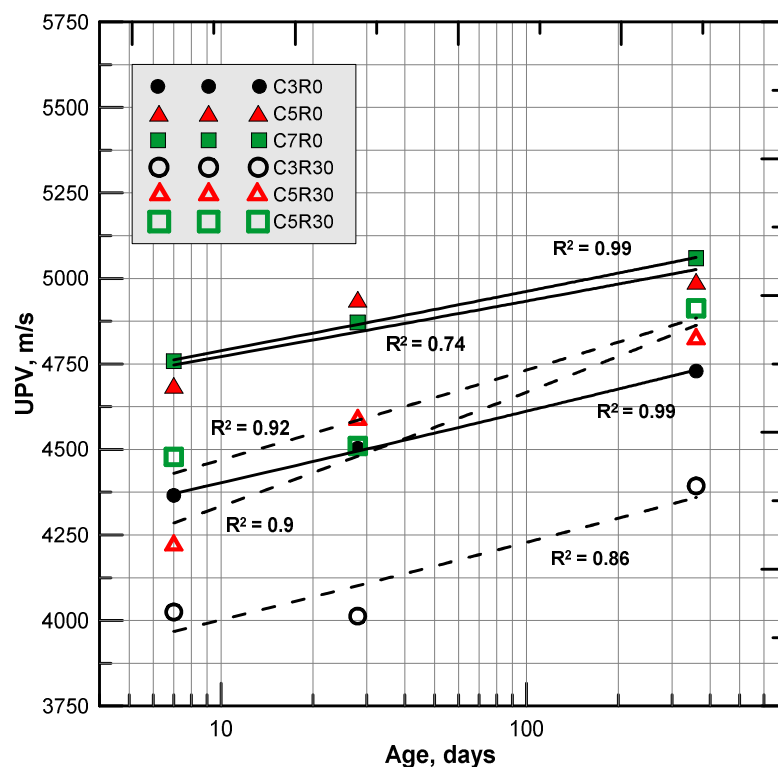


Figure 7.8: Effect of age and cement content on the UPVs

Figures 7.9 and Figure 7.10 reveal an exponential relationship between the strength in terms of UCS and ITS and UPV value. [Shariq et al. \(2013\)](#) and [Su et al. \(2013\)](#) have also reported such a relationship for normal concrete and cementitious-stabilized mixtures, respectively. In pavement design, it necessary in case of unavailability of complex testing or to reduce the cost, to use the correlation between the advanced tests and a simple test, as recommended by the mechanistic–empirical design through Input Level 2. Figure 7.11 through Figure 7.14 illustrate some correlations that have been developed to estimate the important parameter for pavement design from the non-destructive testing. It can be seen from these figures that there is a strong relationship between these parameters and non-destructive one which means that allow all of the parameters to be estimated reliably. These also may be used to ascertain if the strength/stiffness in the field meets the specification or structural design assumptions. The best way to do the latter is by using the ultrasonic pulse velocity test and their associated correlations since the latter test is customarily used to assess the civil engineering structural elements non-destructively.

The developed correlation between ITS value and UPV is very important to estimate the stress ratio at which to test a sample for resilient modulus or for fatigue in the indirect tensile mode as discussed latter in Section 7.5.

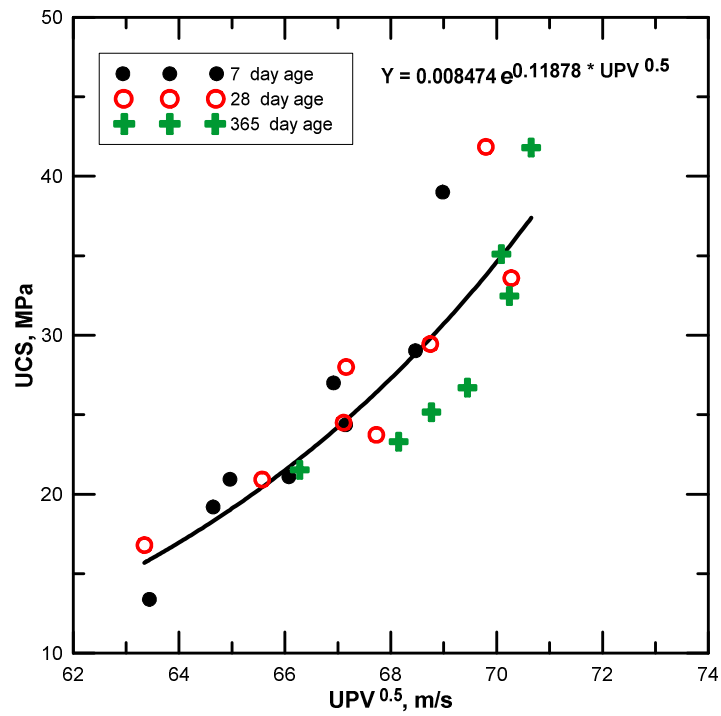


Figure 7.9: Variation of UPVs versus UCSs

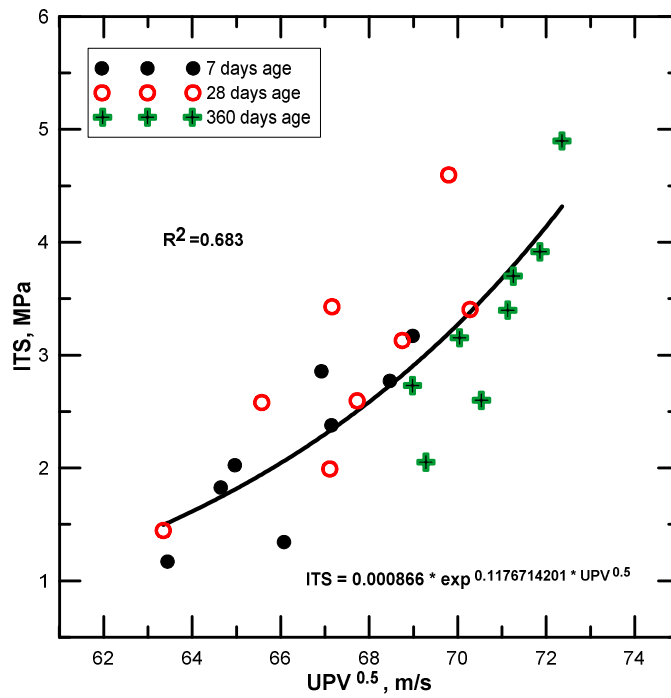


Figure 7.10: Variation of UPVs versus ITSs

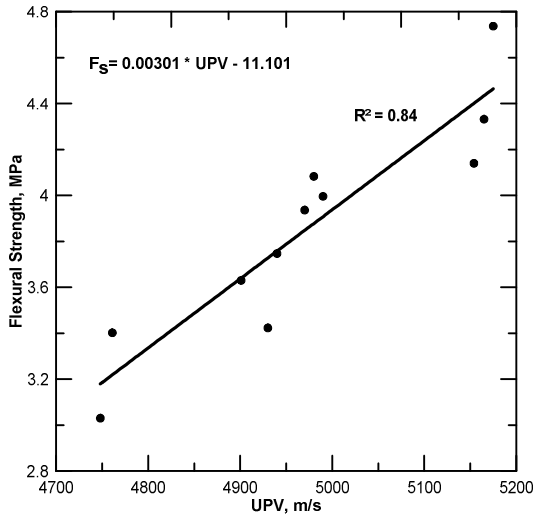


Figure 7.11: Variation of UPVs versus flexural strength @ 5% cement content

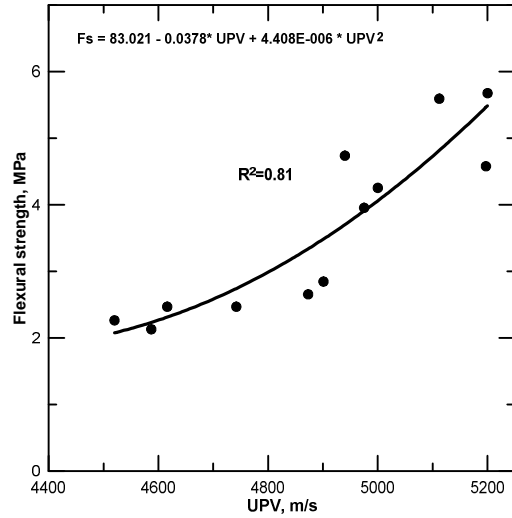


Figure 7.12: Variation of UPVs versus flexural strength @3% and 7% cement

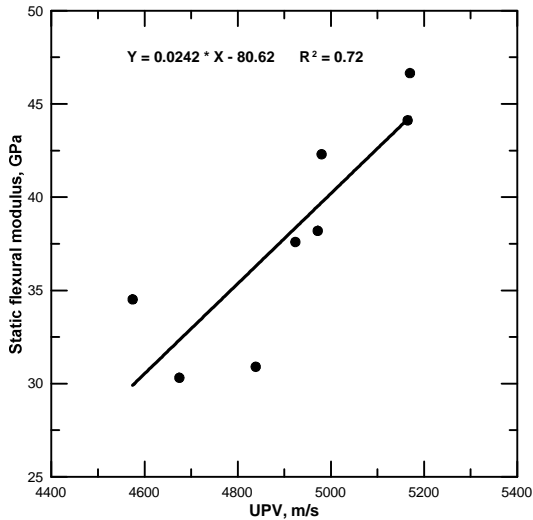


Figure 7.13: Variation of UPVs versus static flexural modulus

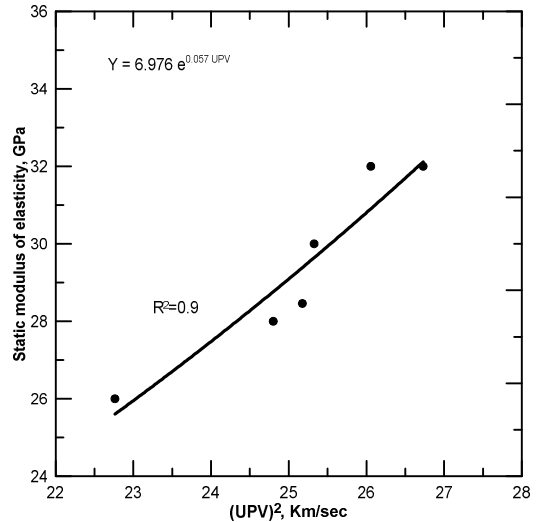


Figure 7.14: Variation of UPVs versus static indirect tensile modulus

### 7.5.3 Dynamic modulus of elasticity

Dynamic modulus of elasticity can also be estimated from the ultrasonic pulse velocity using the following formula (Mardani-Aghabaglou et al. 2013):

$$E_{du} = \frac{\rho \text{UPV}^2(1+\nu)(1-2\nu)}{1-\nu} \quad (7.5)$$

where  $\rho$  and  $\nu$  are the density and Poisson's ratio, respectively. The bulk density of the fabricated beams was estimated using the water displacement method. Since the effect of rubber and cement on the dynamic modulus of elasticity follows the same trend as that of the UPV, therefore this effect is not presented. However, to show the typical values for these modified mixtures and compare these with the typical values resulted from other stiffness modulus testing modes, these typical values and the relationship with results obtained from other testing procedure will be presented in Chapter 9.

#### **7.5.4 Dynamic modulus of elasticity, dynamic shear moduli and dynamic Poisson's ratio**

Similar to the static modulus of elasticity results, there was a decrease in both dynamic modulus of elasticity and dynamic shear modulus due to rubber replacement, as shown in Figure 7.15. This is because these two moduli depend on mixture density and type of aggregate. However, these parameters decreased linearly at all replacement levels. This, in fact, supports the above hypothesis regarding the possible effect of rubber accumulation at higher rubber replacement i.e., C5R45. This was also evidenced in Chapter 6 when the rubber distribution was studied. During non-destructive testing, there was zero applied stress which eliminates the formation of micro-cracks and possible creep (Najim and Hall 2012). In other words, it depends on the mixture constituents and mixture fabrication alone. For this reason, it can be concluded that non-destructive test results do not depend, to a large extent, on rubber

distribution as compared with the sensitivity of the results of destructive tests to rubber distribution.

Regarding the impact of cement on the dynamic properties and similarly to the static modulus of elasticity, there was an increase in both dynamic modulus of elasticity and that of rigidity due to increase in mixture cement content, as depicted in Figure 7.16. Despite the higher dynamic moduli of elasticity values as compared with static ones, the former tends to be highly consistent with the latter where both of them confirm that the reduction in the moduli values due to rubber inclusion is greater at low cement content as compared with higher contents. This, in fact, demonstrates the ability of the non-destructive testing to distinguish between different modified mixtures containing different amounts of cement and their high sensitivity to the small change in the aggregate structure due to incorporation of a small amount of rubber.

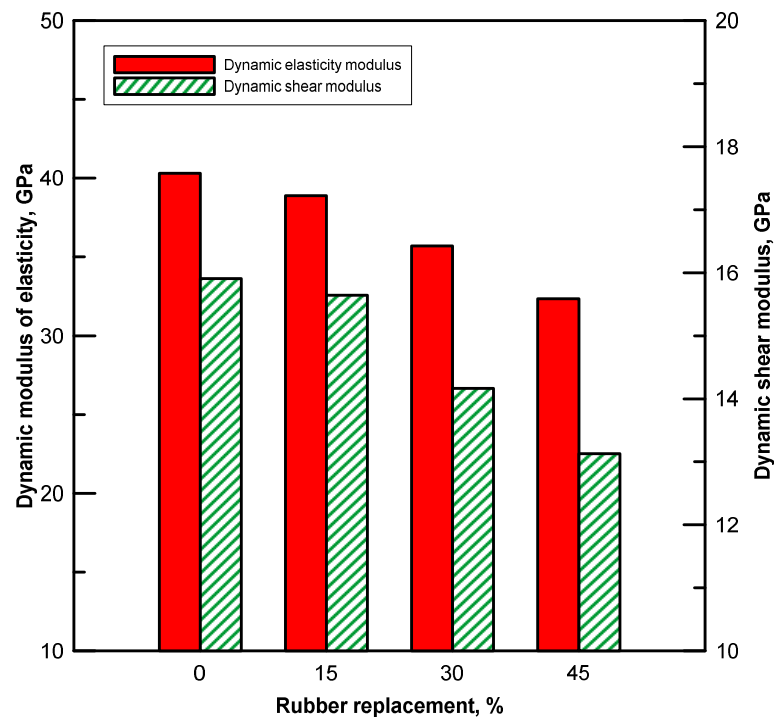


Figure 7.15: Effect of rubber replacement level on dynamic modulus of elasticity and shear modulus

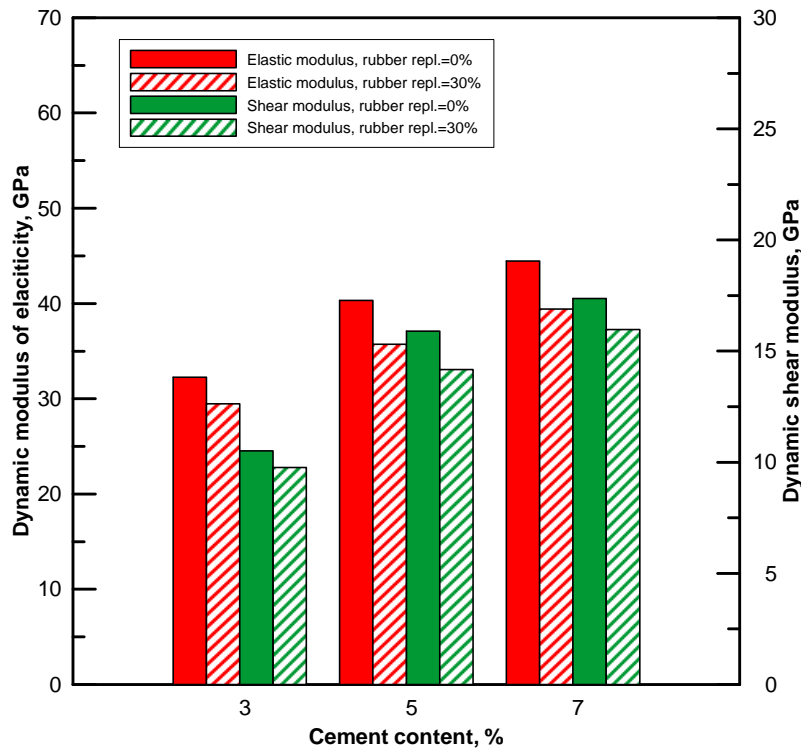


Figure 7.16: Effect of cementation level on dynamic modulus of elasticity and shear modulus

With regard to dynamic Poisson's ratio, Figure 7.17 shows a broad decline in the value of this parameter as the rubber content increases in the mixture. [Nehdi and Khan \(2001\)](#) have reported in their review paper that some authors found that incorporating rubber in a normal concrete mixture resulted in a drop in the Poisson's ratio value while, on the other hand, others reported opposite findings. Since this ratio is the amount of lateral strain with respect to the axial strain, Poisson's ratio from a logical point-of-view should increase due to the introduction of elastic particles, because of the increase in the elasticity of the whole mixture. However, from the author's point-of-view, the above interpretation is valid if the comparison is made between two homogenous mixtures with different degrees of elasticity. RCSAM containing different materials of different strengths and stiffness is a composite material of complex behaviour. Bearing this in mind, the possible

explanations for the decrease in Poisson's ratio comes from the fact that, in case of low rubber content, when the RCSAM is compressed axially, rearrangement, on a mesoscale level, may occur for the compacted particles. As the rubber particles are much softer and compressible than the surrounding materials and natural aggregate, such property might make the rubber particles like venues or spaces into which the aggregate particles may rearrange themselves. This, in turn, will results in less overall lateral deformation and hence a decrease in the Poisson's ratio value. In fact, this explanation depends, to some extent, on the amount of rubber in the mixture.

Figure 7.18 demonstrates the effect of cementation on the Poisson's ratio of both virgin and rubberized mixtures. A decline in Poisson's ratio occurred for both mixtures because the higher stiffness/ lower deformability due to high cement content and fewer tendencies for particle rearrangement will cause a decrease in the overall lateral deformation which in turn reduces the Poisson's ratio.

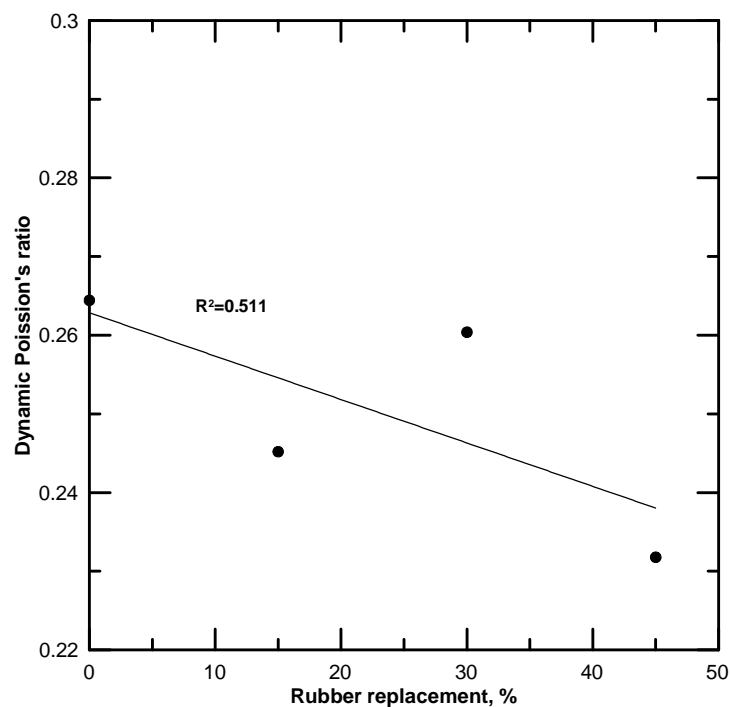


Figure 7.17: Effect of rubber replacement level on dynamic Poisson's ratio

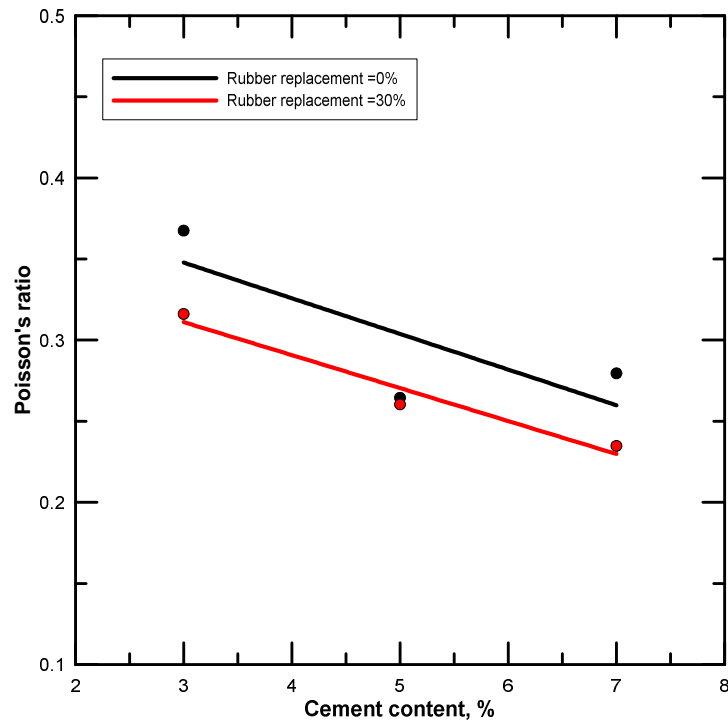


Figure 7.18: Effect of cement content on dynamic Poisson's ratio

#### 7.5.4.1 Effect of sample size on stiffness and shear moduli from resonant-frequency testing

Even for normal concrete where the resonant frequency test was used extensively, little information was found in the literature regarding the effect of sample size on the moduli values. [Kesler and Higuchi \(1954\)](#) as reported by [Malhotra and Carino \(2003\)](#) observed that the resonating frequencies of longer concrete beams is more than that of smaller beams resulting in higher moduli for the former.

In this research, to quantify the effect of different sample size on resonant frequency output, the test was conducted on cylindrical samples 150 mm in diameter by 300 mm high. The same trend as discussed in Section 5.4.3 was obtained. However, comparing and contrasting the moduli values that resulted from both sample sizes

revealed higher values for these parameters when measured using the prisms samples. Figure 7.19 illustrates the relationship between dynamic moduli from prisms and that from large cylinders. From this figure it can be concluded that the moduli measured from the prisms is higher than obtained using large cylinders by 14.5%. Another important conclusion that can be drawn from this comparison is the independency of the relationship (between moduli from two different sample sizes) on the aggregate composition or cementation degree, as data points for different mixtures follow the same relationship.

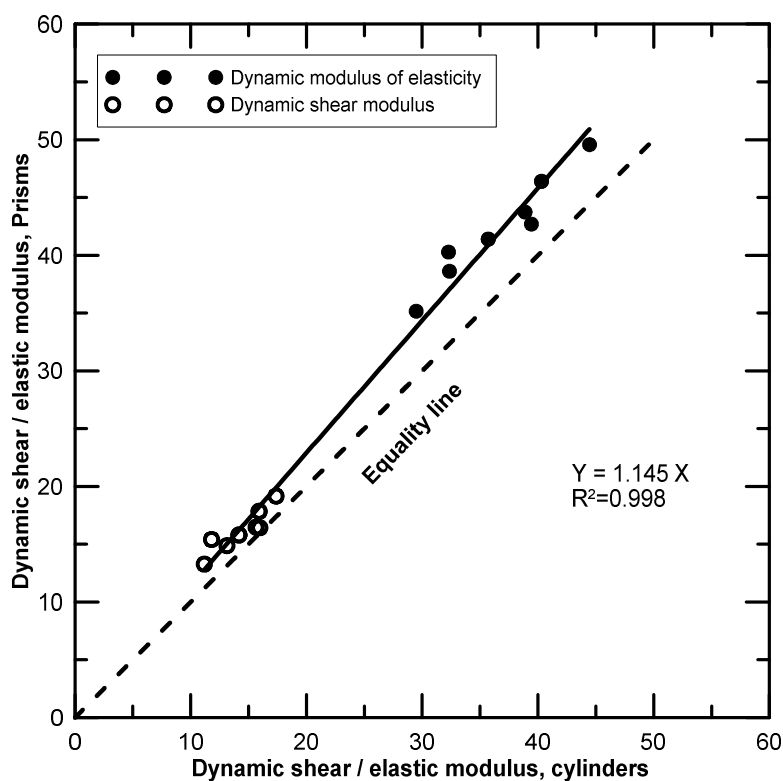


Figure 7.19: Dynamic moduli for large cylinders versus prismatic samples for different rubberized and reference samples under different stabilization degrees

## 7.6 New proposed application for non-destructive testing

Mechanistic pavement design is significantly dependent on the fatigue performance of the cementitiously stabilized mixtures, and the stress ratio at which they are called

to operate. Stress ratio can be defined as the ratio between the applied flexural stress and the flexural strength. In fatigue characterization, the conventional approach is to measure first the flexural strength of the mixture based on the static flexural test testing program and then to estimate the stress ratios to be applied to the different specimens in flexural fatigue tests. However, due to the heterogeneity of CSAMs, this approach does not necessarily ensure that a representative flexural strength is obtained and applied. [Balbo \(1997\)](#) attributed the dispersion in the results of fatigue test to the definition of the materials' strength and hence the S-N relationship. [Sobhan and Das \(2007\)](#) tried to overcome this problem by correlating the flexural strength of full-sized beams to the flexural and compressive strengths of beams and cubes sawn from fatigue failed specimens. In this way they were able to estimate the actual flexural strength and, hence, stress ratio of the fatigued specimens. However, the latter methodology needs large beams to be tested and contains several cutting processes which would incur additional time, cost and effort. In this research, to overcome the heterogeneity of the CSAMs and to better estimate the actual flexural strength and hence stress ratio and fatigue characteristics accordingly, the following methodology is proposed:

1. Measure the UPVs of the samples to be tested for static flexural strength.
2. Measure the flexural strength by performing the static flexural test for different samples.
3. Making a correlation between the UPVs and the static flexural strengths for different samples.

4. In the fatigue test, measure the UPVs for the samples to be tested, then using the correlation developed in 3, estimate the flexural strength for the same sample that will be tested for fatigue.
5. The average of the static flexural strength from the static flexural testing program and the estimated flexural strength from the correlation (4) should be used to estimate the stress ratio.

This methodology, in fact, is not limited only to the fatigue test but can be used also to estimate the stress ratio for the stiffness modulus determination under cyclic loading both in indirect tensile, direct tensile or flexural testing modes. Furthermore, it permits estimation with less effort and cost since the ultrasonic test is cheap and available and can be used for different samples sizes. More importantly, due to the fact that some samples are normally tested after a specific time, using this methodology may overcome the inaccuracy due to adopting the same static flexural test results for samples cured for 28 days as for fatigue samples cured for more than 28 days due to the delay of fatigue testing.

To permit estimation, and due to the fact that the current investigation includes different aggregate compositions or degrees of compaction and different cementation levels, the developed correlation in this research can be used to estimate the flexural strength of cement-stabilized aggregate materials and to estimate the stress ratio without conducting the static flexural testing program. The current methodology will be used for further characterization of fatigue behaviour presented in Chapter 9.

## 7.7 Concluding Remarks

1. A new application and methodology was proposed for using of non-destructive tests as a tool to overcome the CSAMs' heterogeneity and hence to gain accurate fatigue or elastic modulus estimation by accurately determination the actual materials' strength and hence stress ratio.
2. Good correlations were observed between the mechanical properties (mainly strength and stiffness) from different testing modes and the properties obtained from non-destructive tests. These can be used to estimate both simple and advanced test results easily and non-destructively with less time and effort. It can be used also to estimate the properties of the materials in the field for quality control purposes.
3. Incorporating rubber in cement-stabilized mixtures, even at small content levels, caused a noticeable reduction in both UPV value and dynamic modulus of elasticity and shear modulus estimated by the resonant frequency method.
4. An increased in the dynamic modulus of elasticity and shear modulus was observed as a result of increasing the cement content for both virgin and rubberized cement-stabilized aggregate mixtures.
5. Increasing the curing age caused an increase in the UPV values estimated from ultrasonic testing for all investigated rubber and cement contents.

6. Poisson's ratio measured from resonant-frequency method decreases as the rubber content in the mixture increases. Similarly, this ratio also increases as a result of cementation level increase.
7. There were only slight differences in the trend of stiffness moduli evaluated by non-destructive testing methods and destructive methods. These differences were attributed to rubber distribution. The values of moduli determined by both methods were sensitive to the amount of rubber in the mixture. Taken together this implies that the non-destructive methods are suitable for evaluation the quality of CSAMs and RCSAMs both in laboratory and for field quality control.
8. Effect of specimen size on resonant-frequency is addressed and a relationship between moduli (elastic modulus and shear modulus) values was established. In general, a linear relationship exist between them where the moduli measured using the cylindrical sample of size (150 mm x 300 mm) is smaller than that measured from (100 mm x 100 mm x 500 mm) prisms.
9. It seems that the relationship between different sample sizes is not affected by neither aggregate composition/degree of compaction nor the content of cement used to bind the mixture. From this, it can be inferred that there is a unique relation between moduli measured using different sizes of samples.
10. The correlations formulated in this chapter are summarized in the table below.

Table 7.2: Developed relationships between strength, stiffness and nondestructive parameters

No.	Correlation	Parameters and units	R <sup>2</sup>	Figure No.
1	$UCS = 0.008474e^{0.11878 * UPV^{0.5}}$	UCS= unconfined compressive strength, MPa UPV=Ultrasonic pulse velocity. m/s	0.82	7.9
2	$ITS = 0.000866e^{0.11767 * UPV^{0.5}}$	ITS=indirect tensile strength, MPa	0.68	7.10
3	$F_s = 0.00301 * UPV - 11.101$ for 5% cement content	F <sub>s</sub> = flexural strength, MPa	0.84	7.11
4	$F_s = 83.021 - 0.0378 * UPV + 0.00000044 * UPV^2$ for 3% and 7% cement content	Same as above.	0.81	7.12
5	$E_f = 0.0242 * UPV - 80.62$	E <sub>f</sub> = static flexural modulus, GPa	0.72	7.13
4	$E_{it} = 6.976 e^{0.067 * UPV}$	E <sub>it</sub> = static indirect tensile modulus, GPa	0.9	7.14

## 7.8 References

- Applied Research Associates, I. (2004). Guide for Mechanistic-Empirical Design of New and Rehabilitated Pavement Structures. Illinois.
- Balbo, J. T. (1997). High quality cement treated crushed stones for concrete pavement bases. Proceedings of the Sixth International Purdue Conference on Concrete Pavement November.
- Bogas, J. A., M. G. Gomes and A. Gomes (2013). "Compressive strength evaluation of structural lightweight concrete by non-destructive ultrasonic pulse velocity method." *Ultrasonics* 53(5): 962-972.
- Hassan, A. and S. Jones (2012). "Non-destructive testing of ultra high performance fibre reinforced concrete (UHPFRC): A feasibility study for using ultrasonic and resonant frequency testing techniques." *Construction and Building Materials* 35: 361-367.
- Hilbrich, S. and T. Scullion (2007). "Rapid alternative for laboratory determination of resilient modulus input values on stabilized materials for AASHTO mechanistic-empirical design guide." *Transportation Research Record: Journal of the Transportation Research Board*(2026): 63-69.
- Lav, A. H., M. A. Lav and A. B. Goktepe (2006). "Analysis and design of a stabilized fly ash as pavement base material." *Fuel* 85(16): 2359-2370.
- Malhotra, V. M. and N. J. Carino (2003). Handbook on Nondestructive Testing of Concrete Second Edition, CRC press.
- Mandal, T., J. M. Tinjum and T. B. Edil (2014). non-destructive testing of cementitiously stabilized materials using ultrasonic pulse velocity test 2. Transportation Research Board 93rd Annual Meeting.

- Mardani-Aghabaglou, A., Ö. Andiç-Çakir and K. Ramyar (2013). "Freeze–thaw resistance and transport properties of high-volume fly ash roller compacted concrete designed by maximum density method." *Cement and Concrete Composites* 37: 259-266.
- Mohammad, I. K. (2011). *Non-Destructive Testing for Concrete: Dynamic Modulus and Ultrasonic Velocity Measurements*. Advanced Materials Research, Trans Tech Publ.
- Najim, K. B. and M. R. Hall (2012). "Mechanical and dynamic properties of self-compacting crumb rubber modified concrete." *Construction and Building Materials* 27(1): 521-530.
- Nehdi, M. and A. Khan (2001). "Cementitious composites containing recycled tire rubber: an overview of engineering properties and potential applications." *Cement Concrete and Aggregates* 23(1): 3-10.
- Nunn, M. (2004). *Development of a more versatile approach to flexible and flexible composite pavement design : prepared for highways agency, TRL report*.
- Popovics, S. (1998). *Strength and related properties of concrete: A quantitative approach*, John Wiley & Sons.
- Shariq, M., J. Prasad and A. Masood (2013). "Studies in ultrasonic pulse velocity of concrete containing GGBFS." *Construction and Building Materials* 40: 944-950.
- Sobhan, K. and B. M. Das (2007). "Durability of soil–cements against fatigue fracture." *Journal of Materials in Civil Engineering* 19(1): 26-32.
- Solis-Carcaño, R. and E. I. Moreno (2008). "Evaluation of concrete made with crushed limestone aggregate based on ultrasonic pulse velocity." *Construction and Building Materials* 22(6): 1225-1231.

Su, Z., D. Fratta, J. M. Tinjum and T. B. Edil (2013). Cementitiously Stabilized Materials Using Ultrasonic Testing. Transportation Research Board 92nd Annual Meeting.

Yesiller, N., J. Hanson, A. Renner and M. Usmen (2001). "Ultrasonic testing for evaluation of stabilized mixtures." Transportation Research Record: Journal of the Transportation Research Board(1757): 32-42.

Zheng, L., X. Sharon Huo and Y. Yuan (2008). "Strength, Modulus of Elasticity, and Brittleness Index of Rubberized Concrete." Journal of Civil Engineering , ASCE.

### **Specifications**

ASTM C597-09, Standards test method for pulse velocity through concrete

ASTM D2845-95, Standards test method for laboratory determination of pulse velocities and ultrasonic elastic constants of rock.

ASTM C 1018, Standards test method for flexural toughness and first crack strength of fibre-reinforced concrete

## **Chapter Eight**

### **Development of fatigue testing facility**

#### **8.1 Introduction**

Construction materials are normally evaluated using different testing types and modes. The accuracy of performance prediction of materials depends on how close these types and modes simulate the boundary conditions of loading, stress state and supporting system. Therefore, unlike ordinary concrete mixtures where the majority of applied loading is static loading, highway mixtures are normally characterized under repeated or cyclic loading. This is because these mixtures, forming the pavement structure, are subjected to vehicular loading. From a structural point of view, if the applied load is less than the structural capacity then no failure may occur. However, repeating a load that is less than the structural capacity may cause a fatigue failure after a certain number of load repetitions. Accordingly, the evaluation of the

fatigue performance of the structures expected to carry repeated load is of utmost importance to better simulate the field pavement condition.

The purpose of this chapter is to discuss the development of a test facility for cyclic flexural loading. This also includes the instrumentation setup and mounting arrangement. Since this facility will be used for flexural modulus under cyclic load and to investigate fatigue behaviour of selected mixtures, some initial investigation will be included in this chapter. Finally, the methodology to deal with the large volume of data from fatigue test will be also presented.

## **8.2 Fatigue testing configuration and previous studies**

A number of testing methods have been developed to characterize the fatigue behaviour of constructional materials. These includes two point bending, three point bending, four point bending, supported beam, indirect tensile, direct tensile, compressive, tension-compression and wheel tracking method. Figure 8.1 summarizes different fatigue test methods. In their pioneering study to evaluate fatigue test procedures, [Tangella et al. \(1990\)](#) compared different fatigue testing methods in terms of simplicity, ability to simulate the real pavement condition and ability to correlate the laboratory results with in-service pavement structure response. Based on their results, they ranked these methods with the flexural fatigue receiving the highest ranking followed by direct and then indirect tensile testing. However, [Di Benedetto et al. \(2004\)](#) concluded that the fatigue life measured by indirect tensile testing was the shortest as compared with other methods which was, as they claimed, due to the significant permanent deformation accumulation rate. Consequently, they

drew a conclusion that the fatigue lives are highly affected by the testing method and mode of testing.

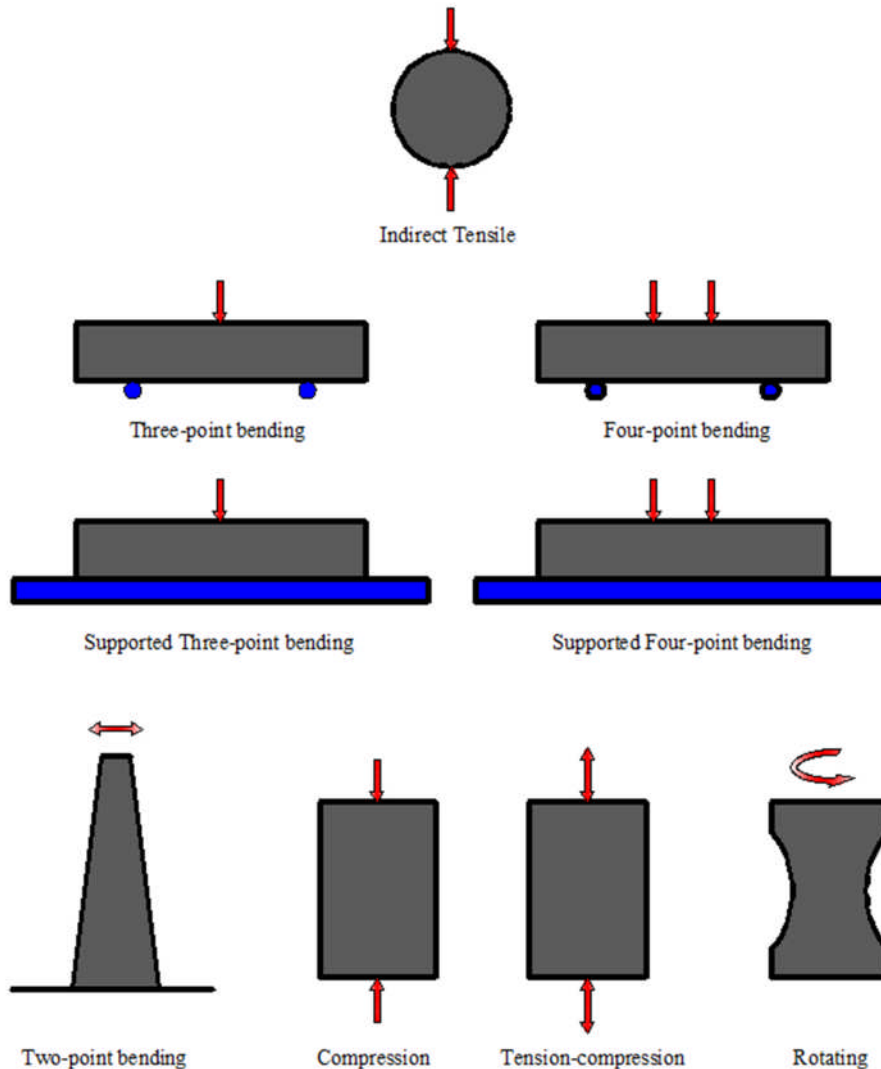


Figure 8.1: Different fatigue test arrangements

### 8.3 Wave form and fatigue testing mode

There are different wave forms that can be applied during the fatigue test. These include sinusoidal, haversine, square and triangular waveforms. Amongst these, sinusoidal and haversine waveform are the most widely used in pavement mixtures characterization during the dynamic modulus or fatigue life estimation as reported by

Huang (2004). In addition, [ASTM D-7460](#) adopts the haversine waveform for asphaltic mixtures testing. Therefore, it will be used in this research for performance characterization under cyclic loading.

Regarding the mode of load, fatigue test is conducted either in controlled stress or controlled strain modes. In the former mode, the stress amplitude is maintained while the strain amplitude increases due to the cyclic application of the stress. In the controlled strain mode, on the other hand, the amplitude of strain is kept constant while the resulting stress decreases due to crack initiation. The applicability of either stress or strain controlled modes depends on the field situation that is to be simulated. Controlled stress mode is normally used for mixtures intended to be used in thick pavement layers. In contrast, the other mode is utilized to simulate the mixtures used in thin layers.

#### **8.4 Fatigue failure analysis criteria**

Various definitions were found in the literature regarding the fatigue failure point. These definitions depend, to some extent, on the fatigue test mode. In a stress controlled fatigue test, the failure is assumed to occur either at the full fracture of the samples or at the point at which the mixture stiffness reaches 10% of its original value ([Rowe 1996](#)). In strain controlled mode, on the other hand, the failure point corresponds to the number of cycles at which the initial stiffness drops by 50% ([Rowe 1996](#)). The reason for adopting 10% stiffness reduction in stress controlled mode as compared with 50% in the strain controlled mode is because, in the stress controlled mode, the cracks are propagated very quickly after their initiation which

makes the number of cycles at 50% stiffness reduction approximately equals to that at which the collapse occur (Li 2013) as shown in Figure 8.2. Van Dijk (1975) considered the number of cycles corresponding to a strain equal to twice the initial strain as the failure point. Although the 50% stiffness reduction is the failure criterion most widely accepted (AASHTO T321-03; BS EN 12697-24, 2004; (Pais and Minhoto 2010) by the asphalt mixtures community, this has been criticized by some scholars who claim that this basis does not reflect any change in the mixture properties. Consequently, other authors attempted to define the failure point more clearly by suggesting new fatigue criteria. Rowe and Bouldin (2000), for example, adjusted Hopeman's energy ratio methodology by plotting the cycle multiplied by the dynamic modulus at that cycle as y-axis versus the cycle number. From this graph, the fatigue failure point was defined as the peak point on that curve. This definition is applicable for both stress and strain controlled testing. Arizona State University proposed a new methodology based on the Rowe and Bouldin's suggestion. In this modification, the values of Rowe and Bouldin's y-axis should be divided by the initial stiffness (Prowell et al. 2010).

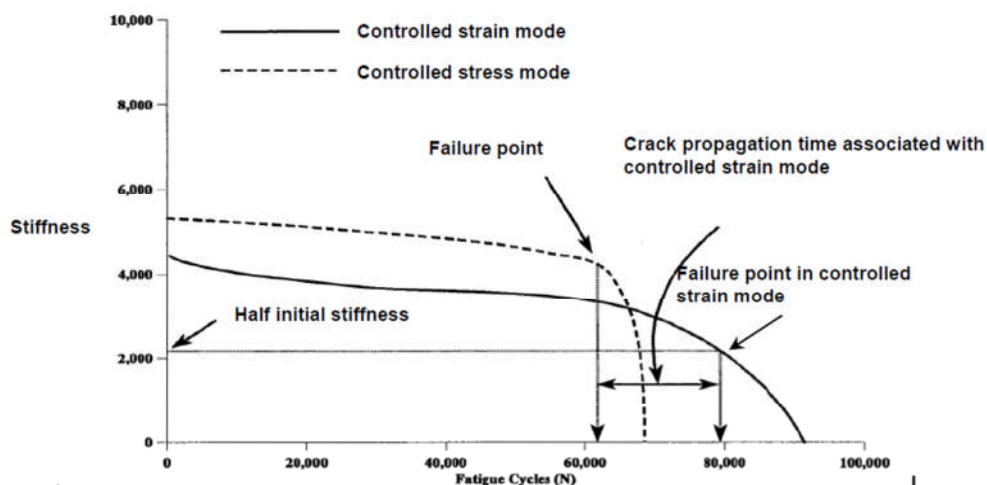


Figure 8.2: Idealized illustration of stress and strain controlled failure points (Li 2013).

### **8.5 Initial stiffness**

Some diversity regarding the definition of the initial stiffness for use in the fatigue test has been found in the literature. [Sobhan and Mashnad \(2003\)](#) considered the initial modulus to be that calculated at 5% of the fatigue life. As a justification of this claim, they pointed out that after this point the rate of permanent deformation become more stabilized. [Jitareekul \(2009\)](#) also reported that the initial reduction in the sample stiffness occurred at 5% of the fatigue life. On the other hand, other authors like [Li \(2013\)](#) reported that the initial stiffness is the one that can be calculated after a few cycles (50-100) from the beginning of the test. Australian practice ([Jameson and Howard 2012](#)) computes the elastic modulus from the resilient deformation after 100 pulses. From a practical point of view, it seems that the evaluation of dynamic stiffness at a specific number of cycles is more logical than the other suggestions. This is because, customary, it is required to evaluate the modulus in a short term test without conducting long term testing (i.e., fatigue). Therefore it is required to adopt such simple evaluation technique.

### **8.6 Development of fatigue testing facility**

This test arrangement used for the work described in this thesis was developed for two purposes. Firstly is to study resilient modulus of the different mixes. Secondly, is to investigate the fatigue characteristics of rubberized mixtures and the ones containing no rubber. According to [Di Benedetto et al. \(2004\)](#), the test development contains many steps including actuator set-up, manufacturing necessary fittings for the test and alignments, data acquisition system and instruments calibration. Each of the above steps will discuss in the following subsections.

### **8.6.1 Actuator installation and set-up**

A 25 kN load capacity actuator manufactured by the Servocone Company was used for cyclic flexural testing. The total stroke for this actuator is  $\pm 100$  mm. The Servocone controller (Figure 8.5) was used which is driven by LabVIEW software. The control software monitor and display the response in real time. During cyclic loading the load is logged from the internal load cell of the actuator, the actuator position from its internal LVDT and test time. In addition, the software is able to provide a two-axis plot of any of these three parameters. Three wave functions can be generated and applied during the cyclic loading: sine, square and triangular.

To set-up a loading system, a steel frame, made of two columns connected by a horizontal beam, was installed by screwing it on the floor slab using 12 x 5 cm bolts then the actuator was attached to the that frame using bolts and plates as shown in Figure 8.3. These bolts and connections were bolted tightened to avoid any slack which may affect the rigidity of the frame and hence affect the accuracy of results. Afterwards the actuator was connected to the central hydraulic system in the structures laboratory at the University of Nottingham.

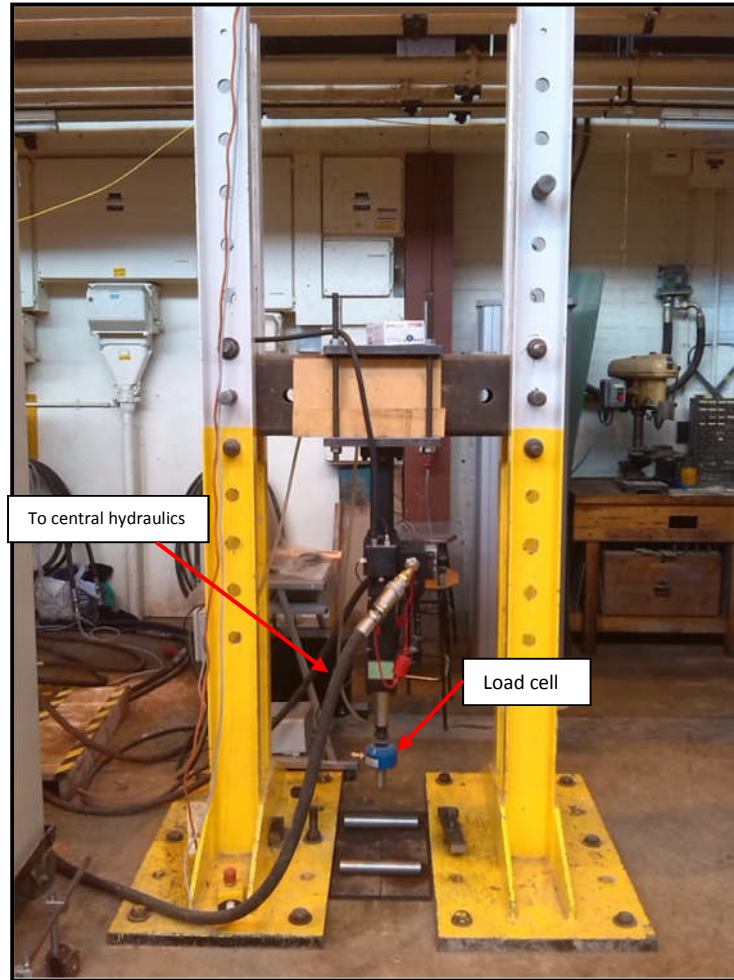


Figure 8.3: Installing testing frame and actuator and the hydraulics.

### 8.6.2 Manufacturing and aligning test fittings

This step consists of manufacturing the bottom and upper parts of the test using plates and rollers (Figure 8.4a) which ensure the same loading configuration that was used in static flexural testing as previously discussed in Chapter 6. The lower part was placed on the floor and screwed to the frame using steel bars and screws. It is worth mentioning that all these steel parts were selected to eliminate any probable deformation that may occur in these parts themselves. Once again, all these were connected tightly to ensure a stiff testing facility. This was done after ensuring that

both rollers lay at the same level using a levelling bulb and aligning so that the actuator head coincided with the centre of the distance between rollers. All these process are shown in Figure 8.4b.

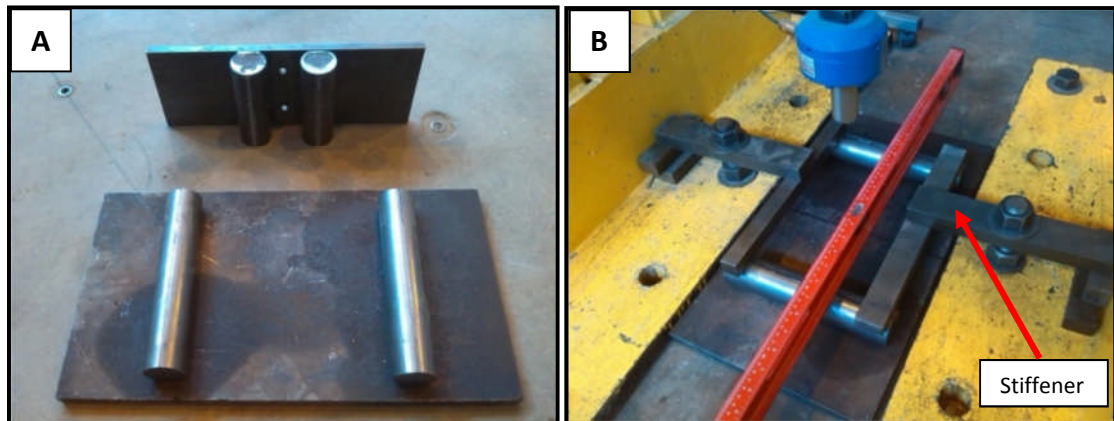


Figure 8.4: Manufacturing and installation of test fittings: a. top and bottom parts; b. installation and alignment.

### 8.6.3 Data acquisition system and instruments calibration

Unlike traditional fatigue testing where the parameters of interest are the number of cycles that cause failure and the repeated flexural load, the current testing program intends to investigate the degradation that occurs in the materials due to repeated loading. This is assessed in terms of stiffness reduction as a result of permanent strain accumulation. This purpose requires a higher level of data acquisition for load-deflection during the test than for traditional fatigue testing. Consequently, an external data acquisition system manufactured by Servocone was utilized to acquire load-deflection data at frequency of 20 Hz. Because the adopted loading frequency is 2 Hz., this will ensure recording 10 points per cycle. Due to the limited ability of the actuator controller to acquire data (load and position) at the required frequency, the actuator controller was connected to the external data logger to move and acquire

both the load and the actuator position readings with the required logging frequency. Accordingly, the recorded data comes from four channels. These are load from actuator load cell, two linear variable differential transducers (LVDTs) and actuator position. All of these data are monitored in real time utilizing the data logger software. The two LVDTs (LVDT 1 and LVDT 2) were used to record the value of beam deflection at the mid-span and the average value was considered as the value of deflection. However, to reduce the size of the logged data file and hence facilitate data handling and processing, only one LVDT was used to log the deformation at the mid-span of the prism. This is also justified since the sample was trimmed and prepared so as to eliminate any big difference in the reading of the two LVDTs as investigated in the initial trials. The configuration of these connections is as follows: the LVDTs are connected directly to the data acquisition system while both the load signal from the load cell and the actuator position signal were moved from the actuator controller to the data acquisition box due to limited capability of data logging. The data acquisition output file contains four columns corresponding to load, position, LVDT reading. Figure 8.5 provides a schematic representation of all the connections while Figure 8.6 shows the test arrangement.

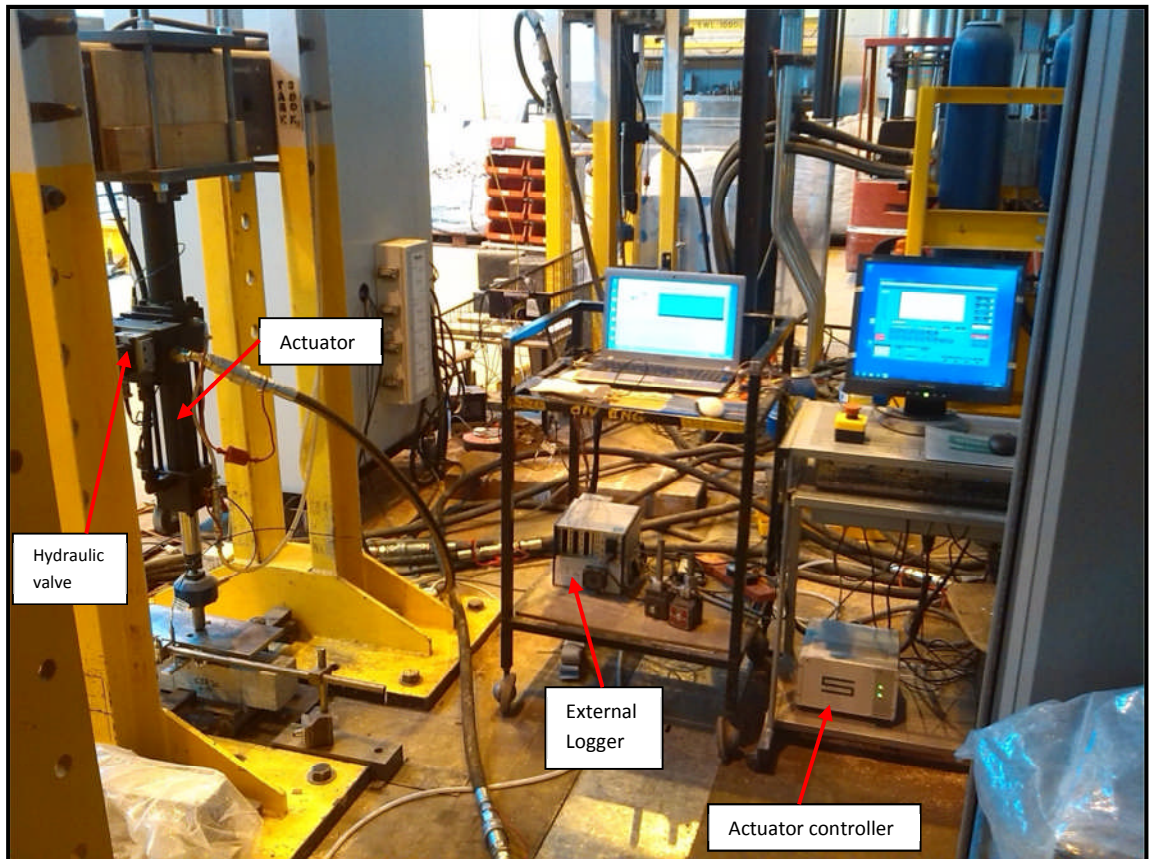


Figure 8.5: Fatigue test facility developed during the course of this study

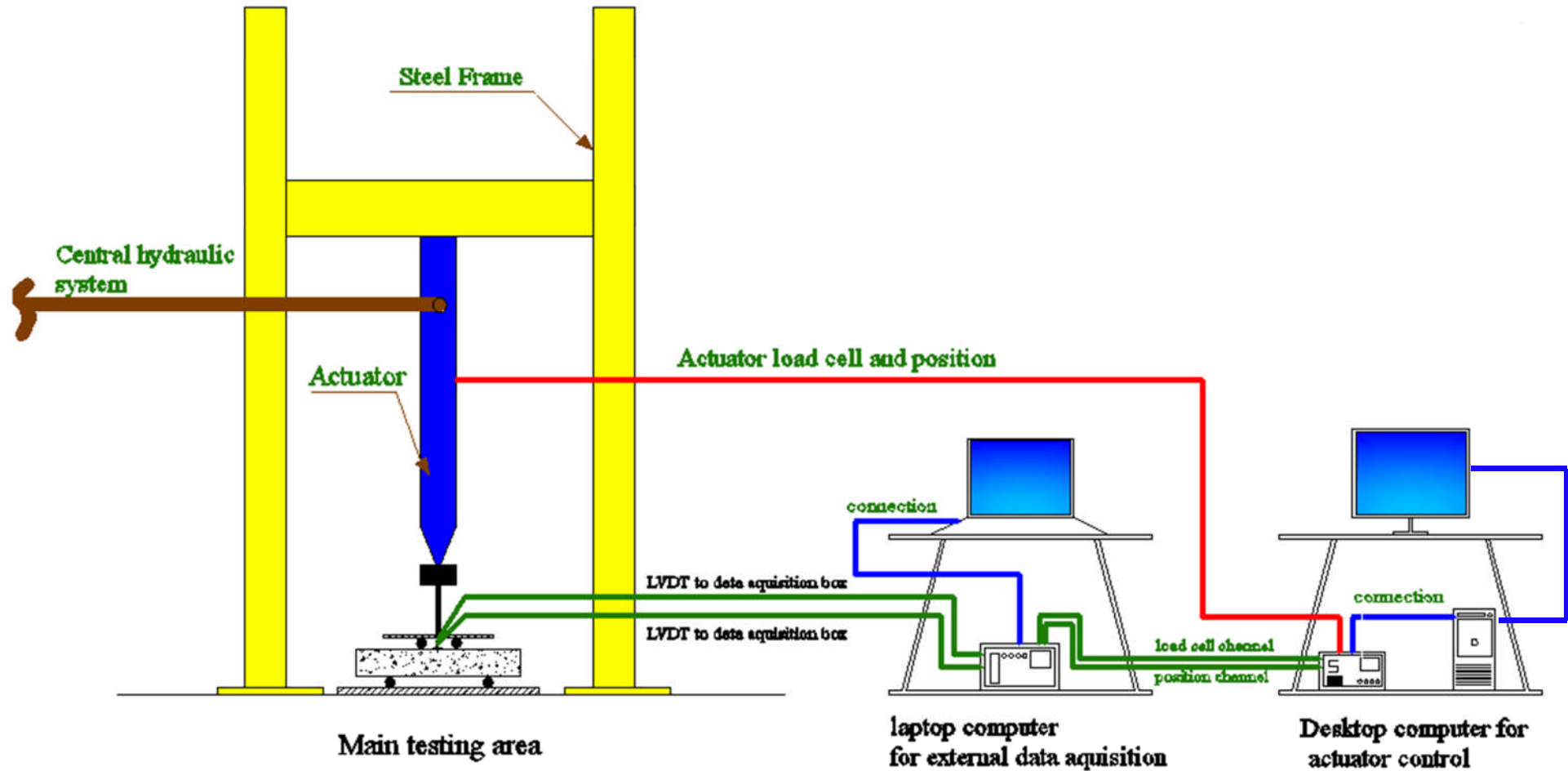


Figure 8.6: Schematic technical representation for the developed fatigue test facility.

#### 8.6.4 Instrumentation mounting and LVDTs Calibration

The mid-span deflection was measured using the two LVDTs, manufactured by DRP Company, UK. In this part of study, to protect the instrumentations it was decided to measure the deformation externally as used by many authors (Sobhan and Mashnad 2000; Khoury 2005; Triches 2009; Mandal 2012; Alderson and Jameson 2014; Wen Haifang 2014). Due to the expected small rate of deformation, it was decided to avoid any source of vibration around the test facility that may be generated by other testing or by personnel movement around the test facility. This was done by mounting the LVDTs firmly using two magnetic stands connected by steel rod. Both of these stands were placed on heavy steel parts having a square cross section and separated from the floor by rubber sheets. This mounting system is shown in Figure 8.7. A thick aluminium plate was glued on top of beam, as performed by Fu et al. (2009). The movement of the LVDT head will generate a voltage output. Both LVDTs were calibrated using calibration blocks (Figure 8.8) and a calibration equation was formulated to convert the voltage output to corresponding displacement. Figure 8.9 is the calibration curves for both LVDTs.

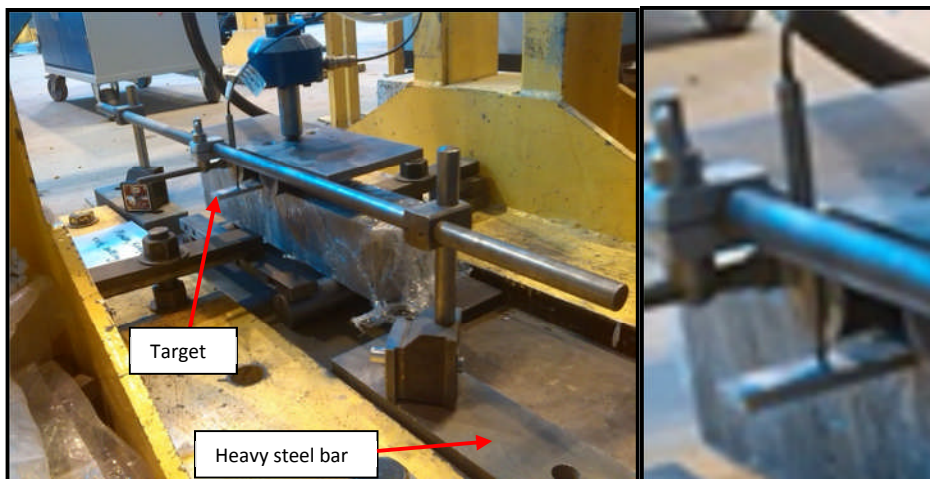


Figure 8.7: Instrumentation mounting arrangement.



Figure 8.8: Illustration of LVDT calibration using blocks of known thickness

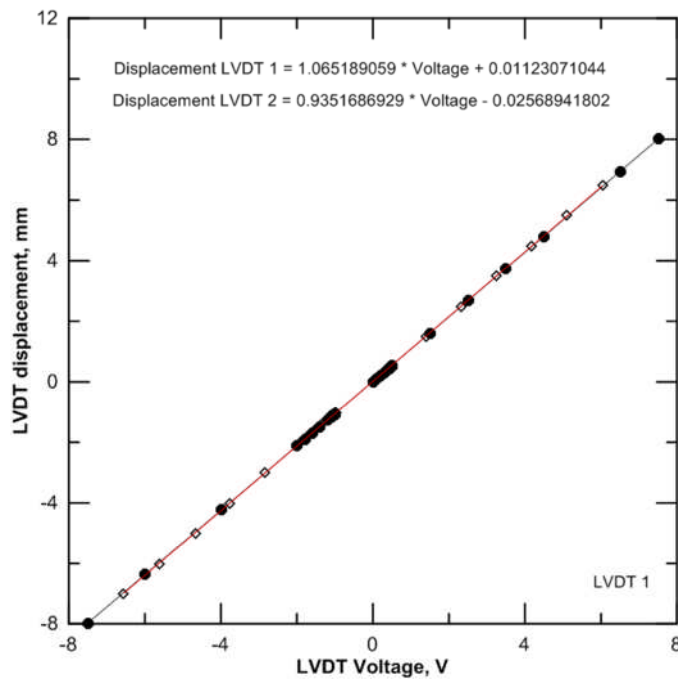


Figure 8.9: Calibration curves for LVDT 1 and LVDT 2.

### 8.6.5 Initial investigations results

In these trials, the tests were conducted under stress-controlled mode whereby the stress was cycled with a maximum value less than the material strength. As stated

previously, the stress ratio is defined as the ratio between the maximum applied stress and the strength of the material, expressed as a percentage.

Figures 8.10 and Figure 8.11 illustrate the load and the corresponding deformation waveform for the CSAM containing 30% rubber and 5% cement (i.e C5R30) subjected to stress ratio of 90%. From this figure it can be seen that the stress was successfully applied at a constant amplitude and frequency. However, observing the rate of deformation and comparing and contrasting this with that obtained during the static flexural test revealed that there was large deformation during this test. The difference was about 400% which would indicate a supposed reduction in the stiffness modulus by 31 GPa as compared with the static one (see Chapter 6). [Paul et al. \(2015\)](#) pointed out that the external mounting of the LVDTs causes underestimation of the material stiffness due to deformation overestimation. Therefore it was important to determine whether this increased strain (or reduced modulus) was a result of the loading or was artefact of the instrumentation arrangements.

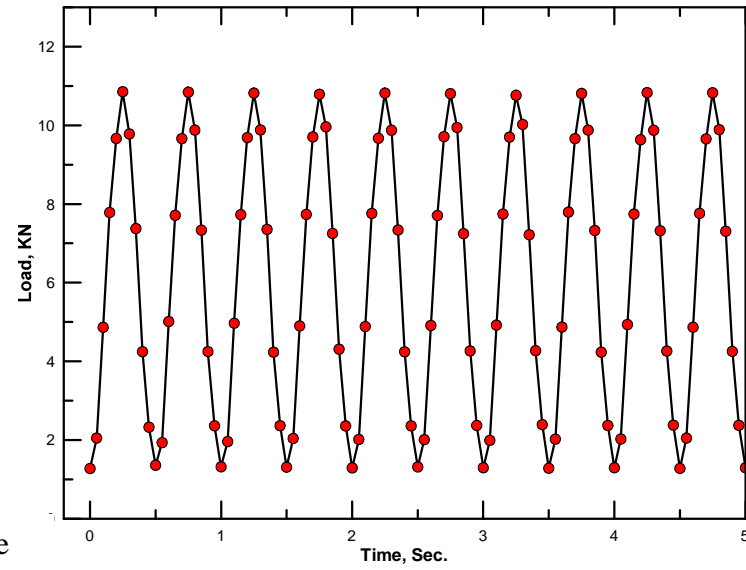
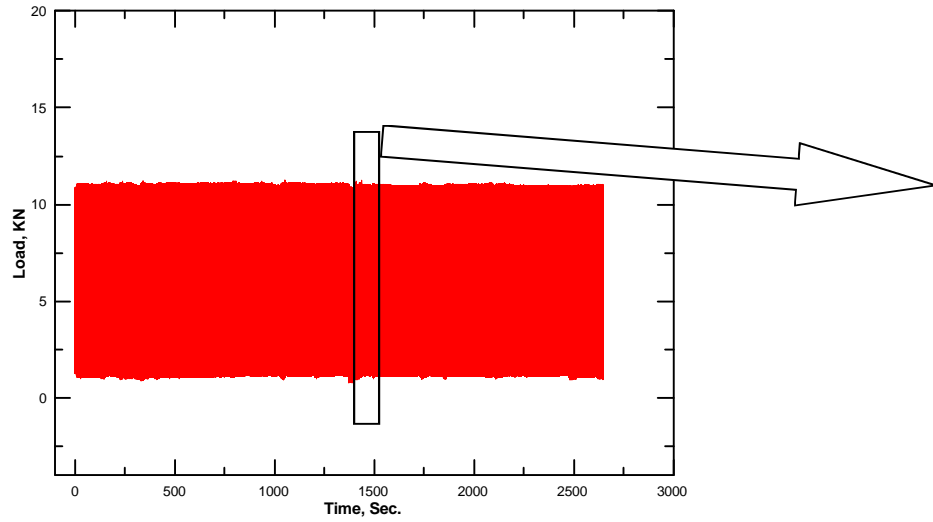


Figure 8.10: Load waveform generated during fatigue testing of constant amplitude

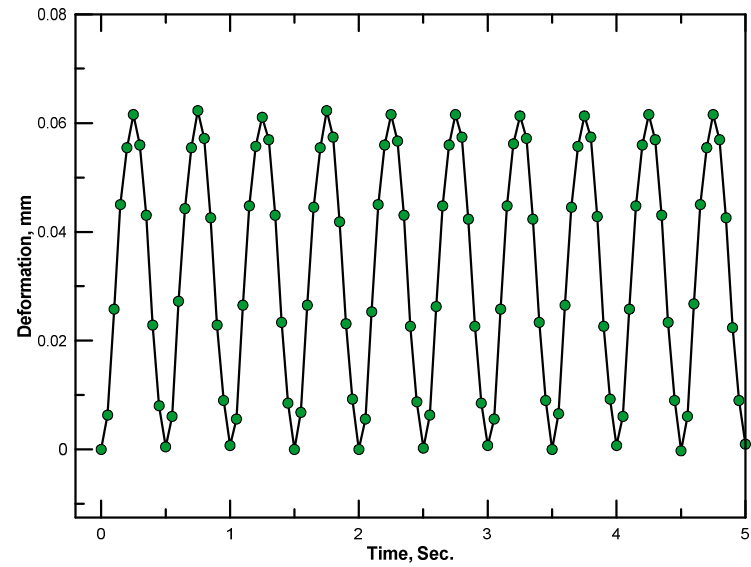
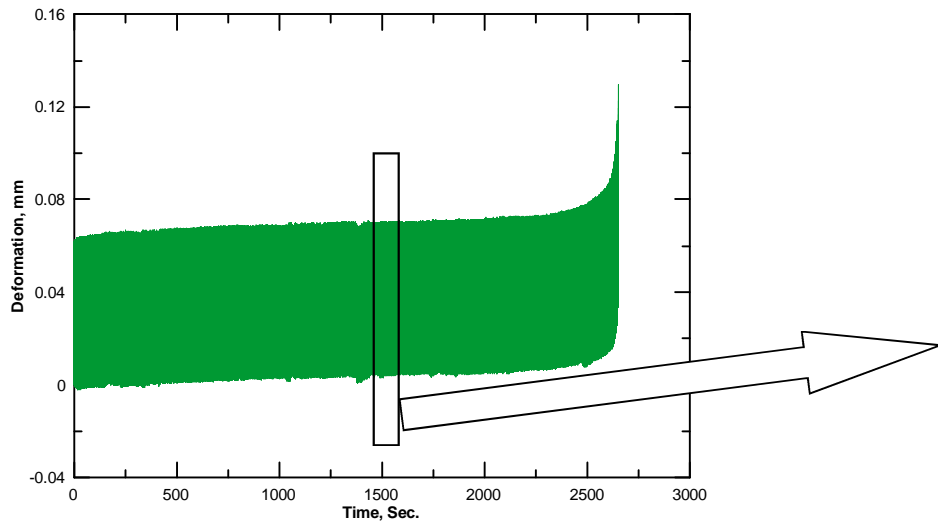


Figure 8.11: Deformation waveform corresponding to the load waveform

For this reason, it was decided to use another measurement tool to check whether there was a problem with the instrumentation or the mounting system. To achieve this, some trial prisms were instrumented using two strain gauges (PL-60-11) having range of 60 mm manufactured by Sokki Kenkyujo Company. These were glued on the bottom of the sample via Araldite<sup>®</sup> 2000 PLUS adhesive glue. Leaving one day to ensure that the glue had hardened, connections, wiring up and electrical testing were conducted. Figure 8.12 illustrates some of the strain-gauging stages. After that, the gauges were connected to the data acquisition system to log data from these strain gauges.

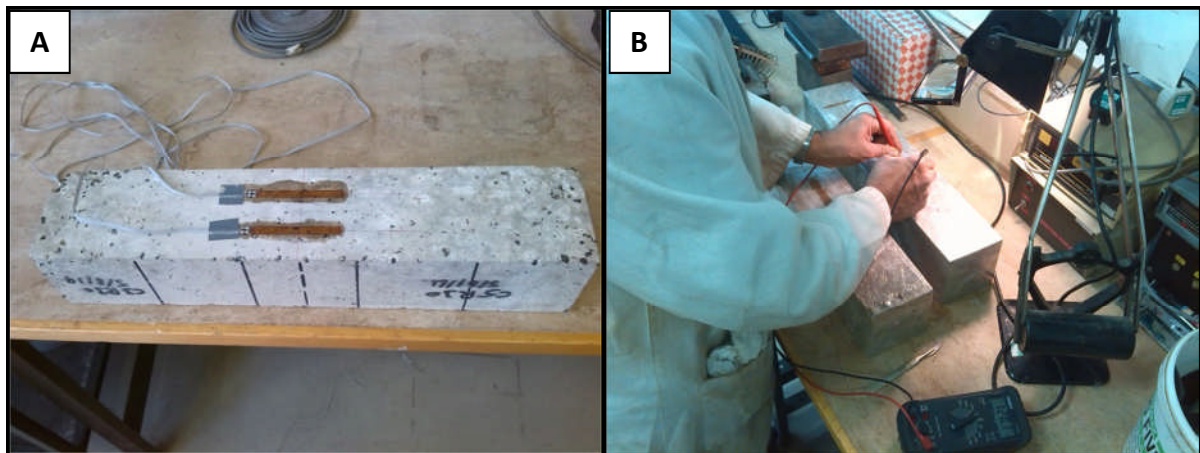


Figure 8.12: Strain gauging: a. Strain gauges and wired sample; b. Electrical circuit testing.

To compare with the static testing program, ensure more accuracy and to eliminate any variability due to repeated load application, two steps were conducted. The first is to include the on-sample instrumentation (i.e. yoke) arrangement used in the static flexural program (Figure 8.13). The second step is to apply the load monotonically at a constant deformation rate of 0.06 mm/min. Since the horizontal extreme fibre strain was read from the strain gauges, the LVDT vertical deformation reading was converted to the equivalent strain ( $\epsilon_t$ )

using beam bending theory to make the results comparable with each other. This was done using the following equation:

$$\varepsilon_t = \frac{12\delta h}{3L^2 - 4a^2} \quad (8.1)$$

Where  $\varepsilon_t$  = tensile strain (mm/mm);  $\delta$  = vertical deflection at the mid-span (mm);  $a$  = distance between load application point ( $a=L/3$ ) (mm) and  $h$  = average sample height (mm).



Figure 8.13: On-sample instrumentation arrangement.

The results and comparison between different measurement means and arrangements are shown in Figure 8.14. Based on that figure, it can be concluded that there was a big difference between the on-sample instrumentation and external instrumentation. Furthermore, the result obtained from LVDT through on-sample arrangement is highly consistent with the strain

measured via the strain gauge. This in turn gives validity to the use of the yoke arrangement in flexural testing. In addition, comparing and contrasting the on-sample results with the results presented in Chapter 6 reveals the reliability of the on-sample results in comparison with the response measured from the external measurement.

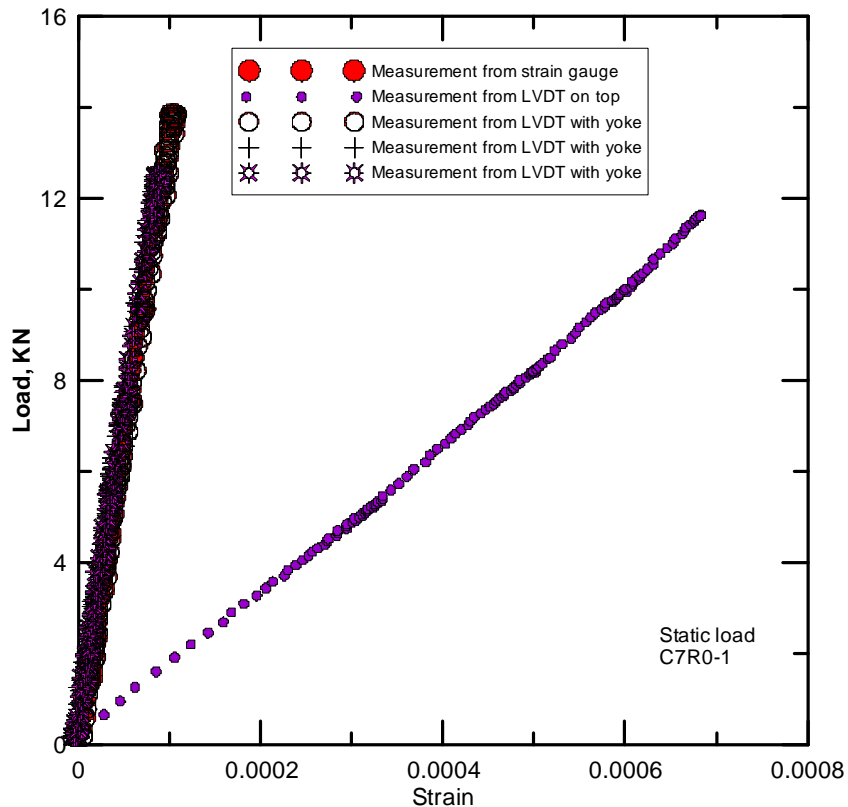


Figure 8.14: Comparison between different instrumentation arrangements

### 8.6.6 Data handling and processing

One objective of this research was to investigate the performance of the selected mixture during the fatigue test in terms of permanent deformation increase, decrease in stiffness modulus and the rate of damage accumulation. So, it is necessary to log data points within each cycle to facilitate tracking of the performance as fatigue develops. Consequently, the data were logged and stored as a text file during the fatigue test in a frequency that ensures

following the characteristics described below can be assessed with a reasonable accuracy. However, as this means the acquisition of a huge amount of data, the processing, calculation and plotting using Microsoft Excel was unsuccessful since the latter has a limited capacity in terms of number of cells that can be processed and/or plotted. For this reason, a computer code was written in Microsoft QuickBasic programming language for processing and analysing fatigue data. Once the analysis was completed, Grapher 11 software developed by Golden Software Company was used for the purpose of data plotting due to its ability to accommodate and plot huge amounts of data (around 1,000,000,000 points).

### **8.7 Concluding remarks**

1. Based on the review of literature, it was revealed that the flexural fatigue testing method is the preferred method in terms of its simulative nature to the in-service pavement and due to its simplicity.
2. Instrumentation setup has a significant impact on the assessment of the final response during fatigue testing. The external measurement arrangement overestimates the mid-span deformation. This would result in an underestimation of the mixture stiffness which may result in uneconomical pavement design. However, on-sample instrumentation using strain gauges and yoke arrangements are substantially identical and will form the basis of the instrumentation used in the test described in the later chapters.
3. A smooth load waveform was generated and applied to the trial specimens with a fairly smooth corresponding deformation wave. These initial investigations confirm the applicability and validity of the developed cyclic load facility to characterize the mixtures under cyclic loads.

4. For better tracking the fatigue performance throughout the test, and since the fatigue test generates a large data file, a computer code was written for handling and processing the fatigue data.
  
5. It is necessary to provide a standardized form of the fatigue test procedure. This test protocol should include all the test details starting from sample preparation and ending with the method of interpretation of test results.

## 8.8 References

- Alderson, A. and G. Jameson (2014). Cemented materials characterisation: final report, Austroad project TT1664, Report no. AP-R462/14.
- Di Benedetto, H., C. De La Roche, H. Baaj, A. Pronk and R. Lundström (2004). "Fatigue of bituminous mixtures." *Materials and Structures* 37(3): 202-216.
- Fu, P., D. Jones, J. T. Harvey and S. A. Bukhari (2009). "Laboratory test methods for foamed asphalt mix resilient modulus." *Road Materials and Pavement Design* 10(1): 188-212.
- Huang, Y. H. (2004). *Pavement analysis and design*, Second edition, Prentice Hall Publishing company, 792 pages.
- Jameson, G. and A. Howard (2012). Preliminary investigation of the influence of micro-cracking on fatigue life of cemented materials.
- Jitarekul, P. (2009). *An Investigation into Cold In-Place Recycling of Asphalt Pavements*, PhD Thesis, University of Nottingham, Department of Civil Engineering.
- Khoury, N. N. (2005). *Durability of cementitiously stabilized aggregate bases for pavement application*. PhD thesis, The University of Oklahoma.
- Li, N. (2013). *Asphalt Mixture Fatigue Testing: Influence of Test Type and Specimen Size*. PhD Thesis, TU Delft, Delft University of Technology.
- Mandal, T. (2012). *Fatigue behavior and modulus growth of cementitiously stabilized pavement layers*. MSc Thesis.
- Pais, J. and M. Minhoto (2010). The prediction of fatigue life of asphalt mixtures using four-point bending tests. 24th APRB conference. Melbourne, Australia, ARRB Group limited
- Paul, D. K., M. Theivakularatnam and C. Gnanendran (2015). "Damage Study of a Lightly Stabilised Granular Material Using Flexural Testing." *Indian Geotechnical Journal*: 1-8.

Prowell, B. D., E. Brown, R. M. Anderson, J. S. Daniel, A. K. Swamy, H. Von Quintus, S. Shen, S. H. Carpenter, S. Bhattacharjee and S. Maghsoodloo (2010). Validating the fatigue endurance limit for hot mix asphalt, Transportation Research Board.

Rowe, G. M. (1996). Application of the dissipated energy concept to fatigue cracking in asphalt pavements. PhD Thesis, University of Nottingham.

Rowe, G. M. and M. G. Bouldin (2000). Improved techniques to evaluate the fatigue resistance of asphaltic mixtures. 2nd Eurasphalt & Eurobitume Congress Barcelona.

Sobhan, K. and M. Mashnad (2000). "Fatigue durability of stabilized recycled aggregate base course containing fly ash and waste-plastic strip reinforcement." Final Rep. Submitted to the Recycled Materials Resource Centre, Univ. of New Hampshire.

Sobhan, K. and M. Mashnad (2003). "Fatigue behavior of a pavement foundation with recycled aggregate and waste HDPE strips." Journal of geotechnical and geoenvironmental engineering 129(7): 630-638.

Tangella, S. R., J. Craus, J. Deacon and C. Monismith (1990). Summary report on fatigue response of asphalt mixtures. No. SHRP-A-312. 1990. Institute of Transportation studies, University of California.

Triches, G. (2009). The fatigue behavior of rolled compacted cobcrete for composite pavements. 2nd workshop on four-point bending, University of Minho, Recored No. 276.

Van Dijk, W. (1975). "Practical fatigue characterization of bituminous mixes." Journal of the Association of Asphalt Paving Technologists 44: 38-72.

Wen Haifang, M. B., Wang Jingan, Li Xiaojun, Edil Tuncer, Tinjum James (2014). Characterization of Cementitious Stabilized Layers for Use in Pavement Design and Analysis. Washington, DC, National cooperative highway research program

## **Specifications**

AASHTO T321-03, Test standards for determining the fatigue life of compacted hot-mix asphalt subjected to repeated flexural bending

BS EN 12697-24:2012, Bituminous mixtures-Test methods for hot mix asphalt-Part 24: Resistance to fatigue

ASTM D-7460, Standard test method for determining fatigue failure of compacted asphalt concrete subjected to repeated flexural bending

## **Chapter Nine**

### **Fatigue and dynamic modulus performance**

#### **9.1 Introduction**

Highway pavements in the field are subjected to dynamic loading as a result of the movement of vehicles. These moving loads produce stresses, typically, that are less in magnitude than the material strength. However, repetition of these relatively small stresses a certain number of times may produce fatigue failure. Fatigue is the primary mode of failure for cementitious pavement layers and for the whole pavement structure. Accordingly, fatigue behaviour of materials should be evaluated (and considered at the design stage) to better simulate the realistic pavement condition.

The purpose of this chapter is to investigate the performance of the modified mixtures under cyclic loading to understand how rubber, cement and their combination may affect fatigue responses. This will include determination of the fatigue equation (also known as the S-N curve) and the mechanism by which the pavement structure will be damaged. This will be achieved by estimating the permanent deformation accumulation and the degradation of pavement stiffness across pavement life. In addition, it is intended to show the applicability of the dissipated energy ratio approach for cementitious materials. In this Chapter, the information from Chapter 6 and Chapter 7 will be used in estimating flexural strength. In addition to the objectives previously mentioned, the results of this chapter will be used as a prerequisite for the pavement analysis and design phase of the study which will be presented in Chapter 10 to show the design implications of this research.

## **9.2 Pavement fatigue failure**

Fatigue cracking is one of the main load-induced distresses that may occur as a result of the application of cyclic loading due to traffic movement. Therefore, this type of cracking can be considered as one form of structural failure that may occur in flexible and semi-rigid pavements.

Regarding the potential fatigue failure in cementitiously stabilized layers, practices adopted by different countries express different points of view about the form of this failure. For example, the South African design practice ([Theyse et al. 1996](#)) suggests two potential locations for this type of failure. These are either compression fatigue

at the top of the cemented layer or tensile fatigue at the bottom of this layer. According to this practice, the first type may occur for pavements with thin surface courses and/or lightly cemented base courses. On the other hand, the current mechanistic-empirical pavement design guide ([Applied Research Associates 2004](#)), only adopts tensile fatigue at the bottom of the cemented layer.

In fact, there is no absolute point of view regarding the potential fatigue failure location (compression on top or tensile at bottom of the layer) because the behaviour is complex and depends on several factors including thickness and relative stiffness of the different layers, the degree of cementation and the condition of underlying courses. Consequently, the key approach is to perform structural analysis and, based on the pavement responses, the critical criteria can be assessed.

### **9.3 Interpretation of fatigue performance**

There is no doubt that the research conducted regarding the characterization of fatigue performance of asphaltic mixtures is far ahead of that performed for cement-stabilized mixtures ([Liu and Wang 2014](#)). Very limited studies have been conducted to investigate and understand the fatigue behaviour in terms of tracking and quantifying of the damage development during the test. This helps to draw a clear picture of damage accumulation until specimen reach complete failure. This, in turn, may provide vital information regarding the mechanism by which the cement-stabilized mixture fails under cyclic flexural loading. In asphaltic mixture technology, two approaches are normally adopted for fatigue behaviour analysis which are stiffness-based and dissipated energy-based approaches.

### 9.3.1 Stiffness reduction approach

During the application of fatigue loading, the crack development process, and hence induced damage, results in stiffness reduction throughout the fatigue life of the mixtures. This reduction, conceptually, follows three stages of evolution as shown in Figure 9.1. Stage I represents the adaption stage in which rapid stiffness drop may occur. In stage II, the reduction in stiffness is more stabilized and tends to decrease linearly. Finally, fracture cracking by rapid growth of microcracks and formation of macrocracks represents stage III. Different authors have used this approach to define the number or cycles to failure as stated in Chapter 8.

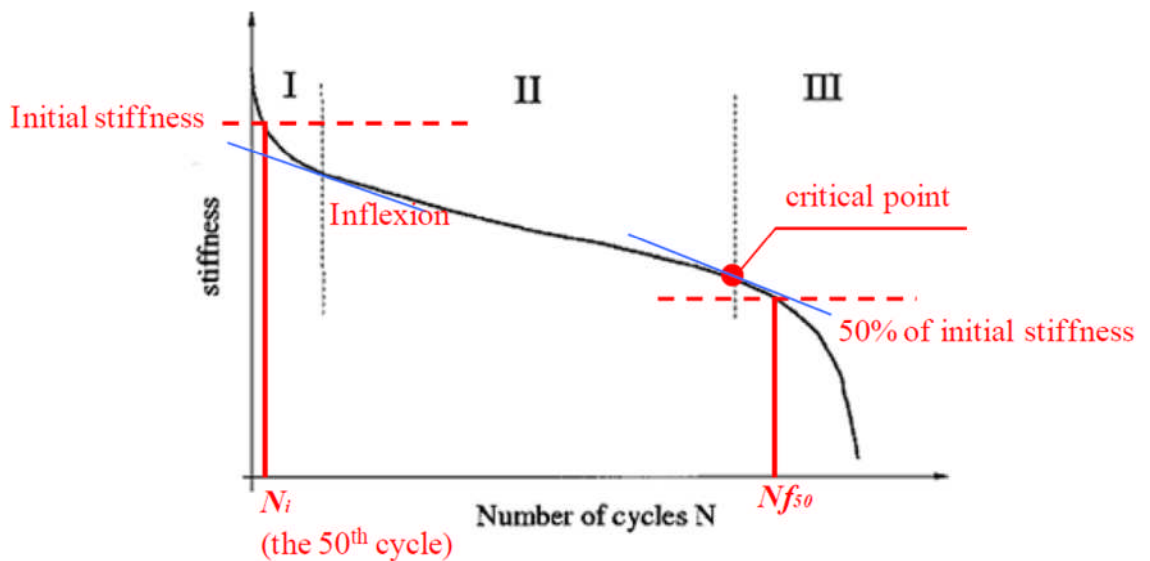


Figure 9.1: Stiffness reduction approach illustration (Wu et al. 2013)

### 9.3.2 Dissipated energy approach

Some authors have criticized the stiffness reduction approach (as illustrated in Figure 9.1) as the latter, they claim, is an arbitrary criterion and does not correspond to any change in the material properties. Therefore, they considered the dissipated energy method as a more reasonable and accurate method to estimate fatigue life.

Sinusoidally loading a beam manufactured from a viscoelastic material will result in a phase lag between the applied load and the measured deformation. In this case, a hysteresis loop will be obtained from the plotted load-deflection relationship as illustrated in Figure 9.2. Hysteresis loops for all specimens at a range of stages during loading are shown in Appendix B. The area inside the loop represents the dissipated energy per loading cycle. This can be calculated as follows:

$$\omega_n = \pi \cdot \sigma_n \cdot \varepsilon_n \cdot \sin\theta_n \quad (9.1)$$

Where:  $\omega_n$  = energy dissipated in cycle n;  $\sigma_n$  = stress amplitude in cycle n;  $\varepsilon_n$  = strain amplitude in cycle n and  $\theta_n$  = phase angle in cycle n ( $\theta_n = 360 \cdot f \cdot \Delta t$ );  $f$  = loading frequency and  $\Delta t$  = time interval between maximum load and maximum deflection. The phase angle is zero or  $90^\circ$  for purely elastic or entirely viscous materials, respectively. Dissipated energy is largely related to the binder viscous flow where the energy is dissipated as heat. Other researchers as reported by [Rowe \(1996\)](#) confirm that this energy is also associated with microcracks and crack surface formation. Many researchers have used this approach to study the behaviour of asphaltic mixtures as discussed in Chapter 8.

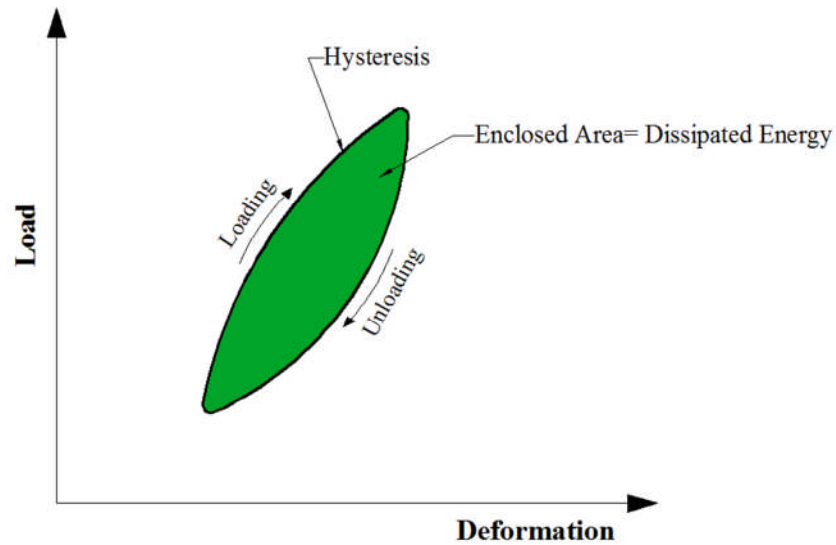


Figure 9.2: Typical hysteresis loop and dissipated energy concept.

This approach was derived based on the theory of viscoelasticity. However, some researchers, as pointed out by [Liu and Wang \(2014\)](#), claimed that cement concrete, which is normally assumed to be an elastic material, has viscoelastic characteristics. Accordingly, [Liu and Wang \(2014\)](#) draw a conclusion that the dissipated energy approach is applicable for studying the fatigue behaviour of the cement-stabilized mixtures due to the similarity between the latter and concrete mixtures.

In this research, it is intended to study how both rubber and/or cement will change the behaviour of the materials under fatigue loading through two objectives. The first is to investigate the combined effect of both rubber and cement on phase angle. The second is to investigate effect of rubber and cement contents on the applicability of the dissipated energy approach.

### 9.3.2.1 Dissipated energy ratio (DER)

One of the criteria that is traditionally used to define the fatigue failure is based on the energy dissipated during the fatigue test. This energy can be estimated by the following expression (Gnanendran and Piratheepan 2009)

$$\text{Energy Ratio} = \frac{w_0}{\left(\frac{w_n}{n}\right)} \quad (9.2)$$

where  $w_0$  =initial dissipated energy at the start of test. The dissipated energy is then calculated using Equation 9.1.

Thus, equation 9.2 above can be rewritten as:

$$\text{Energy Ratio} = \frac{n \cdot (\pi \cdot \sigma_0 \cdot \varepsilon_0 \cdot \sin \theta_0)}{(\pi \cdot \sigma_n \cdot \varepsilon_n \cdot \sin \theta_n)} \quad (9.3)$$

By substitution of  $\varepsilon = \sigma/D_m$  (where  $D_m$  is the dynamic stiffness modulus) into Equation 9.3 gives:

$$\text{Energy Ratio} = \frac{n \cdot (\pi \cdot \sigma_0^2 \cdot D_{mn} \cdot \sin \theta_0)}{(\pi \cdot \sigma_n^2 \cdot D_{m0} \cdot \sin \theta_n)} \quad (9.4)$$

where  $D_{m0}$  and  $D_{mn}$  refer to the dynamic stiffness modulus at the start of test and at the  $n^{\text{th}}$  cycle, respectively.

In a fatigue test conducted under stress-control the value of stress remain constant across the testing which means that  $\sigma_0 = \sigma_n$ . As shown later (Section 9.9.1), the change in  $\sin \theta$  is zero. By substituting these in Equation 9.4, the equation below results:

$$\text{Energy Ratio} = \frac{n \cdot D_{mn}}{D_{m0}} \quad (9.5)$$

As the idea is to plot the Energy Ratio against number of cycles to identify the peak of the curve which is taken to be the failure point (Artamendi and Khalid 2013), for plotting purposes the denominator of the above equation can be ignored (Gnanendran and Piratheepan 2009). The results for all mixtures are presented in Appendix C.

#### 9.4 Materials, mixture design and sample preparation

Materials, mix design and all sample preparatory steps were kept as previously discussed in Chapter 6. All samples were tested at 28 days. In the dynamic modulus testing program, duplicate samples were manufactured and tested for each mixture.

Regarding the number of beams that should be tested to represent the fatigue behaviour of the mixture, Ghuzlan and Carpenter (2000) stated that to establish a representative fatigue curve, at least four samples must be tested. Li and Dong (2011) also used four beams to establish the fatigue line of cement-stabilized recycled aggregate. Due to the time-consuming nature of the fatigue test, several researchers (Sobhan and Mashnad 2003; Oliveira 2006; Jitarekul 2009) have also used one beam per stress ratio. In this research, for each mixture, four beams of 100 mm x 100

mm x 500 mm dimension were prepared in such a way that one beam is tested per stress ratio. Based on sample fatigue testing trials, the approximate time required to repeatedly load each fatigue specimen was estimated, then the beam specimens were manufactured with the aim of ensuring that they reached an age of 28 days on the day of testing. However, delays in commencing fatigue testing for some samples, by between 3 and 7 days, were unavoidable. Similar observation was reported by [Sobhan and Mashnad \(2003\)](#) who mentioned that a delay of one week in sample testing occurred during their fatigue testing program. Inaccuracies arising from this have been mitigated by a procedure described later in Section 9.7.1.

### **9.5 Load application and configuration**

Based on the aforementioned discussion regarding the suitability of fatigue testing mode to simulate the field condition, it was decided to use the four-point flexural testing method performed under stress controlled testing mode. The frequency of load was selected as 2 Hz since this will better simulate the real traffic loading ([Sobhan and Mashnad 2000](#)). The load was applied at different stress ratios. The stress ratio can be defined as the ratio between the applied maximum load and the material strength. During the cyclic test the load amplitude cycles between maximum and minimum values. The maximum value was computed based on the required stress ratio for that test which is calculated based on the estimated flexural strength while the minimum load was adopted as 10% of the required maximum load ([Sobhan and Mashnad 2000](#)). Thereby compression-compression actuator application was ensured. The reason behind applying the minimum load is to prevent any probable impact loading which, in turn, may affect the LVDT readings detrimentally.

### 9.6 Resilience, permanent and total deformation, and dynamic modulus

When the load is applied on a CSAM sample, it will deform proportionally to that load although each material type will behave differently from others. For pure elastic materials, all this deformation will be recovered when the load is removed. For viscoelastic materials, not all the deformation may be recovered and some permanent deformation will arise as shown in Figure 9.3. Some researchers, as documented by [Liu and Wang \(2014\)](#), who studied the behaviour of concrete mixtures, claimed that concrete showed such a viscoelastic behaviour. Based only on the recoverable deformation, the flexural dynamic modulus is normally calculated using the following equation:

$$E_d = \frac{23P_d L^2}{108bh^3 \delta_r} \quad (9.6)$$

Where:  $E_d$  = flexural dynamic modulus;  $P_d$  = applied dynamic load;  $L$  = beam span; distance between supports  $a = L/3$ ; in the test report here  $\delta_r$  = recoverable dynamic deformation and  $I$  = Beam cross section moment of inertia. Hence:

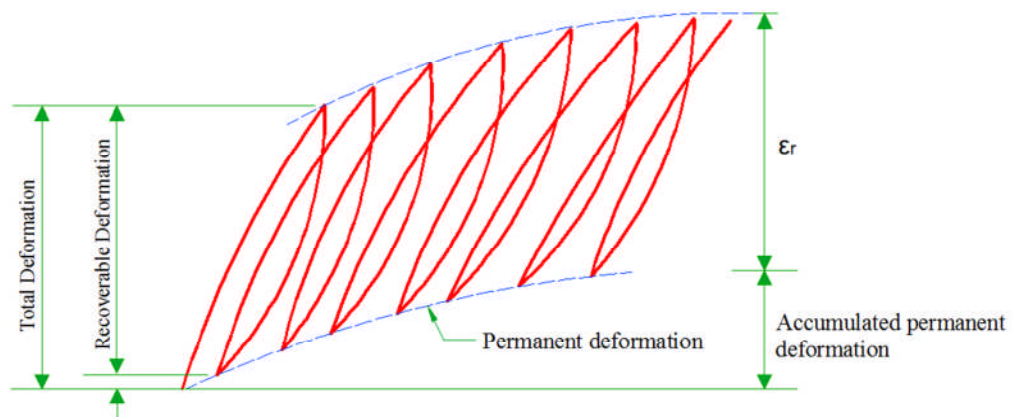


Figure 9.3: Total, elastic and permanent deformation during cyclic loading (redrawn from [Huang 2004](#))

## **9.7 Testing methodology and procedures**

### **9.7.1 Estimation the actual strength of the mixture**

Estimation of the actual flexural strength is an important step for dynamic modulus estimation and characterization of fatigue performance. This is because improper estimation of this parameter may lead to misleading or inaccurate results since the applied load in both procedures is normally computed as a percentage of the materials strength. Therefore, in both dynamic modulus and fatigue testing procedures, the methodology suggested in Chapter 7 (Section 7.10) will be used to estimate the actual flexural strength of the samples to be tested in this chapter.

### **9.7.2 Flexural dynamic modulus and fatigue testing**

Up to now, there is no widely adopted test to estimate the dynamic modulus of prisms ,manufactured from cement-stabilized materials, under dynamic flexural loading (Khoury 2005). For the program described here, at the end of curing period, the specimen was trimmed by diamond saw to achieve a 100 mm height as discussed in the flexural testing program (Chapter 6). Then, the density of each specimen was measured using the water-displacement method to confirm uniform densities as this enables reliable comparison between results. After that, the UPVs for different samples were measured according to the procedure explained previously in Chapter 7. The required applied stress was estimated based the required stress ratio and estimated flexural strength. The latter was computed as the average of the static flexural strength (Chapter 6) and the flexural strength computed on the basis of the developed correlation between flexural strength and the measured UPV value (Section 7.5.2.1). To avoid the probable sudden failure due to the turbulence in the

hydraulic oil, especially at the beginning of actuator powering, a dummy wooden sample was first used until the uniformity of oil supply and circulation was ensured. The sample was then mounted and all necessary instruments were fixed and connected. In fatigue and dynamic modulus characterization, the stress-controlled mode was adopted by applying a constant flexural stress computed on the basis of the required stress ratio. A stress ratio of 40% was used to measure the flexural dynamic modulus. This will guarantee testing within the elastic range of the material (Gonzalez et al. 2010; Arnold et al. 2012; Alderson and Jameson 2014). In this testing program 100 load pulses were applied and the average of the recoverable deformation during the second 50 cycles (Gonzalez et al. 2010) was used for flexural dynamic modulus calculation.

Regarding fatigue testing, four stress ratios were used. These were 90%, 85%, 80% and 75% of the static flexural strength. Due to the limited time available for this project, it was intended to characterize fatigue behaviour and produce transfer functions for only two mixtures. These were C5R0 and C5R30. To investigate the effect of other rubber contents and the effect of cement on both reference and rubberized mixtures, the other six mixtures were only tested under 90% and 85% stress ratios. Figure 9.4 illustrates the adopted plan for the fatigue testing program.

Using the actuator software, a haversine wave-form was selected to apply a flexural load that cycled between the minimum and maximum values. Utilizing data acquisition software, load cell, position and LVDTs were configured and defined. Immediately after starting the application of the repeated loads, the data acquisition

system was started to acquire and generate the data file which was then converted to a text file for further calculation and processing.

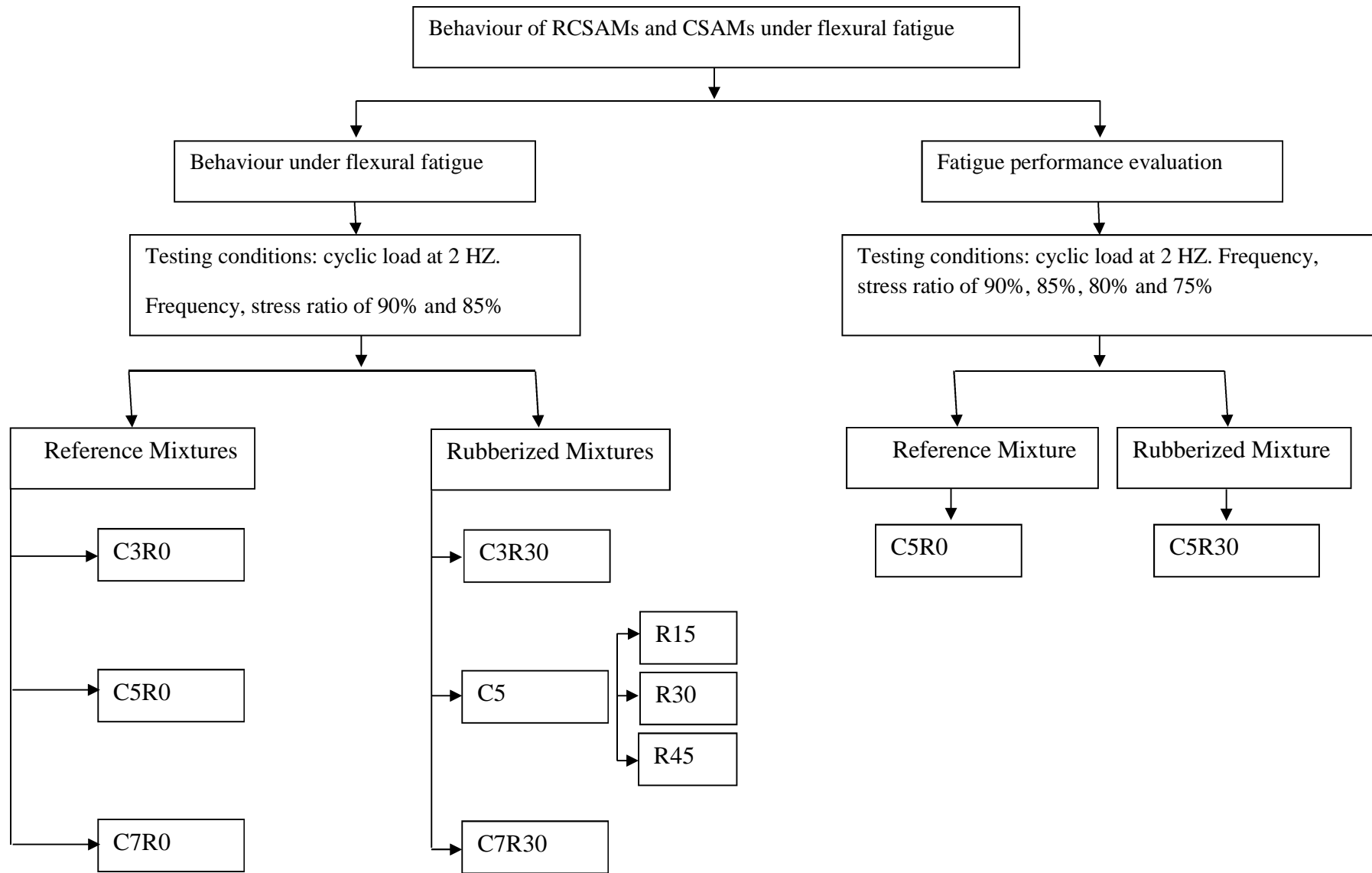


Figure 9.4: Testing planning for the behaviour under flexural cyclic loading.

### **9.8 Flexural dynamic modulus and comparison with other methods**

Table 9.1 shows the experimental results of the dynamic flexural modulus testing program. As can be seen from that table, there is uniformity in the manufactured samples in terms of the measured densities and the flexural strengths estimated from the ultrasonic testing. The dynamic flexural modulus estimated from this mode of testing follows the same trend as previously discussed under different methods and modes of testing (Section 5.4.5 and Section 7.5.4).

To compare between different testing methods and modes, all previously presented data are summarized in Table 9.2. It can be concluded from this summary that the dynamic modulus is larger than the static one in the case of both indirect tensile and flexural testing modes. The difference between static and dynamic flexural modulus seems to be cement content-dependent where, in the case of flexural testing, the difference between the latter and former increases as cement content increases. However, no such behavior occurred in the case of indirect tensile testing.

Regarding the highest and lowest moduli values measured by six different methods (Table 9.2), the modulus measured by indirect tensile and ultrasonic methods showed the lowest and highest values, respectively. The relationships between stiffness moduli estimated using different testing modes are shown in Table 9.3 and Appendix D. Based on the figures shown in Table 9.2, it can be concluded that the resonant frequency method provides approximately the same results as the dynamic flexural testing. This means that in terms of test cost, difficulty and availability of testing, the

dynamic modulus estimated by means of resonant frequency can be used reliably for pavement analysis and design.

Table 9.1: Densities, UPVs and estimation of the actual flexural strength for dynamic flexural modulus.

Mix ID	Density (kg/m <sup>3</sup> )	SR <sub>req'd</sub> (%)	FS <sub>SF</sub> (MPa)	UPV, (m/s)	FS <sub>UT</sub> (MPa)	FS Design (MPa)	Maximum applied load, (kN)	Minimum applied load, (kN)	Frequency, (Hz)	Dynamic modulus (average) (GPa)
C5R0-1	2526.4	40	4.4	5107	4.26	4.33	5.773	0.6	2	44.9
C5R0-2	2520.6	40	4.4	5102	4.245	4.323	5.76	0.6	2	
C5R15-1	2497.2	40	4	5020	4.1	4.05	5.34	0.5	2	43.3
C5R15-2	2489	40	4	5015	3.98	4	5.12	0.5	2	
C5R30-1	2458.7	40	3.6	4985	3.9	3.75	5.1	0.51	2	44.5
C5R30-2	2458.57	40	3.6	4985	3.9	3.75	5	0.5	2	
C5R45-1	2428	40	3.28	4798	3.33	3.3	4.14	0.4	2	38.5
C5R45-2	2423	40	3.28	4770	3.246	3.26	4.7	0.47	2	
C3R0-1	2501.5	40	2.657	4812	3	2.8	3.72	0.35	2	38.8
C3R0-2	2514.2	40	2.657	4730	2.70	2.68	3.57	0.35	2	
C7R0-1	2527.3	40	5.282	5165	5.22	5.25	7	0.7	2	51.55
C7R0-2	2529.9	40	5.282	5175	5.29	5.285	7	0.7	2	
C3R30-1	2452.64	40	2.29	4670	2.48	2.385	3.31	0.331	2	34.6
C3R30-2	-	-	-	-	-	-	-	-	-	
C7R30-1	2463.6	40	4.135	5020	4.2	4.16	5.55	0.6	2	47.9
C7R30-2	2458.5	40	4.135	5015	4.165	4.15	5.534	0.6	2	

SR<sub>req'd</sub>: required stress ratio.

FS<sub>UT</sub>: estimated flexural strength based on ultrasonic correlation (Chapter 7)

FS<sub>SF</sub>: flexural strength based on static flexural testing program (Chapter 6).

FS<sub>Design</sub>: estimated design flexural strength to be applied.

Table 9.2: Summary of comparison between different stiffness modulus (in GPa) characterization methods.

Mixture	Static testing		Dynamic non-destructive testing		Dynamic testing	
	Indirect tensile	Static flexural	Ultrasonic testing	Resonant frequency	Indirect tensile	flexural
<b>C5R0</b>	32	44.12	65.45	46.4	43.67	44.9
StdDev.	1.6	3.67	1.24	0.85	1.21	2.28
CoV	4.9%	8.3%	1.86%	1.8%	2.77%	5.1%
<b>C5R15</b>	30	42.30	62.45	43.70	42.58	43.3
StdDev.	1.96	9	0.53	0.61	0.45	0.21
CoV	6.5%	21.2	0.8%	1.4%	1.06%	0.4%
<b>C5R30</b>	28	37.60	60.85	41.40	41.80	44.5
StdDev.	6.65	4.62	0.69	0.6	1.06	2.9
CoV	23.6%	12.2	1.1%	1.45%	2.53%	6.5%
<b>C5R45</b>	29	30.31	55.8	38.61	35.95	38.5
StdDev.	2.53	1.1	0.67	0.84	0.63	4.95
CoV	8.6%	3.64%	1.2%	2.2%	1.77%	12.8%
<b>C3R0</b>	26	39.10	57	40.27	39.85	38.8
StdDev.	3.76	14.16	1.27	1.55	0.98	1.77
CoV	14.4%	36.2%	2.2%	3.7%	2.46%	4.5%
<b>C3R30</b>	14	34.52	53.4	35.15	35.27	
StdDev.	5.6	4.4		0.78	4.42	34.6
CoV	41.4%	12.8%		2.1%	12.5%	
<b>C7R0</b>	32	43.86	67.4	49.57	44.15	51.55
StdDev.	0.25	6	0.28	1.31	0.73	0.176
CoV	0.8%	13.6%	0.4%	2.6%	1.67%	0.3%
<b>C7R30</b>	28.5	38.19	61.55	42.70	41.75	47.9
StdDev.	0.26	4.05	0.35	1.35	0.88	0.16
CoV	0.9%	10.6%	0.5%	3.1%	2.105%	0.3%
CoV range	0.8%- 41%	3.6%- 36.2%	0.4% - 2.2%	1.4% - 3.7%	1.06%- 12.5%	0.3%- 12.8%
CoV Mean	12.6%	14.8	1.1%	2.3%	3.3%	4.3%

It can be observed from Table 9.2 that for different investigated mixtures and under different testing regimes, the maximum mean of the coefficient of variation is below 14.8% which can be considered acceptable and normal in laboratory characterization. However, except for the static testing, the COV means for all other characterization techniques are below 5%. Furthermore, the non-destructive testing showed less variability as compared with other

techniques while greater variability was observed in the case of testing under static loading. Also, it can be concluded that, firstly, the possible dynamic modulus range of the lightly stabilized mixtures is 26-40.2 GPa. For moderately cemented mixtures this range is from 28 GPa to 46.4 GPa. Finally, heavily stabilized mixtures have dynamic moduli ranging between 28 GPa and 49 GPa. These above possible ranges apply for different cement stabilized crushed fractioned aggregate mixtures having different ranges of densities.

Table 9.3: The relationships between moduli of elasticity estimated under static, dynamic and nondestructive testing.

No.	Relationship	R <sup>2</sup>	Parameters	Figure No.
1	$E_d = 1.1055 * E_f$	0.99	$E_d$ =dynamic flexural modulus $E_f$ =static flexural modulus	D.1
2	$E_d = 1.02 * E_{dr}$	0.99	$E_{dr}$ =dynamic modulus estimated by resonant frequency method	D.2
3	$E_d = 1.05 E_{du} - 20.57$	0.84	$E_{du}$ =dynamic modulus estimated by ultrasonic method	D.3
4	$E_d = 1.426 * ITST - 14.91$	0.76	ITST= indirect tensile stiffness modulus estimated under cyclic indirect tensile loading	D.4
5	$E_d = 1.53 * E_{it}$	0.99	$E_{it}$ =Static indirect tensile modulus	D.5

## 9.9 Fatigue testing program

### 9.9.1 Effect of rubber and cement on phase angle of cement-stabilized aggregate

From observing both loading and deformation amplitudes of tested mixtures, it was noticed that for different cement and rubber contents, there is no time lag between loading and resulting deformation curves. This confirms that the phase angle remain zero regardless of cement or rubber contents. Recently, [Nusit et al. \(2015\)](#) measured the dynamic modulus (in

compressive mode) for cement-stabilized granular materials utilizing the same procedure frequently used for asphaltic mixtures. They reported that the measured phase angle was ranging between  $1.63^\circ$  and  $5.2^\circ$  and, accordingly, they drew a conclusion that cement stabilized materials are pure elastic materials since the measured angle is close to zero.

## **9.10 Fatigue testing program results**

### **9.10.1 Fatigue lives**

#### ***9.10.1.1 Effect of rubber on the fatigue behaviour of CSAMs***

Table 9.4 and Table 9.5 show the measured densities, UPVs and corresponding estimated flexural strength, design flexural strength, loading details and fatigue lives for different mixtures. As can be seen from that table, the densities of different sample belonging to different mixtures are comparable with the measured densities of the samples used in the static flexural testing program (Chapter 6). This confirm the uniformity of specimen manufacturing which in turn indicates the accuracy in adopting the static flexural results as a prerequisite for fatigue testing so as to estimate the flexural strength of the samples to be tested for fatigue. Based on these, it can be seen that the estimated flexural strength (from the correlation with ultrasonic testing) is close to that of the static flexural strength.

Figure 9.5 and Figure 9.6 illustrate the effect of rubber replacement level and effect of cement on fatigue lives, respectively. The general trend that can be concluded from Figure 9.5 is that the fatigue lives of the mixtures improved as a result of rubber inclusion, where the more the rubber content the longer the fatigue lives. Interestingly, it seems that this degree of improvement depends, to some extent, on the applied stress ratio. As is clear from the latter

figure at high stress ratio (i.e., 90%) there is no clear behaviour where, except for the mixture C5R30, the fatigue life remains constant or may decrease as a result of rubber inclusion. For lower stress ratios (below 90%), on the other hand, there is an obvious increase in the fatigue life for all replacement levels as compared with the reference mixture. This behaviour may be attributed to the duration of the microcracking stage. It is thought that this microcracking period, in a stress-controlled experiment, increases as the stress ratio decreases. Evidence was presented in Chapter 5 and Chapter 6 that the cracks are almost developed and/or propagating through the aggregate particles and, accordingly, it is suggested that the mechanism of toughness improvement is by retarding the crack propagation as the stress developed at the crack tip is absorbed/relieved by rubber particles, especially at microcracking level. Also, it was reported by [Modarres and Hosseini \(2014\)](#) that there is a strong relationship between toughness and performance under cyclic loading.

Table 9.4: Densities, UPVs and estimation of the actual flexural strength for fatigue tests.

Mix ID	Density (kg/m <sup>3</sup> )	SR <sub>req'd</sub> (%)	FS <sub>SF</sub> (MPa)	UPV, (m/s)	FS <sub>UT</sub> (MPa)	FS Design (MPa)	Maximum applied load, (kN)	Minimum applied load, (kN)	Frequency, (Hz)	Cycles to failure, N <sub>f</sub>
C5R0-90	2529.2	90	4.4	5219	4.6	4.5	13.5	1.3	2	130
C5R0-85	2526.4	85	4.4	5107	4.26	4.33	12.2	1.2	2	3890
C5R0-80	2524.5	80	4.4	5197	4.53	4.46	12	1.2	2	36500
C5R0-75	2527.3	75	4.4	5165	4.45	4.4	11	1.1	2	113500
C5R30-90	2460	90	3.6	4935	3.742	3.67	11	1.1	2	5000
C5R30-85	2452.5	85	3.6	4980	3.84	3.72	10.4	1	2	50445
C5R30-80	2459.3	80	3.6	4970	3.847	3.84	10.24	1	2	146907
C5R30-75	2458.3	75	3.6	4970	3.78	3.7	9.2	0.9	2	550000
C5R15-90	2490	90	4	5144	4.371	4.39	13.2	1.3	2	33
C5R15-85	2497	85	4	5133	4.378	4.37	12.3	1.2	2	45000
C5R45-90	2426.3	90	3.28	4975	3.86	3.5	10.6	1	2	120
C5R45-85	2425	85	3.28	4911	3.67	3.475	9.8	1	2	55726

SR<sub>req'd</sub> : required stress ratio.

FS<sub>UT</sub> : estimated flexural strength based on ultrasonic correlation (Chapter 7)

FS<sub>SF</sub>: flexural strength based on static flexural testing program (Chapter 6).

FS<sub>Design</sub> : estimated design flexural strength to be applied.

Table 9.5: Densities, UPVs and estimation of the actual flexural strength for fatigue tests.

Mix ID	Density (kg/m <sup>3</sup> )	SR <sub>req'd</sub> (%)	FS <sub>SF</sub> (MPa)	UPV, (m/s)	FS <sub>UT</sub> (MPa)	FS Design (MPa)	Maximum applied load, (kN)	Minimum applied load, (kN)	Frequency, (Hz)	Cycles to failure, N <sub>f</sub>
C3R0-90	2507	90	2.66	4798	3.33	2.99	9	1	2	199
C3R0-85	2492	85	2.66	4812	2.66	2.66	7.54	0.7	2	-
C7R0-90	2527.3	90	5.282	5165	5.22	5.25	15.70	1.5	2	3696
C7R0-85	2529.9	85	5.282	5175	5.29	5.285	15.80	1.5	2	1538
C3R30-90	2452.6	90	2.282	4670	2.48	2.385	7.4	0.75	2	5403
C3R30-85	2438	85	2.28	4901	3	2.64	7.5	0.75	2	1655
C7R30-90	2458.5	90	4.135	5076	4.57	4.57*	12.9	1.3	2	4120
C7R30-85	2463.6	85	4.135	5138	5.13	5.13	14.5	1.5	2	116796

SR<sub>req'd</sub> : required stress ratio.

FS<sub>UT</sub> : estimated flexural strength based on ultrasonic correlation (Chapter 7)

FS<sub>SF</sub>: flexural strength based on static flexural testing program (Chapter 6).

FS<sub>Design</sub> : estimated design flexural strength to be applied.

\*Static value was ignored because the delay in testing at the specific age.

In fact, the findings observed during the fatigue testing agree with the mechanism suggested previously regarding the toughness improvement. This is supported by Figure 9.5 which shows some increase in the fatigue life (at moderate and low levels) when rubber is added.

#### ***9.10.1.2 Combined effect of cement and rubber on the fatigue behaviour of CSAMs***

Regarding the effect of cement on the fatigue life, Figure 9.6 shows the fatigue life, in general, improved due to rubber inclusion at all cement contents with the highest improvement occurring at high cement content. This is consistent with finding of toughness improvement mentioned in Chapter 5 (Figure 5.36). This appears to indicate that the fatigue life is broadly proportional to the toughness of the mixture.

The question that arises now is: "Will the reduction in the mixture strength, due to rubber incorporation, be compensated by the improvement in fatigue life and the reduction of stress attractiveness due to the reduction in the stiffness modulus?" To answer this question it is necessary to investigate the practical implications of rubber inclusion by combining the observed stiffness, strength and fatigue performance through pavement analysis and design.

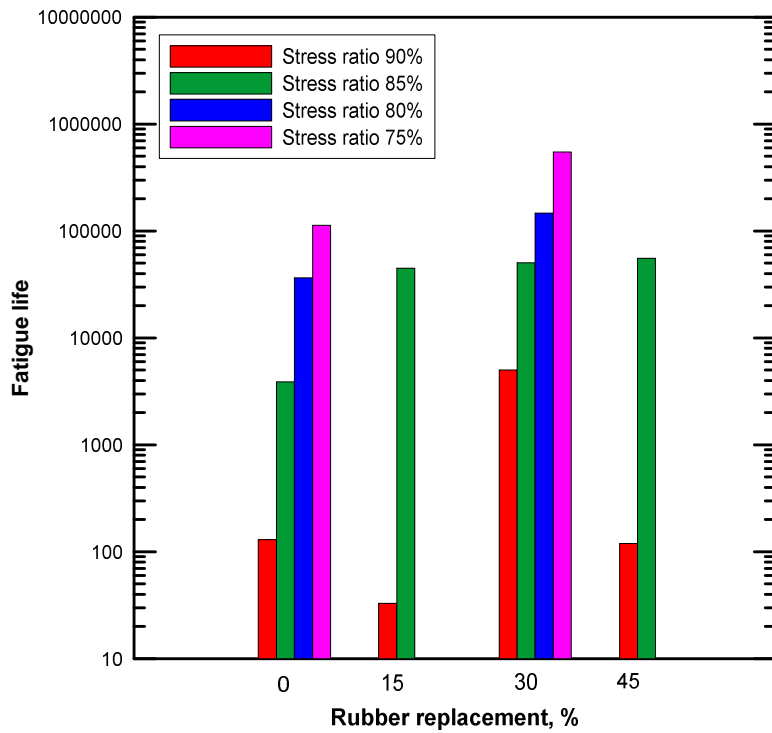


Figure 9.5: Effect of rubber contents on fatigue lives of CSAMs

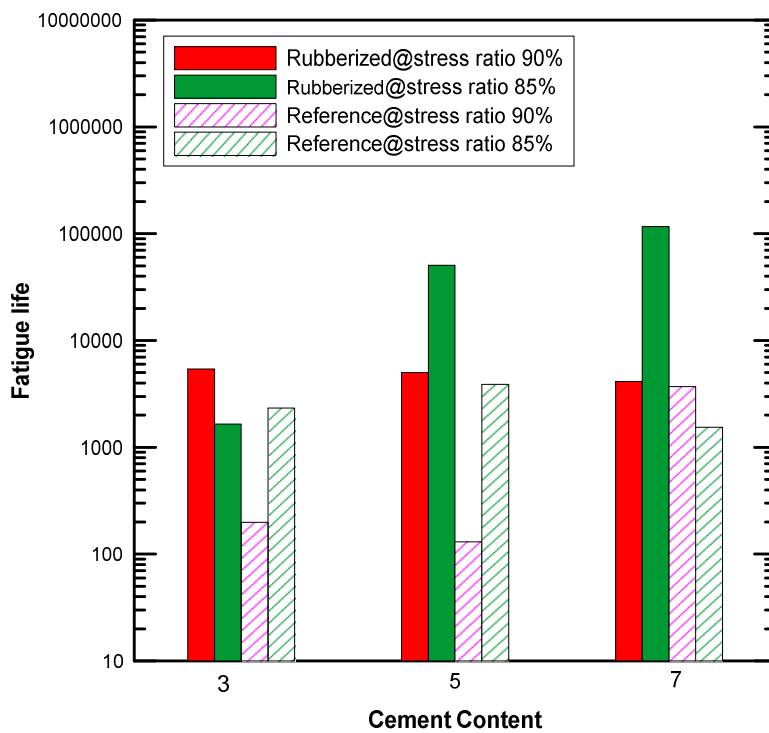


Figure 9.6: Effect of cement content on fatigue lives of reference and rubberized mixtures @ 90% and 85% stress ratios

### 9.11 Dynamic deformations

During repeated loading, the total deflection was recorded for each cycle including the recoverable and permanent deformation (see Figure 9.3). Figure 9.7 through Figure 9.12 illustrate the measured vertical dynamic deformation at mid-span for the tested prisms for selected mixtures. Appendix A shows the vertical dynamic deformation for all mixtures. Utilizing the developed computer code for fatigue data processing (Chapter 8), the maximum and minimum deformation was extracted for each cycle along with the fatigue life. These values were drawn (Figure 9.7 through Figure 9.12 and Appendix A), as illustrated in red and green lines, respectively. From these two values, the recoverable deformations were calculated at each cycle to quantify the development of dynamic modulus across the fatigue life. It should be noticed, from these figures, that the deformation profile across the fatigue life is composed of three regions, as discussed in Section 9.3.1. From observing the results presented in Appendix A, at higher stress ratios, there are two regions. The first extends from the beginning until 95% of the fatigue life. However, at low cement contents, this only lasted until 90% of the fatigue life. At lower stress ratios, the dynamic deformation curve shows three regions regardless of cement or rubber contents.

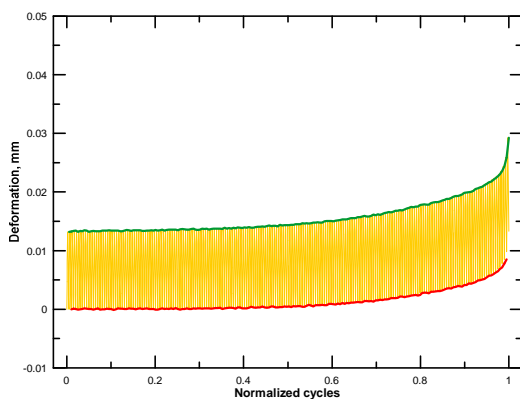


Figure 9.7: Vertical deformation under cyclic loading for C3R0@90% stress ratio

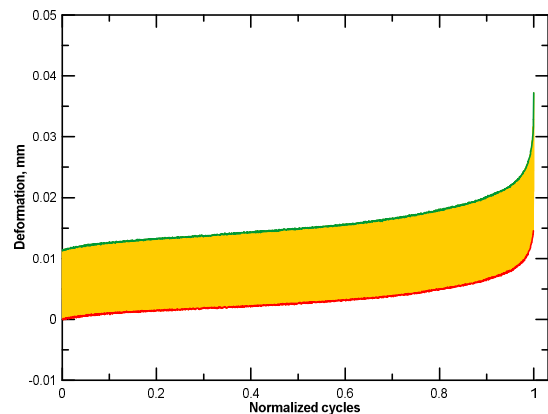


Figure 9.8: Vertical deformation under cyclic loading for C3R30@85% stress ratio

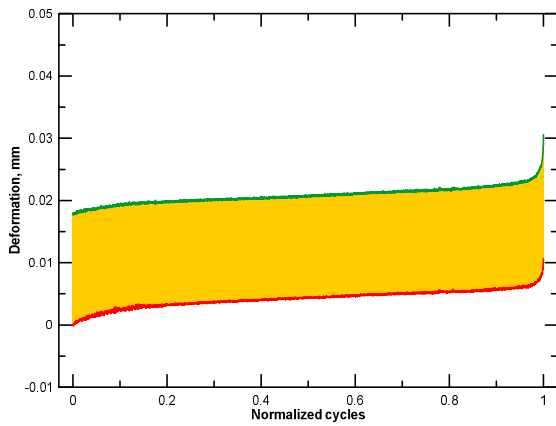


Figure 9.9: Vertical deformation under cyclic loading for C5R0@85% stress

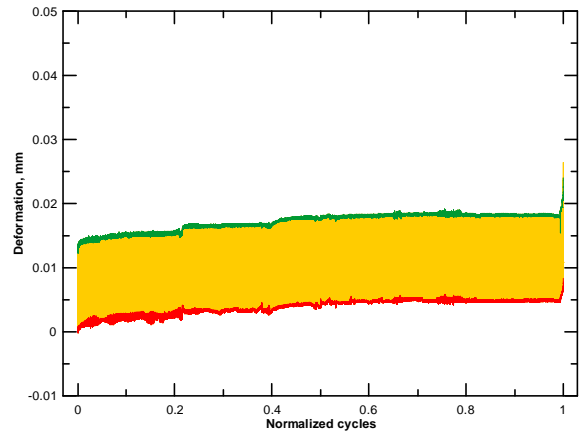


Figure 9.10: Vertical deformation under cyclic loading for C5R30@85% stress ratio

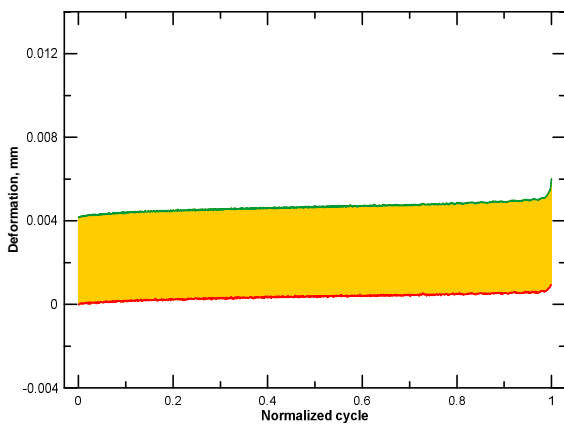


Figure 9.11: Vertical deformation under cyclic loading for C7R0@85% stress ratio

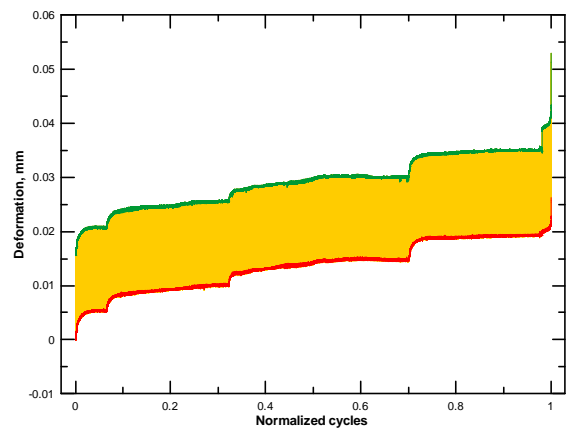


Figure 9.12: Vertical deformations under cyclic loading for C7R30@85% stress ratio

### 9.12 Stress ratio-Number of cycles to failure (S-N) curves

It is customary to express the fatigue test results in terms of stress ratio-fatigue life or S-N curves. The general form of S-N curves is reported in the literature as:

$$SR = a * \ln N + b \quad (9.7)$$

The cycles to failure (in log scale) were plotted against the stress ratio as shown in Figure 9.13. From these, the S-N curves were obtained for both C5R0 and C5R30 as shown in Equation 9.8 and Equation 9.9, respectively.

$$SR = -0.02022 * \ln N + 1 \quad (9.8)$$

$$SR = -0.01748 * \ln N + 1.0155 \quad (9.9)$$

These relationships can be considered as laboratory based transfer functions which are normally incorporated in the mechanistic empirical pavement design procedure for pavement performance prediction. Both Equation 9.8 and Equation 9.9 are good fits to the plotted data as shown in Figure 9.13. This confirms the suitability of the suggested methodology for actual flexural strength estimation, as presented in Chapter 7, and the uniformity of prism manufacturing and other preparatory steps. As is clear from Figure 9.13, at all stress ratios, the fatigue lives of the rubberized mixtures is greater than that of the reference mixture.

### 9.13 Endurance limits and fatigue strength

Endurance limit as defined by [Sobhan and Mashnad \(2003\)](#) is the stress level at which the tested sample can withstand two million cycles without fatigue failure. Based on the developed fatigue equation (Equation 9.8 and Equation 9.9) the endurance limits are 70% and 76% for reference (C5R0) and rubberized (C5R30), respectively. [Sobhan and Mashnad \(2001\)](#) reported that the endurance limit for unreinforced and fibre-reinforced cemented recycled concrete aggregate were 56% and 77% respectively.

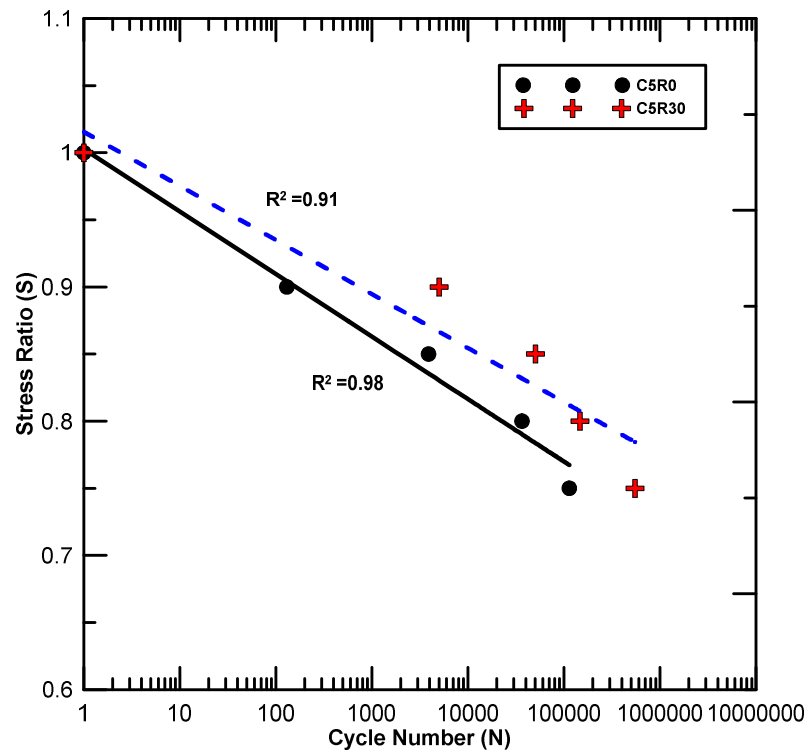


Figure 9.13: S-N curve for reference and rubberized mixtures @ 5% cement content

## 9.14 Evaluation of Damage accumulation

### 9.14.1 Permanent deformation accumulation

Across the fatigue life, permanent deformation accumulates gradually which indicates the accumulation of damage in the mixture (Grzybowski and Meyer 1993). This plastic deformation will contribute directly to the rutting of pavement structure (Sobhan and Das 2007).

Figure 9.14 and Figure 9.15 illustrate the permanent deformation for the stabilized mixtures with different rubber contents at 90% and 85% stress ratios. It is evidenced from the former figures that at 90% stress ratio, the accumulated permanent deformation is smaller for rubberized mixtures. In addition, phase I of the permanent

deformation profile is very short or may not exist. This explains and supports the hypothesis just mentioned regarding the reduction in the fatigue life of rubberized mixture at higher stress ratio which is attributed to the shortness of the microcracking phase. Thus, this was quickly followed by a rapid macrocracking stage and hence failure without excessive deformation.

At lower stress ratios, on the other hand, it can be observed from Figure 9.15 that more deformation was accumulated in rubberized mixtures as compared with reference one. In addition, it can be noticed that there are three regions which was previously discussed (Section 9.3.1). These results are consistent with findings reported in [Shah and Chandra \(1970\)](#). These authors used non-destructive testing methods to observe the occurrence and rate of microcrack growth due to fatigue testing. They found that at low stress ratios (70% and below), there was stable and slow microcracking growth while at higher stress ratios (80% and higher), on the other hand, a faster growth rate of these microcracks occurred.

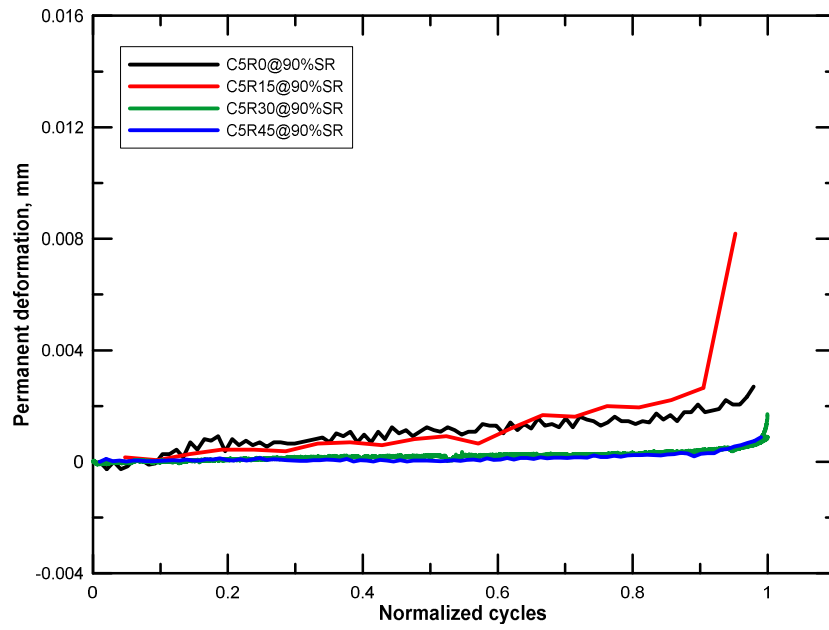


Figure 9.14: Permanent deformation accumulation for mixtures containing different rubber contents @ 90% stress ratio

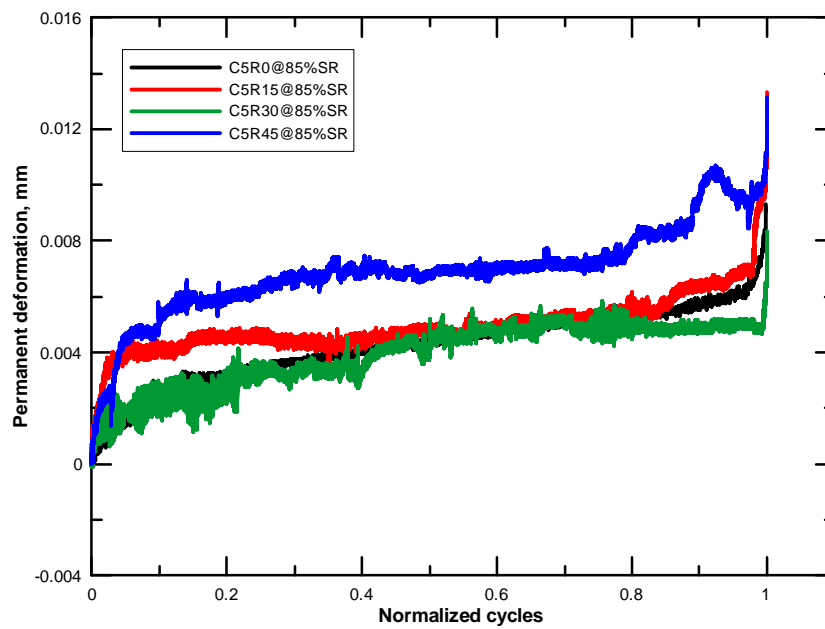


Figure 9.15: Permanent deformation accumulation for mixtures containing different rubber contents @85% stress ratio

Regarding the effect of cement on the permanent deformation accumulation of rubberized mixtures (with 30% rubber replacement), it is obvious from Figure 9.16 that, at high 90% stress ratio, different mixtures showed low levels of permanent deformation with a slightly higher permanent deformation in low cemented mixture as compared with moderately or highly cemented ones. However, at 85% stress ratio, rubberized mixtures of different cementation levels experienced higher permanent deformation levels as compared with those tested at higher stress level with the higher permanent deformation occurring in rubberized mixtures of higher cementation levels. This, in fact, is well agreed with the fatigue lives findings where a better improvement, in terms of fatigue lives, occurred at lower stress ratios. Furthermore, the existence of the three mentioned phases is clearer at low cementation levels for both rubberized and reference mixtures.

On the other hand, it seems that the stress ratio also has the same effect on the permanent deformation accumulation rate of the reference mixtures having different cement contents. Comparing and contrasting the effect of rubber content in mixtures having different cement contents (Figure 9.16 and Figure 9.17 versus Figure 9.18 and Figure 9.19) reveals, at high stress ratios, no big difference between the rates of permanent damage accumulation due to rubber inclusion. However the deformation accumulated at failure is more than in the case of rubberized mixtures at all cement contents. At 85% stress ratio, on the other hand, this rate of accumulation is greater in the case of rubberized mixtures with large improvement occurring at higher cement contents. In addition, there is a big difference in the deformation experienced at failure when the rubber is incorporated.

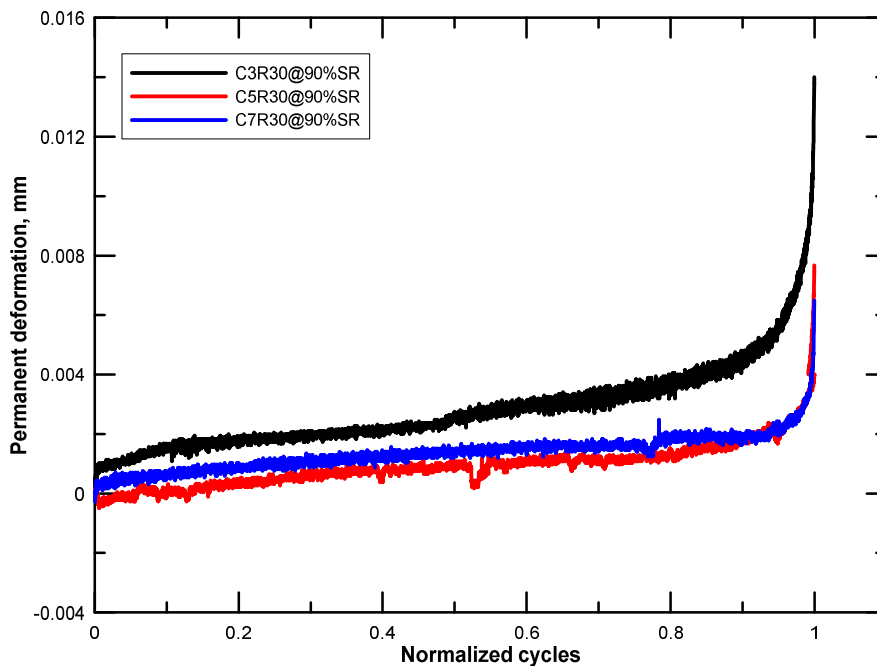


Figure 9.16: Permanent deformation accumulation for rubberized mixtures containing different cement contents @ 90% stress ratio

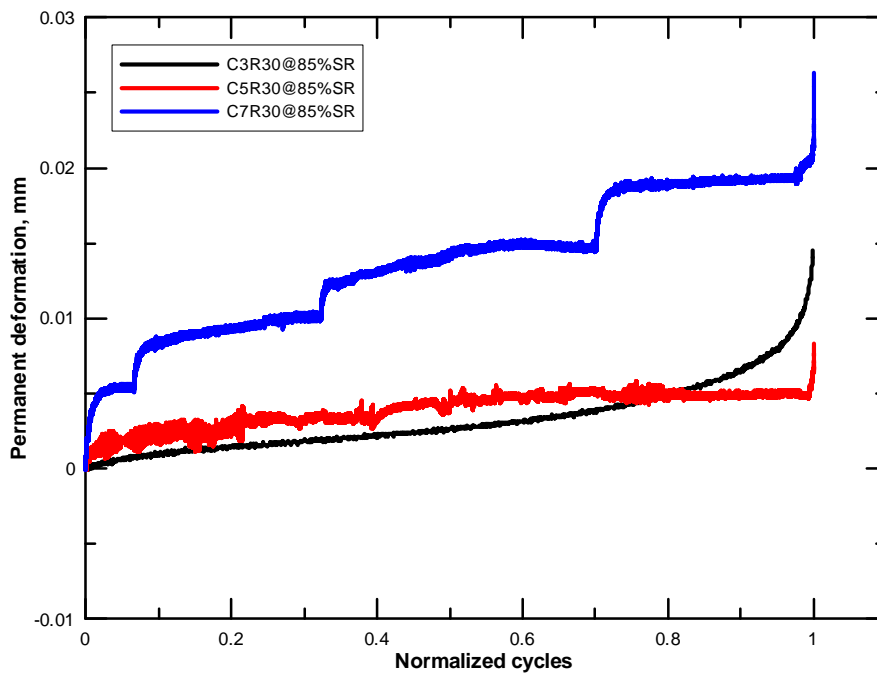


Figure 9.17: Permanent deformation accumulation for rubberized mixtures containing different cement contents @ 85% stress ratio

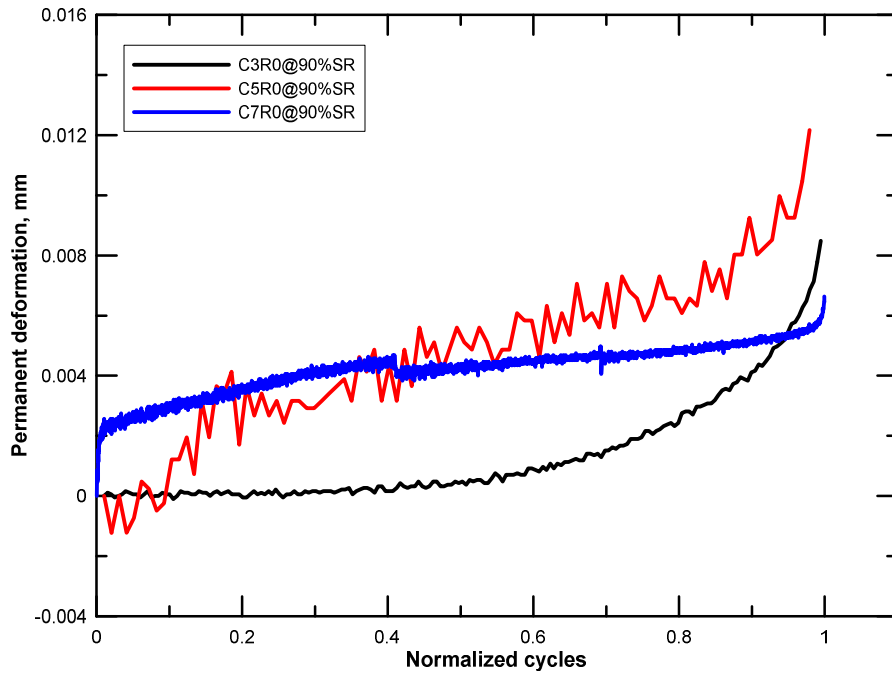


Figure 9.18: Permanent deformation accumulation for reference mixtures containing different cement contents @ 90% stress ratio

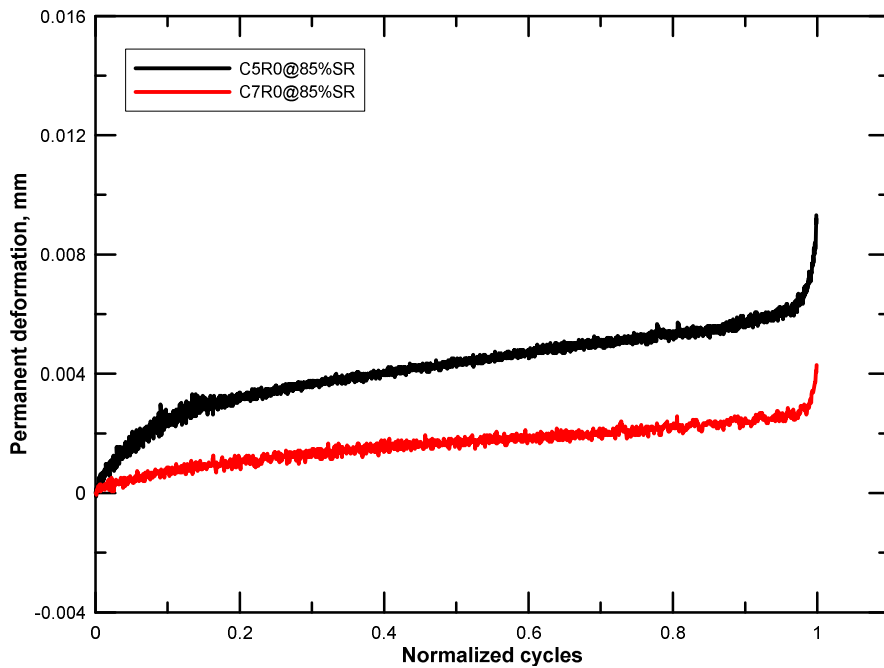


Figure 9.19: Permanent deformation accumulation for reference mixtures containing different cement contents @ 85% stress ratio

From these findings, it can be also concluded that there is a proportional relationship between the rate of damage accumulation and the fatigue life. This means the more the accumulated deformation the more the fatigue life of the mixtures. Sobhan and Mashnad (2002) presented similar permanent deformation growth when they investigated the performance of roller compacted concrete. Also, it has been previously found that the normalized permanent deformation and normalized cycles are related by the following formula (Sobhan and Das 2007; Paul 2011; Gonzalez 2014; Sobhan et al. 2015)

$$\frac{\Delta_p}{\Delta_{pmax}} = c_1 \left( \frac{N_i}{N_f} \right)^{c_2} \quad (9.10)$$

where

$\Delta_p$  = permanent deformation.

$\Delta_{pmax}$  = total accumulated permanent deformation at failure.

$c_1$  and  $c_2$  = regression constants.

$N_i$  = cycles number up to cycle  $i$ .

$N_f$  = total number of cycles up to failure.

Using the permanent deformation experimental data obtained from this investigation, a regression analysis was used to produce relationships between permanent deformation and number of cycles. Table 9.6 shows the regression coefficients for different mixtures. It can see from this table that the coefficient of determination ( $R^2$ ) for all mixtures at all investigated stress ratios (except C5R45@90% SR) is above 0.69. This tends to confirm that at all rubber and cement contents the permanent

deformation still follows the same trend. It is worth mentioning that [Sobhan and Mashnad \(2002\)](#) stated that these equations can be used to predict the permanent deformation at any stage of the fatigue life of the pavement.

Table 9.6: Regression coefficients for permanent deformation of investigated mixtures.

Mixture ID	Stress ratio, %	$c_1$	$c_2$	$R^2$
C3R0	90	0.256381	1.573144	0.69
C7R0	90	0.77607	0.224079	0.94
C3R0	85	-----	-----	-----
C7R0	85	0.59733	0.56883	0.943
C3R30	90	0.277204	0.425193	0.79
C7R30	90	0.303749	0.466041	0.89
C3R30	85	0.378253	0.790576	0.92
C7R30	85	0.719811	0.39564	0.95
C5R0	90	0.746325	0.8815	0.83
C5R15	90	0.306126	1.223147	0.81
C5R30	90	0.239744	1.047187	0.8
C5R45	90	0.193277	0.654556	0.35
C5R0	85	0.669277	0.468734	0.94
C5R15	85	0.441423	0.196214	0.71
C5R30	85	0.638585	0.36552	0.92
C5R45	85	0.680381	0.295584	0.86

#### 9.14.2 Dynamic modulus degradation

Fatigue life of pavement materials in general can be defined as the number of load applications that the materials can sustain at a particular stress/strain level. In addition, in design of a pavement structure, this level of stress/strain should not

exceed the maximum values established for the materials via static tests. Therefore, in the design of pavement structures, it is traditional to increase the layer thickness to ensure that the calculated pavement responses are sufficiently below their maximum values.

In analysis and design of pavement structures, it is normally assumed that the modulus of elasticity remains constant across the fatigue life. This latter assumption is not necessarily correct due to the degradation of the material stiffness throughout its life (Oliveira 2006). Therefore, it can be concluded that it is not only important to investigate the fatigue performance in terms of the number of cycles up to failure, but it is also necessary to observe and monitor the material behaviour throughout the fatigue life to ascertain the accuracy of pavement design assumptions. In addition, observing the behaviour of the materials during the fatigue test may provide vital information to understand the mechanism of their damage under fatigue loading. Therefore, in this part of study, an investigation was performed to investigate the behaviour of the rubberized mixtures containing different amounts of crumb rubber, rubberized mixtures of different degrees of stabilization and reference mixtures with different degrees of cementation under fatigue loading. This was performed in terms of modulus degradation throughout the fatigue life.

Figure 9.20 and Figure 9.21 show the effect of rubber content on the degradation of dynamic modulus of the cemented mixtures subjected to fatigue loading. As can be seen from these figures, at 90% stress ratio, rubber does not have a noticeable effect on the degradability of the modified mixtures where approximately the same modulus was achieved across the majority of the fatigue lives. However, a slight

reduction is observed in the elastic modulus of the mixture with 45% rubber replacement. Similarly, at lower stress ratio, the latter behaviour was also observed in the case of the 45% replacement level. The large degradation in the dynamic modulus would mean an uneconomical layer thickness since similar performance would require a thicker layer to maintain the same level of stress/strains in the underlying and overlying pavement layers. Therefore, in terms of the degradability, the performance of rubberized mixtures does not differ much from that of unmodified mixtures except at high stress states and high rubber replacement percentage.

Regarding the effect of cement content, it can be seen from comparing Figure 9.22 and Figure 9.23 with Figure 9.24 and Figure 9.25 that the rubber has no clear effect on the degradability of flexural dynamic modulus at all examined cement contents. However, it seems that the degradability of mixtures with low cement contents (3%) is larger as compared to mixtures with moderate (5%) and high cement contents (7%). From a practical point of view, this means a need for greater layer thicknesses when constructing using low stabilizer content so as to maintain the same strain/stress levels in the pavement system.

Dynamic modulus degradation curves for the majority of the investigated mixtures showed only two regions. In the other words, the first phase does not exist in these mixtures. This was followed by Phase II which last until 95% and then the rapid degradation Phase III starts. Observations conducted by [Paul \(2011\)](#) for lightly stabilized materials showed similar behaviour.

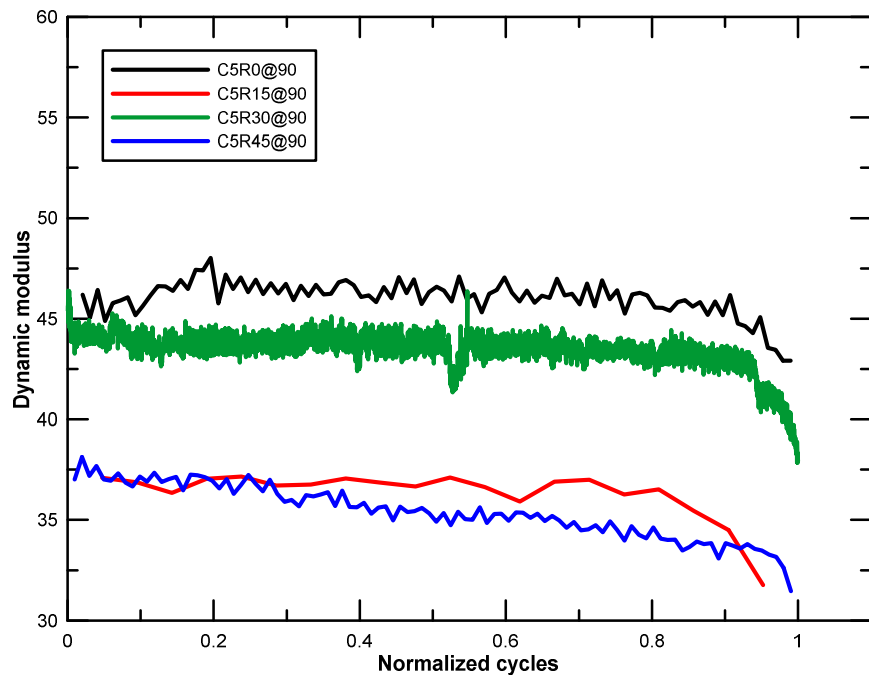


Figure 9.20: Evolution of dynamic modulus of elasticity for CSAMs of different rubber replacement @90% stress ratio

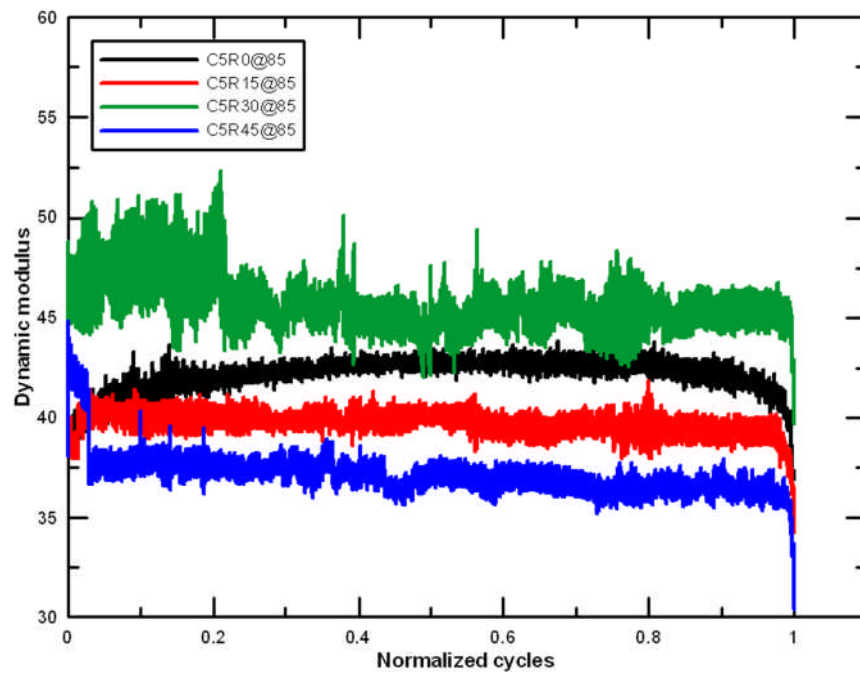


Figure 9.21: Evolution of dynamic modulus of elasticity for CSAMs of different rubber replacement @85% stress ratio.

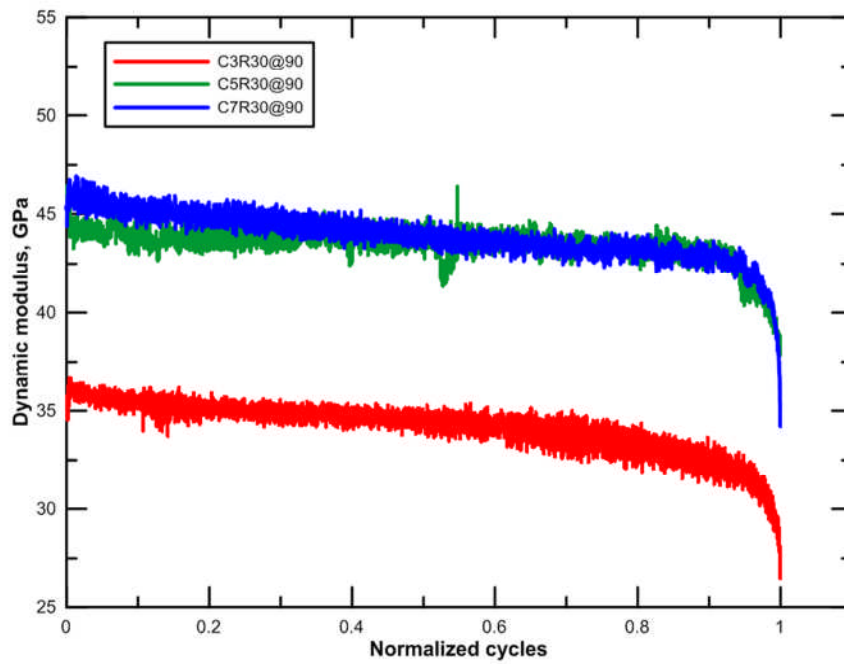


Figure 9.22: Evolution of dynamic modulus of elasticity for RCSAMs of different cement contents @90% stress ratio.

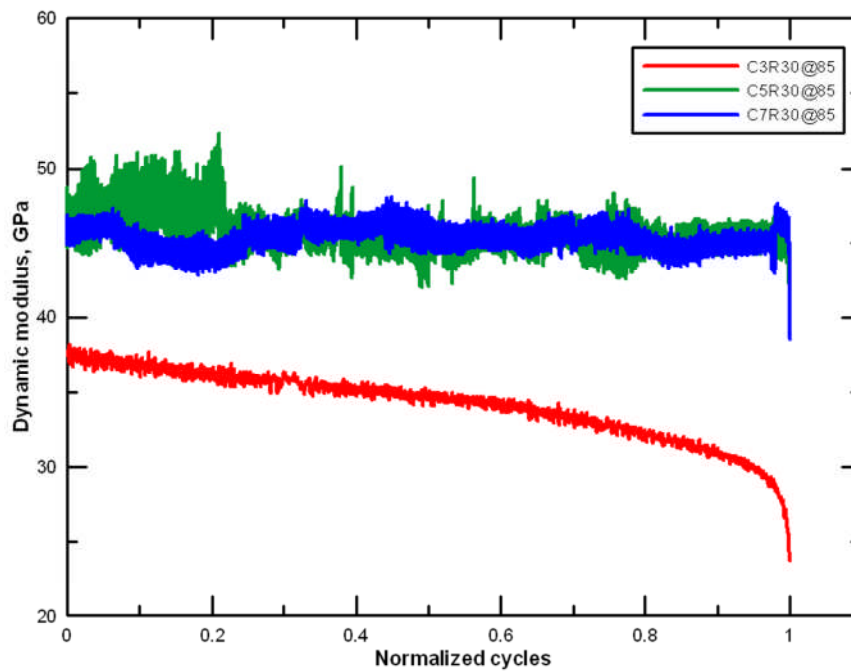


Figure 9.23: Evolution of dynamic modulus of elasticity for RCSAMs of different cement contents @85% stress ratio.

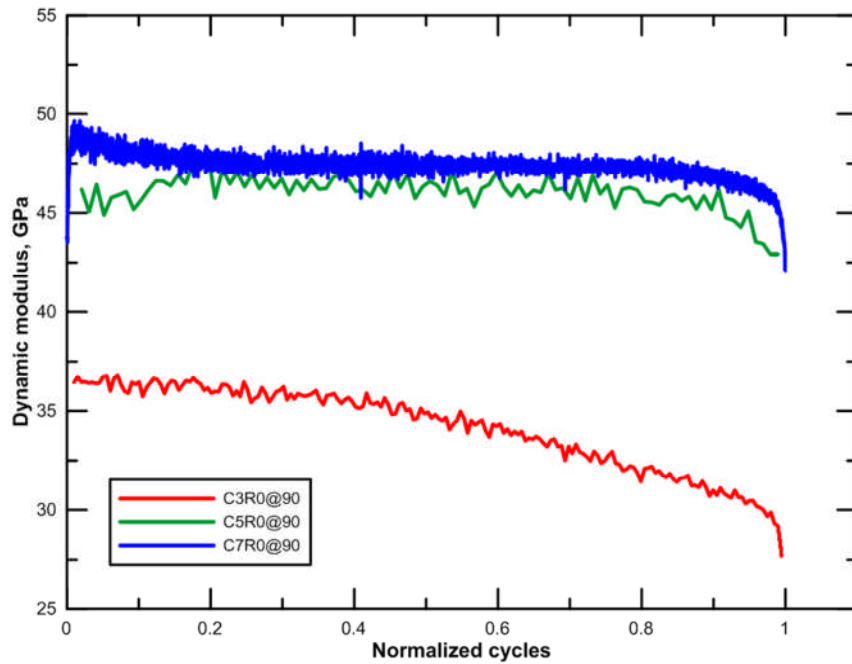


Figure 9.24: Evolution of dynamic modulus of elasticity for CSAMs of different cement contents @90% stress ratio.

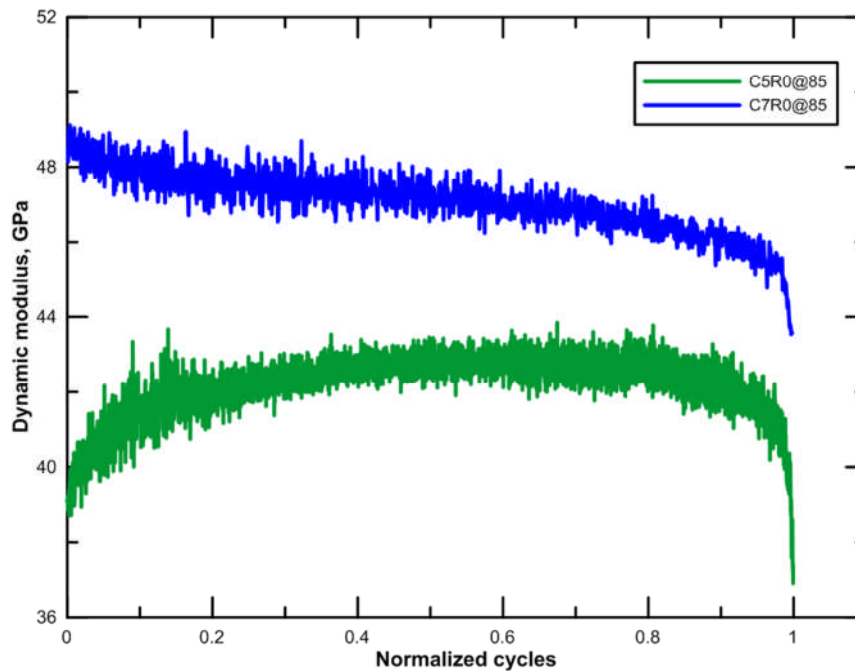


Figure 9.25: Evolution of dynamic modulus of elasticity for CSAMs of different cement contents @85% stress ratio.

### 9.14.3 Dynamic load-deformation hysteresis loops

Figure 9.26 through Figure 9.31 illustrate the typical load-deformation hysteresis for some mixtures while the complete set of hysteresis curves for investigated mixtures at 90% and 85% stress ratios is shown in Appendix B. By comparing and contrasting Figures 9.26, 9.28 and 9.30 with Figures 9.27, 9.29 and 9.31, it can be seen that the dissipated energy (i.e., the area inside the loop hysteresis) is greater due to rubber inclusion at all cementation levels. Furthermore, it seems, from these figures, that more energy was dissipated after 90% of the fatigue life had been consumed for all mixtures. These results are consistent with the permanent deformation findings discussed earlier in Section 9.14.1.

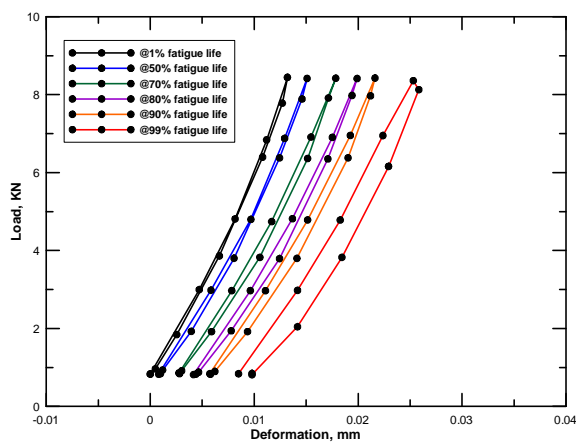


Figure 9.26: Load-deformation hysteresis loops for C3R0@90% stress ratio

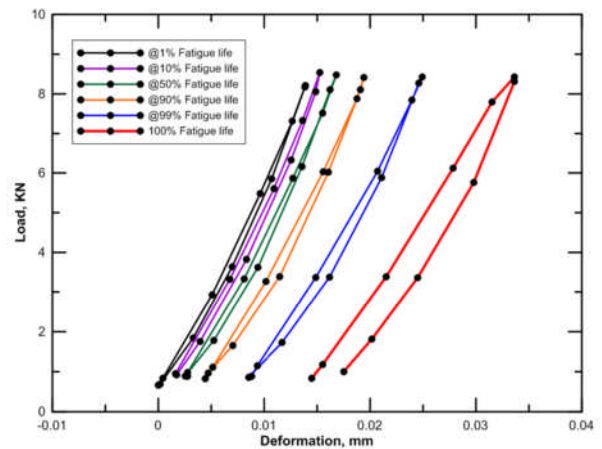


Figure 9.27: Load-deformation hysteresis loops C3R30@90% stress ratio

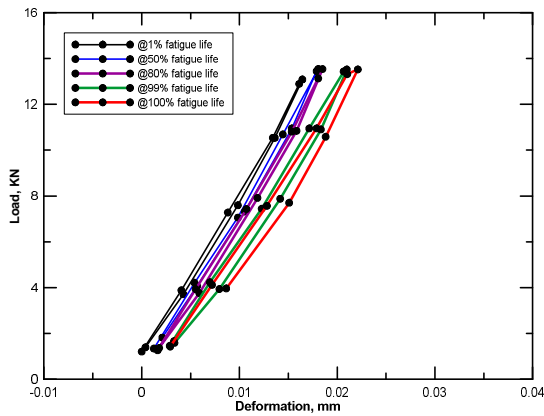


Figure 9.28: Load-deformation hysteresis loops for C5R0@90% stress ratio

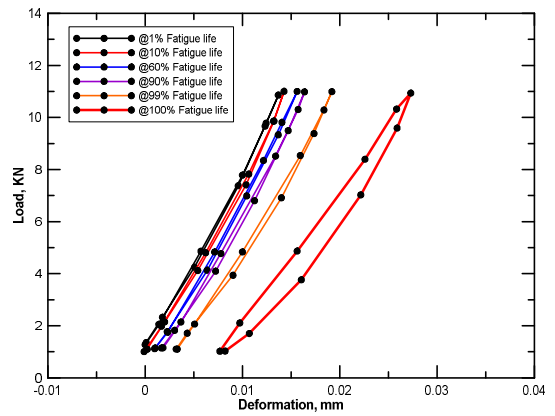


Figure 9.29: Load-deformation hysteresis loops for C5R30@90% stress ratio

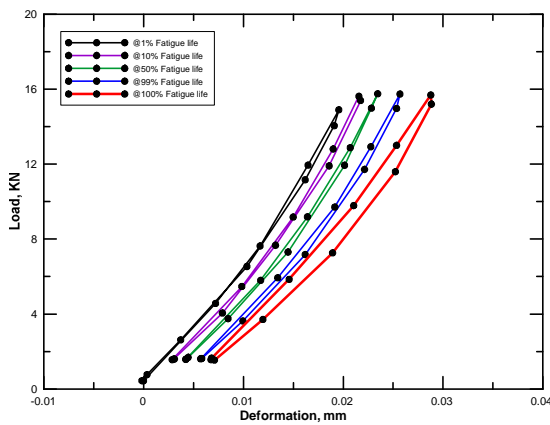


Figure 9.30: Load-deformation hysteresis loops for C7R0@90% stress ratio

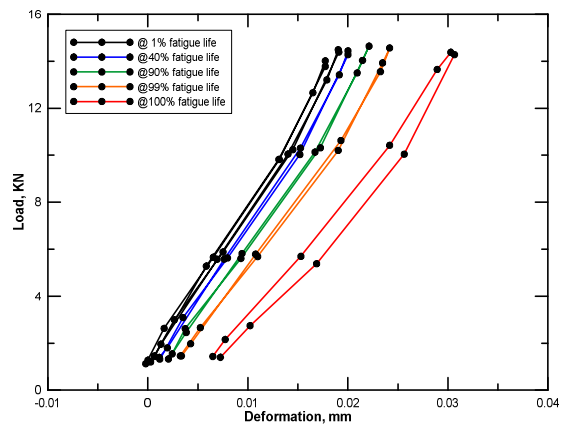


Figure 9.31: Load-deformation hysteresis loops for C7R30@90% stress ratio

#### 9.14.4 Fatigue damage accumulation assessment through dissipated energy approach

There is no doubt that research regarding the fatigue of asphaltic materials and their analysis methods is more advanced as compared with cement-stabilized mixtures. As mentioned earlier, various methods are normally used to define the fatigue failure.

Recently, [Gnanendran and Pirathepan \(2009\)](#) have used the stiffness reduction and

dissipated energy approaches to define the fatigue failure of lightly stabilized materials. Similar results were obtained by these authors using these two approaches. In contrast, the investigations conducted by [Paul \(2011\)](#) in his PhD study for lightly stabilized aggregate showed that the dissipated energy approach results in conservative fatigue lives where these lives were about 86% of those estimated based on complete collapse of the sample.

Due to the limited information regarding the applicability of the dissipated energy approach to define the fatigue failure of cemented materials, it was intended, in this section, to investigate this applicability especially in the light of the mixture variety in terms of aggregate composition and stabilization degree. Also, this approach was introduced very recently in the draft of the new European standards ([BS EN 12697-24:2015](#)) as an alternative criterion to define the fatigue failure life of asphaltic mixtures. The curves presented in Appendix C show the implementation of the dissipated energy ratio method to locate the fatigue failure, as a peak of the curve, for different investigated mixtures. Figure 9.32 through Figure 9.34 represent typical results. To compare between the fatigue lives determined based on the full collapse of the sample and that estimated based on the dissipated energy ratio approach, the latter was plotted against the former to observe the relationships between these two criteria, as shown in Figure 9.35. As can see from this figure, the fatigue life estimated based on dissipated energy approach is close to (around 97% of) that corresponding to the point of sample fracture. This figure also shows that all mixtures, of different cement and rubber contents, follow the same relationship with an extremely high  $R^2$  (0.99); indicating the interchangeability of these two approaches.

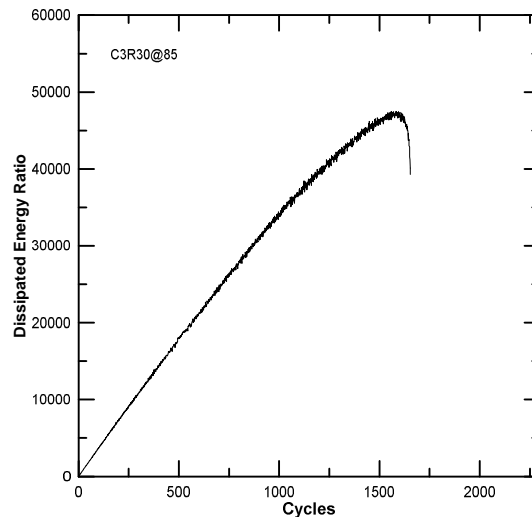


Figure 9.32: Variation in energy ratio versus cycles number for C3R30@85

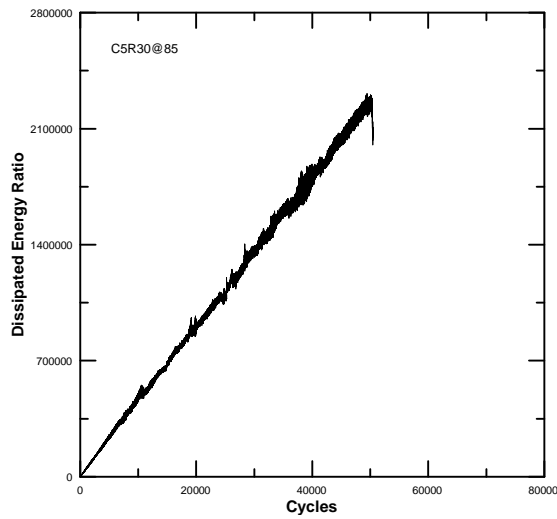


Figure 9.33: Variation in energy ratio versus cycles number for C5R30@85

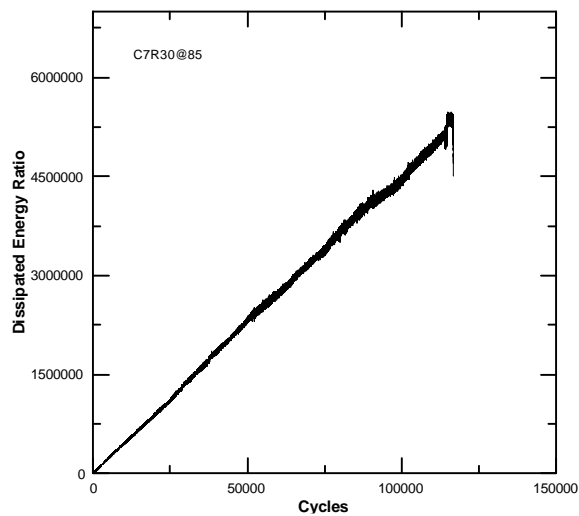


Figure 9.34: Variation in energy ratio versus cycles number for C7R30@85

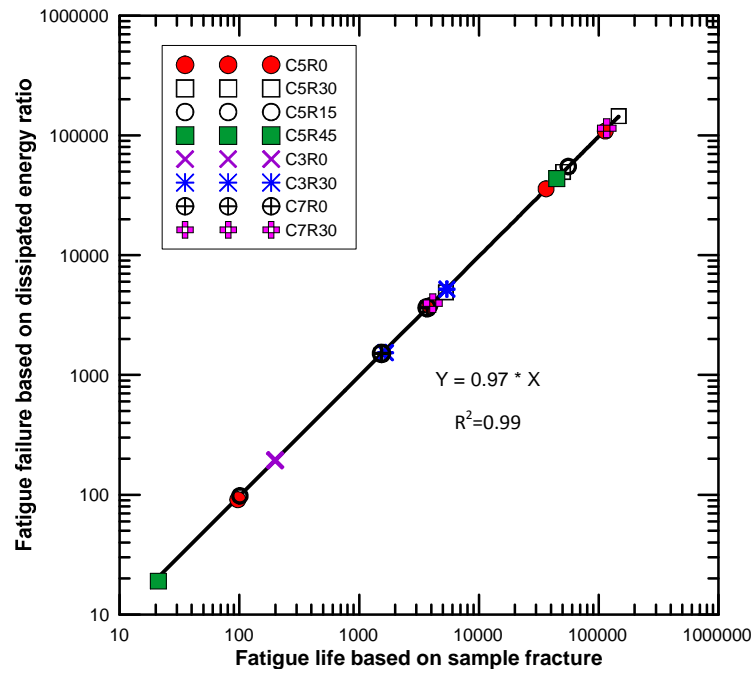


Figure 9.35 Fatigue life based on energy ratio versus cycles number to break the sample.

### 9.15 Concluding remarks

Based on the results presented in this chapter, the following conclusions can be drawn:

1. Inclusion of crumb rubber improves the fatigue lives of the cement-stabilized mixtures. This degree of improvement depends, to some extent, on the stress ratio. In general, the fatigue lives of samples tested at less than 85% stress ratio increase as the rubber content increases. Furthermore, this improvement occurred for all cementation levels with the highest improvement in the case of the highest cement content.

2. More permanent deformation was accumulated as the rubber content increased especially at lower stress ratios (less than 85%). The same behaviour was observed in the case of both the rubberized and reference mixtures at all cement contents.
3. Comparing and contrasting fatigue and permanent deformation accumulated across the pavement life indicates the strong relationship between these two parameters. This suggests that the improvement in fatigue life comes from the fact that more deformation was accumulated in the mixtures.
4. The mechanism of fatigue improvement is probably because the rubber particles delay the crack propagation, especially at the microcracking stage, by absorbing and relieving the stress at the crack tip and by lengthening the crack path. This explanation is supported by the observation that the fatigue life, at lower stress ratios, improved since the microcracks grew more slowly which permits absorbance and relief of the stresses and the crack could take the longest path (as evidenced by more accumulated permanent deformation).
5. The dissipated energy approach was implemented, through the dissipated energy ratio concept, to define the fatigue life of cementitious material, to show the difference between this approach and the complete collapse concept and finally to observe how the rubber, cement and their interaction may affect this behaviour. The results revealed that regardless of the rubber or cementation level the fatigue lives estimated by these two principles are close to each other and very simply and reliably related by a factor of  $0.97L_f=L_e$  where  $L_f$  is the fatigue

life determined on the basis of specimen collapse and  $L_e$  is the life determined by dissipated energy approach.

6. Estimating the actual flexural strength on the basis of ultrasonic pulse velocity is a practical and useful means of accurately estimating applied stress ratio in fatigue tests. This helped to reduce the scatter in results.
7. The possible dynamic modulus range of the lightly stabilized mixtures is 26-40.2 GPa. For moderately cemented mixtures this range is from 28 GPa to 46.4 GPa. Finally, heavily stabilized mixtures have dynamic moduli ranging between 28 GPa and 49 GPa. These above possible ranges apply for different cement stabilized crushed fractioned aggregate mixtures having different ranges of densities.
8. Comparing different stiffness modulus characterization methods (destructive vs. non-destructive) and modes (flexural vs indirect tensile and static vs dynamic) revealed that the resonant frequency testing method can be adopted to estimate reliably the dynamic modulus of elasticity economically and simply for pavement analysis in mechanistic empirical pavement design procedures.
9. The permanent deformation development follows the same trend reported previously for stabilized mixtures at all rubber replacement levels, degrees of stabilization and applied stress ratios.
10. To quantify and optimize the effect of rubber in a pavement structure, it is necessary to investigate if the reduction in the mixture strength will be

compensated by the improvement in the fatigue life and reduction in the stress attractiveness due to stiffness reduction of the rubberized mixtures.

11. In pavement design, the degradability of the layer mixtures should also be taken into consideration. This is because the reduction in the dynamic modulus will reduce the stress attracted to a certain layer which, in turn, may induce more stress/strains in underlying and overlying layers for which they are not designed. This in turn may accelerate the pavement failure and/or reduce the economic ability of the layer if its thickness must be increased to compensate for the effect of reduced modulus.
12. The description of the fatigue behaviour in terms of transfer functions is limited to the comparison between the reference mixture and the rubberized mixture stabilized with 5% cement contents. It is recommended to study the transfer function at different cement contents. This will also help to expand knowledge regarding the effect of cement under other stress ratios.

### 9.16 References

- Alderson, A. and G. Jameson (2014). Cemented materials characterisation: final report, Austroad project TT1664, Report no. AP-R462/14.
- Applied Research Associates, I. (2004). Guide for Mechanistic-Empirical Design of New and Rehabilitated Pavement Structures. Illinois.
- Arnold, G., C. Morkel and G. van der Weshuizen (2012). Development of tensile fatigue criteria for bound materials, NZ Transport Agency report No. 463, New Zealand Institute of Highway Technology.
- Artamendi, I. and H. Khalid (2013). Different approaches to depict fatigue of bituminous materials. ECF15, Stockholm 2004.
- Ghuzlan, K. and S. Carpenter (2000). "Energy-derived, damage-based failure criterion for fatigue testing." *Transportation Research Record: Journal of the Transportation Research Board*(1723): 141-149.
- Gnanendran, C. T. and J. Piratheepan (2009). "Determination of fatigue life of a granular base material lightly stabilized with slag lime from indirect diametral tensile testing." *Journal of Transportation Engineering* 136(8): 736-745.
- Gonzalez, A., A. Howard and R. de Carteret (2010). Cost effective structural treatments for rural highways: cemented materials.
- Gonzalez, L. (2014). Durability of a recycled aggregate concrete base course material under coupled environmental exposure and cyclic loading. PhD thesis, Florida Atlantic University.
- Grzybowski, M. and C. Meyer (1993). "Damage accumulation in concrete with and without fiber reinforcement." *ACI Materials Journal* 90(6).
- Huang, Y. H. (2004). Pavement analysis and design, Second edition, Prentice Hall Publishing company, 792 pages.

- Jitareekul, P. (2009). An Investigation into Cold In-Place Recycling of Asphalt Pavements, PhD Thesis ,University of Nottingham, Department of Civil Engineering.
- Khoury, N. N. (2005). Durability of cementitiously stabilized aggregate bases for pavement application. PhD thesis, The University of Oklahoma.
- Li, X. W. and M. M. Dong (2011). Experimental Research on Pavement Performance of Cement Stabilized Base Recycled Mixture. Applied Mechanics and Materials, Trans Tech Publ.
- Liu, Z. and X. Wang (2014). "Study on the fatigue test of cement bound granular CBG-25." Journal of the Chinese Advanced Materials Society 2(1): 53-69.
- Modarres, A. and Z. Hosseini (2014). "Mechanical properties of roller compacted concrete containing rice husk ash with original and recycled asphalt pavement material." Materials & Design 64: 227-236.
- Nusit, K., P. Jitsangiam, J. Kodikara, H. H. Bui and G. L. M. Leung (2015). "Dynamic Modulus Measurements of Bound Cement-Treated Base Materials." Geotechnical Testing Journal, Vol.38, No.3 38(3): 1-15.
- Oliveira, J. R. M. d. (2006). Grouted macadam: material characterisation for pavement design. PhD Thesis, University of Nottingham.
- Paul, D. K. (2011). "Characterisation of Lightly Stabilised Granular Materials by Various Laboratory Testing Methods." PhD Thesis, University of New South Wales, Australian.
- Rowe, G. M. (1996). Application of the dissipated energy concept to fatigue cracking in asphalt pavements. PhD Thesis, University of Nottingham.
- Shah, S. P. and S. Chandra (1970). Fracture of concrete subjected to cyclic and sustained loading. ACI Journal Proceedings, ACI.

Sobhan, K. and B. M. Das (2007). "Durability of soil–cements against fatigue fracture." *Journal of Materials in Civil Engineering* 19(1): 26-32.

Sobhan, K., L. Gonzalez and D. Reddy (2015). "Durability of a pavement foundation made from recycled aggregate concrete subjected to cyclic wet–dry exposure and fatigue loading." *Materials and Structures*: 1-14.

Sobhan, K. and M. Mashnad (2000). "Fatigue durability of stabilized recycled aggregate base course containing fly ash and waste-plastic strip reinforcement." Final Rep. Submitted to the Recycled Materials Resource Centre, Univ. of New Hampshire.

Sobhan, K. and M. Mashnad (2001). "Roller-compacted fiber concrete pavement foundation with recycled aggregate and waste plastics." *Transportation Research Record: Journal of the Transportation Research Board*(1775): 53-63.

Sobhan, K. and M. Mashnad (2002). "Fatigue damage in roller-compacted pavement foundation with recycled aggregate and waste plastic strips." *Transportation Research Record: Journal of the Transportation Research Board*(1798): 8-16.

Sobhan, K. and M. Mashnad (2003). "Fatigue behavior of a pavement foundation with recycled aggregate and waste HDPE strips." *Journal of geotechnical and geoenvironmental engineering* 129(7): 630-638.

Theyse, H. L., M. De Beer and F. C. RUST (1996). "Overview of South African Mechanistic Pavement Design Method." *Transportation Research Record: Journal of the Transportation Research Board* Volume 1539

Wu, H., B. Huang and X. Shu (2013). "Characterizing fatigue behavior of asphalt mixtures utilizing loaded wheel tester." *Journal of Materials in Civil Engineering*.

BS EN 12697-24:2015, Draft-Bituminous mixtures- test methods- Part 24: Resistance to fatigue

# Chapter Ten

## Pavement Analysis and Design

### 10.1 Introduction

In the mechanistic-empirical pavement design approach, different layer properties are usually involved. The most important ones are strength, dynamic modulus of elasticity and fatigue performance. Modifying cement-stabilized aggregate mixtures with different amounts of rubber and/or cement has resulted, as determined in the previous chapters, in different strengths, moduli and fatigue performances. An interesting question therefore arises: how do the rubber and cement affect the final pavement performance? Or expressed differently, what is the effect of interactions between the different pavement design inputs that result from modification of the aggregate with rubber and cement on the pavement responses and design thickness of different layer(s)? In addition, will the improvement in fatigue performance

compensate for the decline in the materials' strength in the light of the slight reduction in the materials' stiffnesses? To answer these questions it is necessary to implement a mechanistic-empirical design methodology utilizing a multilayer elastic analysis and experimental-derived strength, stiffness and fatigue results.

The purpose of this chapter is to describe such an implementation and to present the responses, mainly in terms of stresses, strains and deflections. Then, these pavement responses are employed with the laboratory transfer functions to gain understanding of the effect of modification on the final layer thickness or the fatigue life of the modified layer. In addition, since the mixtures of different cement contents showed different degrees of degradability, a study was also made of the effect of degradability of the pavement mixture on the performance of different pavement layers.

## **10.2 Pavement arrangements and properties**

To achieve the objectives of this chapter, 64 hypothetical pavement sections (Table 10.1) were taken into consideration to study different pavement arrangements with various layer properties. Pavement sections consist of a Hot Mix Asphalt (HMA) surface course, a CSAM base course, a granular subbase and a soft subgrade. The latter was selected to simulate the worst case in which a rigid layer is logically used. For simplicity, the load is assumed to be applied by a single axle and a single tire. Figure 10.1 illustrates, diagrammatically, the assumed pavement structure. Regarding the pavement properties, these were extracted from the experimental investigation presented in the previous chapters. The thickness range for base course differed,

depending, based on the cement content of these layers. The surface course, subbase course and subgrade were allotted typical properties as documented in the literature. Typical properties and thicknesses for these other layers are presented in Table 10.2.

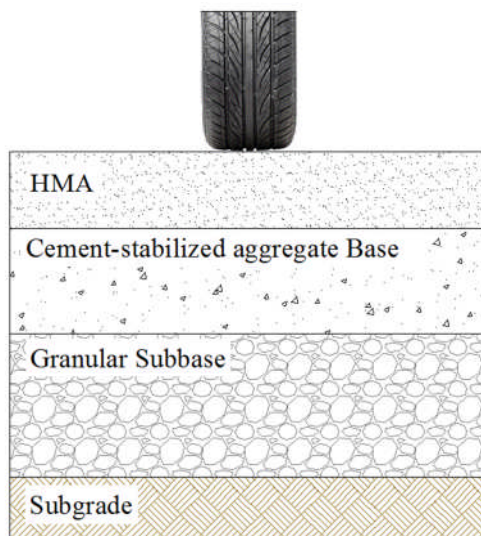


Figure 10.1: Pavement structure configuration (not to scale)

Table 10.1: Analysis and design matrix

Case No.	Surface course thicknesses (mm)	Base course thickness (mm)	Subbase thickness (mm)	Mix type	No. of Pavement sections
Low cement content					
1	40 and 50	175-250 (25)*	200	C3R0	16
2				C3R30	
Moderate cement content					
4	40 and 50	125-170 (15)	200	C5R0	32
5				C5R15	
6				C5R30	
7				C5R45	
High cement content					
9	40 and 50	100-150 (15)	200	C7R0	16
10				C7R30	

\* The number in the brackets represents the thickness increment

Table 10.2: Typical properties for surface, subbase and subgrade courses

Layer	Type	Modulus of elasticity, MPa	Reference
Surface	HMA	2800	<a href="#">Lav et al. (2006)</a>
Subbase	Granular	96.6	<a href="#">Hadi and Bodhinayake (2003)</a>
Subgrade	Soft soil	50	<a href="#">Huang (2004)</a>

### 10.3 Traffic loads and analysis software

Cement-stabilized aggregate bases are normally used in highways that are anticipated to carry heavy traffic loads. Reviewing the criteria of different countries revealed that France, Spain and Belgium use the highest maximum axle load which is 130 kN ([Thøgersen et al. 2004](#)). For the purpose of this study the latter axle load was adopted. The tire pressure was adopted as 750 kPa. The analysis of the structural pavement system was conducted using the KENPAVE software. This was developed by Professor Huang ([Huang 2004](#)) at Kentucky University. KENPAVE consist of two systems which are KENLAYER and KENSLABS used for flexible and rigid pavement analysis and design, respectively. KENLAYER is a multilayer elastic solution system under single, dual, dual-tandem and dual-tridem wheel loads. Each layer can be considered as a linear elastic, nonlinear elastic or viscoelastic material. In this study, all layers are considered as linear elastic materials. This is because the purpose of this study is to show the effect of the relative change in the materials' elastic behaviour resulting from different rubber and cement contents and their combinations.

#### **10.4 Pavement failure criteria**

For successful structural design of any civil engineering structure, including pavement structures, it is necessary to understand their possible failure mode (Brown 2012). The deterioration of the pavement structure normally occurs gradually due the accumulation of damage resulting from different factors including traffic loads and environmental conditions. However, as stated by Brown, traffic loads can be considered as the main reason behind the deterioration of the pavement structure.

In conventional flexible pavement design two critical failure modes occur due to two critical responses. The first mode is fatigue cracking in the bound layer resulting from the tensile stress/strain at the bottom of that later. This can be considered as a structural failure. Rutting of the subgrade due to the excessive compressive stress/strain on its upper surface represents the second failure mode. The latter mode is a functional failure. Since the purpose of pavement structural design is to ensure it serves its role both structurally and functionally, it is necessary to design the pavement to resist both these failure modes. In situations where there is more than one bound layer, the tensile criterion should be checked at the bottom of each bound layer (Figure 10.2). However, in the case of a composite pavement structure, in which there is a rigid base course, it is almost always the tensile stress at the bottom of this layer that is the critical criterion. In this study, the following failure locations will be checked:

1. Bottom of HMA- to check the tensile strain which may cause fatigue cracking.

2. Bottom of CSAMs and RCSAMs- to check the tensile stress which may cause fatigue cracking.

According to the South African mechanistic-empirical pavement design method (Theyse et al. 1996), another possible failure mode is crushing at the top of the cemented layer. This means that the compressive stress must be compared with the unconfined compressive strength of a certain mixture. Therefore, this parameter will also be estimated and checked here. Rutting, that may occur at the top of the subgrade, which is characterized by the compressive strain at the top of the subgrade will be ignored in this investigation due to the high stiffness and hence good load-spreading achieved by the cemented layers.

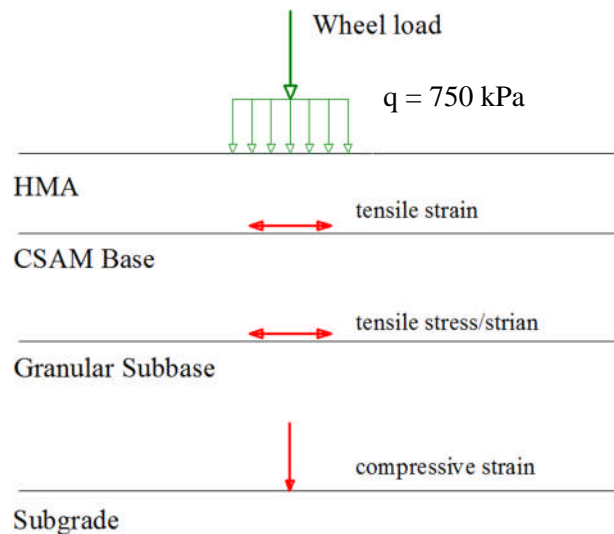


Figure 10.2: Pavement structure critical responses for design

### 10.5 Methodology and Mechanistic pavement design

Unlike the empirical pavement design methods, which are restricted to a specific range of pavement materials and were developed from the observations of the performance of existing pavement structures in full-scale trial sections, the

mechanistic-empirical method permits design for any new material (Lav et al. 2006). It relates the pavement responses from mechanistic analysis with the pavement materials performances measured in the laboratory and is calibrated utilizing specially designed trial pavement sections. The fatigue cracking criteria depend on transfer functions for the different layers in which fatigue cracking may occur. For asphaltic mixtures, the transfer function developed by the Asphalt Institute was adopted as follows:

$$N_f = 0.0796 (\varepsilon_t)^{-3.291} (E)^{-0.854} \quad (10.1)$$

where  $N_f$  is the number of traffic load application to reach fatigue failure,  $\varepsilon_t$  is the horizontal strain at the bottom of asphalt layer and  $E$  is the stiffness modulus of the asphalt surface course. Transfer functions for reference and rubberized cement-stabilized aggregate mixtures will be used as presented in Equation 9.9 and Equation 9.10, respectively. Figure 10.3 demonstrates the methodology adopted in this research and the relationship with other project elements.

## 10.6 Pavement analysis results

### 10.6.1 Vertical stress and strain distributions

The pavement structures in Table 10.1 were adopted to investigate the effect of both rubber and cement on vertical and horizontal stresses and strains. Figure 10.4 illustrates the effect of rubber and cement on the vertical stresses. As expected, there is a reduction in vertical stress as the depth from the pavement surface increases. In addition, neither rubber nor cement has an effect on the vertical stress distribution. Also, the compressive stress levels (that might cause crushing failure at the top of the

cemented layer) are small as compared with the material's compressive strength. Therefore, only the tensile stress at the bottom of the cemented layer is likely to be critical for this layer. Figure 10.5 shows the vertical strain distribution for all the different cementitious base course alternatives. It can be seen from that figure that, as the stiffness of the mixture decreases due to increasing rubber replacement, the stress at the bottom of the cemented layers slightly decreases. However, a considerable increase in the vertical strains applied at the top of the subgrade occurred with this rubber content increase. Similarly, the subgrade becomes less strained as the rigidity of the CSAM/RCSAM increases due to increased cementation.

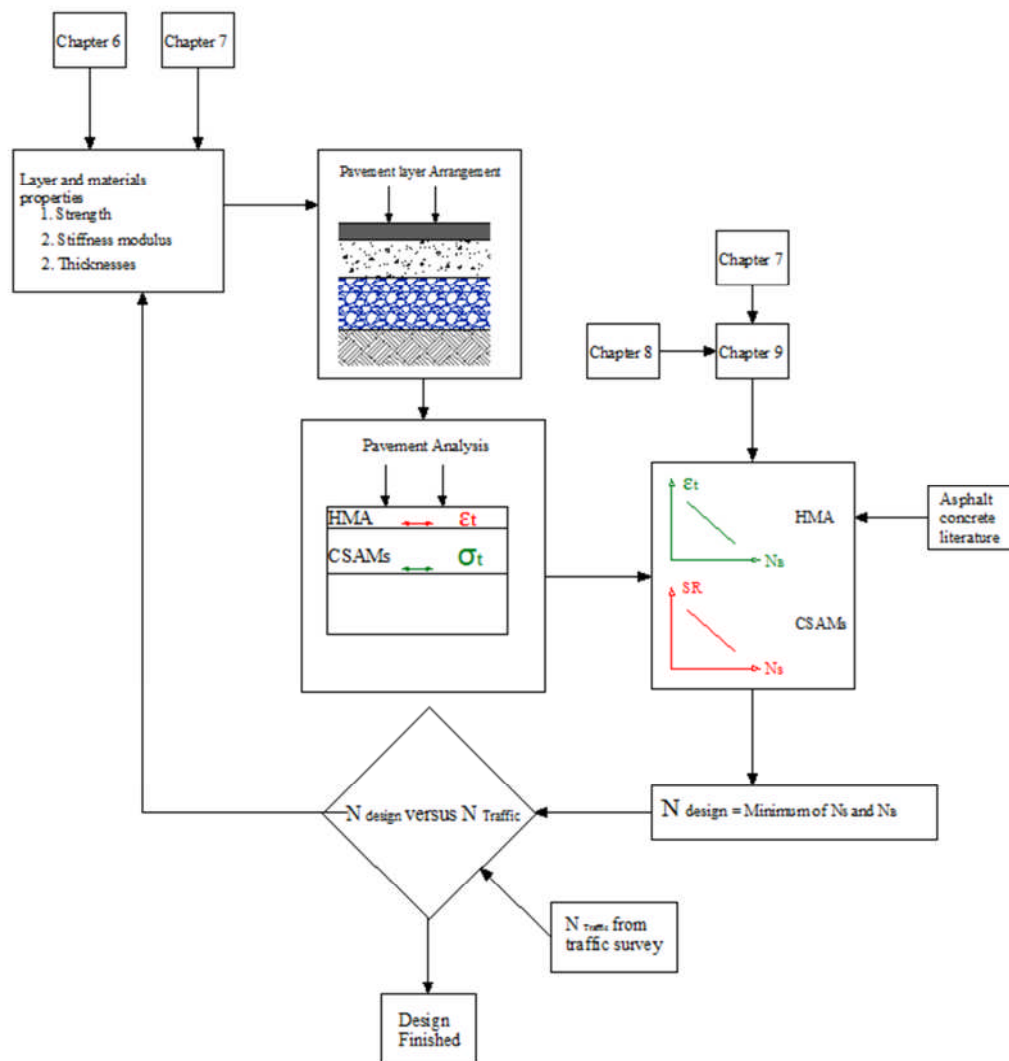


Figure 10.3: Pavement analysis and design methodology adopted.

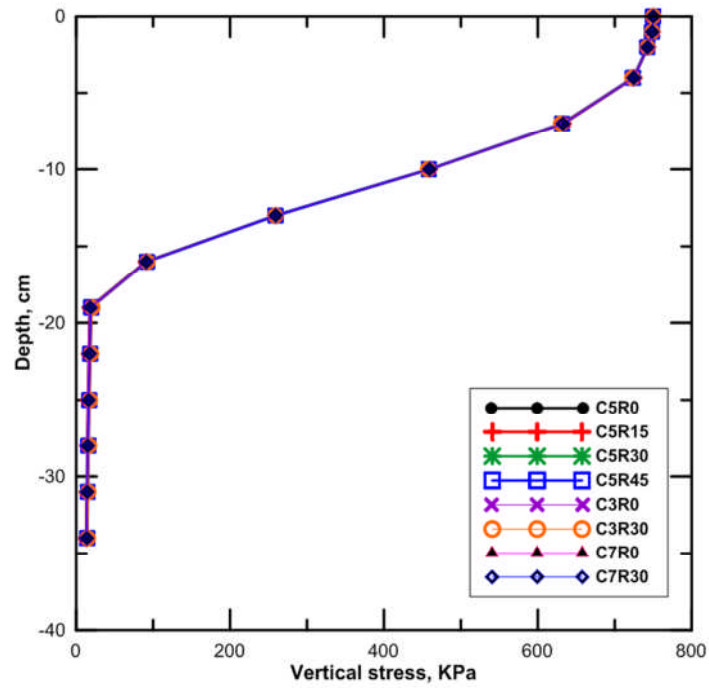


Figure 10.4: Effect of different cemented layer properties on vertical stresses

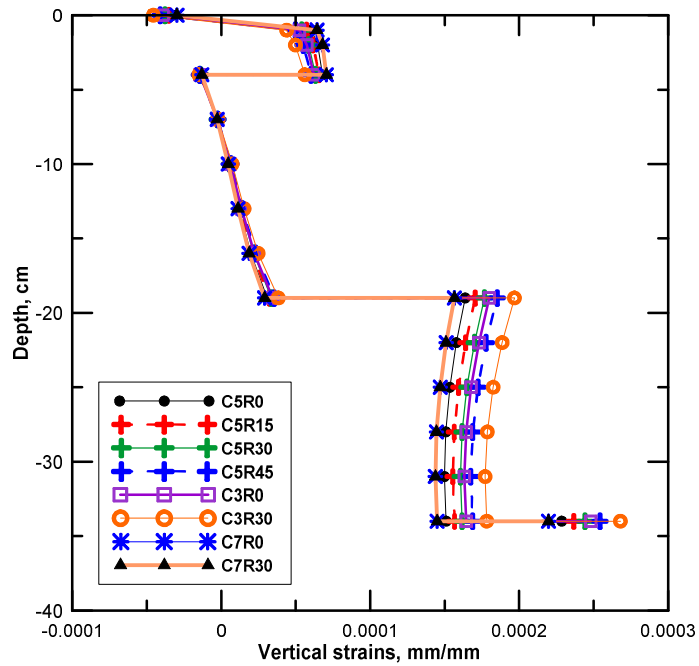


Figure 10.5: Effect of different cemented layer properties on vertical strains

### 10.6.2 Horizontal stress and strain distributions

The horizontal stress distributions for different cementitious base courses of different cement and rubber contents are illustrated in Figure 10.6. It can be seen that the horizontal stress at the bottom of the cemented layer only slightly increases as the amount of rubber increases. On the other hand, there is greater applied stress as the cement content increases. In terms of tensile strains, it can be seen from Figure 10.7 that the strains at the bottom of HMA surface course increase due to incorporation of more rubber in the cemented mixtures while increasing the cementation level of the layer causes a decrease in the strains applied at the bottom of the surface course. The absence of tensile strain at the bottom of the asphaltic surface course Figure 10.7 is partly explained by the assumption that the surface course is in full contact (full friction) with the CSAM base course.

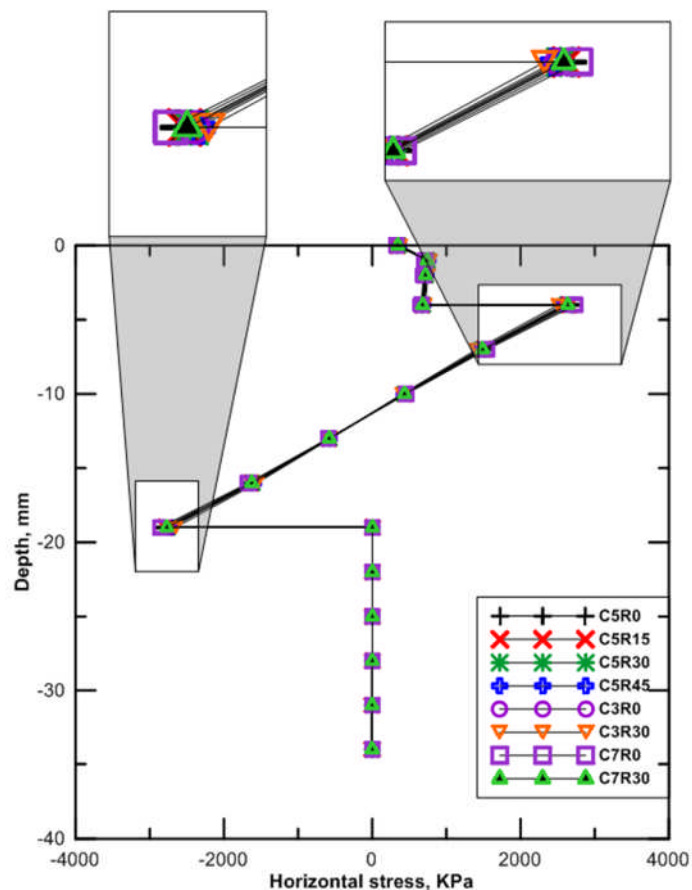


Figure 10.6: Effect of different layer properties on horizontal stresses

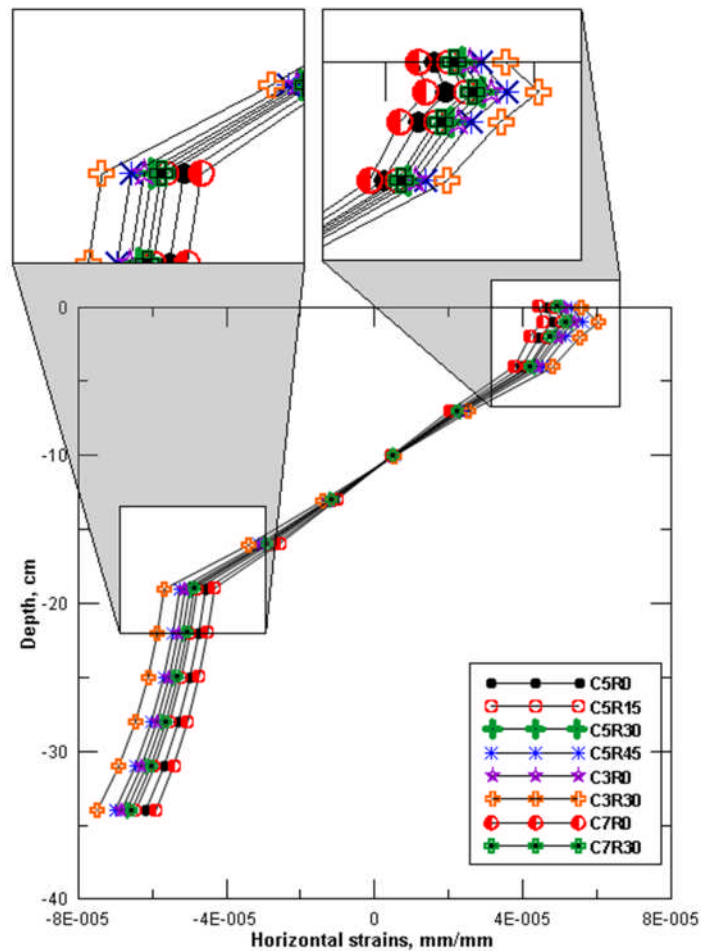


Figure 10.7: Effect of different layer properties on horizontal strains

In the light of this analytical study of the pavement structure, it can be concluded that the reduction in the stiffness of the cemented layer (the main structural element in the pavement structure) increases the horizontal strain at the bottom of the HMA surface layer, decreases in the horizontal stress at the bottom of the layer itself and an increases the vertical strains applied at the top of the subgrade. But the effect of rubber replacement and additional cement ( $> 3\%$ ) is always relatively small. Because the effect of rubber is opposite to the effect of cement, the change in pavement behaviour due to the inclusion of rubber can be offset by greater thickness or more cement so as to keep the same level of strains in the overlaying and underlying layers (surface and subgrade).

### 10.7 Pavement design sensitivity analysis

The effect of rubber replacement level on the CSAM/RCSAM fatigue life is illustrated in Figure 10.8 and Figure 10.9 for 40 mm and 50 mm surface courses, respectively. It can be seen from these figures that, except for the cemented base course of the C5R15 mixture, as rubber content increases the fatigue life of the cemented base course decreases. Practically this means, for the projected design traffic, the required layer thickness increases slightly as the rubber content increases. This, however, can be justified by disposing the waste materials which in turn will reduce the cost of stockpiling and provide a cleaner environment. The layer made from C5R15 presents, approximately, the same performance and hence the same or even less thickness is required.

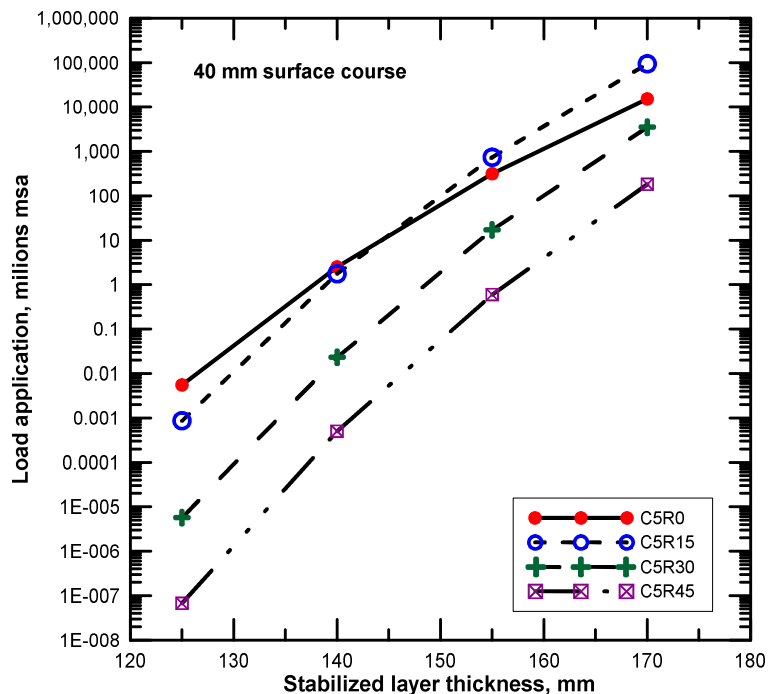


Figure 10.8: Allowable load applications for 40 mm surface course and variable cement-stabilized base thicknesses

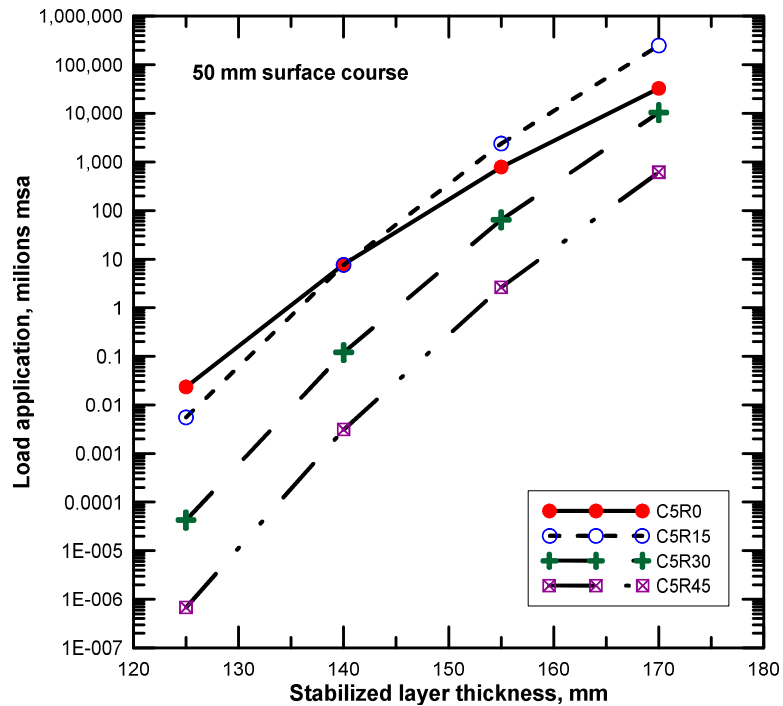


Figure 10.9: Allowable load applications for 50 mm surface course and variable cement-stabilized base thicknesses

Regarding the effect of cement content (Figure 10.10 and Figure 10.11), for the same layer thickness, the rich cement layer has a longer life as compared with those poorly cemented or, in other words, thinner heavily cemented layers can be used for a specific design life as compared to lightly cemented ones. In terms of effect of cementation level on the performance of rubberized mixtures (i.e, CXR30, where X=3, 5 and 7%), it seems that the rubber inclusion reduces the design life of the cemented layers. However, this conclusion is not completely valid for the lightly cementitious materials where the inclusion of rubber improved the design life of these modified mixtures. Furthermore, the thickness of the HMA surface has only a slight effect on the performance of the cemented base. It is noted that in the design figures above some of estimated lives are unrealistically high. These were calculated to demonstrate the behavioural trend only.

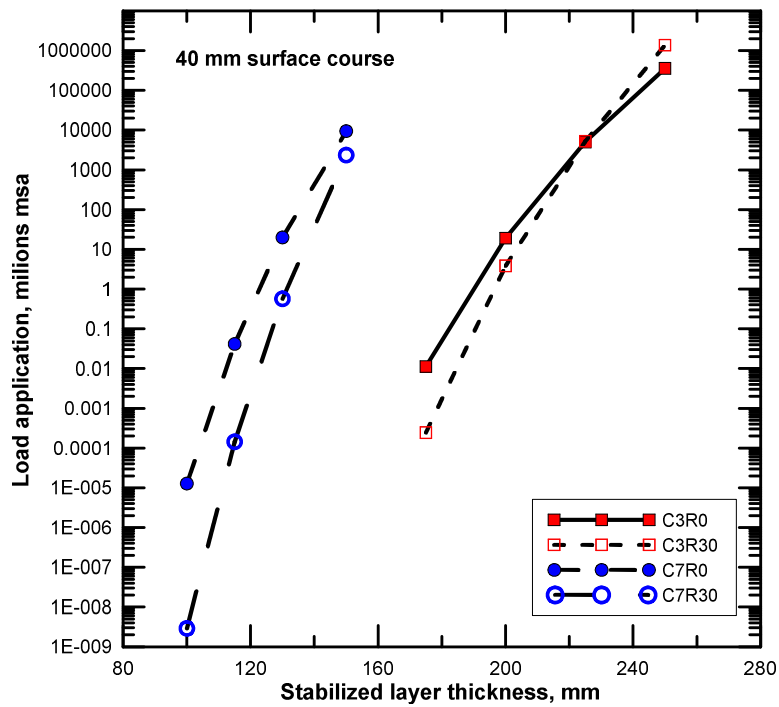


Figure 10.10: Allowable load applications for 40 mm surface course and variable cement-stabilized base thicknesses

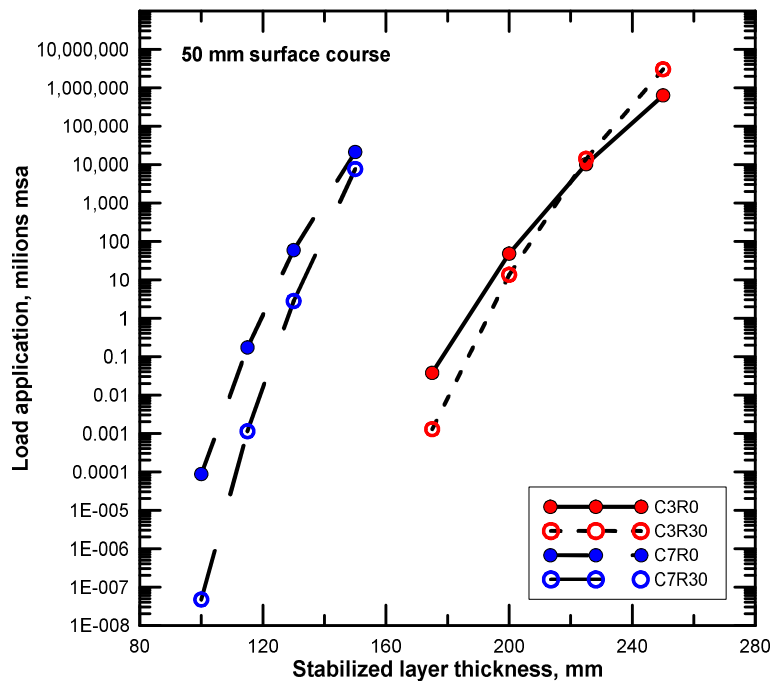


Figure 10.11: Allowable load applications for 50 mm surface course and variable cement-stabilized base thicknesses

### **10.8 Overall discussion regarding pavement design**

As rubber content increases, the fatigue life of the layer in the pavement structure decreases with the exception of the C5R15 mixture (Figure 10.8 and Figure 10.9) for which the fatigue life increases and this increase becomes more significant as the thickness of the layer increases. Even though, for a particular stress, the fatigue life increased (as presented in Chapter 9, Section 9.12) and the stiffness was slightly reduced due to rubber incorporation, there was a drop in the fatigue life of the cemented layer. This is because the reduction in strength overcame the effect of any improvement in fatigue life of the rubberized mixture or of any stress redistribution due to the reduction of stiffness of the modified mixtures. However, this behaviour seems not to be the case for the C5R15 due to the lower reduction in that mixture's strength.

In a similar way, for the same layer thickness, adding more cement improves the design life of the base course layer. This is because the improvement in the strength of the materials results in a decline in the stress ratio and hence an improvement in the design life in terms of fatigue of that layer. For the rubberized cemented layers having light, moderately and heavy cement content, it can be concluded that replacement with rubber has a negative effect on the design life of the modified layer and this effect increases as the cement content increases. This is because, as concluded in Chapter 6, the decrease in flexural strength is more significant for heavily-stabilized materials than for lightly-stabilized ones. Hence, the decrease in the fatigue life in lightly-cemented rubberized mixtures is less significant than in the case of heavily cement-stabilized layers.

In this investigation the three important parameters that help to determine the design life of pavement layers are the stiffness modulus, strength and the fatigue performance. However, for mixtures having different cement contents the fatigue performance was not evaluated. Instead, this fatigue life was estimated based on reference mixture having 5% cement content. Similarly, the transfer function for rubberized cemented mixtures of 5% cement content was adopted to estimate the fatigue life for mixtures of different cement contents. In fact, it is not easy to find in the literature a study about the effect of cement content on the fatigue performance of cement-stabilized aggregate. This may be because the quantity of cement is normally restricted to avoid shrinkage cracking, which may cause only slight differences between cemented layers containing low quantities of cement. This was also concluded by [\(Marradi and Lancieri 2008\)](#) through their study that revealed a slight increase in fatigue performance when 4% instead of 2% cement was added to an aggregate. For soil-cemented mixtures, the Accelerated Load Facility (ALF) testing conducted by [Metcalf et al. \(1999\)](#) revealed that there was a slight increase in fatigue life due to cement content increasing from 4% to 10%. This may be due to microcracking resulting from shrinkage that probably occurs in a highly cemented layer. This may cause a decrease in both strength and fatigue life of the layer. However, these differences have not been included in the computations included in this chapter as the changes in values for the materials studied here are not known and, probably, are small.

### **10.9 Effect of stiffness degradation on pavement analysis and design**

The fatigue life of pavement materials can, in general, be defined as the number of load applications that the materials can sustain at a particular stress/strain level. In addition, in the design of a pavement structure, this level of stress/strain should not exceed the maximum values established, on the basis of the material's strength. Therefore, in the design of a pavement structure, it is traditional to increase the layer thickness to ensure that the calculated pavement responses are sufficiently below their maximum values. In this design approach, as stated by [Oliveira \(2006\)](#), the stress/strain is assumed constant across the fatigue life which is not correct due to the degradation of the material stiffness throughout the pavement's life. It was observed in Chapter 9 that the same level of modulus degradability was achieved after replacement with crumb rubber except in the rich rubber mixture (C5R45). In addition, a considerable degradation occurred in the reference mixtures with low cement contents and even much reduction in the rubberized mixtures with low cementation levels while, on the other hand, less degradation was observed in the case of 5% and 7% cement contents.

Accelerated loading facility (ALF) testing of cemented sections as reported by [Jameson \(2010\)](#) revealed that the modulus of this layer reduced to 10% of its initial value during its fatigue life. In addition, [Theyse et al. \(1996\)](#) also reported a similar reduction value. To take into consideration the effect of modulus degradation or modulus reduction different authors have suggested different procedures.

[Oliveira \(2006\)](#) suggested a cumulative pavement design approach to take the degrading response of the pavement layer into pavement design consideration. This approach was later used by [Kuna \(2014\)](#). Their design calculations, through implementation of the suggested approach, revealed that stiffness reduction causes stress redistribution that results, in turn, in the fatigue life of the layer increasing and hence there is a reduction in the required layer thickness due to the degradation of the layer.

Based on the above conclusion, it seems that the degradability of the layer is a positive phenomenon as far as fatigue considerations are concerned. However, [Oliveira \(2006\)](#) and [Kuna \(2014\)](#) appear to have overlooked the fact that the reduction in the required thickness of the cemented base course will be at the expense of greater requirement in the overlying and underlying layers. This can be explained as follows: fundamentally, if the load is applied on a composite structure, every member in this structure will carry part of that load proportional to its stiffness. This means that the reduction in the stiffness of any member will cause a reduction in the load-carrying capacity of that member. To satisfy the equilibrium condition, this must be accompanied by an increase in stresses/strains in other layers due to the redistribution of stresses. Based on this principle, the reduction in the stiffness of the one particular layer will cause a reduction in the stresses applied to this layer, and hence the stress ratio, which will permit a reduction in the required thickness. This reduction will cause an increase in the horizontal and vertical strains at the bottom and on top of surface course and subgrade, respectively. This, in turn, requires a compensatory increase in the thickness of the surface layer, to bring the stresses and strains in the surface layer back to a permissible value.

It can be concluded that the degradability of the structural pavement layer has a detrimental effect on pavement performance if this not allowed for when designing the layers above or below.

From the above discussion, the following questions arise and need to be answered.

1. To what extent does the degradation of the main structural layer affect the pavement responses?
2. How it is possible to accommodate this phenomenon in pavement analysis and design?
3. Quantitatively, what is the overall impact on design?

An attempt at answering these questions is included in Section 10.10 and 10.11.

### **10.10 Effect of difference between laboratory and field results on pavement design**

In addition to the reduction in the stiffness modulus due to the degradation during cyclic testing, another reduction may occur due to the difference between laboratory and field values of stiffness and strength.

Technically, the transfer functions, which reflect the fatigue behaviour of the mixtures, are normally calibrated by constructing field trial sections to take into consideration the actual fatigue performance. In the previous chapter, a comparison between stiffness moduli resulting from different testing modes showed the typical ranges and values of cement-stabilized aggregate mixtures. However, field results are almost invariably less than those achieved in the laboratory since the latter are normally conducted under controlled conditions (curing, compaction, mixing..., etc.)

which may not be achievable in the field. In addition, shrinkage cracking that may occur after construction may also contribute to reduction in the rigidity of a cemented layer when considered as an extensive sheet rather than as a specimen of small dimensions. For example, laboratory investigation and field trials conducted by (Shahid 1997) revealed that the strengths and stiffnesses achieved in field trials were about two-third of those achieved in the laboratory. Thøgersen et al. (2004) also recommended adoption of a similar difference between the actual and laboratory moduli. Similarly, investigations conducted by the American Portland Concrete Association (PCA) (Scullion et al. 2008) showed that the laboratory stiffness modulus is approximately twice that measured from field cores. Regarding the fatigue life, there was a substantial difference between field and laboratory performance. This difference depends, to a large extent, on the degree of microcracking in the mixture (Jameson and Howard 2012)

To show, quantitatively, the effect of the stiffness reduction on the designed pavement structure comprising a 40 mm surface course ( $E=2800$  MPa), 150 mm CSAM base course (C5R0), 200 mm granular subbase course ( $E=96$  MPa) and soft subgrade ( $E= 50$  MPa), Two cases are considered: firstly, full contact and secondly friction-less interface between pavement layers. It is assumed that the stiffness of the base course gradually decreases and the pavement structure is then reanalysed for each reduction to show its effect on the critical responses. The result of this sensitivity study is illustrated in Figure 10.12 and Figure 10.13 for the above two cases, respectively.

In Figure 10.12, all the new responses were normalized to their initial values before stiffness reduction. As can be seen from the figure, a reduction in the stiffness of the cemented base course to 70% of its original value will result in a decrease in the applied stresses at the bottom of this layer by 25%. This will be accompanied by dramatic increase in the horizontal and vertical strains at the bottom of the surface course and on the top of the subgrade, respectively. These increases are 220% and 180%, respectively. These are both compressive strains. Figure 10.13, on the other hand, shows around 20% reduction in the applied stresses at the bottom of the cemented layer due to the 70% stiffness reduction. In addition, the tensile strain at the bottom of the surface course increased by 30% while an approximate 110% increase in compressive strain occurred on the top of subgrade. In both cases, there is an increase in the compressive strain applied on the subgrade due to the reduction of CSAM base stiffnesses which in turn reduced the load spreading achievable by the rigid layer, as shown in Figure 10.14.

Based on the above discussion it can be concluded that it is not only important to investigate the fatigue performance in terms of the number of cycles to failure, but it is also necessary to observe and monitor the material behaviour throughout the fatigue life to ascertain the accuracy of the pavement design. Secondly, the difference between field and achieved stiffnesses should also be taken into consideration. Neither overestimation nor underestimation of the stiffness modulus of the stiff layer in a composite pavement will ensure a conservative design. For example, if a very low stiffness modulus was assumed during the structural design, this would result in a thinner base layer. Then if the modulus is much bigger than the

assumed value, premature failure would result due to stress attraction to a too-thin layer.

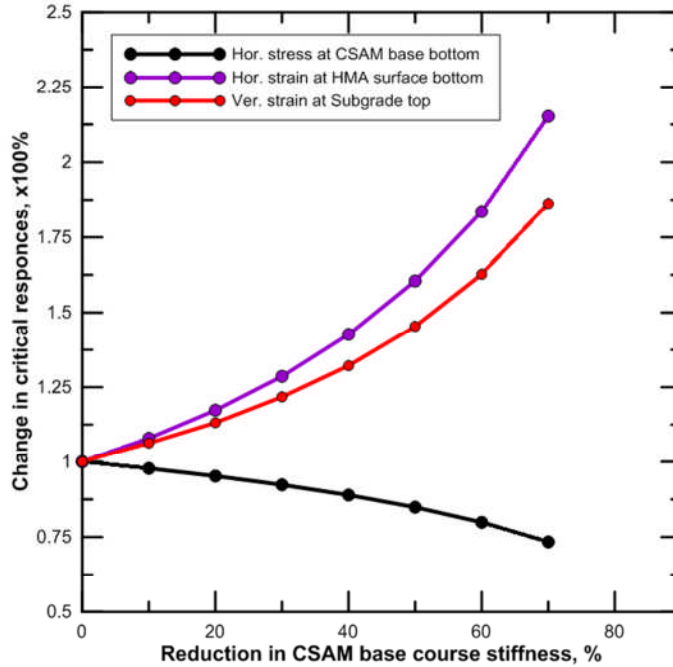


Figure 10.12: Effect of cemented mixture stiffness on pavement critical responses (no bond between layers)

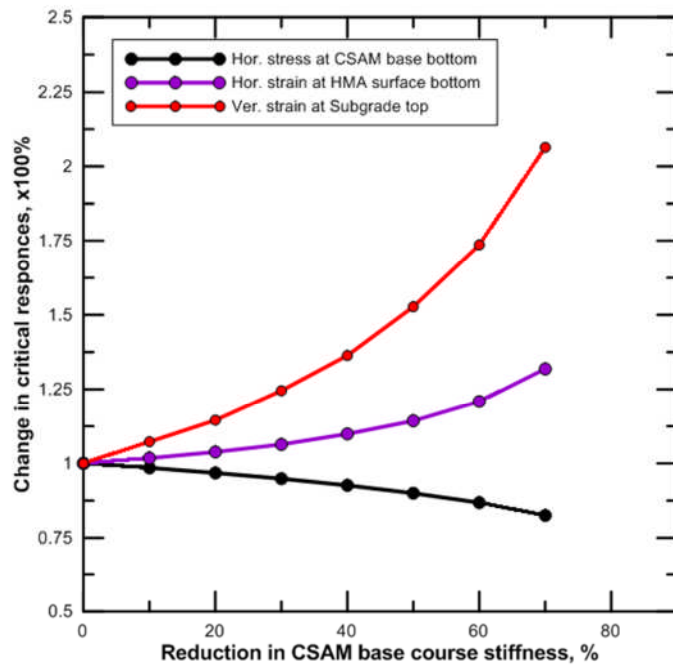


Figure 10.13: Effect of cemented mixture stiffness reduction on pavement critical responses (Fully bonded)

Due to the fact the degradability of the pavement mixtures is different if the test is performed in stress or strain controlled condition, it is recommended to study the degradation of different pavement materials under both stress and strain controlled conditions. This may be beneficial to adjust some adjustment factors to take this parameter in consideration.

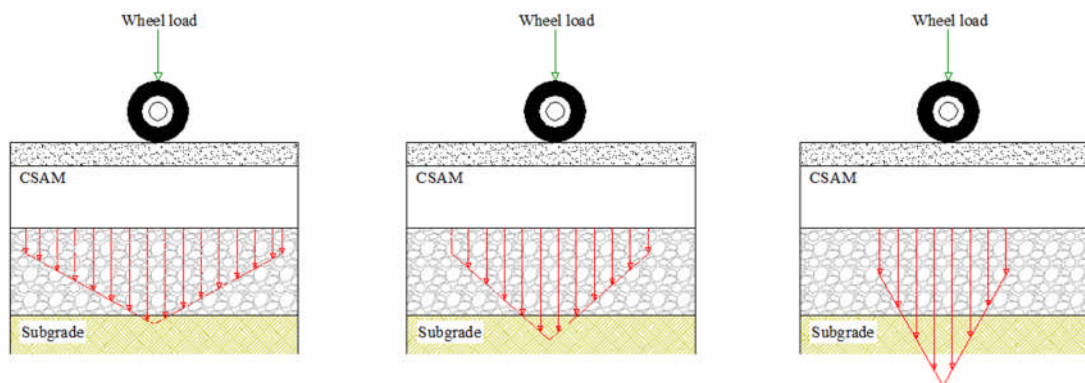


Figure 10.14: Schematic illustration of the effect the cemented base modulus degradation on the stresses applied on the subgrade

### 10.11 Suggested design approach

To accommodate the reductions in stiffness modulus into pavement analysis and design whether due to damage accumulation during the service life or due to the reduction in stiffness resulting from differences between laboratory and field consequential upon shrinkage cracking, the following procedure is suggested. The assumption is that the base layer is the main structural layer in the pavement structure. Firstly, the pavement structure should be analysed with all necessary inputs and the initial dynamic modulus of the cemented layer. Then, the thickness of this layer should be computed based on the calculated stress at the bottom of this layer. After that the pavement structure should be reanalysed with the previously calculated base course thickness and a reduced stiffness of the main structural cement-stabilized

layer, and the necessary asphalt layer thickness computed. Since the adoption of a value of stiffness for the cemented layer at sample collapse (or even slightly before collapse) may be considered to give an uneconomical design, it is suggested that using the stiffness modulus at the end of stage II (Section 9.3.1) would give the appropriate reduced stiffness modulus.

Alternatively, the pavement structure may be analysed using the materials properties with the initial dynamic modulus for the cemented layer as before. Then, the design of all layers should be performed based on the computed responses. After that, reanalyse the pavement structure based on the computed thickness but with the reduced stiffness modulus of the cemented course. Finally, increase the cemented layer thickness until the calculated strains in all other layers are equal to or less than the calculated responses resulted from the first analysis.

An alternative design procedure, to permit consideration of the difference between laboratory and field densities, is as follows. The stiffness of the base course could be measured after construction by a broad, layer-based, graphical method (e.g. the falling weight deflectometer) or by appropriate correlation. Then the thickness of the surface course can be adjusted accordingly so as to maintain the strain level in the asphalt at least as small as in the analysis based on laboratory test values of the cemented layers modulus.

### 10.12 Concluding remarks

1. A slight reduction in the stress induced at the bottom of the cemented layer was observed due to rubber incorporation. This suggests that the replacement of natural aggregate by crumb rubber does not have significant effect on load attraction by the modified cemented layer.
2. It seems that the reduction in a materials' strength due to rubber incorporation over-rides any improvement in layer performance due to the material's fatigue life increase even allowing for a slight reduction in the material's stiffness. However, this was not the case for the mixtures manufactured with the lowest rubber content i.e., C5R15. Adding rubber may, however, be justified if the change in the cracking pattern and the probable improvements in the durability of the mixtures are taken into consideration. These two factors are not included yet in the mechanistic-empirical pavement design guide.
3. Large volumes of crumb rubber extracted from waste tires can be consumed in a pavement structure construction provided that additional cement is used. This increase in the cementation level will compensate for the reduction in the strength due to replacement with the crumb rubber. However, the shrinkage cracking, usually accompanying high cement content, and the difficulties in compaction should be taken into consideration.
4. The design should consider the reduction of the stiffness modulus of the main structural layer (cemented base course) either from degradation during service or due to difference between laboratory and the field conditions. The degradation is

more obvious in the case of low cement content mixtures. Ignoring this issue will result in applying more stresses/strains to the underlying and overlying layers for which they may not be designed.

5. A design approach is suggested to accommodate the above issue which may ensure accurate estimation of layer thicknesses in such a way as to ensure all critical stresses may still lie within limits.
6. It is recommended to analyze the CSAM layer after crack development by modeling the cracks with appropriate calculated load transfer stiffness based on the estimated VSTR.
7. It is recommended to conduct an economic study (after collecting sufficient data regarding the cost of disposing, stockpiling, ..., etc.) to investigate whether the increased thickness of the layers in which the rubber was included will be feasible and economical, as compared with the reference mixture, or not.

### 10.13 References

- Brown, S. F. (2012). "An introduction to asphalt pavement design in the UK." Proceedings of the ICE-Transport 166(4): 189-202.
- Hadi, M. N. and B. Bodhinayake (2003). "Non-linear finite element analysis of flexible pavements." Advances in Engineering Software 34(11): 657-662.
- Huang, Y. H. (2004). Pavement analysis and design, Second edition, Prentice Hall Publishing company, 792 pages.
- Jameson, G. (2010). Towards the revision of Austroads procedures for the design of pavements containing cemented materials.
- Jameson, G. and A. Howard (2012). Preliminary investigation of the influence of micro-cracking on fatigue life of cemented materials.
- Kuna, K. K. (2014). Mix design considerations and performance characteristics of foamed bitumen mixtures. PhD, The University of Nottingham.
- Lav, A. H., M. A. Lav and A. B. Goktepe (2006). "Analysis and design of a stabilized fly ash as pavement base material." Fuel 85(16): 2359-2370.
- Marradi, A. and F. Lancieri (2008). Performance of cement stabilized recycled crushed concrete. First International Conference on Transport Infrastructure ICTI, Beijing, China.
- Metcalf, J., S. Romanoschi, Y. Li, M. Rasouljan, M. Hossain, S. Romanoschi, A. J. Gisi, D. S. Gedafa, S. A. Romanoschi and M. Portillo (1999). The First Full-Scale Accelerated Pavement Test in Louisiana: Development and Findings. CD-ROM), Proceedings of the First International Conference on Accelerated Pavement Testing, Reno, Nev.
- Oliveira, J. R. M. d. (2006). Grouted macadam: material characterisation for pavement design. PhD Thesis, University of Nottingham.

Scullion, T., J. Uzan, S. Hilbrich and P. Chen (2008). "Thickness design systems for pavements containing soil cement bases." PCA R&D Serial(2863).

Shahid, M. A. (1997). "Improved Cement Bound Base Design for Flexible Composite Pavement." PhD Thesis, University of Nottingham.

Theyse, H. L., M. De Beer and F. C. RUST (1996). "Overview of South African Mechanistic Pavement Design Method." Transportation Research Record: Journal of the Transportation Research Board Volume 1539

Thøgersen, F., C. Busch and A. Henrichsen (2004). "Mechanistic Design of Semi-Rigid Pavements - An Incremental Approach." Report 138, Danish Road Institute.

## **Chapter Eleven**

### **Conclusions and Recommendations**

#### **11.1 Introduction**

Mitigation of the environmental issues related to end-of-use tires, contribution in saving the natural resources and modification of the properties of cement-stabilized aggregate mixtures for possible reduction of the shortcomings of cement stabilization are the main three motivations behind this investigation. This research was undertaken to characterize, at macroscale and mesoscale levels, the behaviour of the cement-stabilized aggregate mixtures modified with different rubber contents and to investigate the effect of degree of combined rubberization and stabilization under different modes of static and dynamic loading. In addition, it was also intended to

study the internal structure of these modified mixtures, at mesoscale level, to better understand the mechanism of their failure. This was conducted by developing, suggesting and implementation different testing equipment, methodologies and tools and using them to evaluate the pavement design-related properties and then using them in a pavement analysis and design study to understand the effect of modified layers on the pavement responses and design.

The big picture conclusions drawn based on the analysis of the research findings are presented in Section 11.2. The important conclusions on the basis of individual chapters are grouped into different investigation areas conducted in this study and presented in Sections 11.3 to Section 11.9.

## **11.2 Main Conclusions**

Rubber can be used in the construction of cement-stabilized aggregate mixtures. However, this should be added in small quantities to avoid the difficulties and the need for more compaction which combined with the low specific gravity will reduce the density and strength accordingly. This, in turn, demands more pavement thickness.

Rubber addition reduced compressive strength and tensile strength (both indirect tensile and flexural). At the same time, this modification slightly reduces the stiffness modulus of the modified later. Despite the larger reduction in the material's stiffness once the rubber was added, such modification caused less reduction in the materials strength at low cement content. This reduction was found to be governed by the void-

like behaviour which depends on the relative stiffness between the rubber particles and the surrounding matrices of different cement contents. Since the pavement design is more affected by strength than by stiffness, accordingly, using the rubber in the poorly cemented mixtures would be more useful than in highly cemented ones. Ignoring the probable shrinkage that accompanies high cement content, it is possible to both reduce the thickness of cemented mixtures and keep disposing of waste tire rubber by using more cement.

Cracking investigation utilizing visual inspection of the cracking pattern of the failed samples, 3D fractured surfaces through photogrammetry and the 2D surface crack utilizing the fractal analysis procedure, revealed that addition of rubber modifies the cracking behaviour of the rubber-modified mixture. Cracks (after rubberization) became more tortuous, widely separated and narrow. This will strongly relieve and overcome the reflection cracking due to the reduced stresses generated at less-width cracks. These cracks may develop at a slower rate than in un-rubberized mixtures since the modified mixtures tend to absorb more energy before failure.

Regarding the behaviour under cyclic loading, the modification with rubber has a positive effect on the fatigue life at all investigated cementation levels. The mechanism behind this enhancement seems to be the same that resulted in toughness improvement. The degradability is not affected by rubber addition. However, both reference and rubberized mixtures showed greater degradability at lower stabilization degree.

A study of the amount of rubber on the flexural-induced fractured surfaces, and of the internal structure of the ITS-failed samples, showed that the mechanism of failure of the rubberized mixtures involved preferential propagation of cracks through, or around, the rubber particles. This behaviour was observed at all cement contents.

Quantitative evaluation of the rubber distribution revealed broadly uniform rubber distribution. However, the rich rubber mixture showed a larger degree of non-uniformity in rubber distribution which further confirms the conclusion just mentioned above regarding the undesirability of using high rubber content. Uniform rubber distribution indicates that rubber *distribution* has no effect on the strength reduction. Propagation of the cracks through rubber particles contributed (especially at microcracking level) to the delay and lengthening of the crack propagation which, in turn, improved the toughness under static loading and prolonged the fatigue life of the mixtures. These improvements in rubber-modified mixtures' toughnesses and fatigue lives were observed at all investigated cement contents.

Analytical study and experimental results showed that the reduction in strength due to rubberization overcame the improvement in stiffness and fatigue life. However, the lowest rubber mixture showed similar or better behaviour to that of the comparable un-rubberized mixtures.

Lastly, regarding techniques, methodologies and tools developed in this study, it can be concluded that:

- The manufacturing procedure showed a high degree of consistency.

- The NAT machine and the suggested methodology can be used to characterize cement-stabilized mixtures.
- Fractal analysis was found to be a useful tool to discriminate between different cracking patterns and to judge roughly the fracture energy of cement-stabilized mixtures.
- Photogrammetry procedures form an important tool to study the fractured surfaces which in turn can be used to investigate the three dimensional cracking response and to estimate the load-transfer efficiency in advanced analytical studies.
- The cyclic loading facility together with the selected instrumentation system was found to be adequate to study, comprehensively, the fatigue behaviour of cemented mixtures and to estimate the dynamic flexural modulus.
- Utilization of the suggested fatigue testing methodology incorporating nondestructive testing proved its effectiveness in accurately evaluating the fatigue behaviour by reducing data scatter.

### **11.3 Conclusions related to mix design and sample preparation**

1. The reduction in the density of the cement-stabilized aggregate mixtures is partly because of the lower density of the rubber particles as compared with the natural aggregate and partly due to reduced compaction efficiency due to the damping or high elasticity of the crumb rubber particles. This suggests avoiding high rubber replacements.

2. The cement strengthening mechanism comes from the binding effect due to cement hydration and from enhancement of the mixture compactibility due to its filling action.
3. It is possible to use the experimental porosity method (used normally for concrete mixtures) to evaluate the compacity of the cement-stabilized aggregate mixtures provided that 5% cement content or more is used. However, for lower cement content this method underestimates the compacity of the mixture. This can be used as an indirect method to judge the bond nature between the aggregate and surrounding materials.
4. Comparison between different manufactured samples (small cylinders, big cylinders and prisms) proved that the manufacturing method of cement-stabilized aggregate mixtures produced uniform densities. This permits reliable comparison between different mixtures' properties and use of correlations to estimate the advanced test results from the results of simple tests.

#### **11.4 Conclusions related to static mechanical characterization**

1. There was a reduction in unconfined compressive, indirect tensile and flexural strengths when adding crumbed rubber. This reduction is due to the low strength and stiffness of the rubber particles and due to the reduction in the achieved density. From the strength point-of-view, the addition of rubber affects the pavement design detrimentally. This, in turns, means a need for a thicker pavement. However, other factors like stiffness and fatigue performance must also be considered.

2. Increasing cement content improves the strength of reference and rubberized mixtures. However, the behaviour of rubberized cement-stabilized mixtures is governed by the relative stiffness between rubber particles and the surrounding materials. This was observed through different testing methods. At low cement contents, the reduction in the strength, due to rubber incorporation, is less than that at higher cement content. This is due to the higher relative stiffness which makes rubber particles behave like voids in the latter case and hence leads to more stress concentrations. Therefore, from the strength point of view, replacement of natural aggregate by crumb rubber is more feasible at low cement contents.
3. Comparison with the previously suggested correlations revealed that the relationship between compressive and tensile strengths seems not affected by aggregate composition or degree of cementation of these mixtures.
4. Rubberization of cement-stabilized mixtures has a positive effect on the toughening of these mixtures. Two mechanisms are behind toughness improvement: first, through delaying the crack propagation by stress relief at the crack tip. Secondly, through lengthening of the crack path. This improvement was observed and evidenced at all cementation levels.

### **11.5 Conclusions related to fracture pattern, internal structure and mechanism of failure**

1. Regarding the failure patterns, the rubberized mixtures showed, during different testing modes, ductile behaviour as compared with the brittle behaviour of the

reference mixtures. In addition, high integrity and narrow cracking was also observed in case of rubberized mixtures. This behaviour is more obvious at 5% and 7% cement content. This suggests the addition of rubber may mitigate the detrimental cracking pattern of the cementitious materials having higher cement content.

2. Inclusion of rubber increases the fractal dimension of the cement-stabilized mixtures which indicates, based on the analysis of surface crack, more dissipated energy during the fracture of these mixtures.
3. Internal structure observations at mesoscale level of the failed samples from indirect tensile testing and quantification of the rubber quantity through flexural-induced fractured surfaces indicated that the failure mechanism of this type of mixture is by preferential propagation of the cracks through or around the edge of the rubber particles. This mechanism is valid at all levels of cementation.
4. Characterization of the fractured surface revealed an increase in the crack roughness and tortuosity and greater VSTR in the case of rubberized mixtures as compared with the reference mix. However, the rubber distribution plays an important role in the variation between different mixtures. This also demonstrates the reason for less brittle mixtures. From the point-of-view of load transfer efficiency (through cracks) it can be said that rubber incorporation has a beneficial effect on this efficiency.
5. Quantitative analysis, through intensive X-ray scanning and image analysis, of the internal structure indicated uniform rubber distribution both vertically and

radially for all replacement levels. However, less uniformity was observed in the case of the richest rubber mixture.

6. Based on the mechanical characterization results it can be suggested that, in rubberized cement-stabilized aggregate mixtures, the cracks start and propagate through or around the edge of the rubber particles. The cracks attractiveness to the rubber particles comes from higher relative stiffness between these soft particles and surrounding stiff medium. This mechanism was evidenced and proved based on internal structure investigation at mesoscale level, fractal analysis, quantitative study of fractured surfaces and quantification of rubber on the fractured surfaces. These were conducted by studying the failed samples under indirect tensile and flexural testing methods.
  
7. The mechanism of fatigue improvement is due to the rubber particles delaying the crack propagation, especially at the microcracking level, by absorbing and relieving the stress at the crack tip and by lengthening the crack path. For this reason, it was observed that the fatigue life, at lower stress ratio, improved since the microcracks grew slowly which permits absorbance and relief of the stresses, and the crack took a longer path which was evidenced by more accumulated permanent deformation.

### **11.6 Conclusions related to nondestructive testing of cementitious materials and comparison with static and dynamic testing**

1. Ultrasonic pulse velocity dropped noticeably as a result of rubber incorporation. In addition, both modulus of elasticity and shear modulus,

measured through resonant frequency, declined due to rubber incorporation. Taken together, this reveals the importance of the aggregate composition and degree of stabilization on the performance as measured by nondestructive testing.

2. Increasing the curing period has a positive effect on both reference and rubberized cementitious materials. This indicates that the inclusion of rubber particle does not have a detrimental effect on the strength development.
3. Incorporation of rubber particles reduces the stiffness of cement-stabilized mixtures for all cement contents. However, a larger drop was noticed at 3% cement content whereas less reduction occurred at 5% and 7% cement contents. This suggests, from a stiffness point-of-view, that the inclusion crumb rubber is more beneficial at 5% and 7% cement contents since, at these cementation levels, the stress attraction by the cemented layer may not be greatly affected by rubber inclusion since the latter has less impact on the stiffness modulus.
4. Comparing different stiffness modulus characterization methods (destructive vs. nondestructive) and modes (flexural vs indirect tensile and static vs dynamic) showed that the resonant frequency testing method may be adopted to estimate the dynamic modulus of elasticity accurately, economically and simply for pavement analysis in mechanistic empirical pavement design procedures.

### **11.7 Conclusions related to fatigue testing facility and characterization tests and techniques**

1. The developed fatigue testing facility was found to be adequate to characterize the fatigue performance of the cementitious materials. Comparison between instrumentation setups, by comparing the developed facility results with other methods, indicates that on-sample instrumentation provided more accurate results.
2. Fractal analysis was observed as a good tool for evaluating the cracking patterns and fracture energy of cement-stabilized mixtures. This was able to discriminate between different mixtures at different rubber contents. It seems that the fractal analysis in terms of fractal dimension is more sensitive to aggregate composition than to cement content.
3. Innovative utilization of photogrammetry techniques proved to be a reasonable and accurate means of acquiring measurements of fractured surfaces.
4. Utilization of the NAT machine can be considered as an efficient method to characterize cement-stabilized mixtures under dynamic load conditions. However, adoption of the asphaltic mixtures procedure is inaccurate for characterization of cementitious materials. Instead, the methodology and procedure suggested in this study can be used to ensure proper characterization of CSAMs and RCSAMs.
5. Characterization of the internal structure of the rubberized cement-stabilized aggregate mixture through X-ray scanning, combined with the image processing

technique, was found to be an effective tool to study and differentiate between different mixtures in terms of crack propagation and rubber distribution.

6. The suggested methodology for estimating the actual flexural strength utilizing the nondestructive testing was found to be very useful, accurate, cost-effective and simple.
7. The higher sensitivity of nondestructive characterization methods to the small changes in the mixtures' internal structures, due to aggregate composition change and degree of stabilization, indicates those methods' suitability to characterize such mixtures, especially in the light of their comparable results to destructive testing.

### **11.8 Conclusions related to fatigue performance and pavement analysis and design**

1. From a fatigue life prospective, incorporation of crumb rubber in cement-stabilized aggregate has a positive impact. This behaviour is observed at all investigated cement contents under stress ratios of lower than 85%. This improvement is accompanied by increasing the permanent deformation.
2. Implementation of the dissipated energy approach to identify the fatigue failure life and comparison with fatigue life, estimated on a full collapse basis, revealed no significant difference between the two approaches regardless of rubber content or degree of cementation.

3. Combining the experimental program analysis results with the pavement analysis and design procedures revealed that the reduction in strength overcomes all other enhancements resulting from either fatigue life increase or reduction in the layer stiffness modulus. However, this is not the case for a base course manufactured from C5R15 (a mixture contains 5% cement content and 15% replacement of the 6 mm natural aggregate fraction size) where the improvement of the fatigue life compensates the strength reduction.
4. The degradability of the stiffness modulus should be considered in pavement analysis and design since ignoring this phenomenon will accelerate pavement failure due to the application of additional stress/strains on underlying and overlying layers as stress is less attracted to the cemented layer resulting from its stiffness degradation.
5. Replacement of natural aggregate by the crumb rubber does not have an effect on degradability of the modified cemented mixture. However, the rich rubber mixtures showed slight degradation across the fatigue life. On the other hand, large degradation was observed in the poorly cemented mixtures as compared with mixtures having moderate and high cement contents.

### **11.9 Recommendations for future research**

Due to the limited time and resources available for this study, some research areas need more investigation to validate the use of crumb rubber extracted from waste tires within cement-stabilized aggregate layers. These can be summarized as follows

1. It is suggested to investigate the durability of the modified mixtures under different testing protocols to ensure that the effect of both rubber and cement, and their combination, is understood.
2. Investigation of the fatigue performance of rubberized mixtures under other cement contents (i.e., 3% and 7%) will be of great importance so as to identify the most suitable degree of stabilization for rubberized cement-stabilized mixtures.
3. It is recommended to construct a trial pavement section or large scale experiment to evaluate the in-situ performance of a flexible pavement structure containing rubberized cement-stabilized base course. Such a study will be useful for evaluating site construction, nature of cracking and evaluating the load-transfer efficiency across the cracks after their formation.
4. It is suggested to investigate the effect of stress ratio and loading frequencies on the flexural dynamic modulus of cemented mixtures with different cement and rubber contents. This may show to what extent the stiffness moduli of the mixtures having different aggregate composition and cement content are affected by the frequency or by the stress ratio.
5. Since the present study was limited to one aggregate type and gradation, it is recommended to study other aggregate types and gradations, as well as other rubber types and gradations, to better understand the effect of the interaction between aggregate type and gradation with rubber replacement.

6. Studying the second phase of rubberized mixtures' performance after failure is important to understand the effect of rubber on the behaviour of this layer after transferring from acting as fully bound to a fragmented layer.
  
7. It is suggested to investigate the effect of rubber incorporation on the shrinkage characteristics of cement-stabilized aggregate mixtures.

## Appendix A

### Vertical deformation histories under cyclic loading

The vertical deformation histories under cyclic loading, described in Chapter 9, for different investigated mixtures are presented in Figure A.1 through Figure A.18

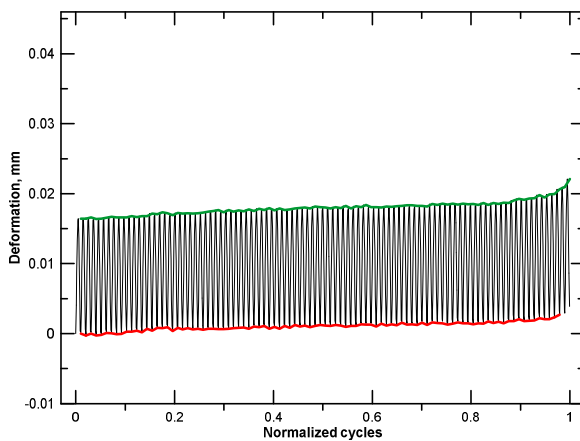


Figure A.1: C5R0@90% stress ratio

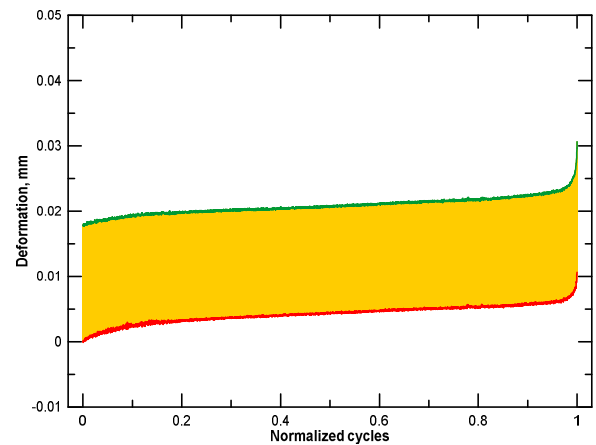


Figure A.2: C5R0@85% stress ratio

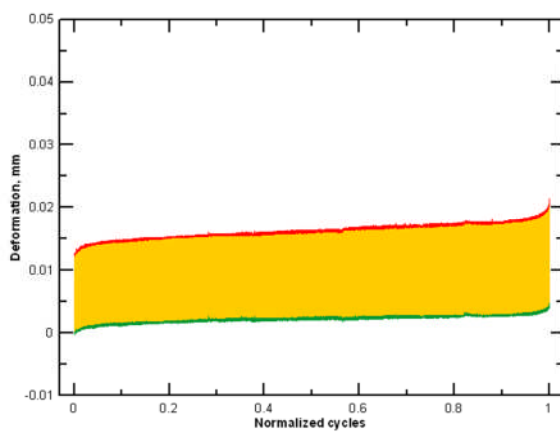


Figure A.3: C5R0@80% stress ratio

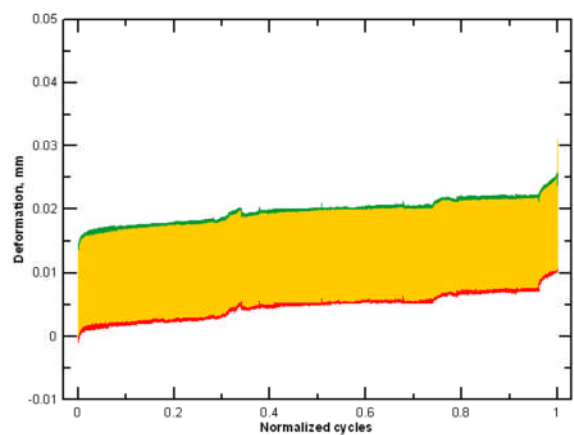


Figure A.4: C5R0@75% stress ratio

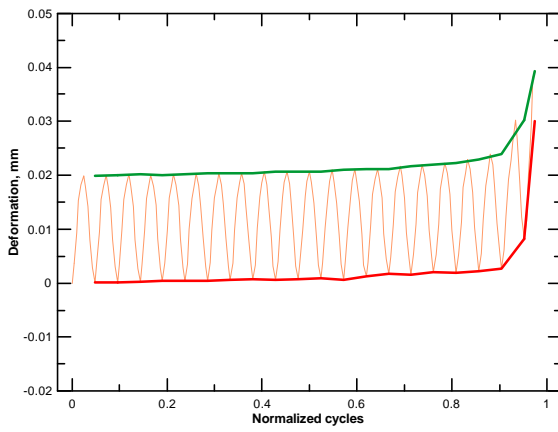


Figure A.5: C5R15@90% stress ratio

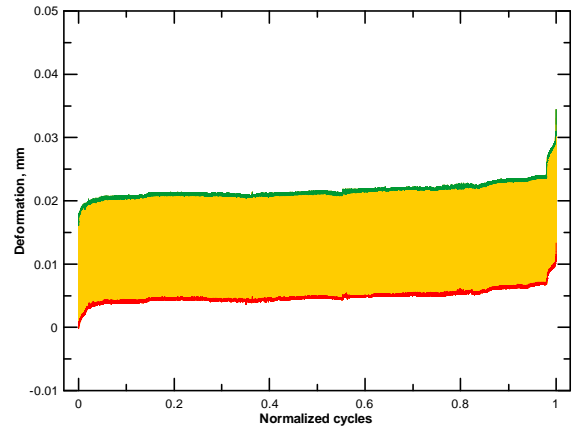


Figure A.6: C5R15@85% stress ratio

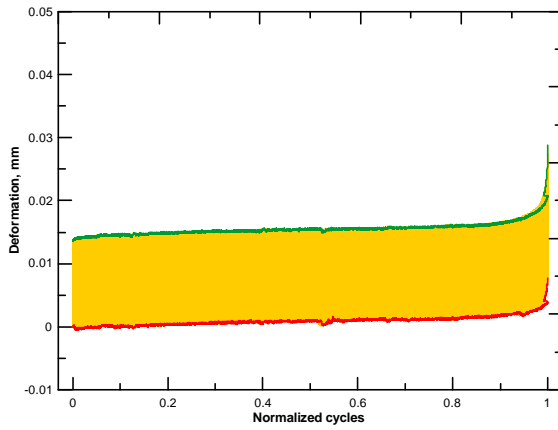


Figure A.7: C5R30@90% stress ratio

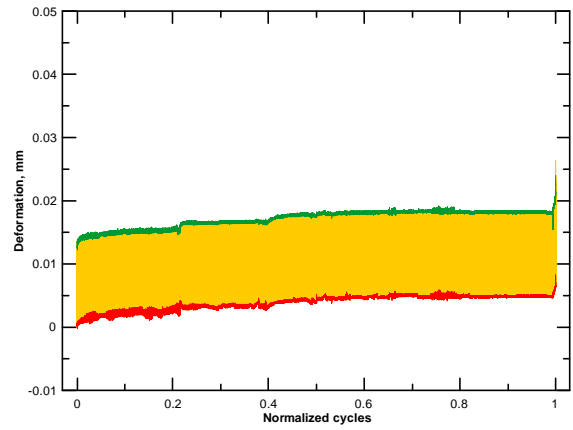


Figure A.8: C5R30@85% stress ratio

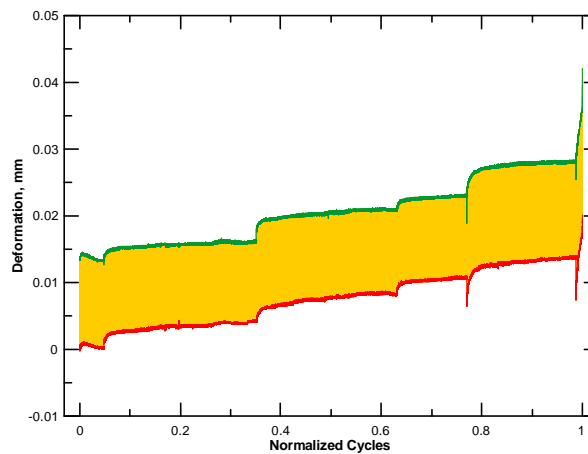


Figure A.9: C5R30@80% stress ratio

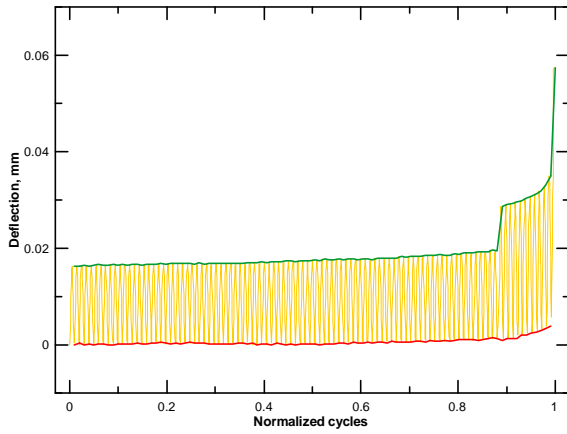


Figure A.10: C5R45@90% stress ratio

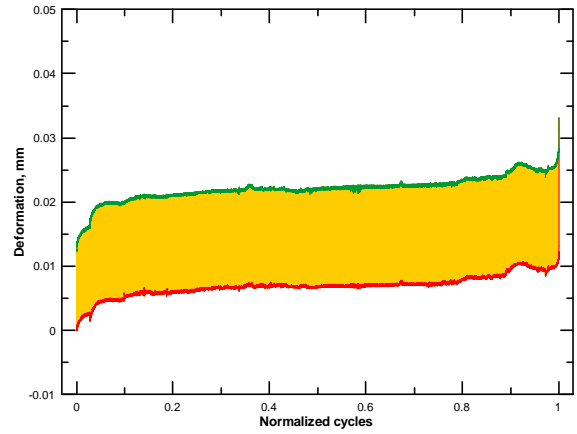


Figure A.11: C5R45@85% stress ratio

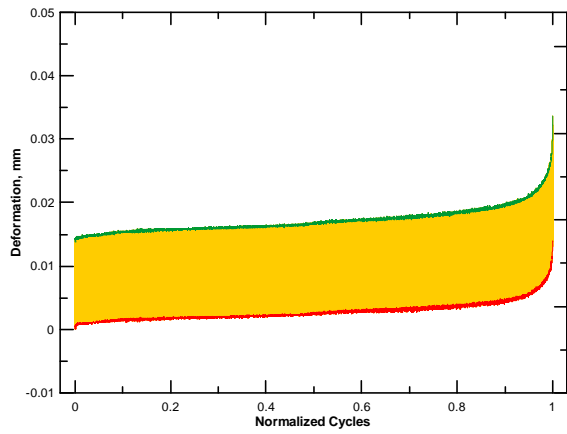


Figure A.12: C3R30@90% stress ratio

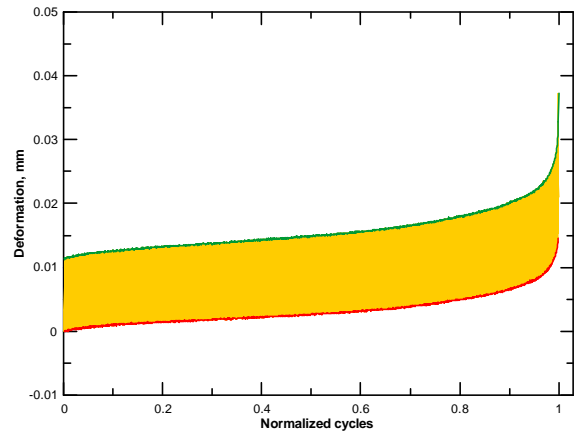


Figure A.13: C3R30@85% stress ratio

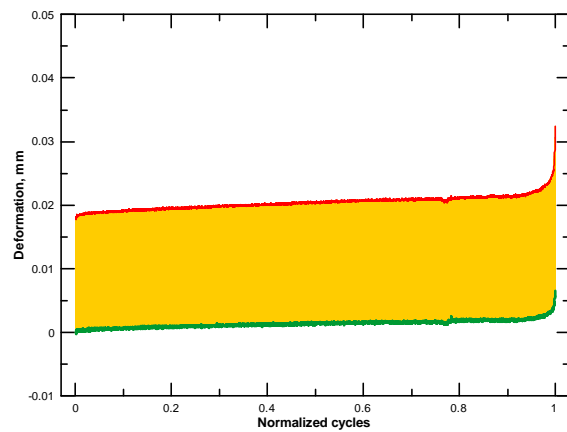


Figure A.14: C7R30@90% stress ratio

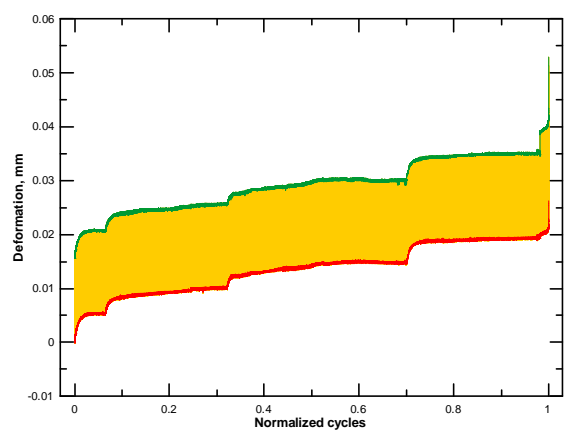


Figure A.15: C7R30@85% stress ratio

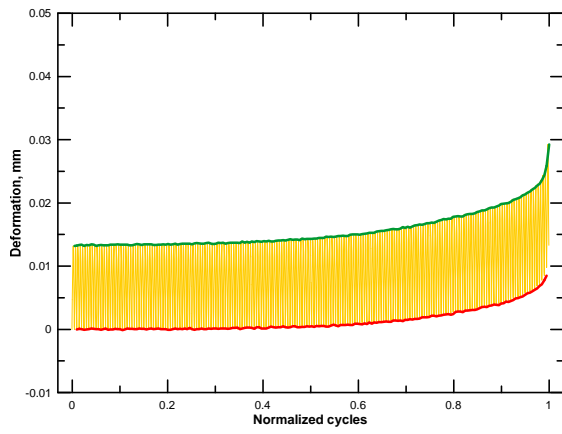


Figure A.16: C3R0@90% stress ratio

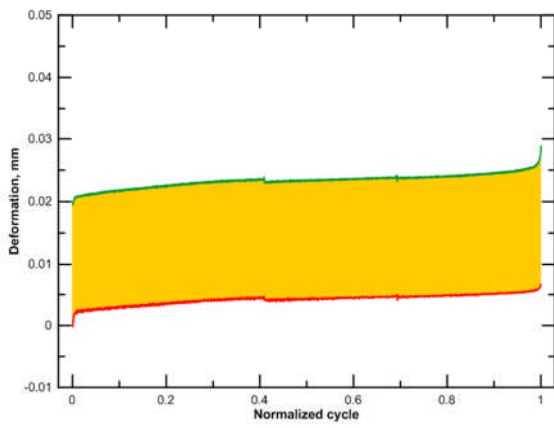


Figure A.17: C7R0@90% stress ratio

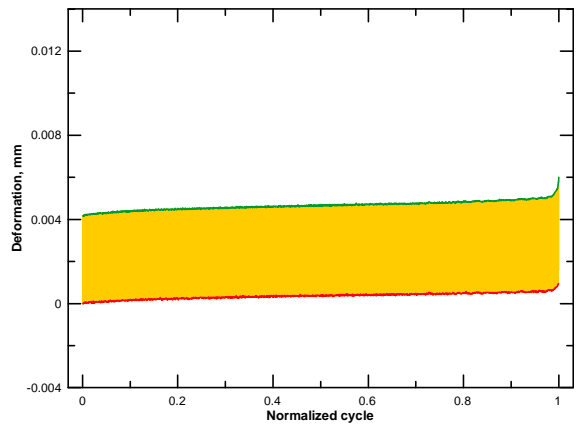


Figure A.18: C7R0@85% stress ratio

## Appendix B

### Load-deformation hysteresis loops

The load-deformation hysteresis loops for different investigated mixtures are presented in Figure B.1 through Figure B.17

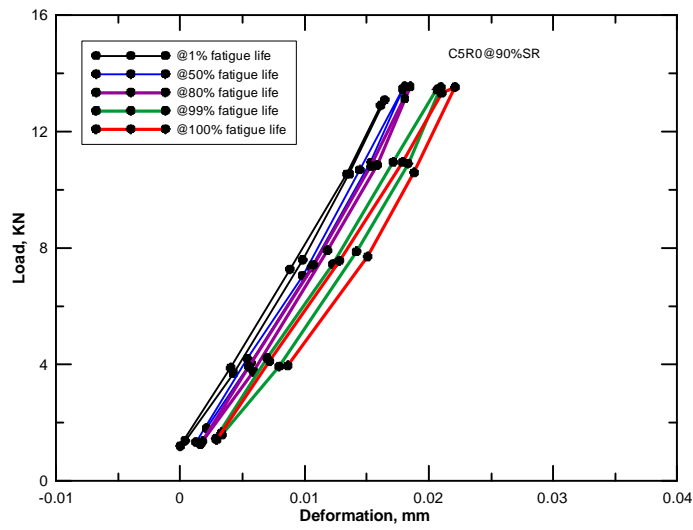


Figure B.1: C5R0@90% stress ratio

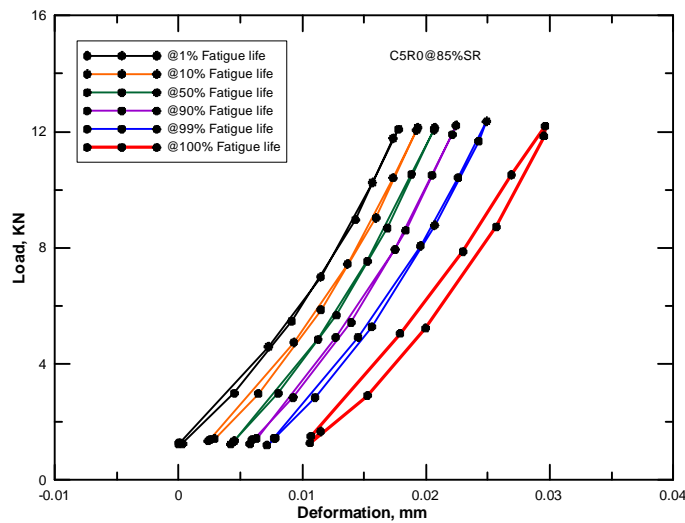


Figure B.2: C5R0@85% stress ratio

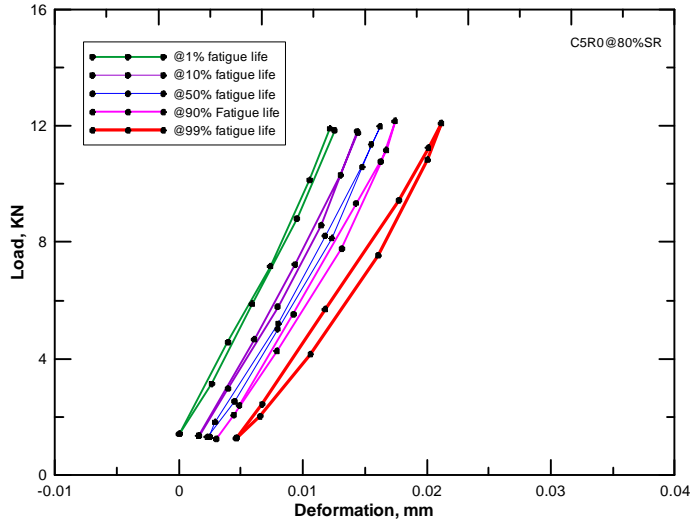


Figure B.3: C5R0@80% stress ratio

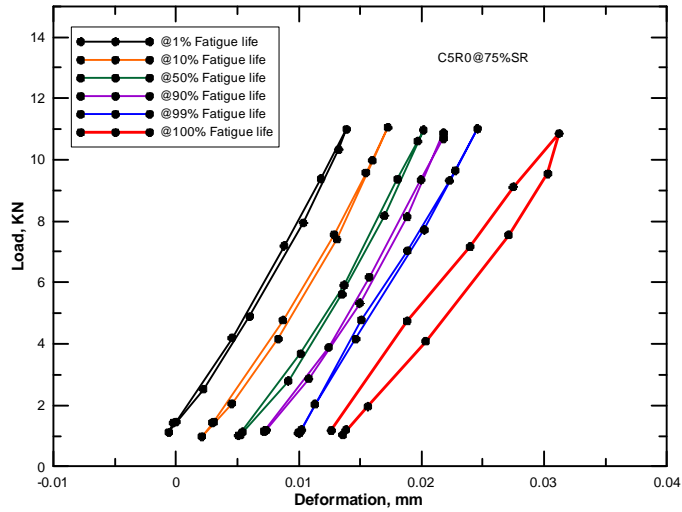


Figure B.4: C5R0@75% stress ratio

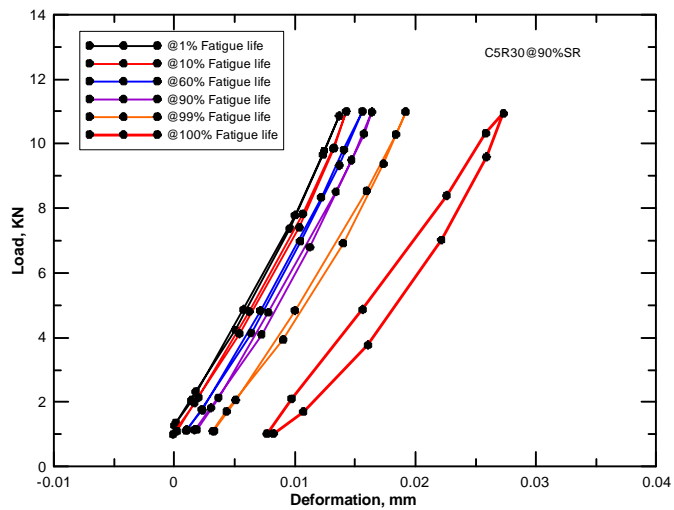


Figure B.5: C5R30@90% stress ratio

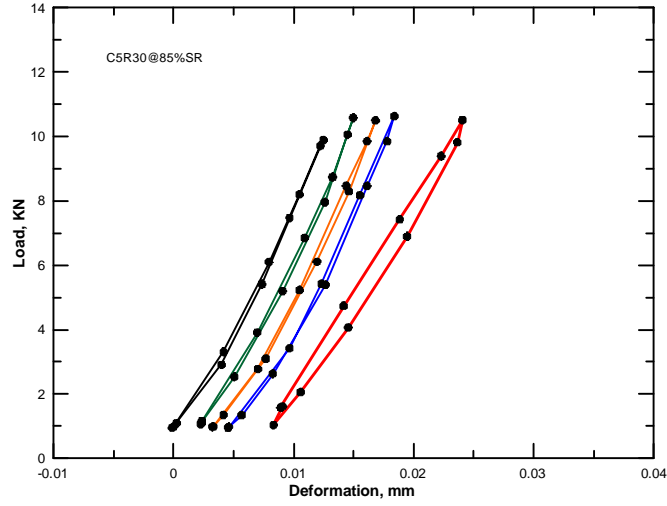


Figure B.6: C5R30@85% stress ratio

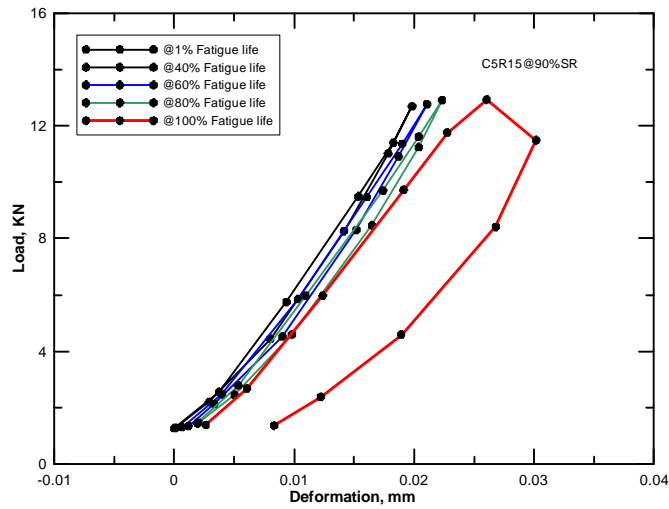


Figure B.7: C5R15@90% stress ratio

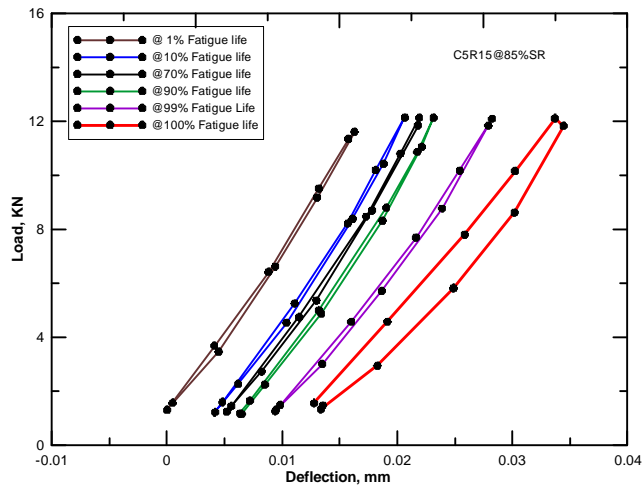


Figure B.8: C5R15@85% stress ratio

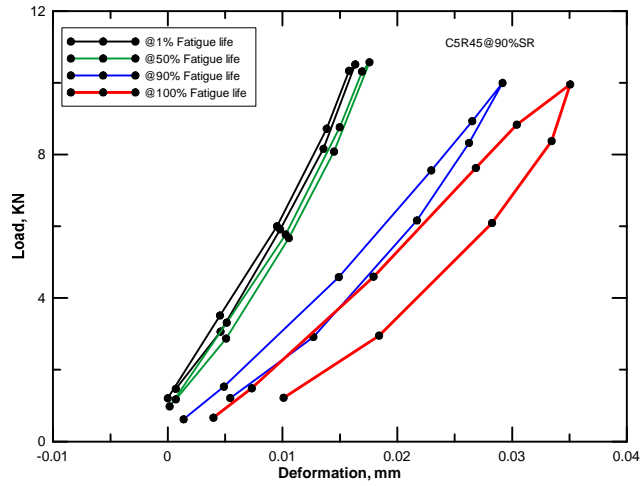


Figure B.9: C5R45@90% stress ratio

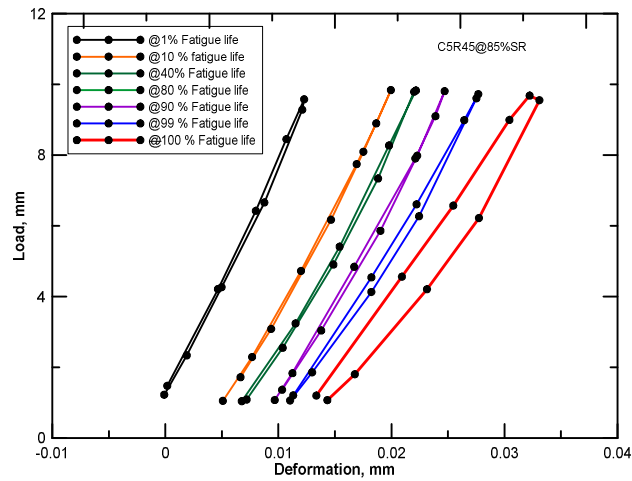


Figure B.10: C5R45@85% stress ratio

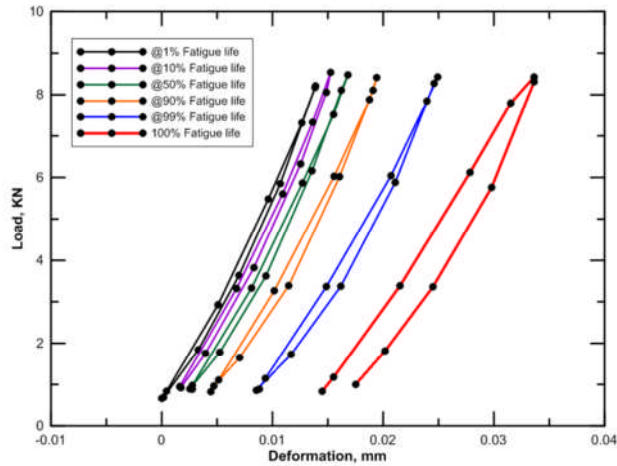


Figure B.11: C3R30@90% stress ratio

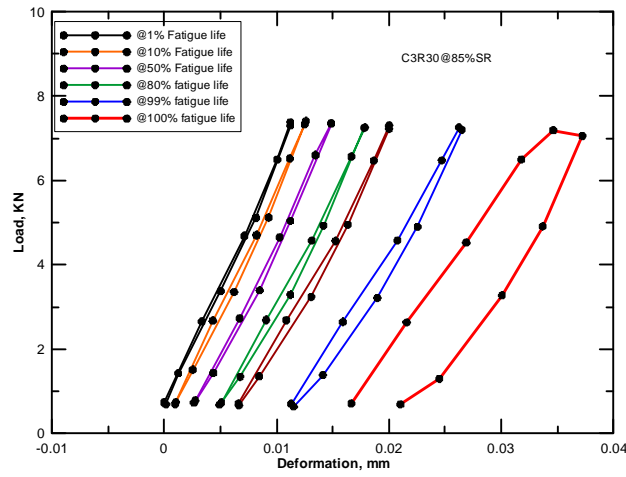


Figure B.12: C3R30@85% stress ratio

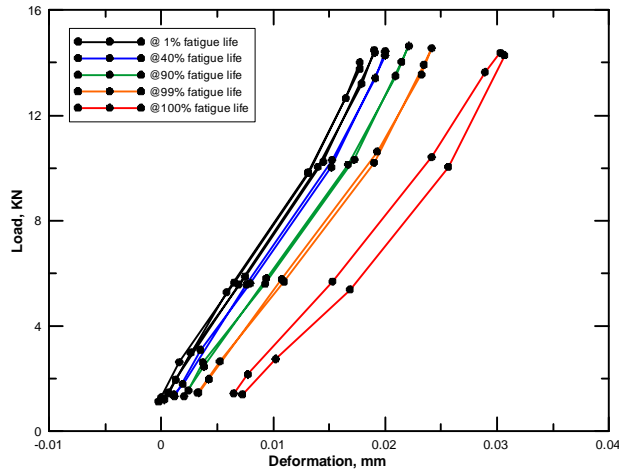


Figure B.13: C7R30@90% stress ratio

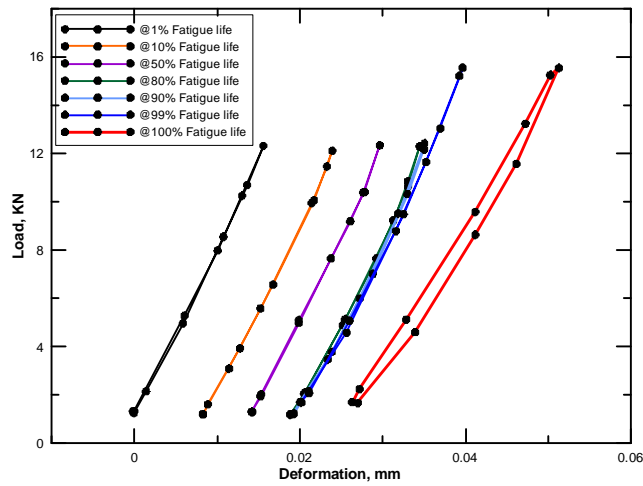


Figure B.14: C7R30@85% stress ratio

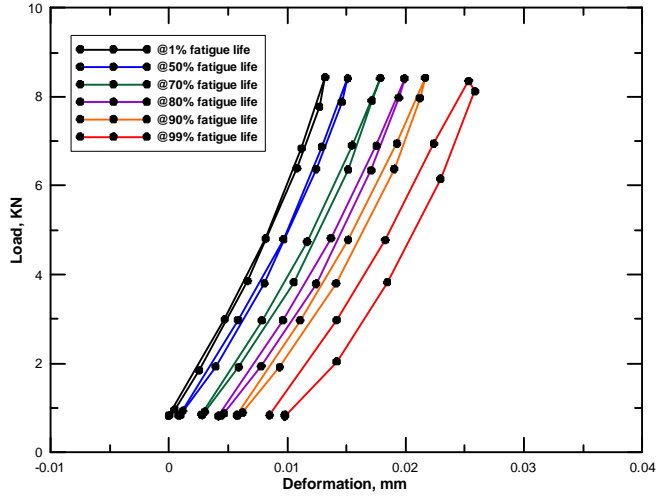


Figure B.15: C3R0@90% stress ratio

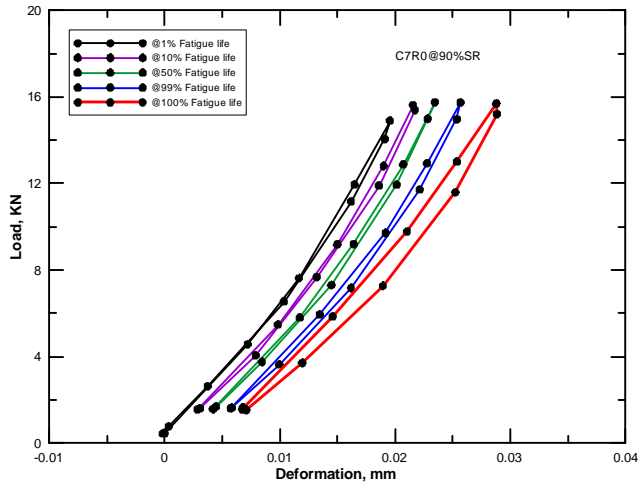


Figure B.16: C7R0@90% stress ratio

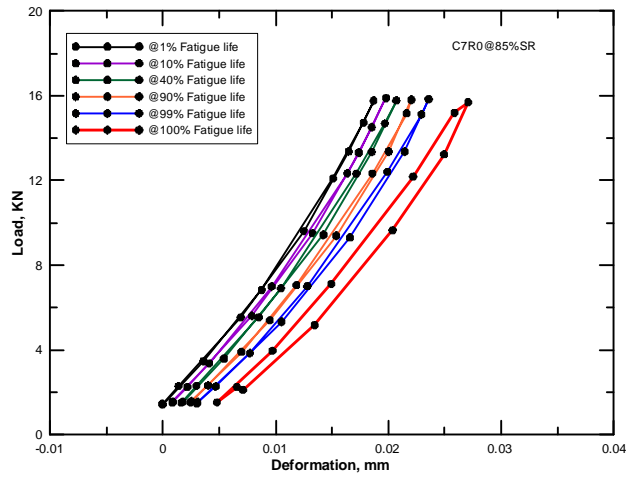


Figure B.17: C7R0@85% stress ratio

## Appendix C

### Dissipated energy approach results

The dissipated energy approach was used in Chapter 9 to determine the fatigue life for different mixtures as presented in Figure C.1 through Figure C.17.

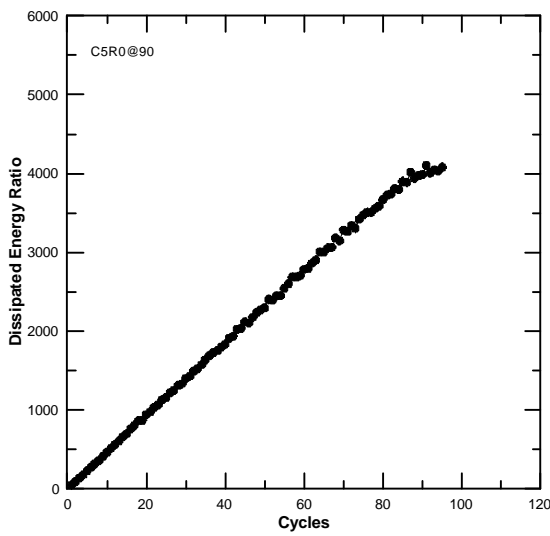


Figure C.1: Variation in energy ratio versus cycles number for C5R0@90

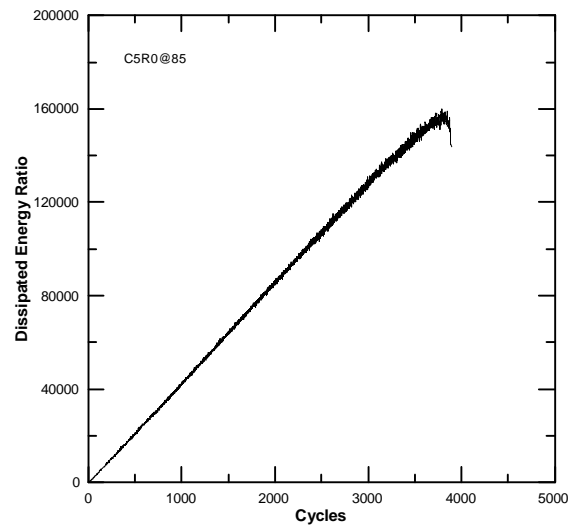


Figure C.2: Variation in energy ratio versus cycles number for C5R0@85

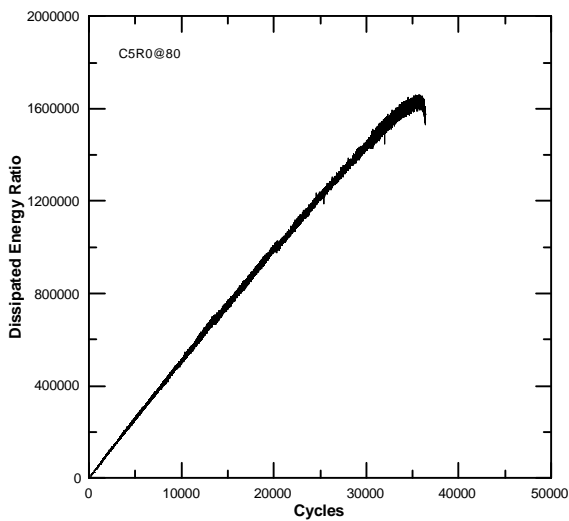


Figure C.3: Variation in energy ratio versus cycles number for C5R0@80

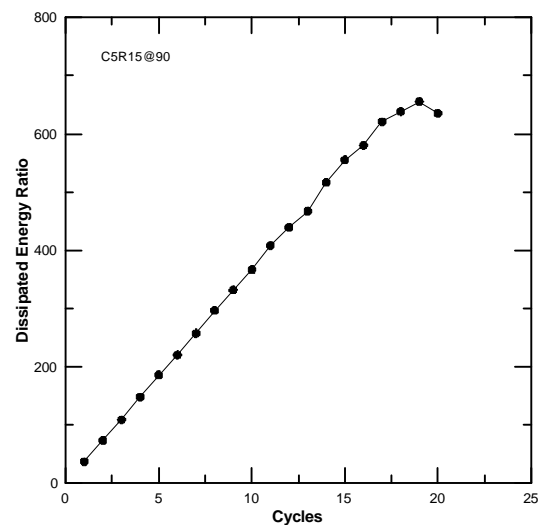


Figure C.4: Variation in energy ratio versus cycles number for C5R0@90

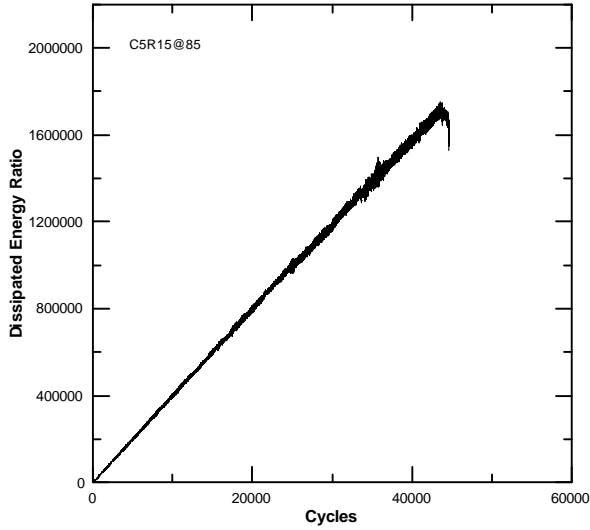


Figure C.5: Variation in energy ratio versus cycles number for C5R15@85

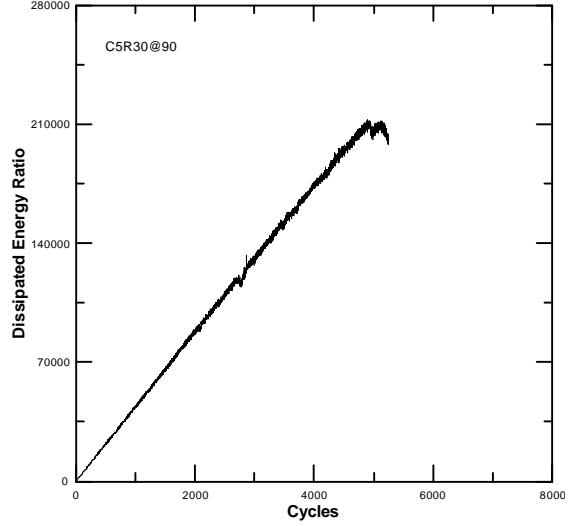


Figure C.6: Variation in energy ratio versus cycles number for C5R30@90

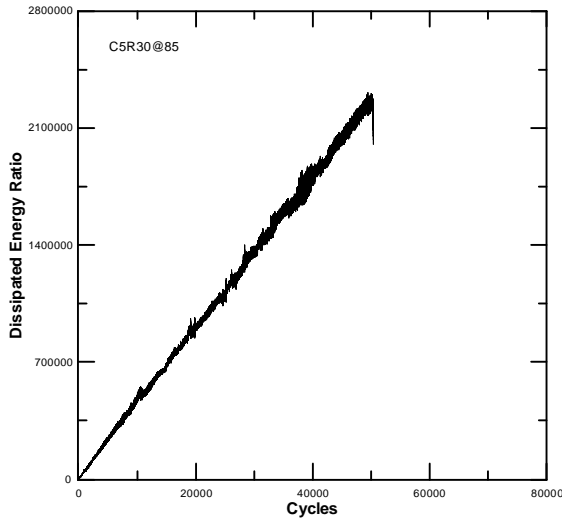


Figure C.7: Variation in energy ratio versus cycles number for C5R30@85

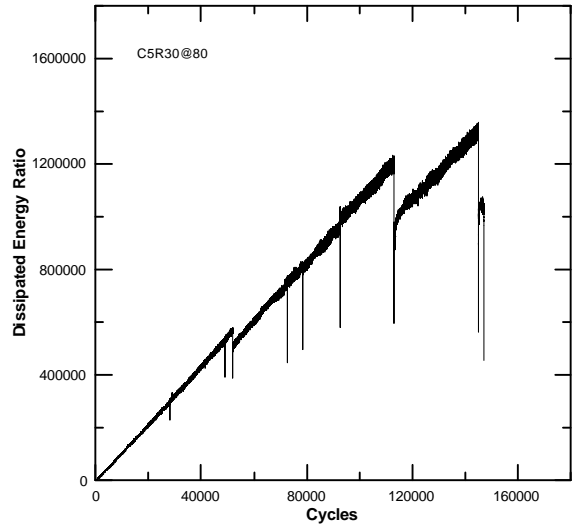


Figure C.8: Variation in energy ratio versus cycles number for C5R30@80

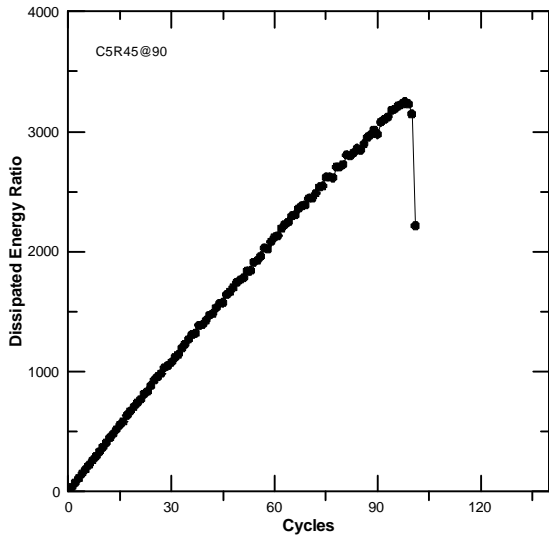


Figure C.9: Variation in energy ratio versus cycles number for C5R45@90

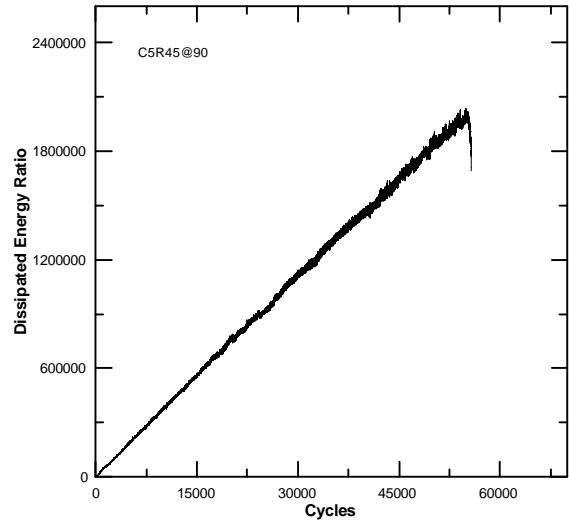


Figure C.10: Variation in energy ratio versus cycles number for C5R45@85

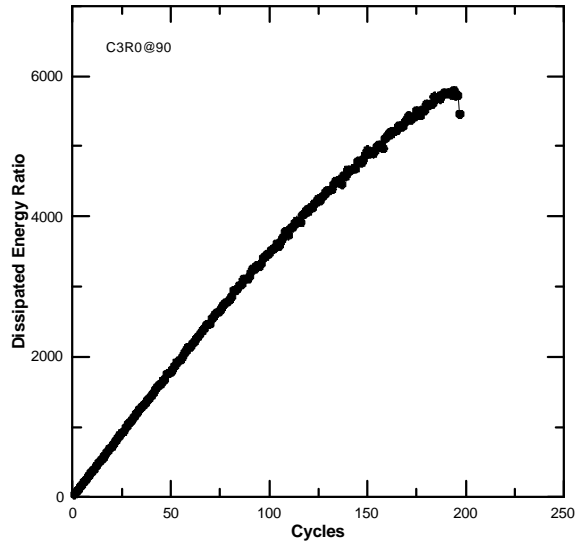


Figure C.11: Variation in energy ratio versus cycles number for C3R0@90

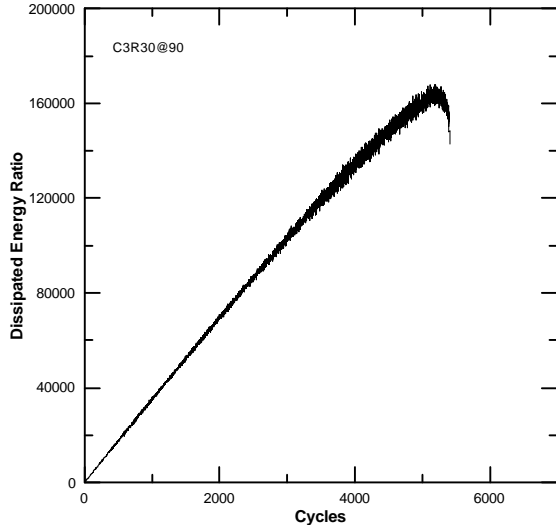


Figure C.12: Variation in energy ratio versus cycles number for C3R30@90

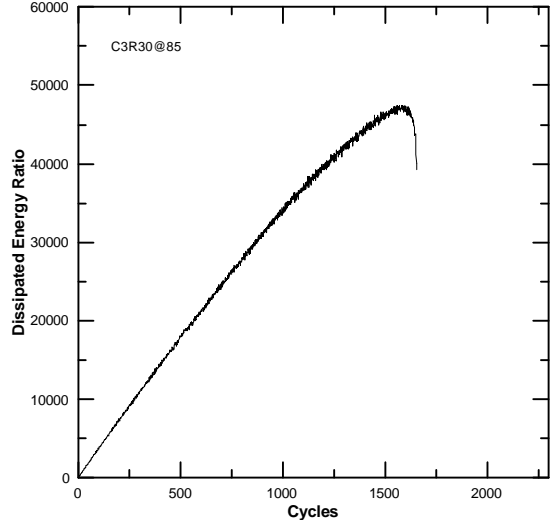


Figure C.13: Variation in energy ratio versus cycles number for C3R30@85

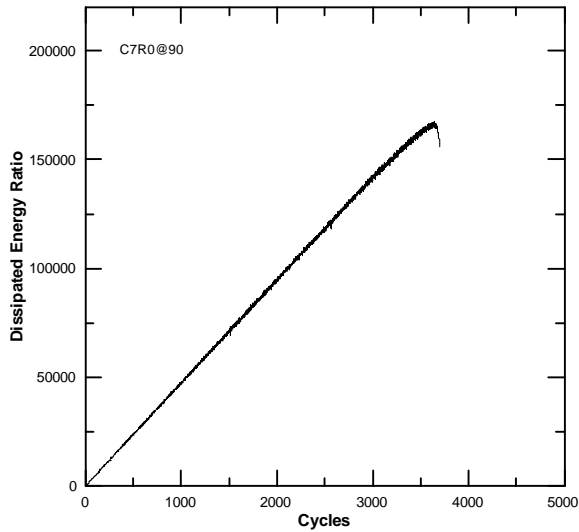


Figure C.14: Variation in energy ratio versus cycles number for C7R0@90

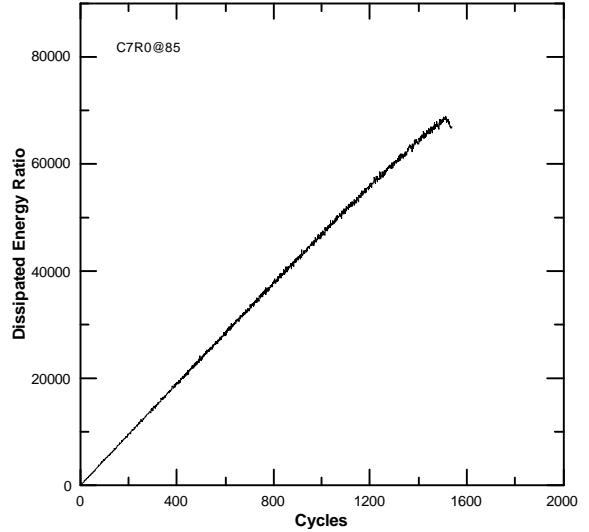


Figure C.15: Variation in energy ratio versus cycles number for C5R0@85

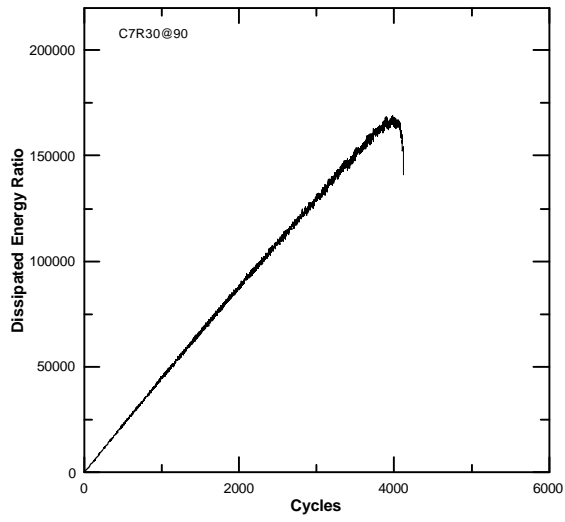


Figure C.16: Variation in energy ratio versus cycles number for C7R30@90

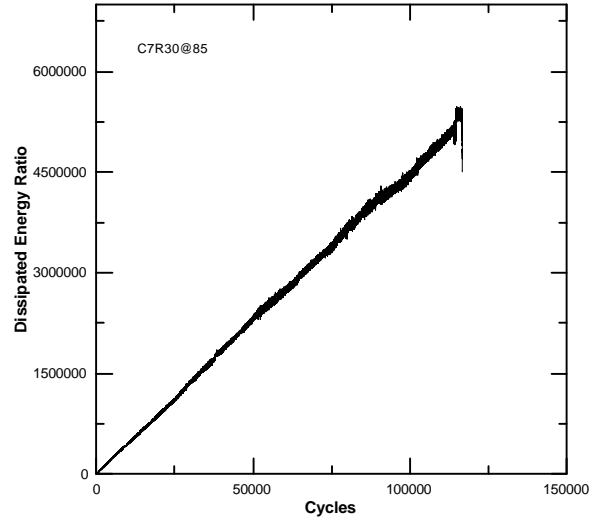


Figure C.17: Variation in energy ratio versus cycles number for C5R30@85

## Appendix D

The relationships between different moduli of elasticity estimated by static, dynamic and nondestructive testing were described in Chapter 9. The graphical representations are illustrated in Figure E.1 through Figure E.5.

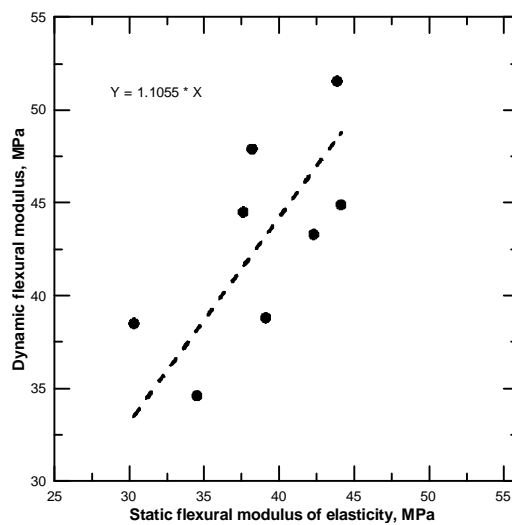


Figure D.1: Relationship between dynamic flexural modulus and static flexural modulus

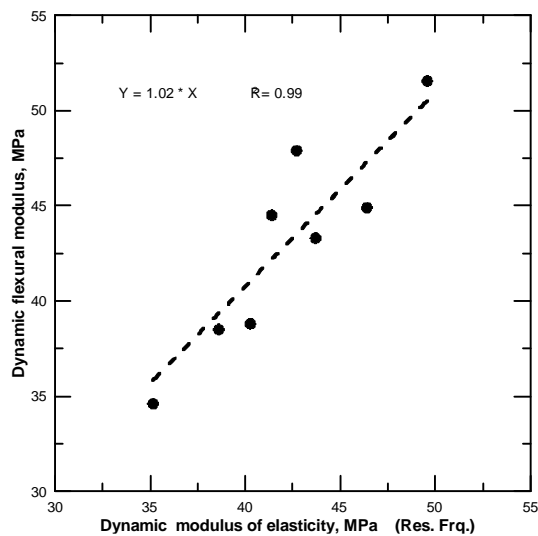


Figure D.2: Relationship between dynamic flexural modulus and dynamic modulus estimated by resonant frequency method

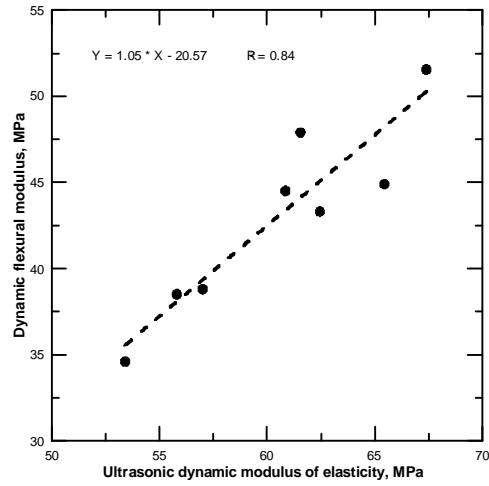


Figure D.3: Relationship between dynamic flexural modulus and dynamic modulus estimated by ultrasonic method

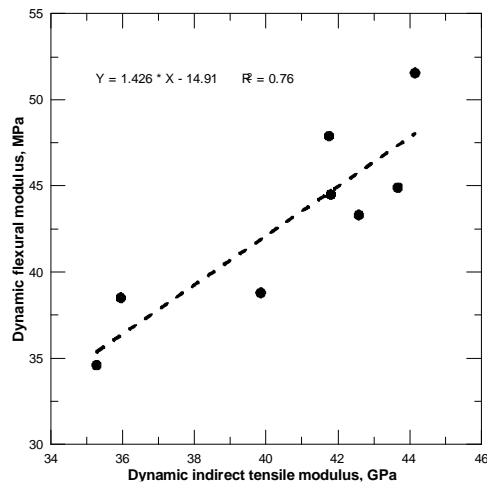


Figure D.4: Relationship between dynamic flexural modulus and dynamic indirect tensile modulus

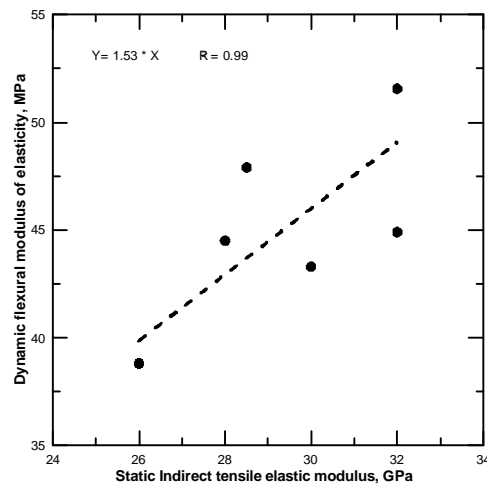


Figure D.5: Relationship between dynamic flexural modulus and static indirect tensile modulus